



APPENDIX

K

**TALBINGO AND
TANTANGARA RESERVOIRS
PHYSICAL LIMNOLOGY
REPORT**



Talbingo and Tantangara Reservoirs Physical Limnology

Snowy 2.0 Main Works
Environmental Impact Statement

599181511

Prepared for
EMM Consulting Pty Ltd

13 September 2019



Contact Information

Cardno (NSW/ACT) Pty Ltd

ABN 95 001 145 035

Level 9 - The Forum

203 Pacific Highway

St Leonards NSW 2065

Australia

www.cardno.com

Phone +61 2 9496 7700

Fax +61 2 9439 5170

Document Information

Prepared for	EMM Consulting Pty Ltd
Project Name	Snowy 2.0 Main Works Environmental Impact Statement
File Reference	59918111_Snowy2_Reservoirs Physical Limnology Rev1.docx
Job Reference	599181511
Date	13 September 2019
Version Number	Rev1

Author(s):



David van Senden
APAC Water Director

Effective Date 13/09/2019

Approved By:



Lachlan Barnes
Environmental Management Team Lead

Date Approved 13/08/2019

Document History

Version	Effective Date	Description of Revision	Prepared by	Reviewed by
V0F	6 June 2019	Preliminary Draft	David van Senden	
V0K	1 July 2019	Draft	David van Senden	Lachlan Barnes
RevA	23 July 2019	Final Draft	DvS / Tanja Mackenzie	Chris Scraggs
RevB	2 August 2019	Final Draft	David van Senden	Belinda Crichton
Rev0	28 August 2019	Final	David van Senden	Belinda Crichton
Rev1	13 September 2019	Final	David van Senden	Belinda Crichton

© Cardno. Copyright in the whole and every part of this document belongs to Cardno and may not be used, sold, transferred, copied or reproduced in whole or in part in any manner or form or in or on any media to any person other than by agreement with Cardno.

This document is produced by Cardno solely for the benefit and use by the client in accordance with the terms of the engagement. Cardno does not and shall not assume any responsibility or liability whatsoever to any third party arising out of any use or reliance by any third party on the content of this document.

Our report is based on information made available by the client. The validity and comprehensiveness of supplied information has not been independently verified and, for the purposes of this report, it is assumed that the information provided to Cardno is both complete and accurate. Whilst, to the best of our knowledge, the information contained in this report is accurate at the date of issue, changes may occur to the site conditions, the site context or the applicable planning framework. This report should not be used after any such changes without consulting the provider of the report or a suitably qualified person.

Executive Summary

Snowy Hydro Limited (Snowy Hydro) proposes to develop Snowy 2.0, a large-scale pumped hydro-electric storage and generation project which would increase hydro-electric capacity within the existing Snowy Mountains Hydro-electric Scheme (Snowy Scheme). Snowy 2.0 is the largest committed renewable energy project in Australia and is critical to underpinning system security and reliability as Australia transitions to a decarbonised economy. Snowy 2.0 will link the existing Tantangara and Talbingo reservoirs within the Snowy Scheme through a series of underground tunnels and a new hydro-electric power station will be built underground.

The proposed Snowy 2.0 upgrade (the project) involves the construction of a new underground, 2,000 MW hydroelectric power generation station in line with a tunnel connecting Tantangara Reservoir to Talbingo Reservoir. The project aims to generate power during peak demand periods and utilise cheaper power, during periods of low demand and excess generation, to pump water back to Tantangara Reservoir and thereby form an efficient, re-useable, and reliable energy source.

The aim of this report is to characterise the physical limnology of the existing Talbingo and Tantangara reservoirs to provide a sound basis for comparing future predictions of potential change to the ecosystem that may be attributed to the Snowy 2.0 development.

A comprehensive data collection exercise commenced in May 2018 and continues to provide detailed measurements of the behaviour of the reservoirs. In addition to these recent data sets, historic information on weather, reservoir characteristics and operational regime has been collated to provide a basic description of the factors that determine the reservoirs' thermal structure and mixing characteristics – the physical limnology of the reservoirs.

The results of this study indicate that the water mixing regime within both reservoirs is influenced by the energy imparted from the surface winds into the water column, energy inputs from surface heat fluxes, energy contributions from the river inflows, and energy imparted by the water transfers. The surface heat fluxes show strong seasonal trends with spring/summer heating leading to warming of surface waters and development of thermal stratification and the autumn/winter cooling leading to heat loss from the water to the atmosphere with gradual erosion of stratification by surface mixing processes and deepening of the surface mixed layer. During stratified periods diurnal winds excite internal seiche (long-wave motions) that transfer energy from surface to the deeper waters. These motions effectively transfer energy to the deeper waters of the reservoir which then cascades to smaller scales of motion contributing to turbulent mixing then ultimately dissipating into heat energy. As the stratification varies through the summer the natural frequency of the internal motions changes and stratification itself impedes vertical mixing and exchange of water between thermal strata.

In Talbingo Reservoir the Tumut 2 (T2) Power Station discharges to the upper Tumut River arm and the Tumut 3 (T3) Power Station transfers (both out of the reservoir for power generation and pump-back into the reservoir) near the dam lead to mixing within the lower reaches of the reservoir. Because of its depth and thermal mass Talbingo reservoir retains its thermal structure for longer than the shallow Tantangara Reservoir where the thermal structure is typically homogenised by autumn cooling by April each year.

The deepest waters of Talbingo Reservoir (70 to 130 m depth) retain the previous seasons thermal structure through to August when snow melt leads to cold inflows from the unregulated rivers and the water transfers from Tumut 2 Pondage. These cold inflows move along the lake bed, as density currents, down the old river valley to displace the deepest waters near the dam wall. It is likely that during dry years this process is weakened and the deeper water of the reservoir may be retained over the next year. The deeper waters are subject to gradual warming from early October through to the following August, by around 0.05°C per month, by molecular diffusion that transfers heat from warmer surface waters down into the deeper waters, albeit at a very slow rate.

Due to the regular winds, water transfers and annual cooling both reservoirs are subject to regular mixing and the resultant dispersion effectively transfers water borne constituents throughout both reservoirs. The timescale for mixing of the whole body is longer for the deeper waters of Talbingo Reservoir during the stratified summer period.

Water quality of both reservoirs is characterised by relatively low turbidity and chlorophyll-a with some evidence of algal blooms, although the causal relationships of algal blooms is not well understood. Light attenuation measurements collected during three days of vertical profiling indicate a strong relationship between light extinction coefficient and turbidity. Assuming these measurements reflect the relationship

for the rest of the year then it is likely that any increase in turbidity would lead to reduced light penetration and likely reduce primary productivity. The photic depth (depth at which underwater light reduces to 1% of its surface intensity) is typically less than about 10 m. It appears that the waters of both reservoirs contain relatively high colour content (typically due to the presence of dissolved organic compounds in the water, such as tannins) that contributes to the relatively shallow photic depth.

In Talbingo Reservoir, the water transfers for current power generation at T2 and T3 power station typically occur during the high demand periods in the early morning and daylight hours with pump-back flows from T3 power station typically occurring in the late night and pre-dawn period. These flows involve significant water discharges that can lead to turbulent mixing in the Tumut arm due the T2 discharge and rapid lowering and raising of reservoir water levels. In Tantangara Reservoir, water transfers occur at a more constant rate via operation of the Murrumbidgee-Eucumbene tunnel which transfers water from the Murrumbidgee catchment to Eucumbene Reservoir. In Talbingo Reservoir, which is situated in a steep sided river valley with a large surface area, the change in water level has limited effect on the change in shoreline inundation and exposure areas. By contrast, Tantangara Reservoir is situated in a broader floodplain and rapid changes in water level across the gently sloping shoreline lead to rapid changes in shoreline inundation and exposure.

This description of the physical limnology of the existing reservoirs provides a sound basis for assessing the effects of introducing the proposed water transfers between Tantangara and Talbingo Reservoirs. °°

Glossary and Abbreviations

ADCP	Acoustic Doppler Current Profile
AHD	Australian Height Datum, m (~ standard height measurement for Australian construction) approximately mean sea level
AWS	Automatic Weather Station
BoM	Bureau of Meteorology
Cardno	Cardno NSW/ACT Pty Ltd
CSSI	critical State Significant Infrastructure
CTD	Conductivity-Temperature-Depth
DO	Dissolved Oxygen
DoEE	Commonwealth Department of the Environment and Energy
DPIE	NSW Department of Planning, Industry and Environment
ECVT	Egress, Cable and Ventilation Tunnel
EPBC Act	Commonwealth <i>Environment Protection and Biodiversity Conservation Act 1999</i>
EIS	Environmental Impact Statement
EMM	EMM Consulting Pty Ltd
EP&A Act	NSW <i>Environmental Planning and Assessment Act 1979</i>
FSL	Full Supply Level
GL	Gigalitre; 1,000 megalitres
ha	Hectares
HC	Heat Content, measured in Joules (J)
hr	Hour
Hyperlimnion	Deep layer below the main part of the temperature stratification in a lake
km	kilometres
km ²	square kilometres
KNP	Kosciuszko National Park
LGAs	local government areas
LW	Long wave solar radiation
m	metres
m ³	Cubic metres
MAT	main access tunnel
Metalimnion	The middle stratified layer encompassing the thermocline in a lake
ML	Megalitres
MNES	matters of national environmental significance
MOL	Minimum Operating Level
MW	Megawatts
NTU	Nephelometric Turbidity Units
PAR	Photosynthetically available radiation
ROW	River Outlet Works – typically a variable level offtake for environmental flow releases

SEARs	Secretary's Environmental Assessment Requirements
Snowy Hydro	Snowy Hydro Limited
Snowy Scheme	Snowy Mountains Hydro-electric Scheme
SRD SEPP	<i>State Environmental Planning Policy (State and Regional Development) 2011</i>
SSI	State significant infrastructure
SW	Short wave solar radiation
T1 (Power Station)	Tumut 1 Underground Power Station
T2 (Power Station)	Tumut 2 Power Station
T3 (Power Station)	Tumut 3 Power Station
Talweg	Valley floor – the deepest part of the cross section through a river valley
TKE	Turbulence kinetic energy

Table of Contents

Executive Summary	iii
Glossary and Abbreviations	v
Table of Contents	vii
Appendices	viii
Tables	ix
Figures	ix
1 Introduction	1
1.1 The Project	1
1.2 Project Location	2
1.2.1 Project Area	2
1.3 Proponent	3
1.4 Purpose of this Report	3
1.5 Related Projects	3
1.6 Report Structure	4
2 Overview of the Snowy Scheme	5
2.1 Existing Snowy Hydro Scheme	5
2.2 Weather	8
3 Talbingo Reservoir and Tantangara Reservoir	9
3.1 Physical Limnology	9
3.2 Talbingo Reservoir	12
3.3 Tantangara Reservoir	15
4 Methodology	17
4.1 Available Data	17
4.2 Field Program 2018-19	17
4.3 Analysis	21
4.3.1 General	21
4.3.2 Meteorological Data	21
4.3.3 Reservoir Heat Content and Surface Heat Fluxes	21
4.3.4 Thermal Structure	22
4.3.5 Seiches	23
4.3.6 Light Extinction	24
5 Results	25
5.1 Introduction	25
5.2 Overview of Historic Operations	25
5.2.1 Water Levels	25
5.2.2 Inflows	26
5.2.3 Annual Water Budget	26

5.3	Talbingo Reservoir 2018-19	31
5.3.1	Weather and Surface Heat Flux	31
5.3.2	Thermal Structure	31
5.3.3	Inflows and Outflows 28 September to 4 October 2018	36
5.3.4	Spatial Structure (CTD Surveys)	39
5.3.5	Water Density and Intrusions	41
5.3.6	Seiches and Mixing	42
5.4	Tantangara Reservoir 2018-19	42
5.4.1	Weather and Surface Heat Fluxes	42
5.4.2	Thermal Structure	43
5.4.3	Underwater Light and Extinction Coefficient	47
6	Discussion	50
6.1	Temperature Comparison – Talbingo and Tantangara Reservoirs	50
6.2	Summary of Key Processes	51
7	References	54

Appendices

Appendix A	Monitoring Program
Appendix B	Heat Flux Methods
Appendix C	Inflows and Transfers
Appendix D	Meteorological Figures
Appendix E	Thermistor String Figures
Appendix F	CTD Profiles
Appendix G	CTD Long Sections
Appendix H	Water Quality Time Series
Appendix I	ADCP Current Meter Figures
Appendix J	Monthly Snapshots

Tables

Table 3-1	Key features of Talbingo and Tantangara reservoirs	9
Table 3-2	Tumut 2 Pondage, Talbingo Reservoir and Jounama Pondage inlets and outlet structures and capacities	14
Table 3-3	Tantangara Reservoir inlets and outlet structures	15
Table 4-1	Available data – Talbingo and Tantangara Reservoirs	18
Table 5-1	Water level variability in Talbingo and Tantangara reservoirs expressed in m below dam FSL (Talbingo FSL 543.2 m AHD and Tantangara FSL 1,228.7 m AHD)*	25
Table 5-2	Long-term flow information for Talbingo Reservoir	27
Table 5-3	Long-term flow information for Tantangara Reservoir	27
Table 5-4	Monthly heat flux components (see Section 6.3 for definitions) and the total heat flux in Talbingo Reservoir	31
Table 5-5	Monthly heat flux components (see Section 4.3.3 for definitions) and the total heat flux in Tantangara Reservoir	43
Table 5-6	Coefficients relating extinction coefficients to chlorophyll-a and turbidity using reliable data (44 points)	48
Table 5-7	Light Extinction, Photic Depth versus Turbidity	48

Figures

Figure 2-1	Infrastructure and interconnections of the Snowy-Murray (top) and Snowy-Tumut (bottom) components of the Snowy Scheme	6
Figure 2-2	General topography and catchment boundaries of Talbingo and Tantangara Reservoirs and the Snowy Scheme infrastructure	7
Figure 3-1	Talbingo and Tantangara reservoirs bathymetry.	10
Figure 3-2	Schematic diagram of Talbingo Reservoir indicating the key processes that determine reservoir dynamics, mixing and dispersion	11
Figure 3-3	Schematic diagram of Tantangara Reservoir indicating the key processes that determine reservoir dynamics, mixing and dispersion.	12
Figure 3-4	Tumut 2 Power Station discharge to Tumut River in the upper Talbingo Reservoir (~25 km upstream of the dam wall).	13
Figure 3-5	Hypsography of Talbingo Reservoir (minimum bed elevation 401 m AHD)	14
Figure 3-6	Hypsography of Tantangara Reservoir (minimum bed elevation 1193 m AHD)	16
Figure 4-1	Talbingo Reservoir moorings and profiling sites. Distances are chainage from the dam wall along the thalweg	19
Figure 4-2	Tantangara Reservoir moorings and sampling sites. Distances are chainage from the dam wall along the thalweg	20
Figure 4-3	Overview of the heat exchange mechanisms at a water body surface (Deltares, 2019)	22
Figure 5-1	Water levels in Talbingo (top) and Tantangara (bottom) reservoirs for 20 years 1999 to 2019	25
Figure 5-2	Total annual rainfall, mean stream discharge and total discharge measured at Talbingo Reservoir between 1993 and 2018	29
Figure 5-3	Historical mean rainfall and stream inflow and discharge at Tantangara Reservoir (1993 - 2019)	30
Figure 5-4	Monthly averaged surface heat fluxes (W/m ²) for Talbingo Reservoir	31

Figure 5-5	Temperature isotherms derived from 10-minute samples at 50 thermistors deployed over the total depth near the dam wall at Talbingo Reservoir (TAL01)	33
Figure 5-6	Thermistor String surface and bottom temperatures at the three sites	34
Figure 5-7	Temperature profiles in Talbingo Reservoir derived from thermistor strings at the 3 sites on 29 July 2018 at 6 hr intervals.	35
Figure 5-8	Daily average velocity vectors derived from the ADCP deployed in Talbingo Reservoir at TAL_ADCP_02 in the Tumut Arm 1 km upstream of Tumut/Yarrangobilly confluence.	36
Figure 5-9	Thermal Structure - Temporal a) Yarrangobilly River stream discharge (top), b) T3 extraction and pumpback and T2 inflow (middle), and c) Talbingo Reservoir water level (bottom)	37
Figure 5-10	Easterly and northerly wind speeds (top) and air temperature (bottom) at Talbingo Reservoir (TAL_01) near the dam wall	38
Figure 5-11	Isotherm depths, 8°C and 9°C at Tal_01 near the dam wall Tal_02 near Long Creek and Tal_03 in the Yarrangobilly arm	38
Figure 5-12	Longitudinal currents at ADCP site TAL_01 in the Yarrangobilly arm	39
Figure 5-13	Daily averaged current vectors at each depth at the two ADCP sites	39
Figure 5-14	Longitudinal/depth contours on 2 October 2018 derived from vertical profiles (sites indicated). Lower panel zoomed in to 50 m depth. Triangles and numbers indicate the profiles sampling locations.	40
Figure 5-15	T3 inlet/outlet channel and transects	41
Figure 5-16	Monthly heat flux components and the net heat flux for Tantangara Reservoir	43
Figure 5-17	Temperature isotherms derived from 10 min samples at 30 thermistors deployed over the total depth near the dam wall at Tantangara Reservoir	44
Figure 5-18	Isotherm depths at the two thermistor sites in Tantangara Reservoir	45
Figure 5-19	Longitudinal currents at ADCP site TAL_ADCP_01 in Tantangara Reservoir	46
Figure 5-20	Vertical profiles collected on 4 October 2018 in Tantangara Reservoir at CTD profiling sites 1, 4, 6, 8 and 10	47
Figure 5-21	Light Extinction coefficient versus chlorophyll-a and Turbidity derived from CTD profiles in both Reservoirs	48
Figure 6-1	Temperature at different depths near the dam walls in Tantangara and Talbingo reservoirs	50

1 Introduction

1.1 The Project

Snowy Hydro Limited (Snowy Hydro) proposes to develop Snowy 2.0, a large-scale pumped hydro-electric storage and generation project which would increase hydro-electric capacity within the existing Snowy Mountains Hydro-electric Scheme (Snowy Scheme). Snowy 2.0 is the largest committed renewable energy project in Australia and is critical to underpinning system security and reliability as Australia transitions to a decarbonised economy. Snowy 2.0 will link the existing Tantangara and Talbingo reservoirs within the Snowy Scheme through a series of underground tunnels and a new hydro-electric power station will be built underground.

Snowy 2.0 has been declared to be State significant infrastructure (SSI) and critical State significant infrastructure (CSSI) by the former NSW Minister for Planning under Part 5 of the NSW *Environmental Planning and Assessment Act 1979* (EP&A Act) and is defined as CSSI in clause 9 of Schedule 5 of the *State Environmental Planning Policy (State and Regional Development) 2011* (SRD SEPP). CSSI is infrastructure that is deemed by the NSW Minister to be essential for the State for economic, environmental or social reasons. An application for CSSI must be accompanied by an environmental impact statement (EIS).

Separate applications are being submitted by Snowy Hydro for different stages of Snowy 2.0 under Part 5, Division 5.2 of the EP&A Act. This includes the preceding first stage of Snowy 2.0, Exploratory Works for Snowy 2.0 (the Exploratory Works) and the stage subject of this current application, Snowy 2.0 Main Works (the Main Works). In addition, an application under Part 5, Division 5.2 of the EP&A Act is also being submitted by Snowy Hydro for a segment factory that will make tunnel segments for both the Exploratory Works and Main Works stages of Snowy 2.0.

The first stage of Snowy 2.0, the Exploratory Works, includes an exploratory tunnel and portal and other exploratory and construction activities primarily in the Lobs Hole area of the Kosciuszko National Park (KNP). The Exploratory Works were approved by the former NSW Minister for Planning on 7 February 2019 as a separate project application to NSW Department of Planning, Industry and Environment (DPIE)(SSI 9208).

This description of the physical limnology of the existing Talbingo and Tantangara Reservoirs has been prepared to accompany an application and supporting EIS for the Snowy 2.0 Main Works. As the title suggests, this stage of the project covers the major construction elements of Snowy 2.0, including permanent infrastructure (such as the underground power station, power waterways, access tunnels, chambers and shafts), temporary construction infrastructure (such as construction adits, construction compounds and accommodation), management and storage of excavated rock material and establishing supporting infrastructure (such as road upgrades and extensions, water and sewage treatment infrastructure, and the provision of construction power). Snowy 2.0 Main Works also includes the operation of Snowy 2.0.

Snowy 2.0 Main Works, if approved, would commence before completion of Exploratory Works.

The Snowy 2.0 Main Works do not include the transmission works proposed by TransGrid (TransGrid, 2018) that provide connection between the cableyard and the NEM. These transmission works will provide the ability for Snowy 2.0 (and other generators) to efficiently and reliably transmit additional renewable energy to major load centres during periods of peak demand, as well as enable a supply of renewable energy to pump water from Talbingo Reservoir to Tantangara Reservoir during periods of low demand. While the upgrade works to the wider transmission network and connection between the cableyard and the network form part of the CSSI declaration for Snowy 2.0 and Transmission Project, they do not form part of this application and will be subject to separate application and approval processes, managed by TransGrid. This project is known as the HumeLink and is part of AEMO's Integrated System Plan.

With respect to the provisions of the Commonwealth *Environment Protection and Biodiversity Conservation Act 1999* (EPBC Act), on 30 October 2018 Snowy Hydro referred the Snowy 2.0 Main Works to the Commonwealth Department of the Environment and Energy (DoEE) and, on a precautionary basis, nominated that Snowy 2.0 Main Works has potential to have a significant impact on matters of national environmental significance (MNES) and the environment generally.

On 5 December 2018, Snowy 2.0 Main Works were deemed a controlled action by the Assistant Secretary of the DoEE. It was also determined that potential impacts of the project will be assessed by accredited assessment under Part 5, Division 5.2 of the EP&A Act. This accredited process will enable the DPIE to manage the assessment of Snowy 2.0 Main Works, including the issuing of the assessment requirements for the EIS. Once the assessment has been completed, the Commonwealth Minister for the Environment will make a determination under the EPBC Act.

1.2 Project Location

Snowy 2.0 Main Works are within the Australian Alps, in southern NSW, about mid-way between Canberra and Albury. Snowy 2.0 Main Works is within both the Snowy Valleys and Snowy Monaro Regional local government areas (LGAs).

The nearest large towns to Snowy 2.0 Main Works are Cooma and Tumut. Cooma is located about 50 kilometres (km) south east of the project area (or 70 km by road from Providence Portal at the southern edge of the project area), and Tumut is located about 35 km north west of the project areas (or 45 km by road from Tumut 3 Power Station at the northern edge of the project area). Other townships near the project area include Talbingo, Cabramurra, Adaminaby and Tumberumba. Talbingo and Cabramurra were built for the original Snowy Scheme workers and their families, while Adaminaby was relocated in 1957 to make way for the establishment of Lake Eucumbene.

The pumped hydro-electric scheme elements of Snowy 2.0 Main Works are mostly underground between the southern ends of Tantangara and Talbingo reservoirs, a straight-line distance of 27 km. Surface works will also occur at locations on and between the two reservoirs. Key locations for surface works include:

- > Tantangara Reservoir - at a full supply level (FSL) of about 1,229 metres (m) to Australian Height Datum (AHD), Tantangara Reservoir will be the upper reservoir for Snowy 2.0 and include the headrace tunnel and intake structure. The site will also be used for a temporary construction compound, accommodation camp and other temporary ancillary activities;
- > Marica - this site will be used primarily for construction including construction of vertical shafts to the underground power station (ventilation shaft) and headrace tunnel (surge shaft), and a temporary accommodation camp;
- > Lobs Hole - the site will be used primarily for construction but will also become the main entrance to the power station during operation. Lobs Hole will provide access to the Exploratory Works tunnel, which will be refitted to become the main access tunnel (MAT), as well as the location of the emergency egress, cable and ventilation tunnel (ECVT), portal, associated services and accommodation camp; and
- > Talbingo Reservoir - at a FSL of about 546 m AHD, Talbingo Reservoir will be the lower reservoir for Snowy 2.0 and will include the tailrace tunnel and water intake structure. The site will also be used for temporary construction compounds and other temporary ancillary activities.

Works will also be required within the two reservoirs for the placement of excavated rock and surplus cut material. Supporting infrastructure will include establishing or upgrading access tracks and roads and electricity connections to construction sites.

Most of the proposed pumped hydro-electric and temporary construction elements and most of the supporting infrastructure for Snowy 2.0 Main Works are located within the boundaries of KNP, although the disturbance footprint for the project during construction is less than 0.25% of the total KNP area. Some of the supporting infrastructure and construction sites and activities (including sections of road upgrade, power and communications infrastructure) extends beyond the national park boundaries. These sections of infrastructure are primarily located to the east and south of Tantangara Reservoir. One temporary construction site is located beyond the national park along the Snowy Mountains Highway about 3 km east of Providence Portal (referred to as Rock Forest).

The area of interest for this report is described in more detail in Chapter 2.

1.2.1 Project Area

The project area for Snowy 2.0 Main Works has been identified and includes all the elements of the project, including all construction and operational elements. Key features of the project area are:

- > The water bodies of Tantangara and Talbingo reservoirs, covering areas of 19.4 square kilometres (km²) and 21.2 km² respectively. The reservoirs provide the water to be utilised in Snowy 2.0;

- > Major watercourses including the Yarrangobilly, Eucumbene and Murrumbidgee rivers and some of their tributaries;
- > KNP, within which the majority of the project area is located. Within the project area, KNP is characterised by two key zones: upper slopes and inverted treelines in the west of the project area (referred to as the 'ravine') and associated subalpine treeless flats and valleys in the east of the project area (referred to as the 'plateau'); and
- > Farm land southeast of KNP at Rock Forest.

The project area is interspersed with built infrastructure including recreational sites and facilities, main roads as well as unsealed access tracks, hiking trails, farm land, electricity infrastructure, and infrastructure associated with the Snowy Scheme.

1.3 Proponent

Snowy Hydro is the proponent for the Snowy 2.0 Main Works. Snowy Hydro is an integrated energy business – generating energy, providing price risk management products for wholesale customers and delivering energy to homes and businesses. Snowy Hydro is the fourth largest energy retailer in the NEM and is Australia's leading provider of peak, renewable energy.

1.4 Purpose of this Report

The purpose of this report is to provide the background description of the physical limnology of Talbingo Reservoir and Tantangara Reservoir to inform the EIS for the Snowy 2.0 project. The scope of this report is to collate, analyse and interpret available reservoir and meteorological data to:

1. Describe the general long-term weather and rainfall patterns that affect reservoir dynamics;
2. Analyse data from the intensive field exercises carried out by Cardno between April 2018 and March 2019;
3. Characterise the existing system surface mixed layer depth, metalimnion and hypolimnion thickness variability;
4. Discuss temporal variability in the vertical level of inflow intrusions (surface, mid-depth or bottom) under different seasonal conditions;
5. Discuss the selective withdrawal process at intakes and its effects on reservoir stratification;
6. Characterise the turbidity, extinction coefficient, light penetration; and
7. Summarise the key mixing and stratification regimes in the existing Talbingo and Tantangara Reservoirs to inform the modelling and aquatic ecology impact assessments.

At the commissioning of this report the available data included measurements prior to March 31, 2019. The preparation of this report was carried out to inform the EIS and hence was mindful of the Secretary's Environmental Assessment Requirements (SEARs) for Snowy 2.0 Main Works, issued on 31 July 2019, as well as relevant government assessment requirements, guidelines and policies.

1.5 Related Projects

There are three other projects related to Snowy 2.0 Main Works, they are:

- > Snowy 2.0 Exploratory Works (SSI-9208) – a Snowy Hydro project with Minister's approval;
- > Snowy 2.0 Transmission Connect Project (SSI-9717) – a project proposed by TransGrid; and
- > Snowy 2.0 – Segment Factory (SSI-10034) – a project proposed by Snowy Hydro.

While these projects form part of the CSSI declaration for Snowy 2.0 and Transmission Project, they do not form part of Snowy Hydro's application for Snowy 2.0 Main Works. These related projects are subject to separate application and approval processes. Staged submission and separate approval is appropriate for a project of this magnitude, due to its complexity and funding and procurement processes.

1.6 Report Structure

This report is structured as follows:

- > Section 2 provides a brief overview of the existing Snowy Scheme and the regional setting including, weather and river flows;
- > Section 3 provides a description of the reservoirs dimensions and their water transfer infrastructure;
- > Section 4 outlines the methodology used for this review, including the analysis techniques applied to the datasets to quantify various processes;
- > Section 5 reports the results of the analyses; and
- > Section 6 summarises the key processes driving the existing system dynamics and general findings.

2 Overview of the Snowy Scheme

2.1 Existing Snowy Hydro Scheme

The Snowy Mountains form the highest mountain peaks of the Great Dividing Range in south eastern Australia with the tallest peak Mt Kosciuszko at 2,228 m AHD. Winter snow covers the peaks down to around 1,400 m during winter before providing spring snow melt that drains to four major river basins that can provide water to various components of the existing Snowy Hydro scheme. These basins include the:

- > Tooma River to the southwest;
- > Tumut River that flows north, then to the west and ultimately joins the Murrumbidgee River;
- > Murrumbidgee River that initially flows east then turns north and ultimately flows to the Murray River; and
- > Snowy River that flows eastwards to the Tasman Sea.

The Murray River flows west and ultimately enters the Southern Ocean some 2,500 km downstream at Goolwa in South Australia. Weathering of the ancient mountain range has led to the steep incised river systems ideal for water storages and hydropower generation.

Planning for the Snowy Scheme commenced in the 1940s. Construction of the Scheme started in 1949 and was completed in 1974. Built in the National interest with the support of the NSW, Victorian, South Australian and Commonwealth Governments, the Snowy Scheme today provides electricity to the National Electricity Market and much needed water storage for drought security. A brief overview of the existing Snowy Scheme and the proposed Snowy 2.0 expansion of the scheme is provided on the project webpage - <https://www.snowyhydro.com.au/our-scheme/snowy20/>.

The Snowy Scheme incorporates the following assets (**Figure 2-1** and **Figure 2-2**):

- > Nine power stations – Murray 1, Murray 2, Blowering, Guthega, Tumut 1 (T1, located 366 m below ground level), Tumut 2 (T2, located 244 m below ground level), Tumut 3 (T3), Jounama Small Hydro Power Station and Jindabyne Mini Hydro Power Station;
- > One pumping station at Jindabyne and a pump storage capability at T3 Power Station;
- > Sixteen major dams with a total storage capacity of 7,000 GL;
- > 145 km of inter-connected tunnels and pipelines and 80 km of aqueducts; and
- > Thirty-three hydro-electric turbines with a generating capacity of 4,100 MW.

These assets provide the vital infrastructure to manage the flow of waters (including snow melt) from the upper catchments of the Murray River, including the Murrumbidgee and Tumut Rivers, and the Snowy River, to generate electricity and provide water for irrigation, the downstream riverine and floodplain environments, and support drinking water supply to a number of small towns. The Murrumbidgee River is a tributary of the Murray River, and the Tumut River is a tributary of the Murrumbidgee River.

Since the Snowy Scheme's completion in 1974, Snowy Hydro has carefully managed the water that flows through the Scheme's dams, tunnels, aqueducts and power stations in accordance with its water licence. Since revision of the Commonwealth *Water Act 2007* Snowy Hydro is required to contribute to the development of annual Water Sharing Plans agreed between stakeholders that then guide the following years' water allocations to water users.

In the Snowy Scheme, water releases and electricity generation are inseparably linked. Each year, Snowy Hydro has to reach certain targets for downstream and environmental water releases in accordance with the Water Licence. Snowy Hydro has operational flexibility day-to-day to strategically manage electricity generation and water releases while at the same time giving long-term security to the downstream users around annual water releases.

The waters within the scheme can be diverted from the Tooma River and Eucumbene Reservoir through trans-mountain tunnels to Tumut Pondage, where they join the waters of the Tumut River and flow through T1 and T2 underground power stations that ultimately discharge into the Tumut River within the upper reaches of Talbingo Reservoir. T3 Power Station is located downstream of Talbingo Dam. Three of the six units at T3 Power Station are equipped with large pumps that can be used to pump water from Jounama Pondage back up into Talbingo Reservoir. In the existing scheme and within the Tumut River system, water cannot be pumped any further uphill than Talbingo Reservoir.

Talbingo Reservoir is one of a six storages on the Tumut River (**Figure 2-1**) with a water surface roughly 540 m AHD. The T2 Power Station discharges to the Tumut Arm of Talbingo Reservoir some 33 km upstream of the Talbingo Dam wall. T2 sources water from Tumut 2 Pondage located at an elevation of around 800 m AHD. Further upstream the T1 underground Power Station sources water from Tumut Pondage where the water surface is about 1,160 m AHD. Tumut Pondage can also source water via the tunnels from the Snowy River catchment at Lake Eucumbene and from Tooma Reservoir in the Upper Murray catchment. Water from Tantangara Reservoir can flow into Lake Eucumbene thereby forming a connection to the Murrumbidgee River.

Tantangara Reservoir is located about 25 km east of Talbingo Reservoir, some 700 m higher at around 1,200 m above sea level in the upper Murrumbidgee River catchment (**Figure 2-1**). Tantangara Reservoir captures natural inflows from the Murrumbidgee River and Mosquito Creek. In addition, transfers from the Goodradigbee River via the Goodradigbee Aqueduct also flow into Tantangara Reservoir. The Goodradigbee River flows northward through the Brindabella Range to the join the Murrumbidgee River at Burrinjuck Reservoir near Canberra. Water from Tantangara Reservoir can be transferred to Lake Eucumbene, via the Murrumbidgee to Eucumbene tunnel, and a discharge via the River Outlet works on the dam wall to facilitate environmental release flows to the Murrumbidgee River downstream.

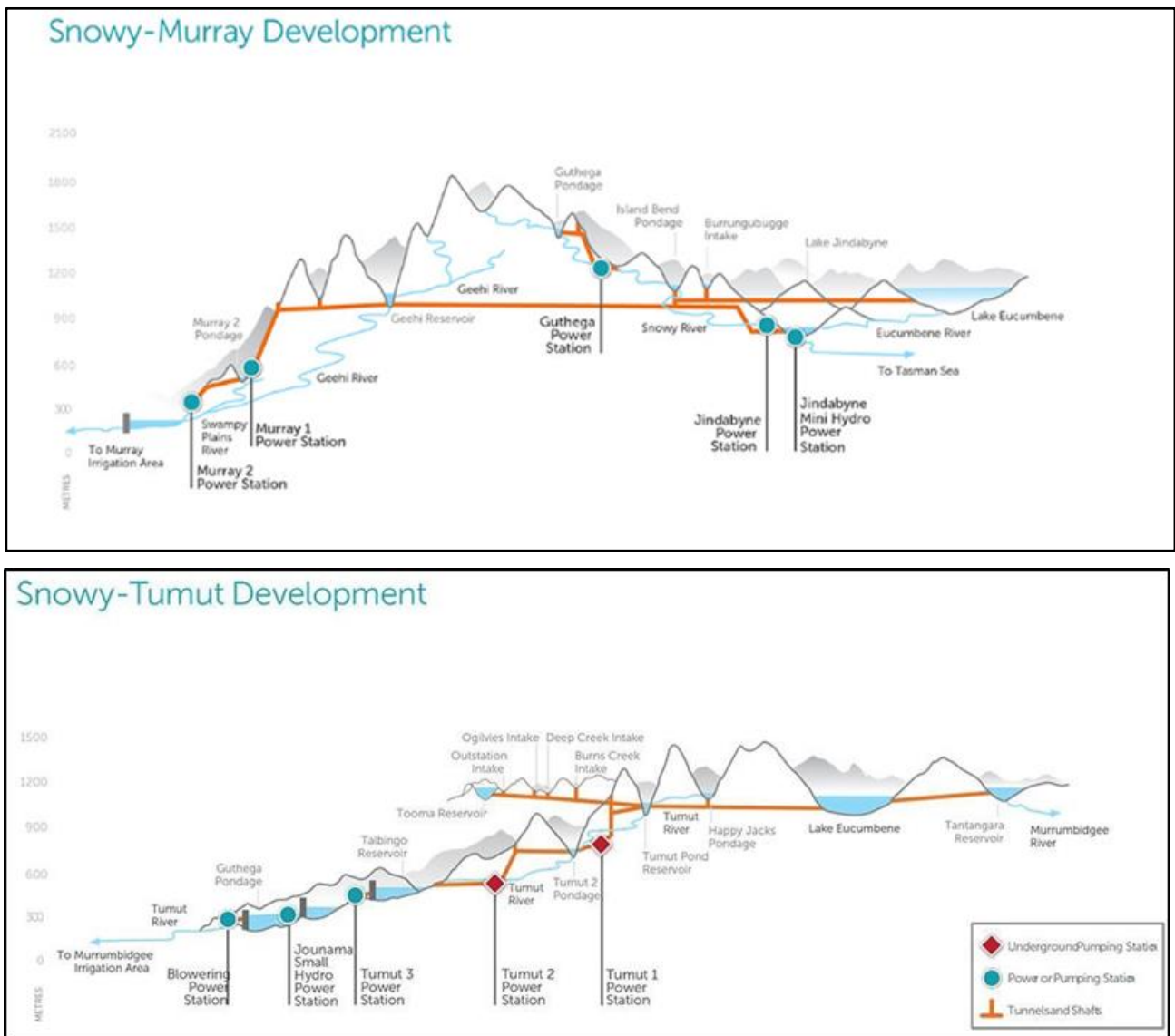


Figure 2-1 Infrastructure and interconnections of the Snowy-Murray (top) and Snowy-Tumut (bottom) components of the Snowy Scheme

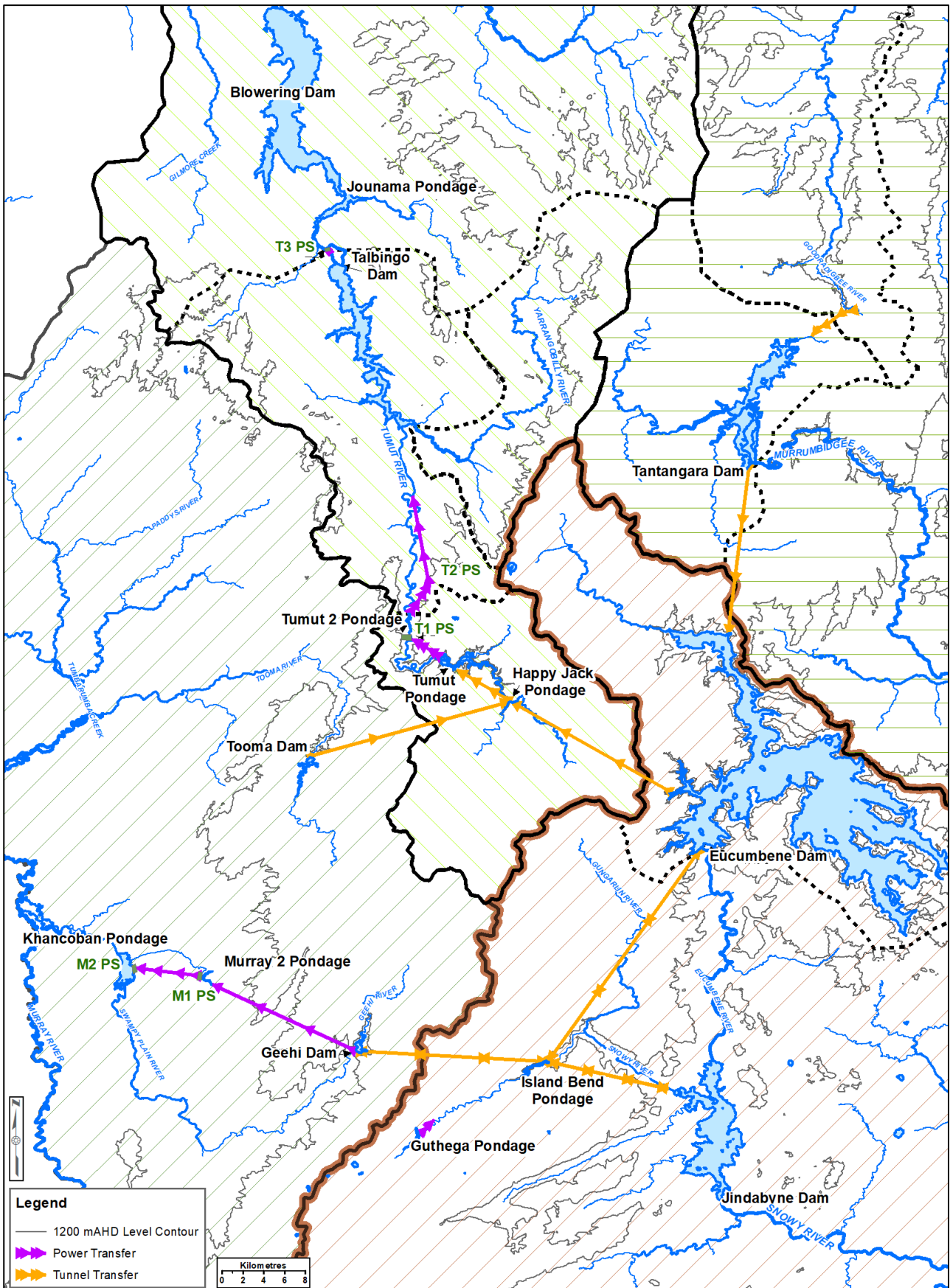


Figure 2-2 General topography and catchment boundaries of Talbingo and Tantangara Reservoirs and the Snowy Scheme infrastructure

2.2 Weather

The meteorological and hydrological characteristics of the study area are described in Snowy Hydro (2017), which analysed available data from weather station records dating back to 1969 (with good quality continuous records from 1993) and reliable reservoir inflow records commencing in 1953 for Tantangara Reservoir and 1948 for Talbingo Reservoir.

The key characteristics reported in Snowy Hydro (2017) of relevance to this review are as follows:

- > The region is characterised by hot dry summers and cold winters with snow falling at higher altitudes;
- > Mean monthly maximum and minimum temperatures at Tantangara are significantly lower than those at Talbingo;
- > While average annual precipitation is similar for both Tantangara and Talbingo, precipitation regularly falls as snow during winter at Tantangara, and snowpack could be expected during the coldest months, although unlikely to persist at depth for long periods. In contrast, at Talbingo snowfall is rare and snow would not persist for any appreciable length of time;
- > There is substantial inter-annual variability in precipitation at both sites;
- > Tantangara Reservoir receives on average 224 GL of inflow per year, peaking between July and October when snow melts and precipitation peaks. There is significant inter-annual variability and over the past 23 years annual flows have ranged from less than 40 GL in drought years to over 300 GL during wetter years ; and
- > Talbingo Reservoir receives on average 1,616 GL of inflow per year, also peaking between July and October. There is significant inter-annual variability, with annual flows ranging from less than 500 GL in drought years, up to over 3,300 GL in wetter years.

The different climatic and inflow characteristics are due in part to the significant difference in elevations between the two reservoirs, with Tantangara Reservoir at 1,200 m AHD and Talbingo Reservoir at 540 m AHD. Another key feature of the climate is the high inter-annual variability. Both factors have a major influence on reservoir physical limnology with flow-on effects on water quality and aquatic ecology.

3 Talbingo Reservoir and Tantangara Reservoir

3.1 Physical Limnology

Key features of Talbingo and Tantangara reservoirs are listed in **Table 3-1** along with brief summary of operational characteristics.

Table 3-1 Key features of Talbingo and Tantangara reservoirs

Characteristic	Talbingo Reservoir	Tantangara Reservoir
Volume at Spillway Crest Level (GL)	921	254
Surface Area at Spillway Crest (ha)	1,936	2,117
Catchment Area (km ²)	1,093	460
Dam Crest Elevation (m AHD)	544.7	1,228.7
Full Supply Level (m AHD)	543.2	1,228.7
Minimum Operating Level (m AHD)	534.4	1,205.8
Licence Operating Range (m)	8.8	22.9
Max Depth (m below Dam Crest)	140	35
Existing Snowy operations	T2 inflows to upper reservoir Tumut River, T3 inflows (pumping) and T3 outflows (generation) near dam wall. River Outlet Environmental flow release near dam wall.	Outflow to Lake Eucumbene via Providence Portal, River Outlet Environmental releases to Murrumbidgee River. Both outlets on Tantangara Dam wall.
Recent operation range	8 m over past 20 years.	Typically 5 to 8 m over the past 8 years - reservoir can experience large variations in water level in response to catchment rainfall, evaporation and releases to Lake Eucumbene.

The bathymetry of each of the two reservoirs is in **Figure 3-1**. Note that both river valleys are aligned roughly north-south with the predominant wind direction. In Talbingo Reservoir the dam is located at the northern end of the northward flowing Tumut River, while in Tantangara Reservoir the dam wall is located at the southern end of the south flowing Murrumbidgee River.

Surface heat fluxes and water clarity (as indicated by turbidity) influence the thermal stratification regime within reservoirs. Surface water inflows from streams and rivers are also important to the reservoir water volume, heat and sediment budgets. The energy available to drive turbulent mixing processes (turbulence kinetic energy or TKE) is derived primarily from the surface winds and inflows to the reservoir. This energy is transferred throughout the reservoir by internal seiches and internal waves. This energy then cascades down to smaller and smaller wave-like motions, ultimately dissipating through turbulent mixing events within the water column and at boundaries. These processes and the general flow of water through Talbingo and Tantangara Reservoirs effectively act to redistribute material in the system affecting the physical dynamics and ecosystem response, and are represented in **Figure 3-2** and **Figure 3-3** respectively.

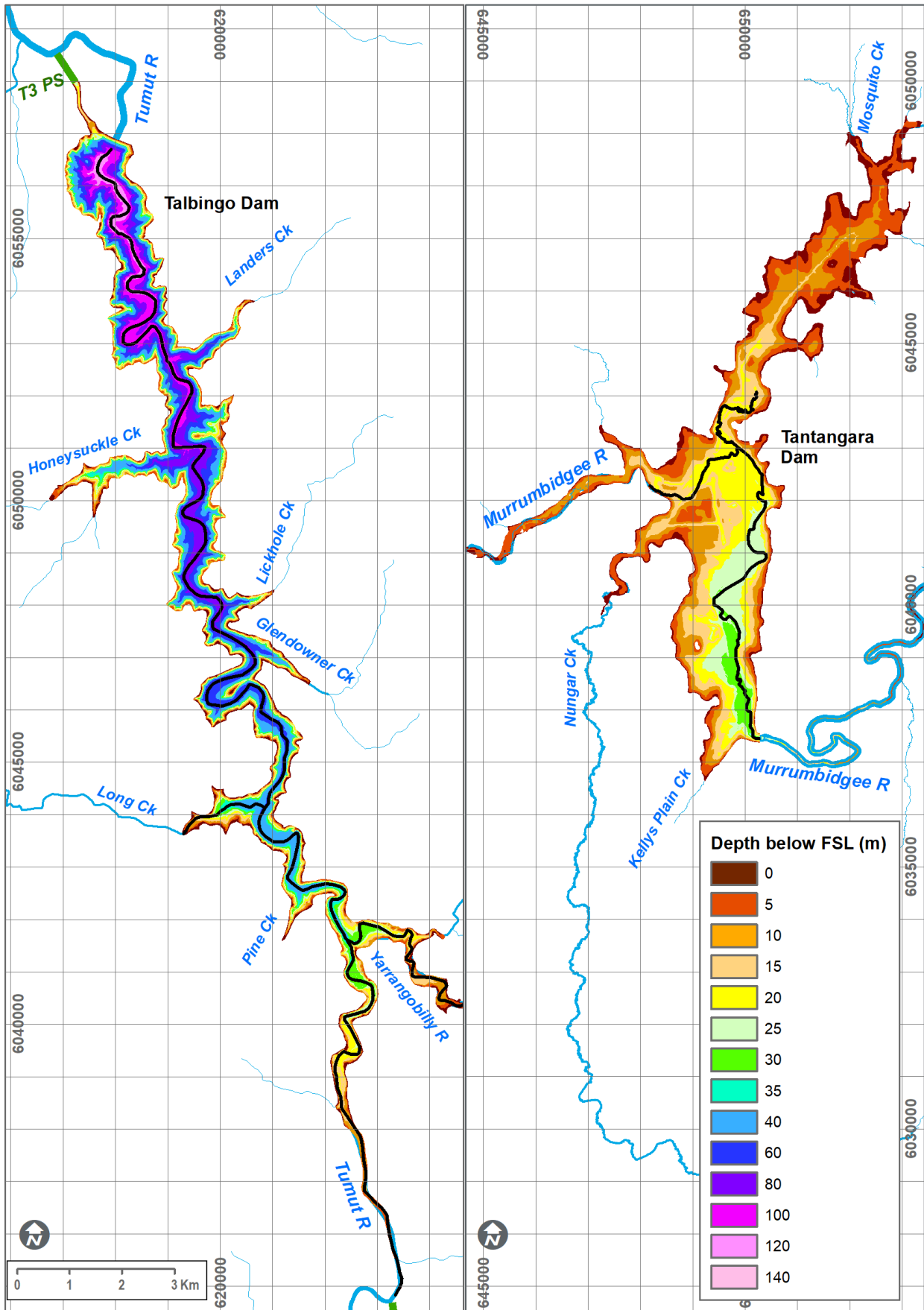


Figure 3-1 Talbingo and Tintangara reservoirs bathymetry.

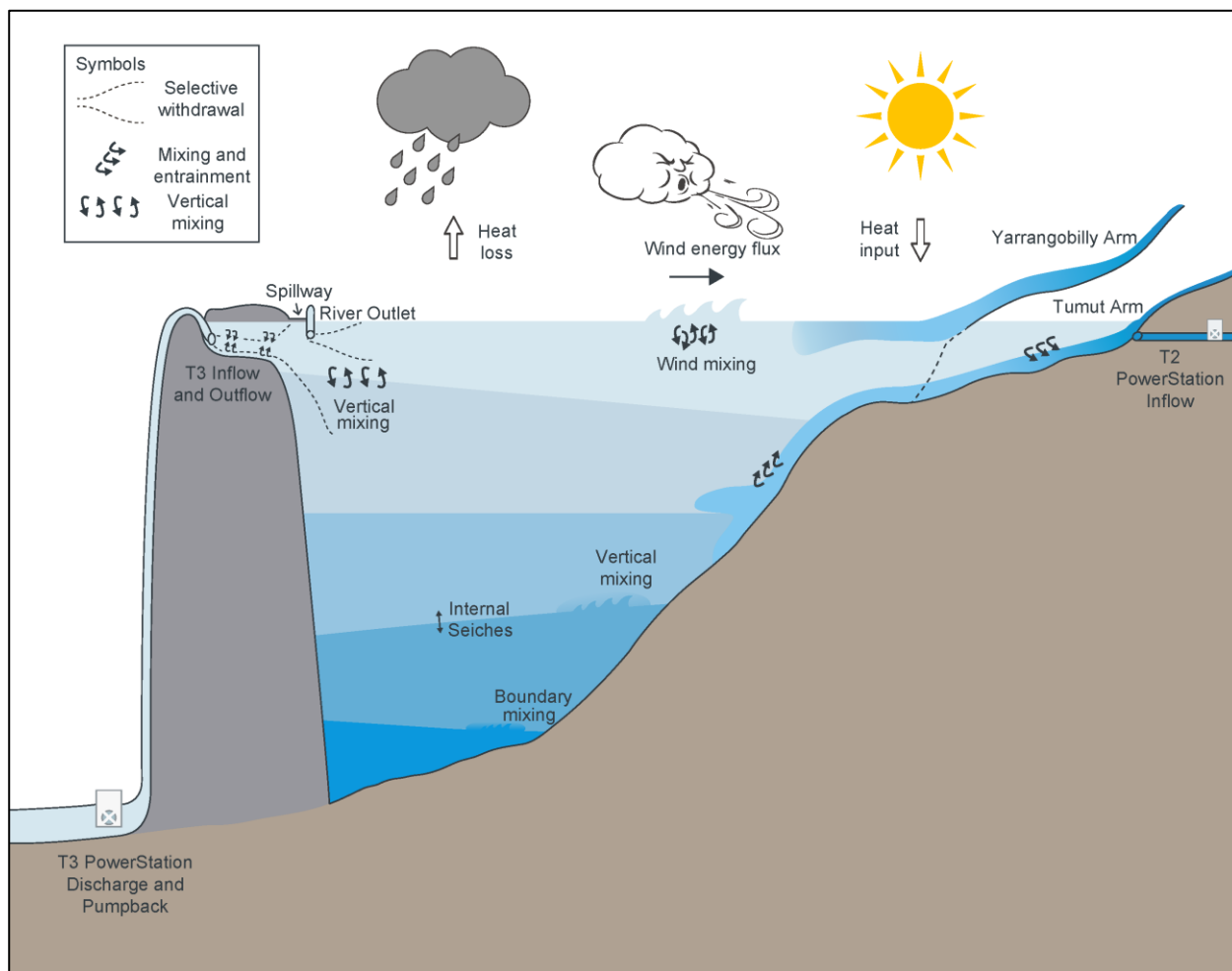


Figure 3-2 Schematic diagram of Talbingo Reservoir indicating the key processes that determine reservoir dynamics, mixing and dispersion

The key potential and kinetic energy inputs to the reservoir include:

- > Solar radiation (produces buoyancy);
- > Wind (imparts energy to the water surface leading to seiching and mixing);
- > Natural inflows and outflows; and
- > Transfers for hydroelectric generation (both inflows and outflows).

This energy is then redistributed within the lake/reservoir by processes including:

- > Internal seiches;
- > High frequency internal waves;
- > Turbulent mixing and TKE dissipation at boundaries and internally; and
- > Density currents intruding into the reservoir at their level of neutral buoyancy.

Wuest *et al.* (2000) demonstrated that the TKE imparted to lake waters by the surface wind stress is dissipated both internally within the water body and at the lake boundary with breaking internal waves leading to small mixing events that collapse as density intrusions into the lake. The overall effect of these processes is consistent across different lakes and stratification regimes.

Inflows also introduce significant mixing associated with the kinetic energy of the inflow. Outflows and selective withdrawal processes effectively extract energy from the water body.

The processes described above lead to turbulent mixing and dispersion of waterborne constituents (e.g. nutrients, metals and particles).

In stratified systems the characteristics of the water withdrawal via an outflow are influenced by the level of the outlet, the intensity of the stratification and withdrawal discharge. Similarly, the inflow characteristics are an important determinant for the level at which water propagates into the reservoir. It is therefore important to understand where the inflows have come from and the water characteristics of that source to determine where the inflow is likely to end up in the reservoir.

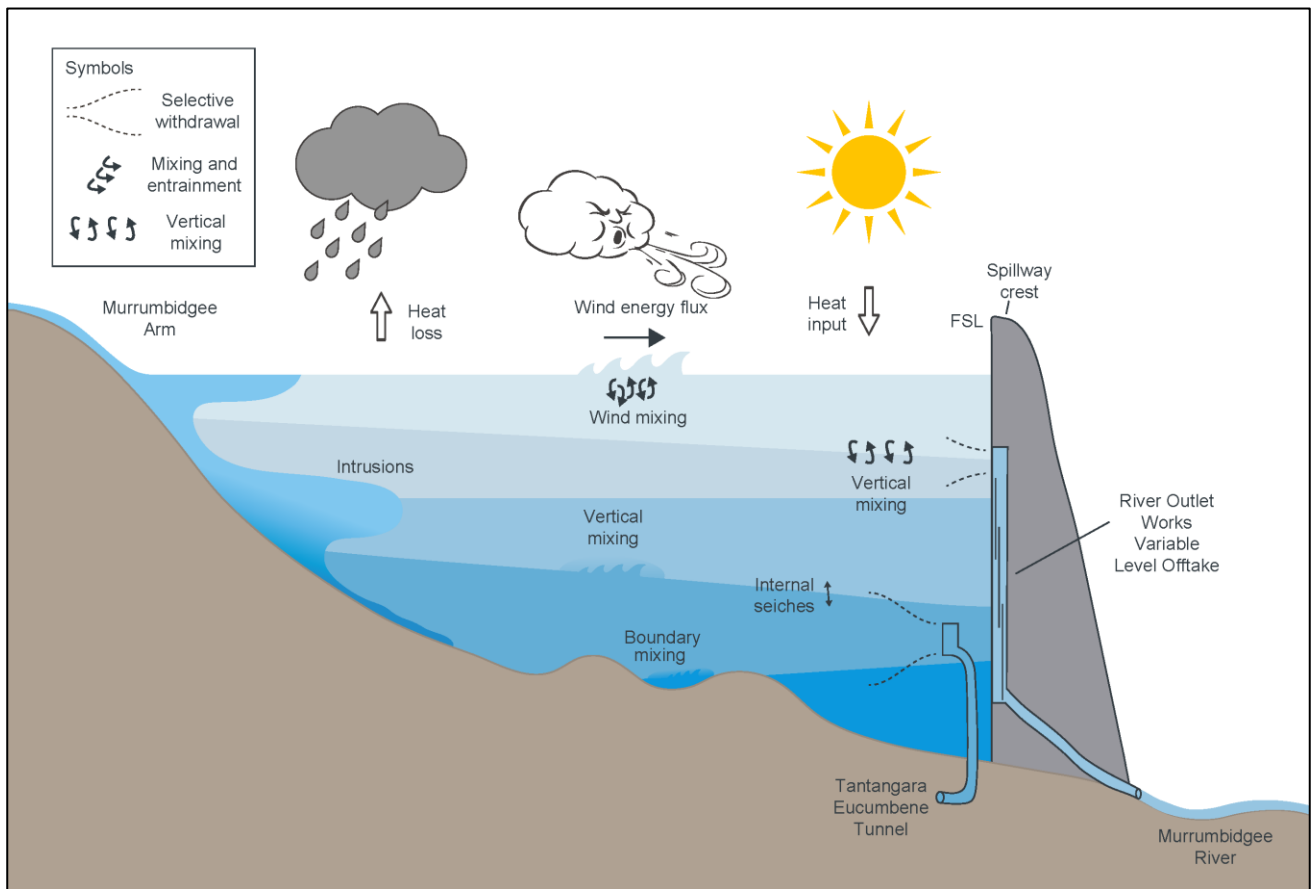


Figure 3-3 Schematic diagram of Tantangara Reservoir indicating the key processes that determine reservoir dynamics, mixing and dispersion.

3.2 Talbingo Reservoir

Talbingo Dam was constructed in 1971 and is located on the Tumut River. The dam wall is 162 m high and 700 m wide at the crest. The main water sources to Talbingo Reservoir comprise natural stream flows, regulated upper Tumut River flows, and pumpback transfers from Jounama Pondage. The highly regulated Tumut River upstream of the reservoir drains about 50% of the total Talbingo Reservoir catchment, the natural flow in the Yarrangobilly River drains about 30% of the catchment and a number of smaller streams drain the remaining 20% of the Talbingo Reservoir catchment.

Discharge from the T2 Power Station feeds into the Tumut River, just downstream of the Elliot Way bridge crossing some 33 km upstream of the dam wall and about 8 km upstream of the Yarrangobilly and Tumut Rivers confluence. The T2 discharge enters the reservoir via a rock lined channel.

The bottom of the T2 Outlet is around 533 m AHD and generally submerged about 8 m below the typical storage water surface level of 542 m AHD. Water discharging from the T2 Outlet is sourced from the small Tumut 2 Pondage at an elevation of around 800 m AHD. The discharge is likely to introduce colder water into the upper Talbingo Reservoir for most of the year, except perhaps in late summer when the smaller volume of T2 Pondage water is likely to become warmer than the Talbingo surface waters. The relatively high flow (**Figure 3-4**) of this water is likely to cause significant mixing within the Tumut Arm of the reservoir. Introduction of the cold water is also likely to lead to density currents flowing downstream along the lake bed.

Adjacent to the dam wall, a 1 km long by 100 m wide by 20 m deep headrace channel feeds water to the inlet structure connecting six pipes to the T3 Power Station. The T3 Power Station is located below the Dam and discharges into Jounama Pondage from which, water can be pumped back into Talbingo

storage via three of the six units. An additional offtake tower, the River Outlet Works is also located near the dam wall to facilitate environmental releases to the Tumut River downstream of the dam that flow into Jounama Pondage.

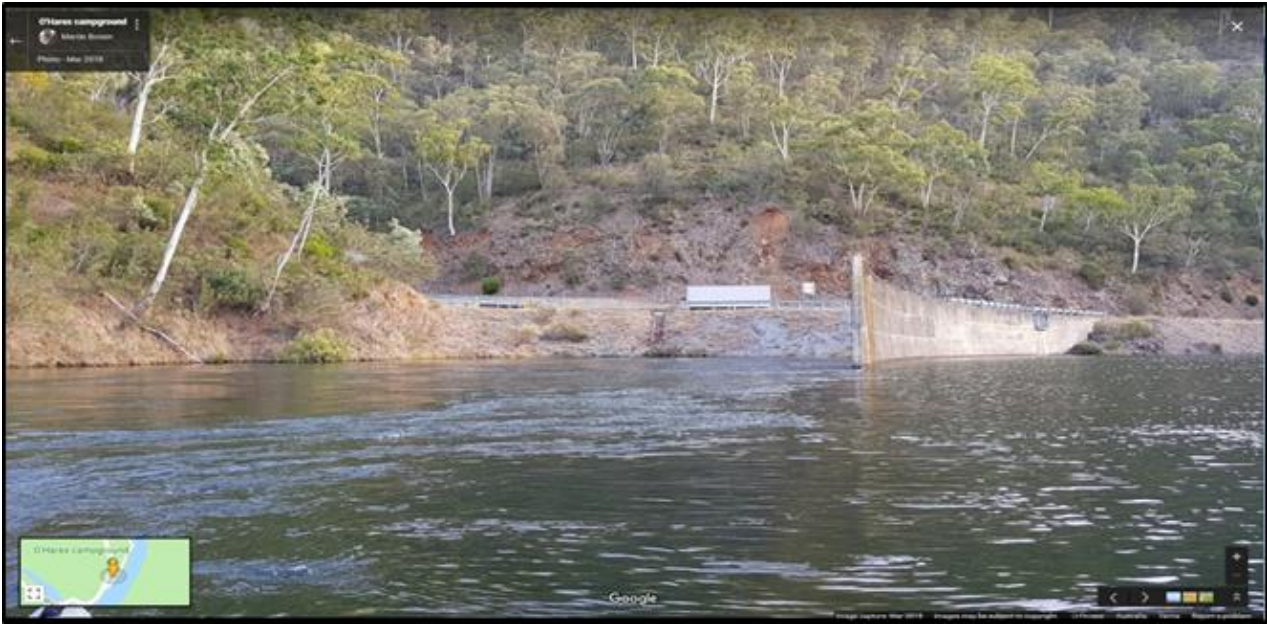


Figure 3-4 Tumut 2 Power Station discharge to Tumut River in the upper Talbingo Reservoir (~25 km upstream of the dam wall).

Yarrangobilly Creek (refer **Figure 3-1**) forms the main tributary with significant undisturbed catchment inflow. The confluence of the Yarrangobilly Creek and the Tumut River is within the storage some 18 km (along the original river thalweg path) upstream of the dam wall.

Key operational infrastructure affecting water flows, storage levels and water quality include the levels and rating curves of the various intakes, catchment inflows and the spillway crest level that is generally only overtopped under extreme flood scenarios. For Talbingo Reservoir this includes the T3 Power Station and River Outlet intakes, the upstream inflows from the natural rivers and the regulated T2 Power Station discharge. These levels are discussed further below, but are included here to provide an indication of the relationship between operating level and storage hypsographic curve (**Figure 3-5**). The water levels indicated by the box and whisker diagram indicate the maximum, 75th percentile, median, 25th percentile, and minimum, and red crosses show outliers of a normal distribution of the data.

The water transfer infrastructure for transfers to/from Talbingo Reservoir are listed in **Table 3-2**. The vertical level and dimensions of the outlet structures are key to understanding the water withdrawal characteristics during outflow from the reservoir, for example, to the T3 Power Station. Likewise, the dimensions and structures at inflow locations and the flow rate are key to understanding the mixing around the inflow points. Transfers of water from the Tumut 2 Pondage via the T2 Power Station effectively transfer water downstream along the Tumut River. The T3 discharge flows into the Jounama Pondage and can be pumped back into Talbingo Reservoir.

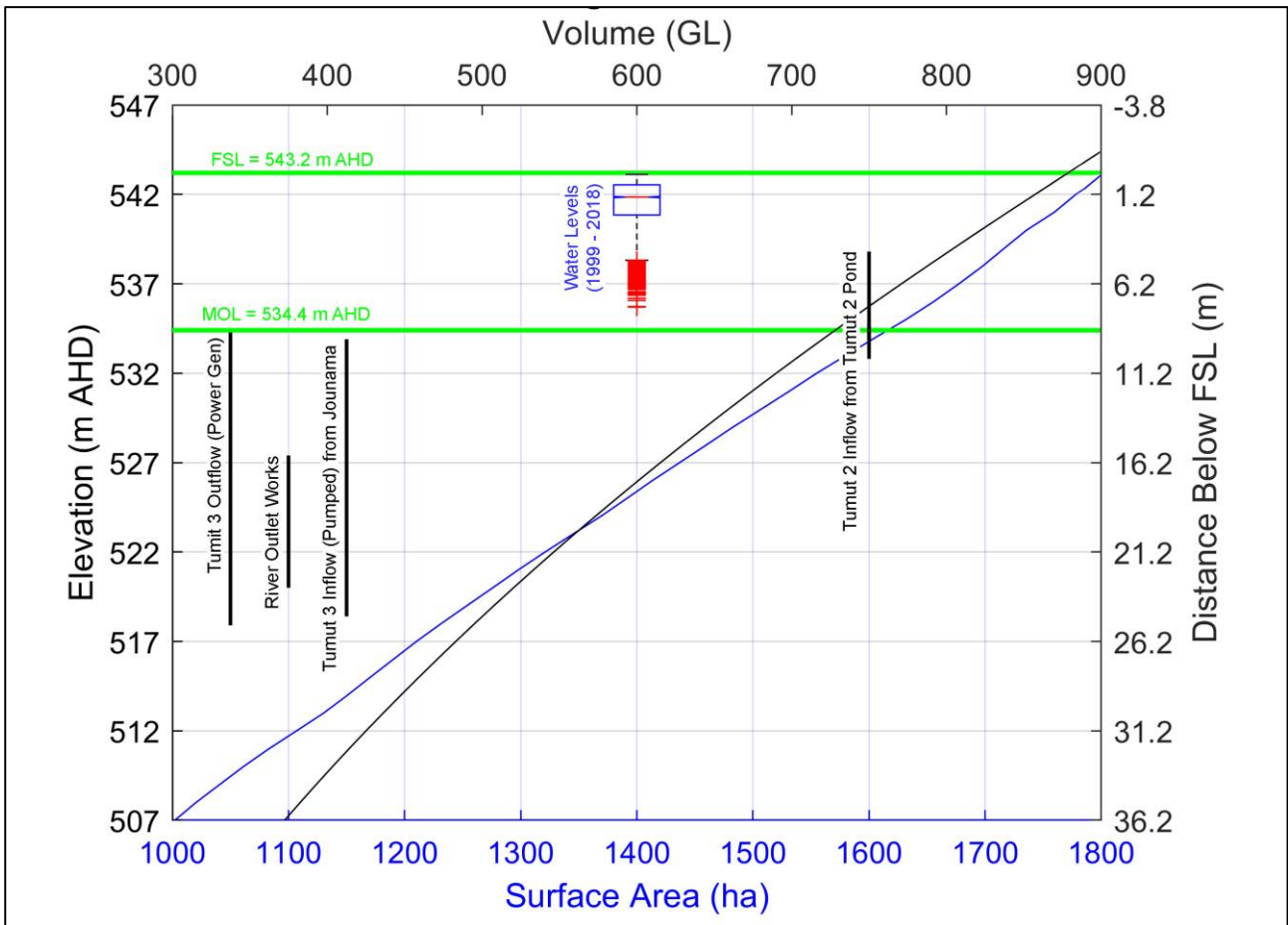


Figure 3-5 Hypsography of Talbingo Reservoir (minimum bed elevation 401 m AHD)

Table 3-2 Tumut 2 Pondage, Talbingo Reservoir and Jounama Pondage inlets and outlet structures and capacities

Structure	Flow	Dimensions	Centreline AHD	Vertical extent (min. - max.)	Capacity (m³/s)	Capacity (ML/hr)
Tumut 2 Pondage						
Tumut 2 Inlet	Out	6 panels each 2.92 m wide x 8 m tall (17.52 m wide x 8 m tall)	813.6	809.6 - 817.6	118.9	428
Talbingo Reservoir						
Tumut 3 Inlet Structure	Out	6 inlets each 9.9 m wide x 16.5 m high (59.4 m wide x 16.5 m tall)	526.1	519.4 - 534.4	1,200	4,320
River Outlet Works	Out	7.32 m high x 4 m wide	523.7	520.0 - 527.4	70.8	255
Spillway	Out	230.4 m long crest with 545.9 m crest elevation	544.7		4,250	15,300
Jounama pumped to Tumut 3 Outlet	In	3 of the T3 pipes with pumps	526.1	518.4 - 533.9	297.3	1,070
Tumut 2 Outlet	In	11 m wide and 6 m tall outlet	535.8	532.8 - 538.8	118.9	428
Jounama Pondage pump back to Talbingo						
Tumut 3 Pump Intake	In	3 inlet channels each 5 m diameter vertical	371.83	371.83	297.3	1,070

3.3 Tantangara Reservoir

Tantangara Dam was constructed in 1959 and is located in the upper catchment of the Murrumbidgee River in an incised floodplain. The dam is 46 m high by 216 m wide at its crest. The original deep pipe river outlet works on the dam wall were upgraded to a variable level offtake in 2006.

The main tributaries of Tantangara Reservoir include the Murrumbidgee River that drains about 60% of the Tantangara Dam catchment, Mosquito Creek that drains about 20% and Nungar Creek that drains the remaining 20%.

The water transfer infrastructure for transfers to/from Tantangara Reservoir are listed in **Table 3-3**. The River Outlet Works is located on the Tantangara Dam wall and comprises a variable level offtake to facilitate environmental releases to the Murrumbidgee River below the dam. The Murrumbidgee to Eucumbene Transfer tunnel inlet is a submerged manifold located on the southern bank about 100 m upstream of the dam wall. The Goodradigbee Aqueduct transfers water from the Goodradigbee River, another tributary of the Murrumbidgee River to the east of Tantangara into Gurrangorambla Creek a tributary of Mosquito Creek.

Table 3-3 Tantangara Reservoir inlets and outlet structures

Structure	Flow	Dimensions	Centreline AHD	Vertical extent (min, max)	Capacity (m ³ /s)	Capacity (ML/hr)
River Outlet Works	Out	Variable level offtake slot opening of 3.2 m wide x 6 m high, level adjustable over vertical range of 17.6 m	Variable from 1,204.9 m to Surface water level.	Variable	28	100.8
Murrumbidgee to Eucumbene Tunnel	Out	7 inlets each 3.1 m wide x 3.1 m tall (21.7 m wide x 3.1 m tall)	1,206.8	1,205.3 – 1,208.4	17 normally 21 if pressurised	61 normally 76 if pressurised

Key operational offtake levels and water levels for the two periods when the operational regime changed are presented along with the hypsographic curve for Tantangara Reservoir in **Figure 3-6**. The water levels indicated by the box and whisker diagram indicate the maximum, 75th percentile, median, 25th percentile, and minimum, and red crosses show outliers of a normal distribution of the data.

For Tantangara Reservoir, transfers to Lake Eucumbene via the Murrumbidgee to Eucumbene tunnel, discharge to the Eucumbene River at Providence Portal. The variable level offtake river outlet works can be adjusted over a vertical range of 17.6 m through manipulation of three baulks each 6 m high by 3.2 m wide. These flows are released to the Murrumbidgee River as part of Snowy Hydro's commitment to the downstream environment.

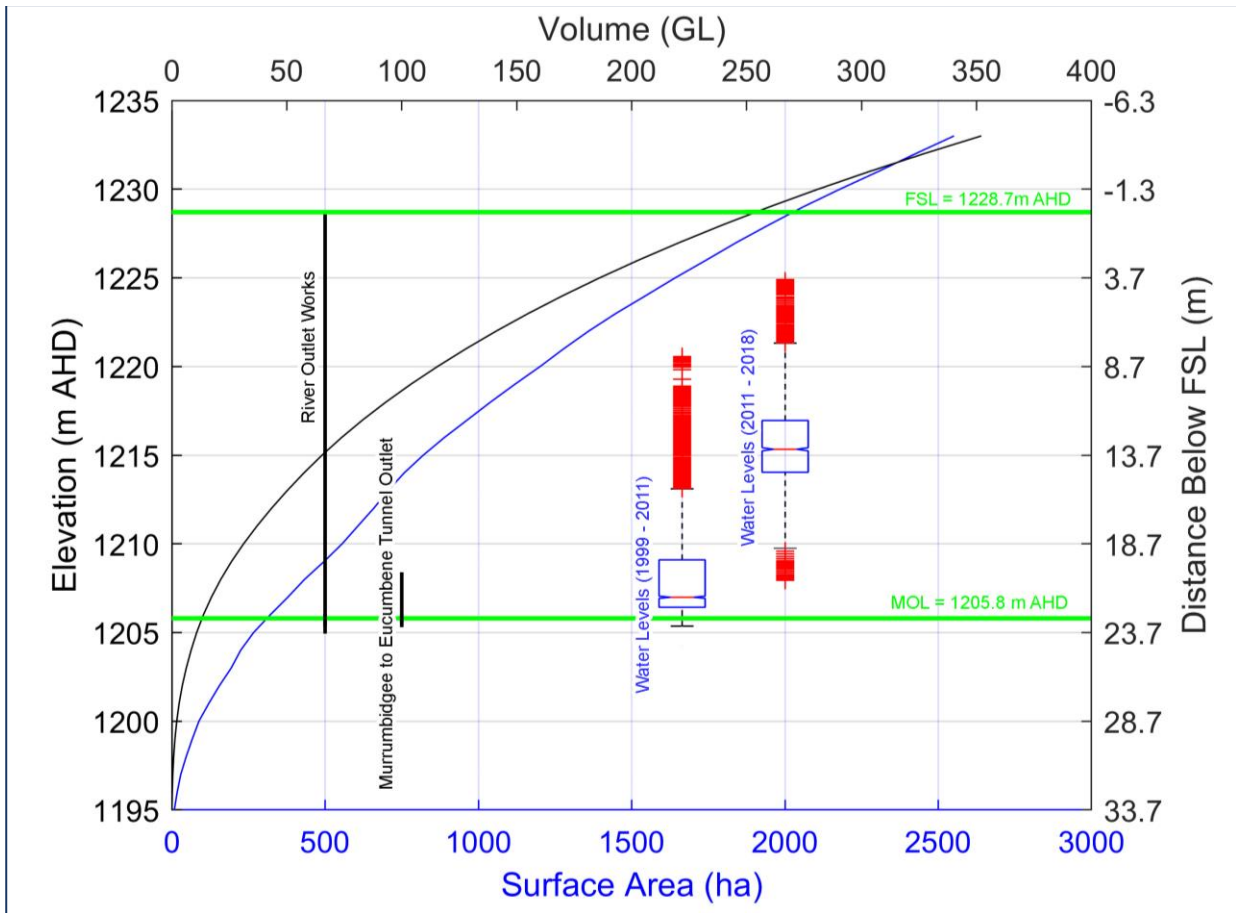


Figure 3-6 Hypsography of Tantangara Reservoir (minimum bed elevation 1193 m AHD)

4 Methodology

4.1 Available Data

To understand the key processes influencing mixing and dispersion in the reservoirs a number of data sets were collated, analysed and interpreted to determine the relative importance of the key drivers and responses as outlined in **Section 3.1**.

The weather and climate patterns described in **Section 2.2** utilised historical data from a number of sources (Snowy Hydro, 2017). Subsets of these data including the Bureau of Meteorology (BoM) and Snowy Hydro weather stations, and Snowy Hydro reservoir sampling sites were provided by Snowy Hydro to supplement the information available for this investigation. A one-year intensive field campaign to sample the reservoir dynamics and water quality commenced in March 2018 and for some of the instruments continued through to July 2019 (**Appendix A**). The field program was designed to support a number of concurrent programs as part of the EIS for the Snowy 2.0 project. The appendices to this report include the suite of data collected relevant to the physical limnology.

Historical data sets have been used describe the past 20 years of weather variability and flow variability to set the context for the description of detailed processes resolved during the field campaign of the past year. The long-term data include:

- > Meteorological data;
- > Flow rate and stream gauge measurements:
 - Tributary inflows and outflows (water transfers),
 - Power Station discharges and Pumped Storage inflows;
- > Reservoir water levels; and
- > Conductivity-temperature-depth (CTD) profiles near the dam walls.

4.2 Field Program 2018-19

A data collection program commenced in March 2018 and finished in July 2019. This program was designed to support a range of programs involved in the Snowy 2.0 EIS, including the anticipated sub-aqueous placement of spoil within Talbingo Reservoir (and possibly Tantangara Reservoir), aquatic ecology investigations and water characterisation. The data collection program comprises the following components:

- > Field campaigns conducted in autumn and spring including:
 - Collection of water quality samples - for determination of a suite of physical and chemical parameters/analytes,
 - Collection of sediment samples – for determination of a suite of physical and chemical parameters/analytes,
 - Physico-chemical profiling (conductivity, temperature, depth, dissolved oxygen (DO), chlorophyll-a, turbidity, pH and photosynthetically available radiation (PAR)) of the water column structure,
 - Collection of aquatic ecology samples (benthic infauna and phytoplankton);
- > Moored instrument deployments collecting time series data including:
 - Thermistor strings, DO, depth, chlorophyll-a and turbidity,
 - Acoustic Doppler Current Profiler (ADCP) instruments, and
 - Reservoir inflows at selected inflow sites.

The data collection report (Cardno 2019; **Appendix A**) describes in detail the methodology for the delivery of these works, covering initial sampling and instrument deployments. Details of the moorings and instrument specifications and sampling setup/configurations are also included in **Appendix A**.

Collected data in the Talbingo and Tantangara reservoirs are summarised in **Table 4-1** and site maps shown in **Appendix A**. Moorings and CTD profile sites are mapped in **Figure 4-1** and **Figure 4-2**.

Water and sediment samples were transferred to analytical laboratories within the appropriate period for determinations of the suite of analytes listed in **Appendix B**. The water sample sites generally formed a subset of the CTD profiling sites in **Figure 4-1** and **Figure 4-2**.

Table 4-1 Available data – Talbingo and Tantangara Reservoirs

Instrument	Number of sites	Deployment
Talbingo Reservoir		
Profiling (CTD, DO, PAR, turbidity)	16	22 Mar 2018
	17	2 & 3 Oct 2018
Water sampling	6	21, 27 & 28 Mar 2018
	8	3 Oct 2018
	4	4 rounds: 1 Nov 2018, 20 Nov 2018, 5 Dec 2018, 16 Jan 2019
Sediment sampling	24	26 & 27 Mar 2018
	11 (Middle Bay)	16 May 2018
Temperature String, CTD mooring deployments	3	2 sites from 17 May 2018 (CTDs only)
		3 sites from 5 & 6 Jun 2018 (Full instrumentation)
ADCP deployments	3	From 18 Apr 2018 (1 relocated from ADCP_02 to ADCP_PCB_03 on 20 Nov 2018)
Inflow monitoring deployments	5	16 & 17 May 2018
		5 Sept 2018
		1 Nov 2018
		4 Dec 2018
Tantangara Reservoir		
Profiling (CTD, DO, PAR, turbidity)	10	20 Mar 2018
	10	4 Oct 2018
Water sampling	5	20 Mar 2018
	5	4 Oct 2018
	4	4 rounds: 1 Nov 2018, 20 Nov 2018, 5 Dec 2018, 16 Jan 2019
Sediment sampling	24	28 Mar 2018
Mooring deployments	2	1 location from 15 May 2018 (CTDs only)
		2 locations from 7 Jun 2018 (Full instrumentation)
ADCP deployments	2	19 Apr 2018
Inflow monitoring deployments	3	15 May 2018
		10 July 2018
		4 Sept 2018

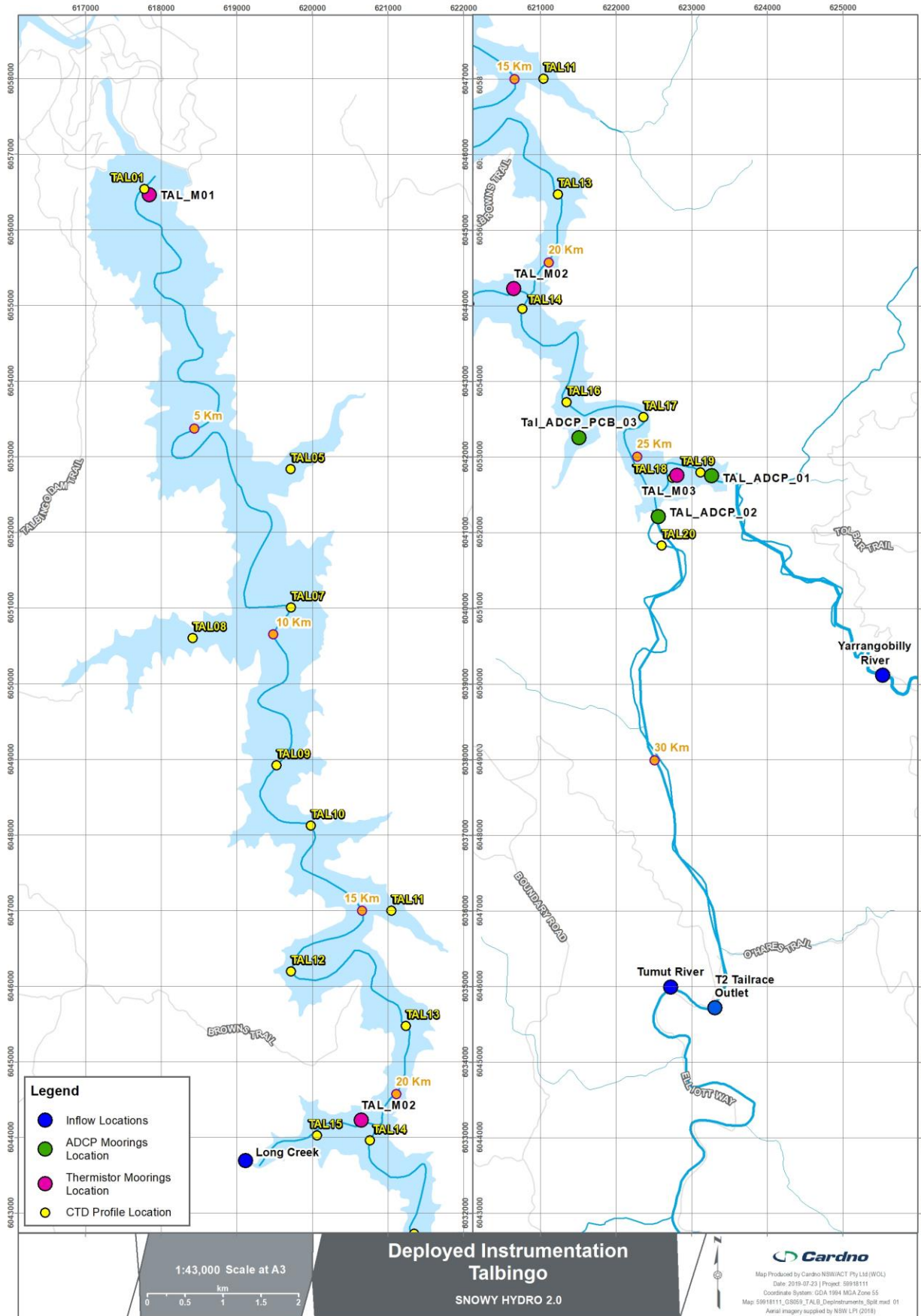


Figure 4-1 Talbingo Reservoir moorings and profiling sites. Distances are chainage from the dam wall along the thalweg

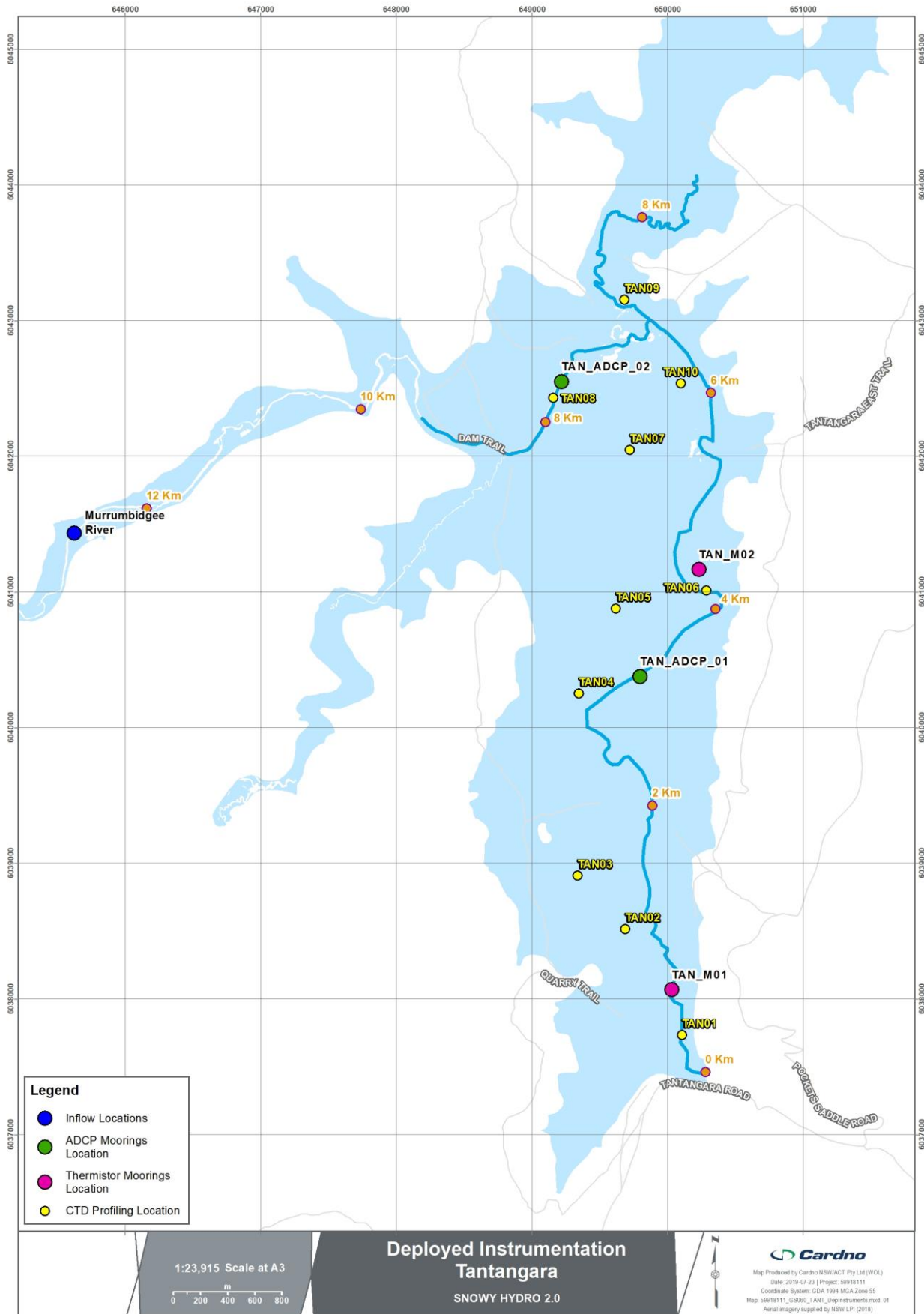


Figure 4-2 Tantangara Reservoir moorings and sampling sites. Distances are chainage from the dam wall along the thalweg

4.3 Analysis

4.3.1 General

The analysis of the meteorological and reservoir data involved a series of initial quality assurance/quality control processes as summarised in the field data collection report (**Appendix A**). Where the analytical routines revealed minor inconsistencies in the data sets, subsequent finer scale checks were applied. These adjustments typically arose from application of vertical fixed bed datum shifts and time coincidence between different instruments.

Standard routines are used for graphical presentations including depth profiles, time series and contouring. To highlight the importance of different time scales, a range of low pass filters and monthly averaging of time series were applied. To compare outputs from different sensors that sample at different time intervals, the shorter time interval was generally used to interpolate the other sequence to match times of both data series.

4.3.2 Meteorological Data

To provide information to support estimates of surface heat fluxes, meteorological measurements from weather stations mounted approximately 1.5 m above the water surface were undertaken at the Talbingo and Tantangara reservoirs. The meteorological instruments were deployed with the thermistor string moorings at locations TAL_M01, TAL_M02 (**Figure 4-1**) and TAN_M02 (**Figure 4-2**). The measurements included:

- > Air temperature;
- > Relative humidity;
- > Barometric pressure;
- > Wind speed (4-minute averages and gusts);
- > Wind direction; and
- > Solar radiation.

In addition to the recorded meteorological data, daily rainfall data, obtained from the BoM site at the Mount Ginini Automatic Weather Station (AWS) was used to supplement the dataset.

4.3.3 Reservoir Heat Content and Surface Heat Fluxes

The heat content (HC) of a reservoir is the potential energy stored in the water body, measured in Joules (J) and may be estimated by integrating the water temperature over the reservoir volume:

$$HC = \int_0^{Surface} \rho C_E T(z) A(z) dz \approx \sum_0^{Surface} \rho C_E T_z A_z \Delta z \quad (\text{Equation 1})$$

Where HC is the heat content [J], ρ is the water density [kg/m^3], C_E the specific heat capacity of water (4.1818 kJ/kgK), $T(z)$ and T_z the water temperature at layer z (K), $A(z)$ and A_z (m^2) the surface area at layer z and dz and Δz the height of discrete layer z (m). HC defines the total heat content in a reservoir at any given time. The change heat content, ΔHC , can be calculated as the difference between HC at any two defined periods:

$$\begin{aligned} \Delta HC &= HC_{in} + HC_{SHF} - HC_{out} \\ &= \rho C_E \int T_{in} Q_{in} dt + \int Q_{net} A_S dt - \rho C_E \int T_{out} Q_{out} dt \end{aligned} \quad (\text{Equation 2})$$

HC_{in} is the heat entering the reservoir through river inflows and water transfers or geothermal heat transfer through the bed (discharge Q_{in} and water temperature T_{in}). HC_{SHF} is the net surface heat flux, Q_{net} , through the water surface of area A_S and HC_{out} is the heat lost through water discharges (releases, spilling flows and transfers of discharge Q_{out} and water temperature T_{out}) from the reservoir.

Surface heat fluxes are the major mechanism of energy exchange between the reservoir and the atmosphere and are directly responsible for the production of thermal stratification in the reservoir. Solar radiation emitted by the sun reaches the earth in the form of electromagnetic waves with wavelengths in the range of 0.15 to 4 μm . In the atmosphere, the radiation undergoes scattering, reflection and absorption by air, clouds, dust and particles. While solar radiation is typically the predominant source of heat to the reservoir, additional processes attributed to latent heat (evaporation) and sensible heat (convection) also contribute to the overall net gain or loss of heat to the system, albeit to a smaller extent.

During the summer months, shortwave solar radiation penetrates the water surface into the water bodies and heat is stored within the upper layers of the water column. This natural process of net heat gain during the summer months leads to the formation of thermal stratification and subsequent mixing near the surface leads to the formation of a thermocline; the depth zone where the water temperature changes rapidly, limiting vertical mixing.

Full details of the adopted heat flux models and the parameters used as input for the determination of surface heat fluxes are documented in **Appendix B**. The various heat flux components discussed in the appendix are shown schematically in **Figure 4-3** (Deltares, 2019) and are defined as:

- Q_{sc} Solar radiation for a clear day (W/m^2)
- Q_{sn} Net incident solar radiation (shortwave) (W/m^2); $- Q_s - Q_{sr}$
- Q_s Solar radiation (shortwave) (W/m^2)
- Q_{sr} Reflected solar radiation (shortwave) (W/m^2)
- Q_{an} Net incident atmospheric radiation (longwave) (W/m^2)
- Q_a Atmospheric radiation (longwave) (W/m^2)
- Q_{ar} Reflected atmospheric radiation (longwave) (W/m^2)
- Q_{br} Surface back radiation (longwave) (W/m^2)
- Q_{ev} Heat loss due to evaporation (latent) (W/m^2)
- Q_{co} Convective (sensible) heat loss (W/m^2)

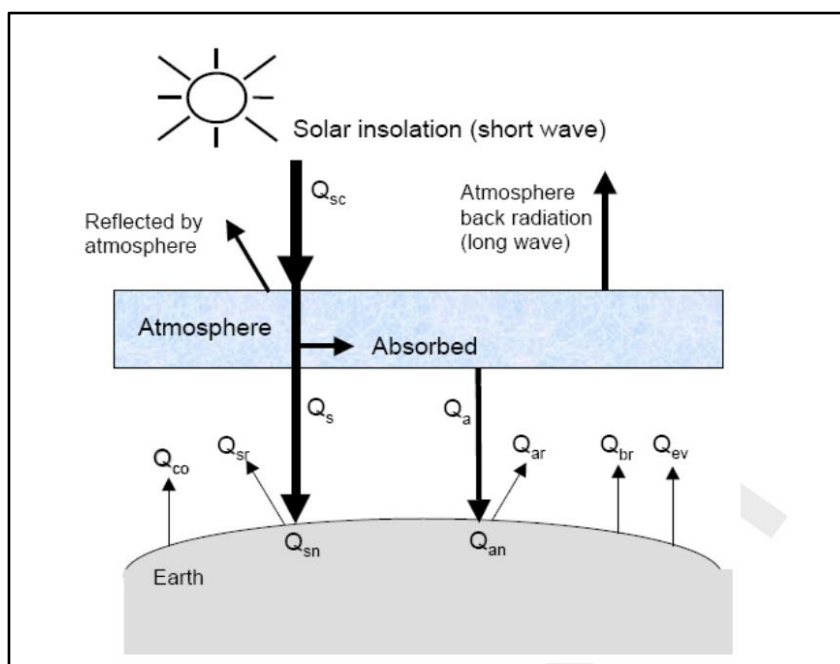


Figure 4-3 Overview of the heat exchange mechanisms at a water body surface (Deltares, 2019)

4.3.4 Thermal Structure

Thermal structure of the reservoir is generally measured using temperature profilers that collect profiles at various locations in the reservoir to characterise spatial variability, and/or fixed mooring thermistor strings that provide time series of the temperature at fixed depths and/or height above the bed. Isotherm depths; i.e., depths where the temperature is the same, provide a useful means of characterising the internal seiches in the reservoir. The depth of a particular isotherm (e.g. 10°C) is effectively computed by interpolating the temperature data over the entire depth of the thermistor string and then searching for the depth at which a specific isotherm occurs.

The thermistor string temperature data for this study are presented as temperature contours highlighting temporal variability at a particular mooring site and CTD profiles are presented as spatial contours at a particular time.

4.3.5 Seiches

When a wind blows on the surface of a lake of length L , the surface waters are pushed downwind and pile up at the downwind shoreline causing a (small) surface slope along the lake. When the wind dies down or changes direction the surface slope relaxes at the speed of a surface gravity wave. Surface seiching in an enclosed water body typically occurs at a period, T , related to the length, L , of the reservoir and gravity wave celerity \sqrt{gh} , where g is the gravitational constant and h the water depth. For a first horizontal mode surface seiche:

$$T = \frac{2L}{\sqrt{gh}} \quad (\text{Equation 3})$$

Internal seiches and their surface counterpart are effectively the natural frequencies of the water body that come into play following some forcing stimulus such as a wind event or sudden inflow. The thermal (or density) structure that determines the internal period as given by the formula:

$$SP = \frac{2L}{c} \quad (\text{Equation 4})$$

SP (s) is the internal seiche period in a basin of length, L (m) is the basin length at the depth of the thermocline and c (m/s) is speed of a long wave.

The seiching motions are generally captured in thermistor string measurements, CTD profiles and ADCP current meters. Seiches effectively transfer energy from the low frequency seiches to higher frequency internal waves. As these smaller length scale internal waves propagate around the system reflecting off the solid boundaries they effectively break and result in mixing and dissipation of the kinetic energy into heat energy. The modal structure of the internal seiches depends on the stratification as characterised by the buoyancy frequency, N (Hz). Vertical modes can be determined from thermistor string data and ADCP current measurements. Determination of horizontal modes requires spatial resolution of the thermal structure that can be obtained from CTD profiling or a number of thermistor strings monitoring at strategic field monitoring sites along the reservoir.

4.3.5.1 Density Currents and Intrusions

The density of the water in inflowing mountain streams generally reflects a combination of atmospheric temperature and the amount of fine suspended material in the water. During summer, warmer temperatures will heat the stream flow and it will become lighter than the reservoir receiving waters while at night the stream becomes colder and heavier, therefore sinking and flowing into the reservoir along the bed. If there are significant concentrations of suspended load contributing to the density, then these form turbidity currents (a type of density current) that flow along the bed of the reservoir. Density currents advance into the reservoir typically at a rate equivalent to the phase speed, c (m/s) of an internal wave given by

$$c = \sqrt{\frac{\Delta\rho}{\rho} g h} \quad (\text{Equation 5})$$

Where $\Delta\rho$ (kg/m^3) is the density difference between the inflow and reservoir waters, ρ (kg/m^3) the inflow water density, g (m/s^2) the gravitational acceleration and h (m) the water depth.

Turbidity is a measure of cloudiness of the water caused by fine suspended particles and colour (dissolved organic compounds such as tannins) and generally measured by optical or acoustic backscattering sensors. Turbidity is of particular interest here as it is likely that construction of the proposed development will lead to an increase in the fine suspended particles concentrations (or turbidity). The turbidity in inflowing streams generally increases water density and these inflows may flow into the reservoir as bottom density currents (also referred to as turbidity currents).

4.3.5.2 Selective Withdrawal Layers

In stratified waters, the flow of water towards an inlet is modified by the presence of the stratification such that water is drawn towards the inlet along constant density surfaces. The vertical thickness of the withdrawal layer, δ (m), at steady state is a function of the strength of the stratification, as measured by the buoyancy frequency N (Hz) and the inlet discharge, Q (m^3/s). For a point sink, δ is given by the formula (Anohin *et al.*, 2006).

$$\delta = 1.42 \left(\frac{Q}{N}\right)^{1/3} \quad (\text{Equation 6})$$

In terms of the inlet structures within Talbingo and Tantangara Reservoirs, this point-sink assumption is probably relevant to the river outlet works and the Murrumbidgee to Eucumbene Tunnel entrance in the Tantangara Reservoir.

For the larger inlet and flows associated with the T3 Power Station the inlet and upstream channel are better approximated by the assumption of a line sink. Jamali and Aghsaei (2007) report on investigations of the characteristics of withdrawal layer thickness for a line sink located downstream of a sill and a contraction in an otherwise uniform reservoir. The inlet channel leading to the T3 inlet structure may be approximated by a 1 km long channel. Moving upstream of the inlet structure the depth gradually decreasing from about 27 m (below FSL) at the inlet to about 12 m (below FSL) some 800 m upstream before then increasing to over 25 m (below FSL) at the 1 km upstream and then sharply to over 100 m in the reservoir. This system may be viewed as a sill of 12 m depth in an inlet channel of 25 m depth at the inlet. The inlet may be approximated as a line sink with discharge, Q (m^3/s), linear density stratification with buoyancy frequency, N (Hz), and the withdrawal layer thickness, δ_L (m), estimated from the equation (Jamali and Aghsaei, 2007):

$$\delta_L = H \left(0.99 \pi F + 0.85 \varepsilon (1 + \sqrt{\pi F}) \right) \quad (\text{Equation 7})$$

The Froude number, F , is given by

$$F = \frac{Q}{N H^3} \quad (\text{Equation 8})$$

And $\varepsilon = H_s/H$, is the ratio of sill depth to total depth.

4.3.6 Light Extinction

The attenuation of light, $I(z)$, with increasing depth, z (m), is characterised by Beer's law:

$$I(z) = I_0 e^{-kz} \quad (\text{Equation 9})$$

where k (m) is the extinction coefficient and I_0 the surface light intensity. The vertical Photosynthetically Active Radiation (PAR) profiles collected using the profiler were analysed to determine the light extinction coefficient and surface light by inverting **Equation 9** and fitting a straight line to the $\ln(I(z))$ versus z . These results were then used to determine the photic depth, z_p (m), the depth at which the light intensity falls to 1% of its surface value.

The relationship between the key variables characterising the water cloudiness – turbidity and chlorophyll-a – and extinction coefficient was determined from linear regression. The turbidity (NTU) and fluorescence chlorophyll-a (mg/L) data were averaged over the photic depth and regressed against the extinction coefficient, k (1/m), to derive the relationship.

$$k = a + b \text{ Chlorophyll } a + c \text{ Turbidity} \quad (\text{Equation 10})$$

Where the coefficients a (1/m), b (L/mg/m) and c (1/NTU/m) are determined through the regression analysis.

5 Results

5.1 Introduction

Sections 5.2 provides an overview of the long-term operations in terms of reservoir water levels, inflows and outflows and the general weather patterns through this period. Results of the 2018-2019 field campaign are then described separately for each reservoir.

5.2 Overview of Historic Operations

5.2.1 Water Levels

The seasonal nature of the water level variability of both storages is indicated by the last 20 years of daily minimum and peak water levels shown in **Figure 5-1**. General statistics derived from these data are listed in **Table 5-1** that reference water levels to each dam's FSL (see **Table 3-1**).

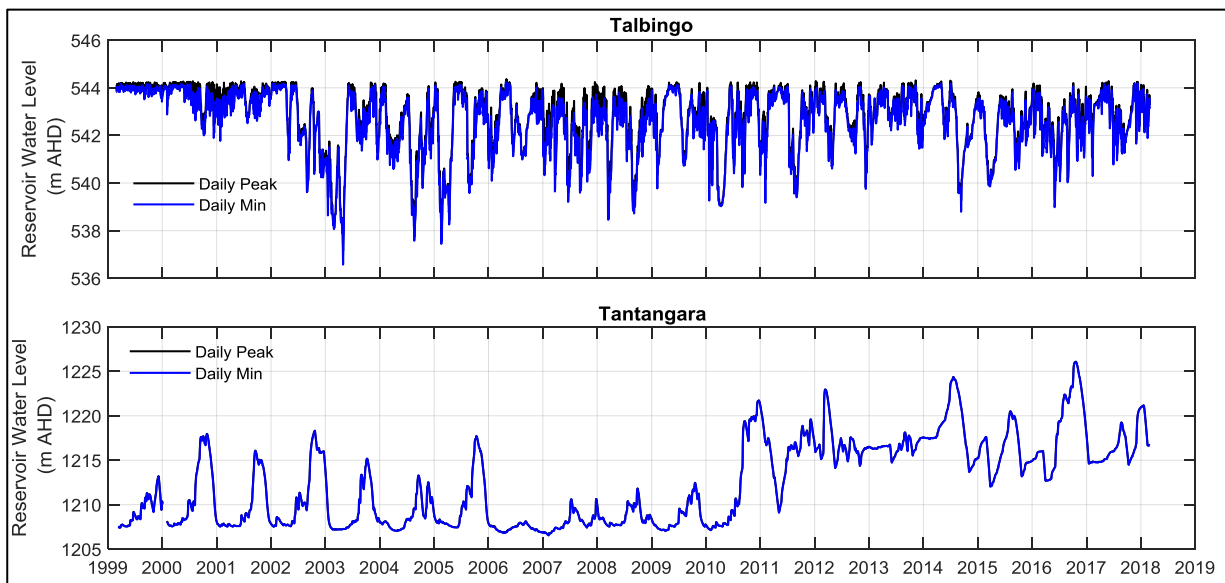


Figure 5-1 Water levels in Talbingo (top) and Tantangara (bottom) reservoirs for 20 years 1999 to 2019

Table 5-1 Water level variability in Talbingo and Tantangara reservoirs expressed in m below dam FSL (Talbingo FSL 543.2 m AHD and Tantangara FSL 1,228.7 m AHD)*

	Talbingo Reservoir		Tantangara Reservoir			
Recording Period	27 Feb 1999 - 1 Mar 2018		10 Mar 1999 - 30 Jun 2010		1 Jul 2010 - 1 Mar 2018	
Daily Water level	Peak (m)	Minimum (m)	Peak (m)	Minimum (m)	Peak (m)	Minimum (m)
Mean	1.90	2.15	19.40	19.47	11.65	11.73
Maximum	0.33	0.47	10.36	10.39	2.60	2.62
90 th Percentile	0.61	0.75	15.33	15.44	7.52	7.57
75 th Percentile	0.87	1.12	18.58	18.71	10.11	10.27
Median	1.56	1.83	20.58	20.62	12.11	12.18
25 th Percentile	2.55	2.85	21.08	21.10	13.49	13.55
10 th Percentile	3.70	3.99	21.45	21.47	14.83	14.90
Minimum	7.54	8.13	22.13	22.15	19.93	19.96
Interquartile Range	1.67	1.73	2.50	2.39	3.38	3.27
Number samples	6943	6943	4103	4103	2801	2801

*Note: Maximum water level is equivalent to minimum depth below FSL.

Key features to note for Talbingo Reservoir are:

- > The 20-year operating range (75th – 25th percentiles, i.e. interquartile) is typically 1.7 m and within 0.3 m of FSL;
- > Mean daily water level change (peak – minimum on each day) is 0.25 m which equates to a volume change, at 1 m below crest level of 4.4 GL/day primarily associated with Hydro Power Station operations; and
- > Water levels are typically maintained at the dam crest level for around six months of the year and lower water levels tend to occur in late winter or spring, although this pattern shifts from year to year.

For Tantangara Reservoir the key features include:

- > A shift in operating level occurred in 2010 with the mean water level being maintained at some 7.8 m higher in the period 2010-2018 than in the preceding 11 years (1999 to 2010);
- > The mean water level was typically around 19.4 m below FSL from 1999 to 2010 and 11.7 m below FSL from 2010 to 2018;
- > Water level tends to peak in spring following spring snow melt and the increased inflow;
- > The interquartile range of operation over the years 1999 to 2010 was 2.4 m, compared with 3.3 m from 2010 to 2018; and
- > The mean daily range is 0.07 m equating to a volume change of roughly 474 ML and surface area change of 3.27 ha.

5.2.2 Inflows

Inflows to Talbingo and Tantangara reservoirs, including both natural catchment flows and transfers over the period between 1993 and 2018, are shown in **Appendix C** and annual volumes presented in **Table 5-2** and **Table 5-3**, respectively.

Inflows to Talbingo Reservoir comprise natural streamflow that peaks in late winter to early spring with snow melt and winter rains. Water temperature of these inflows is generally around 4°C colder than the waters in the reservoir, and as a result the inflow plunges to the bed as it enters the reservoir. As it propagates downstream along the bed of the reservoir, the inflow waters mix with surrounding waters and ultimately equilibrate, then separate from the bottom to intrude into the reservoir at the level of neutral buoyancy.

Sporadic rainfall during summer months is also likely to be colder than the surface waters of the reservoir but the stronger summer thermal stratification causes the inflow to flow into its level of neutral buoyancy sooner and generally around the thermocline level.

The annual transfer discharges, T2 Power Station and Jounama Pondage pumpback, into Talbingo Reservoir and T3 discharge, are typically an order of magnitude larger than the natural inflow from the Yarrangobilly River.

The drought/wet cycles are indicated for Talbingo Reservoir in **Figure 5-2** with the period 2001 to 2009 showing lower rainfalls and stream runoff. The transfer flows also reflect some a decrease during these periods.

For Tantangara Reservoir, data were available for only the Murrumbidgee River flow gauging station just upstream of the reservoir but the transfer of water from the Goodradigbee River was not available at the time of preparing this report. These data indicate a pattern of drought response similar to the Yarrangobilly River.

These inflow and transfers characteristics have been a key determinant in the evolution of the aquatic ecology of the reservoir and adjacent streams since they were constructed and then first filled some 38 years (Talbingo) and 60 (Tantangara) years ago. It would appear there is limited fine sediment runoff from the catchments as turbidity in both reservoirs is generally very low – even following rainfall/runoff events.

5.2.3 Annual Water Budget

Long-term flow information provided by Snowy Hydro has been analysed into annual periods and shown in **Figure 5-2** and **Table 5-2** and **Table 5-3**. Note that the reservoirs are operated in a manner that captures as much water as possible minimising spilling of water during major flood events (e.g. greater than 1:20 year rainfall). Total annual rainfall and annual volumes from inflows to and outflows from Talbingo Reservoir are presented in **Figure 5-2**. River inflow at Ravine is the Yarrangobilly arm only.

Table 5-2 Long-term flow information for Talbingo Reservoir

Year	Total Rainfall (mm)	Annual River Inflow at Ravine (GL)	T3 Power Station Outflow (GL)	T3 Pump back inflow (GL)	T2 Inflow (GL)	Net Power Station Flows (GL)
1994	677	58	1,943	18	1,763	-162
1995	1,296	172	1,737	119	1,216	-402
1996	1,255	174	2,029	433	1,199	-397
1997	778	58	1,255	60	1,119	-75
1998	995	92	1,259	8	1,119	-133
1999	1,115	87	1,289	22	1,140	-128
2000	1,130	166	2,058	602	1,126	-329
2001	890	100	1,689	563	934	-193
2002	763	68	1,217	1	1,092	-123
2003	859	80	1,872	27	1,778	-67
2004	858	89	1,652	1,068	435	-149
2005	757	117	1,788	4	1,550	-234
2006	363	15	1,360	388	1,026	54
2007	924	36	3,276	2,556	655	-65
2008	989	65	2,836	2,120	634	-83
2009	794	63	1,057	416	561	-80
2010	1,559	184	1,706	107	1,196	-403
2011	1,303	158	1,009	338	422	-249
2012	1,136	151	1,764	115	1,368	-281
2013	779	79	1,386	0	1,256	-130
2014	970	84	599	49	438	-113
2015	921	63	861	18	756	-87
2016	1,342	188	2,004	23	1,612	-369

Table 5-3 Long-term flow information for Tantangara Reservoir

Year	Rainfall (mm)	Tantangara to Eucumbene Outflow (GL)	Murrumbidgee River Inflow (GL)
1994	801	107	91
1995	1,345	227	218
1996	1,278	214	210
1997	894	101	88
1998	1,037	117	126
1999	1,061	123	116
2000	1,032	192	184
2001	962	136	126
2002	937	117	109
2003	877	142	108
2004	921	132	122

Year	Rainfall (mm)	Tantangara to Eucumbene Outflow (GL)	Murrumbidgee River Inflow (GL)
2005	787	161	149
2006	579	25	20
2007	1,005	82	81
2008	924	123	118
2009	890	120	115
2010	1,245	205	223
2011	1,109	196	200
2012	1,015	167	189
2013	862	126	116
2014	990	129	125
2015	810	107	99
2016	1,230	227	236

The information presented in **Figure 5-2** and **Table 5-2** provides an indication of the important components of the water budget for Talbingo Reservoir that may be summarised as follows:

- > Transfers into the reservoir from the regulated flows from T2 and T3 pumpback are significantly larger than the inflows from the unregulated inflows;
- > The T3 Power Station operation is the primary discharge while the environmental releases form a very small component of the water budget; and
- > Direct rainfall on the reservoir water surface area and evaporation from this area (not shown) form relatively minor contributions to the water budget.

For Tantangara Reservoir, the information presented in **Table 5-3** indicates:

- > Regulated inflow from Goodradigbee River, unregulated streams and the Murrumbidgee River are the main sources of water; and
- > Transfers to Eucumbene Reservoir and the smaller environmental releases roughly balances the unregulated inflows.

The long term (1993 to 2018) rainfall variability, mean stream discharge and total discharge volume measured at Talbingo reservoir are summarised in **Figure 5-2**. This data highlights the drought/wet cycles with extended drought period of low rainfall between 2001 and 2009. More recently 2016 was classified as a wet year with 2017 and 2018 classified as dry years. During the period of data collection, April 2018 to March 2019 monthly rainfall at the Tantangara weather station (**Figure 5-3**) was typically within the (mean) monthly rainfall at Talbingo reservoir.

Surface heat fluxes between the air and water are a key determinant of the annual and seasonal cycles of reservoir stratification and mixing dynamics. The key meteorological variables that drive the surface heat fluxes and total heat energy within the water body include: solar radiation (SW and LW), air temperature (and its difference to the surface water temperature), humidity, wind speed and direction, air pressure, rainfall and evaporation. The surface heat fluxes are derived from these variables as discussed in **Appendix B** and summarised in **Section 4.3.3**.

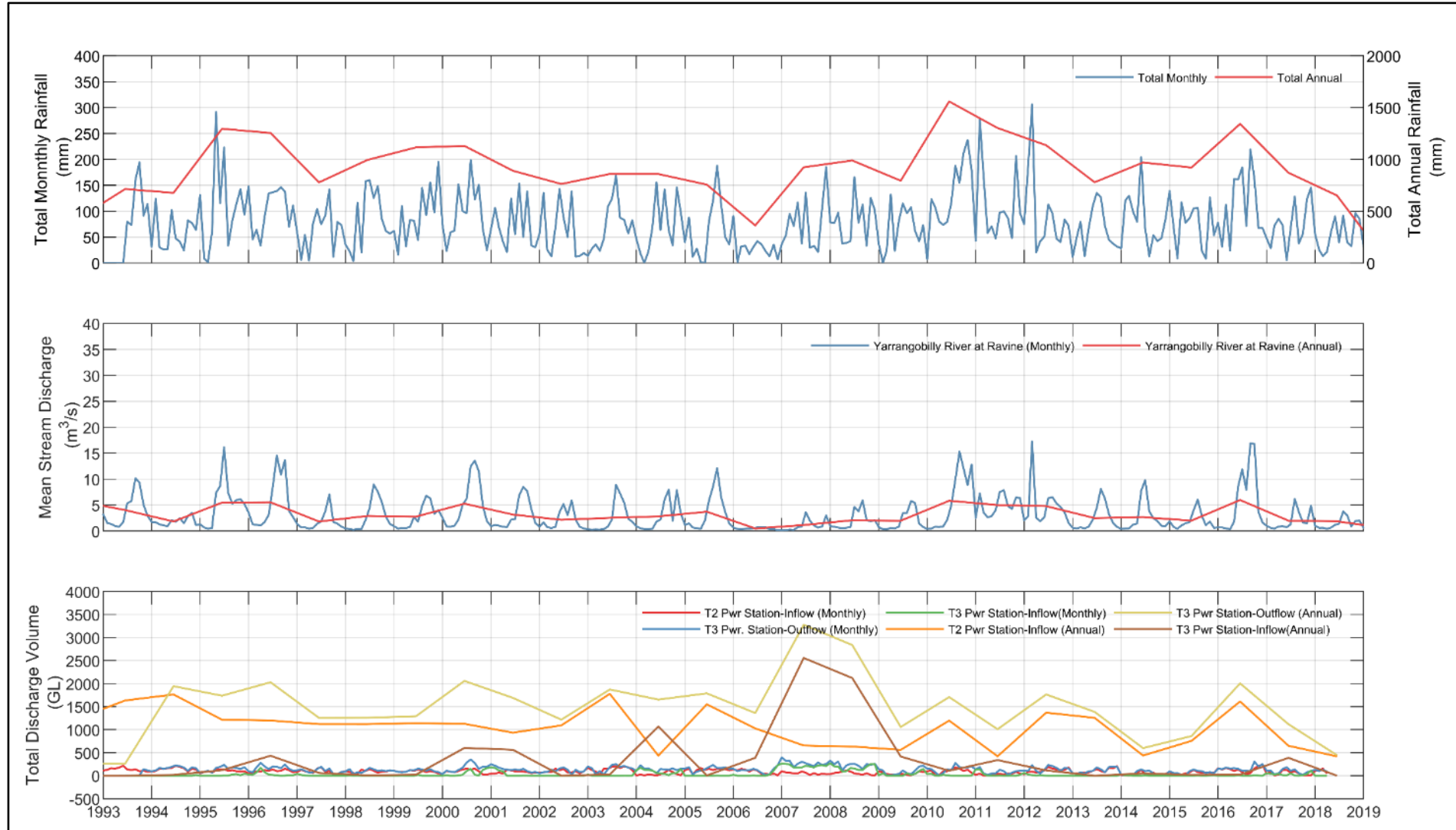


Figure 5-2 Total annual rainfall, mean stream discharge and total discharge measured at Talbingo Reservoir between 1993 and 2018

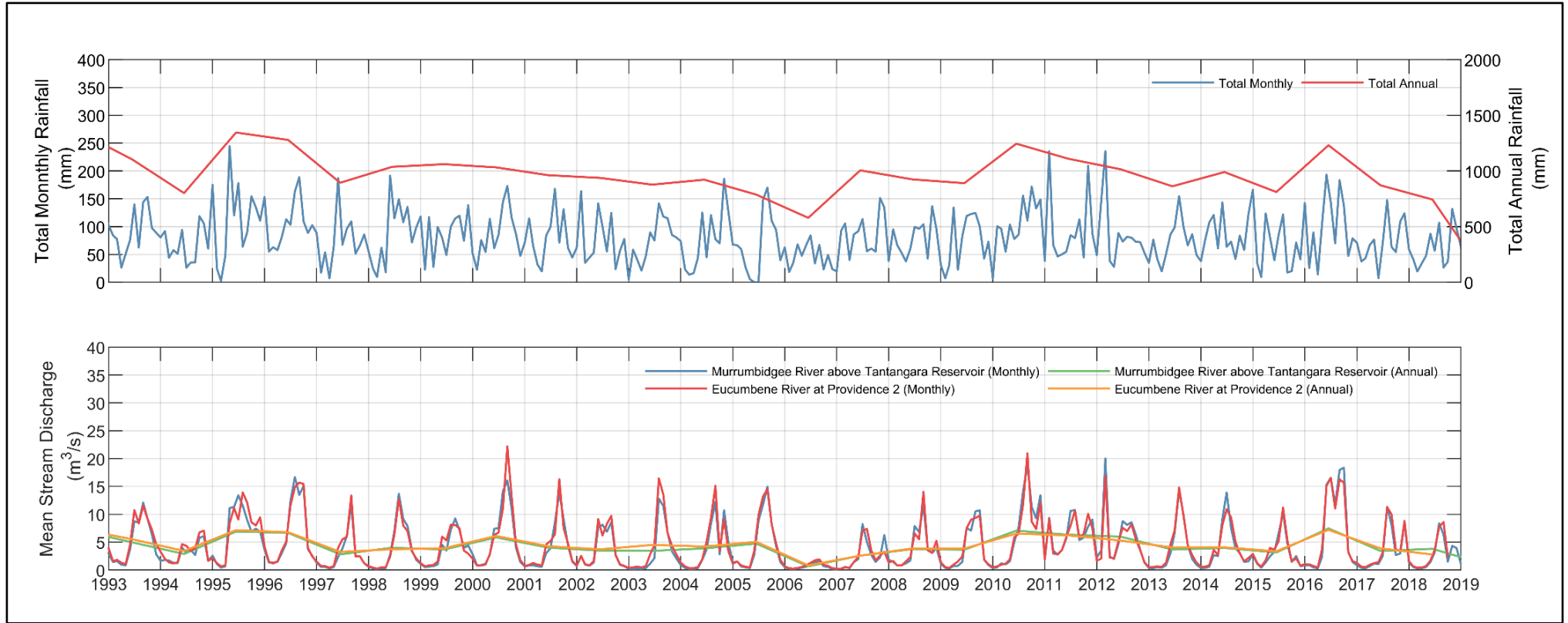


Figure 5-3 Historical mean rainfall and stream inflow and discharge at Tantangara Reservoir (1993 - 2019)

5.3 Talbingo Reservoir 2018-19

5.3.1 Weather and Surface Heat Flux

The 2018-19 field campaign collected data from the time series monitoring sites and intensive field campaigns for over one year. Data for the period April 2018 to March 2019 was available at the time of preparation of this report. Meteorological data collected on Talbingo Reservoir are shown in **Appendix D**. The typical diurnal wind pattern and regular stronger wind events associated with the passage of low pressure systems are a key feature of these data. The dominant north-south wind direction is aligned along the valley. A number of rainfall events occurred during the sampling period leading to natural inflows. These data were utilised to estimate the surface heat fluxes as described in **Section 4.3.3**.

The monthly surface heat fluxes for Talbingo Reservoir derived from the meteorological data are presented in **Figure 5-4** and **Table 5-4**. These indicate the seasonal nature of the surface flux variability including summer heating, winter cooling and transition in spring and autumn. The net heat gain intensifies the stratification during summer and the surface losses (negative net heat flux from the surface) during winter causing vertical mixing and homogenisation of the water column.

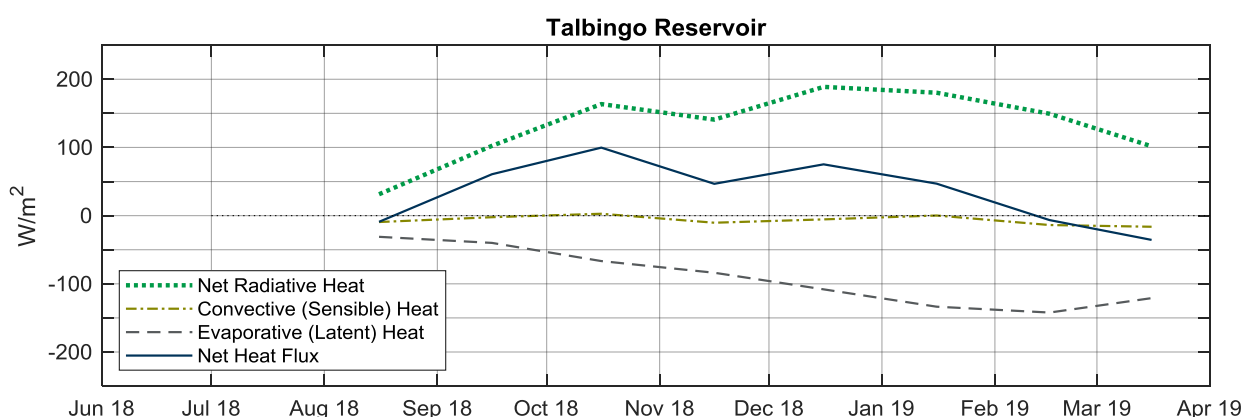


Figure 5-4 Monthly averaged surface heat fluxes (W/m²) for Talbingo Reservoir

Table 5-4 Monthly heat flux components (see Section 6.3 for definitions) and the total heat flux in Talbingo Reservoir

Month	Q _{sn}	Q _{an}	Q _{br}	Q _{ev}	Q _{co}	Q _{tot}
August	256	247	338	31	9	-9
September	257	257	344	40	2	61
October	281	276	366	67	-3	100
November	293	282	385	84	10	47
December	306	300	405	108	6	75
January	321	319	425	134	0	47
February	301	302	415	142	14	-7
March	308	297	409	121	16	-36

5.3.2 Thermal Structure

The thermal structure of the reservoir over the period June 2018 to March 2019, as indicated by the thermistor string measurements closest to the dam wall at site TAL_01, is shown in **Figure 5-5** and the contours for the three thermistor string moorings are provided in **Appendix E**. Note the stratification in Talbingo Reservoir at the deepest point, approximately 130 m deep (**Figure 5-5**), does not completely mix during the winter cooling period. The occurrence of the deep (below 460 m AHD elevation) colder water in early September indicates the flow of colder bottom current from upstream rather than resulting from local vertical mixing, as occurs in shallower systems. Surface heating commences in September and the thermal stratification intensifies through the summer to late February when the shoulder season with periods of cooling and heating leads into the repeating annual cycle.

The typical summer stratified layer extends down to around 30 m deep (510 m elevation) and the thermocline (depth of largest vertical density gradient) occurs at depths of between 5 and 20 m. The other notable feature of the thermal structure in Talbingo Reservoir is the presence of persistent internal waves (vertical fluctuations of the isotherms for example between 490 m and 520 m in the first two weeks of August) at longer periods in the winter and daily cycle through most of the year.

Figure 5-6 compares the surface and bottom temperature time series measurements from the three thermistor string moorings. The location and vertical extent of these moorings is depicted in the inset on **Figure 5-6** and is summarized as:

- > TAL_01, near the dam wall in 135 m water depth;
- > TAL_02, near Long Creek in approximately 65 m water depth some 21 km upstream of the dam wall; and
- > TAL_03 near the confluence of the Tumut and Yarangobilly Rivers in approximately 35 m water depth, about 25 km upstream of the dam wall.

This figure highlights the upstream source of the colder (and heavier) water in spring that propagates down the sloping bottom to displace slightly warmer water previously residing in the deepest layers at the TAL_01 site. Comparing blue lines (surface and bottom temperatures near the dam wall at TAL_01) shows the deep water remains around 6.3°C through the winter, around 2°C colder than surface waters. The bottom temperature shows a gradual warming estimated to be 0.002°C per day, consistent with molecular diffusion of heat through the water column down the vertical temperature gradient of 2°C per 100 m.

Surface and bottom temperatures at TAL_02 (red lines) and TAL_03 (green lines) indicate the upper reaches of the reservoir also remain stratified through the winter. There is considerable structure in the temperature variability with both warm and cold inflows from upstream, and the T2 transfers all intruding into the reservoir. Note the T2 transfers enter the Tumut River arm at about 33 km upstream of the dam wall. After about mid-July colder water associated with T2 inflows leads to colder temperatures in the upper reaches than near the dam wall. It appears this colder water affects the TAL_03 site on 20 July and some five days later affects the TAL_02 site some 5 km further downstream.

From TAL-02 it appears to take about two to three weeks for the colder water to propagate the 20 km downstream and affect the water temperature at TAL_01, near the dam wall (see drop in temperature in blue line ~6 August at TAL_02 July and drop at TAL_01 on 21 August).

In the Tumut River arm just upstream of the Tumut/Yarrangobilly confluence, at site TAL_03, the temperatures again show considerable structure with daily surface heating and night-time cooling of the surface waters. Note the night-time cooling rarely mixes through the whole water column (35 m deep) except for a period in June and early July when the green lines meet on a daily basis, indicating sporadic overnight cooling and vertical homogenisation of the entire water column at this site.

By mid-September the water temperatures at the upstream sites increase above the TAL_01 site and deeper cold water at the dam wall is again isolated from the near surface spring/summer heating processes.

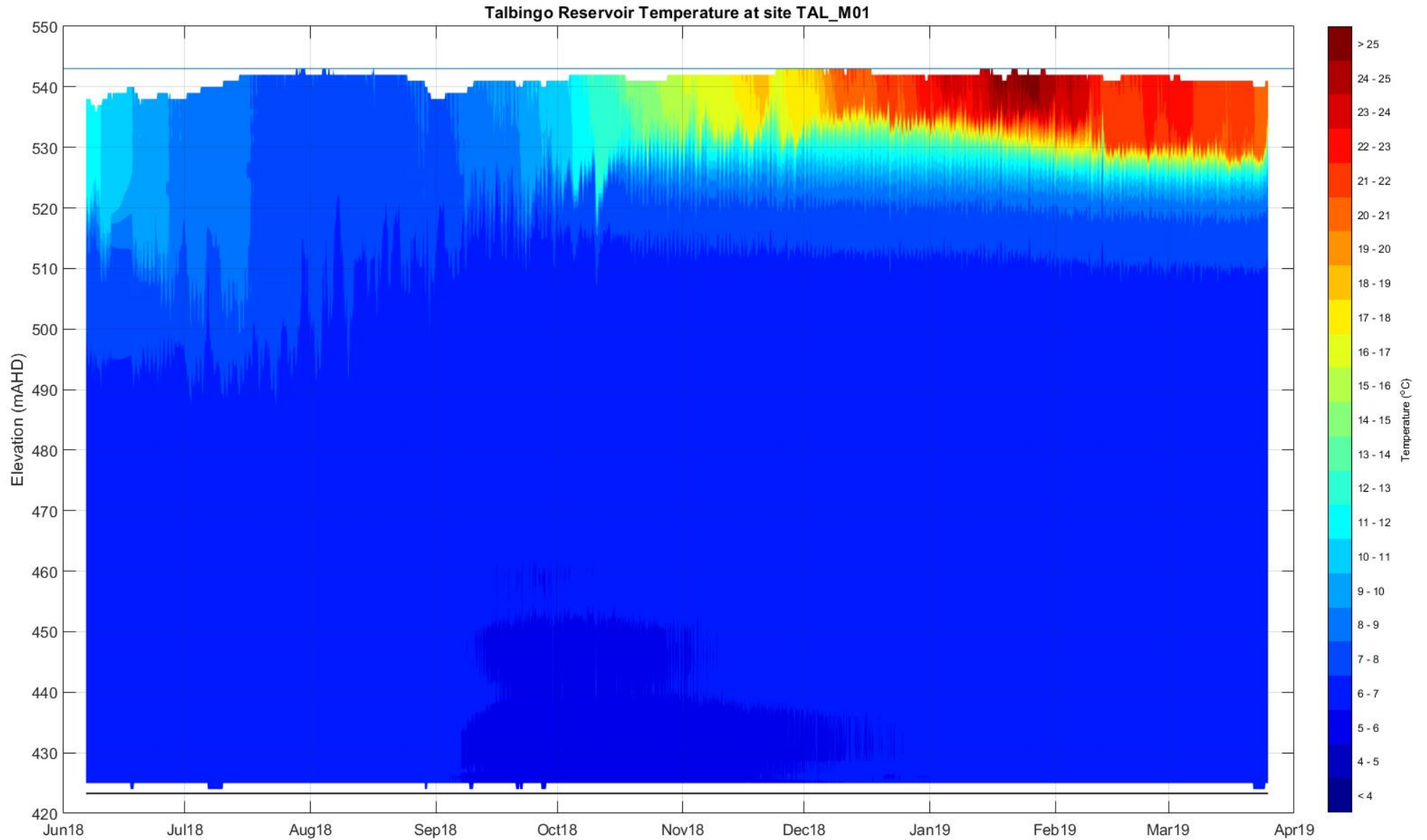


Figure 5-5 Temperature isotherms derived from 10-minute samples at 50 thermistors deployed over the total depth near the dam wall at Talbingo Reservoir (TAL01)

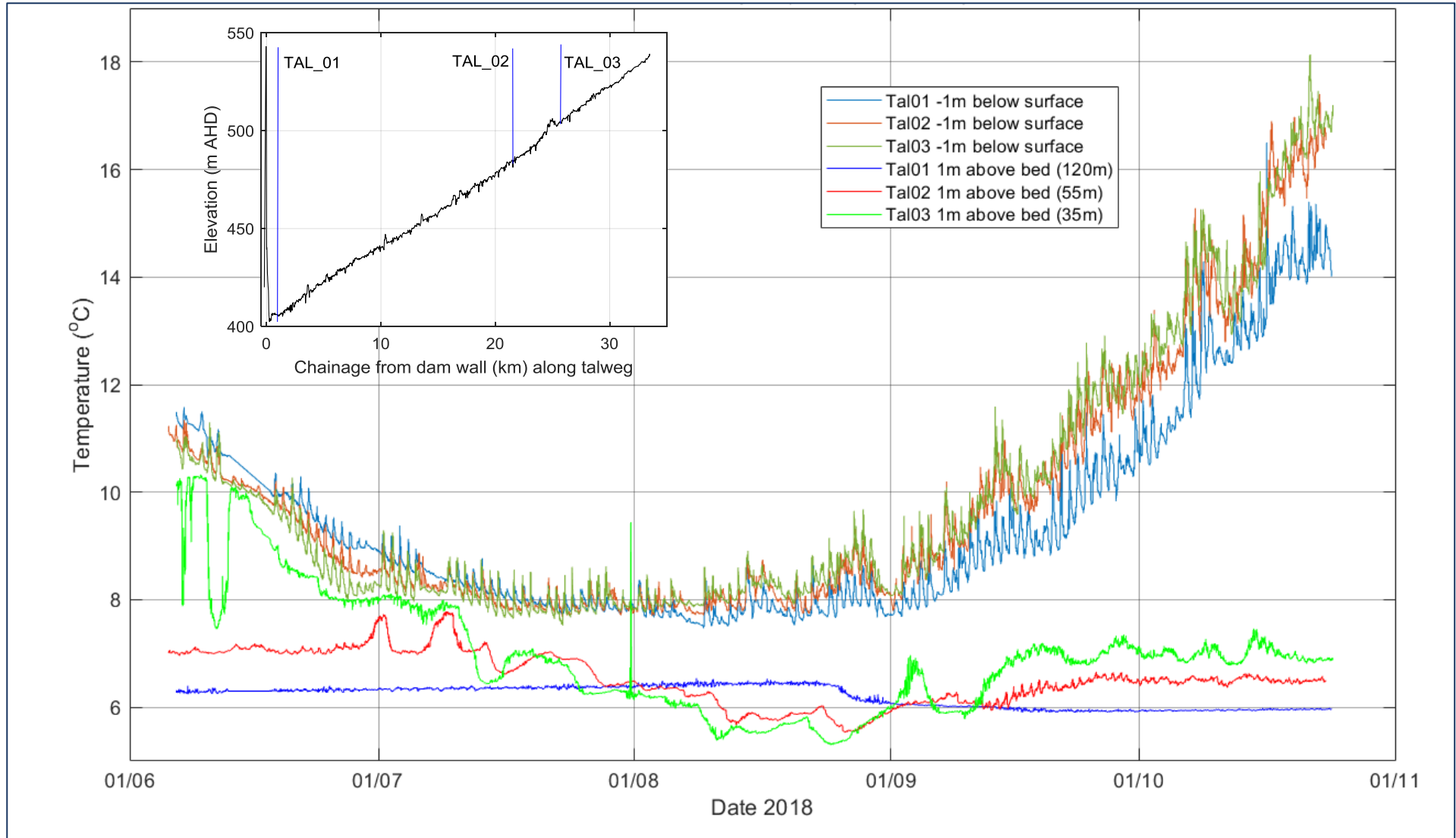


Figure 5-6 Thermistor String surface and bottom temperatures at the three sites

An example of the internal seiche activity in the lower reservoir on 29 July 2018 is shown in **Figure 5-7**. The inset figure shows only the top 40 m of the profile. The figure shows the thermocline near the dam wall (blue lines) moves down from 00:00 to 06:00 and is deepest at 12:00 before returning the original location around 18:00. The vertical oscillation of the thermocline is around 5 m. These internal seiches form a key mechanism for transferring wind and diurnal T3 pumping/release cycle energy from the surface to the benthic boundary layer and the mixing within the reservoir. The thermocline at the upper reaches is considerably higher in the water column indicating the different mixing characteristics between upper and lower reservoir.

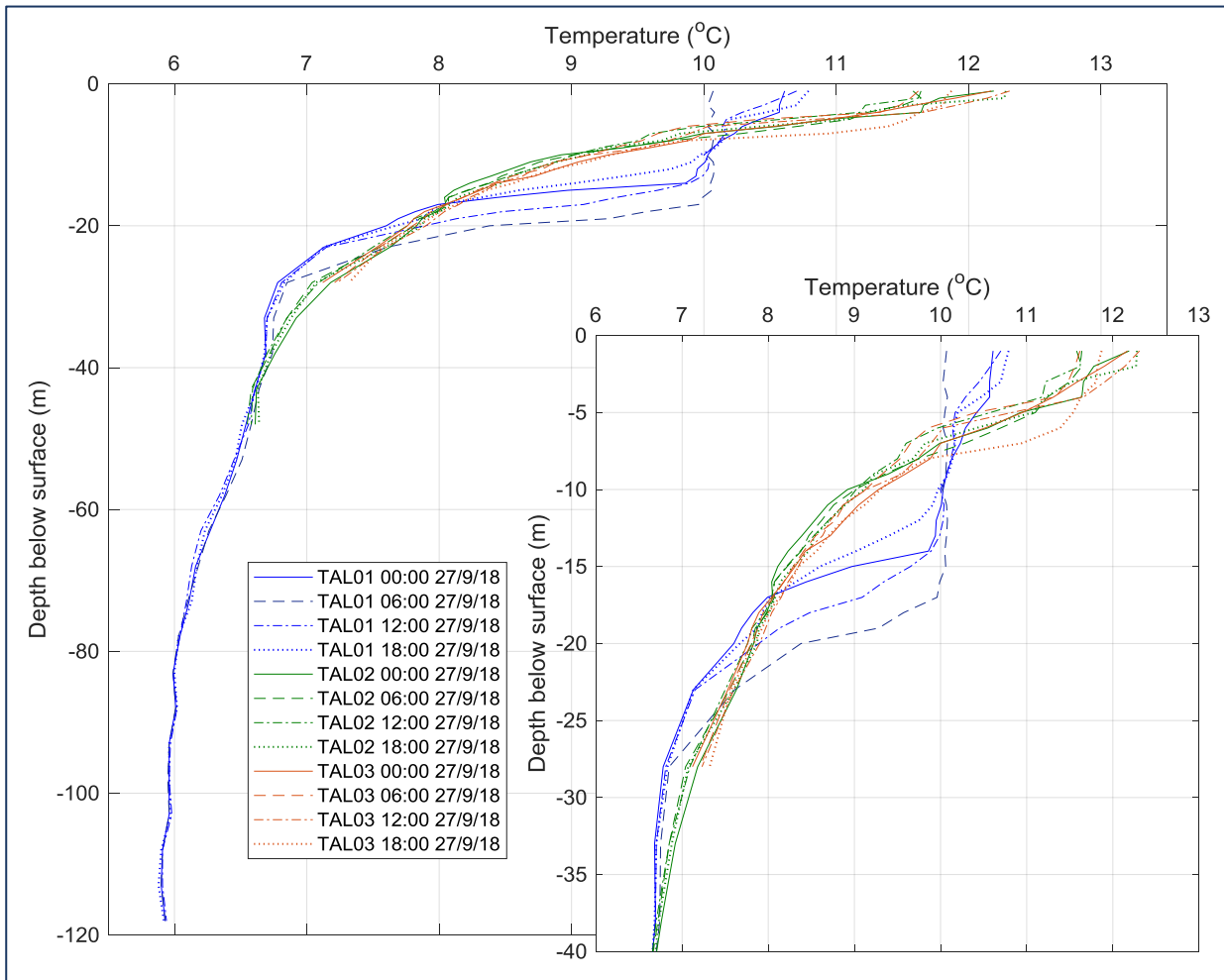


Figure 5-7 Temperature profiles in Talbingo Reservoir derived from thermistor strings at the 3 sites on 29 July 2018 at 6 hr intervals.

The daily average water velocity on the same day at TAL_ADCP_02 in the Tumut Arm about 1 km upstream of the Tumut/Yarrangobilly confluence shown in **Figure 5-8**. This figure indicates the surface water, down to 10 m depth, is flowing downstream (south-eastward flow) and the deeper waters between 10 and 35 m depth flowing upstream (towards the north). The significant vertical shear of the horizontal currents within the stratified layer below the thermocline indicates the considerable mixing potential.

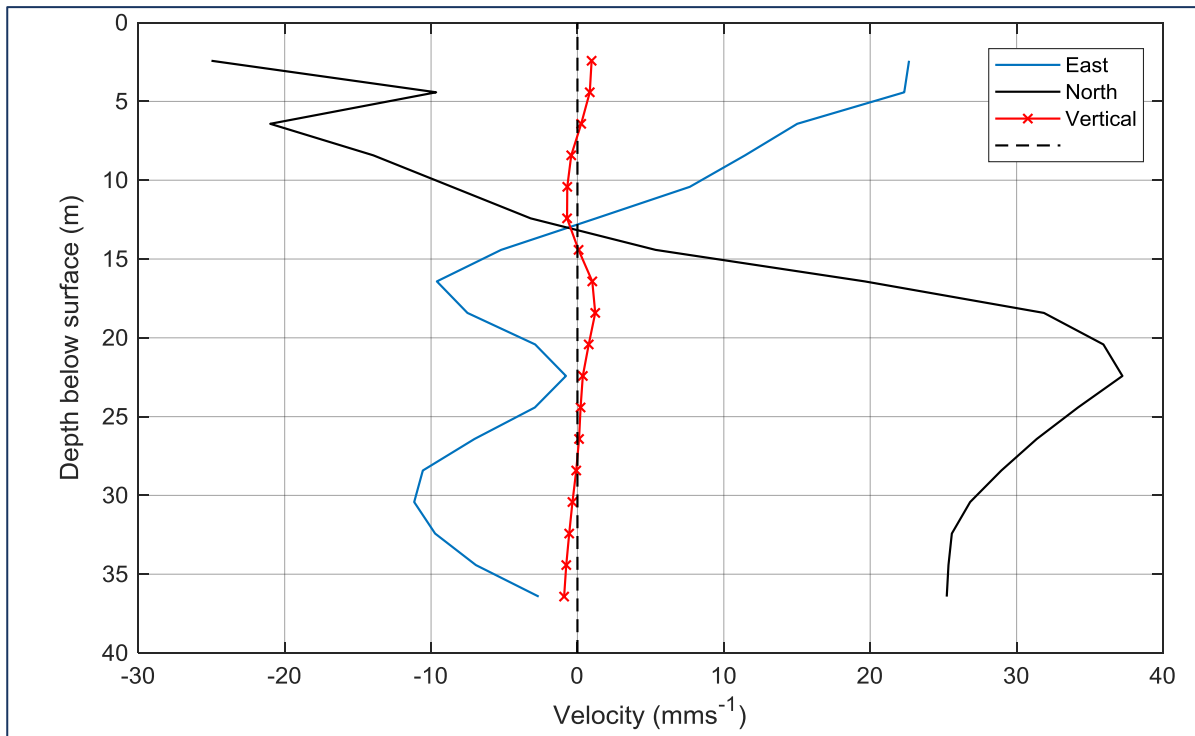


Figure 5-8 Daily average velocity vectors derived from the ADCP deployed in Talbingo Reservoir at TAL_ADCP_02 in the Tumut Arm 1 km upstream of Tumut/Yarrangobilly confluence.

Figure 5-7 and **Figure 5-8** indicate some of the complexity of the mixing regime in the reservoir and time scales of influence that are likely to affect the dispersion of any introduced sediments and dissolved substances.

5.3.3 Inflows and Outflows 28 September to 4 October 2018

An intensive field sampling campaign including vertical profiling of the water column was conducted over the week of 28 September to 4 October 2018 when the spring thermal structure had developed. The time series measurements from moored instruments and the vertical profiles that highlight both the temporal and spatial variability are discussed below. Inflows and outflows to the reservoir during this period are shown in **Figure 5-9**. The discharge in Yarrangobilly River was generally low and less than 2 m³/s for the 7 days. Likewise, there was virtually no inflow from the T2 transfers that enter the reservoir via the Tumut arm in the upper reaches. T3 pumpback inflows from Jounama Pondage into Talbingo occurred on the four days over 28 to 30 September and 1 October 2018 following the power generation release flows. These discharges are typically greater than 100 m³/s and lead to the changing water level shown in the lower frame of **Figure 5-9**.

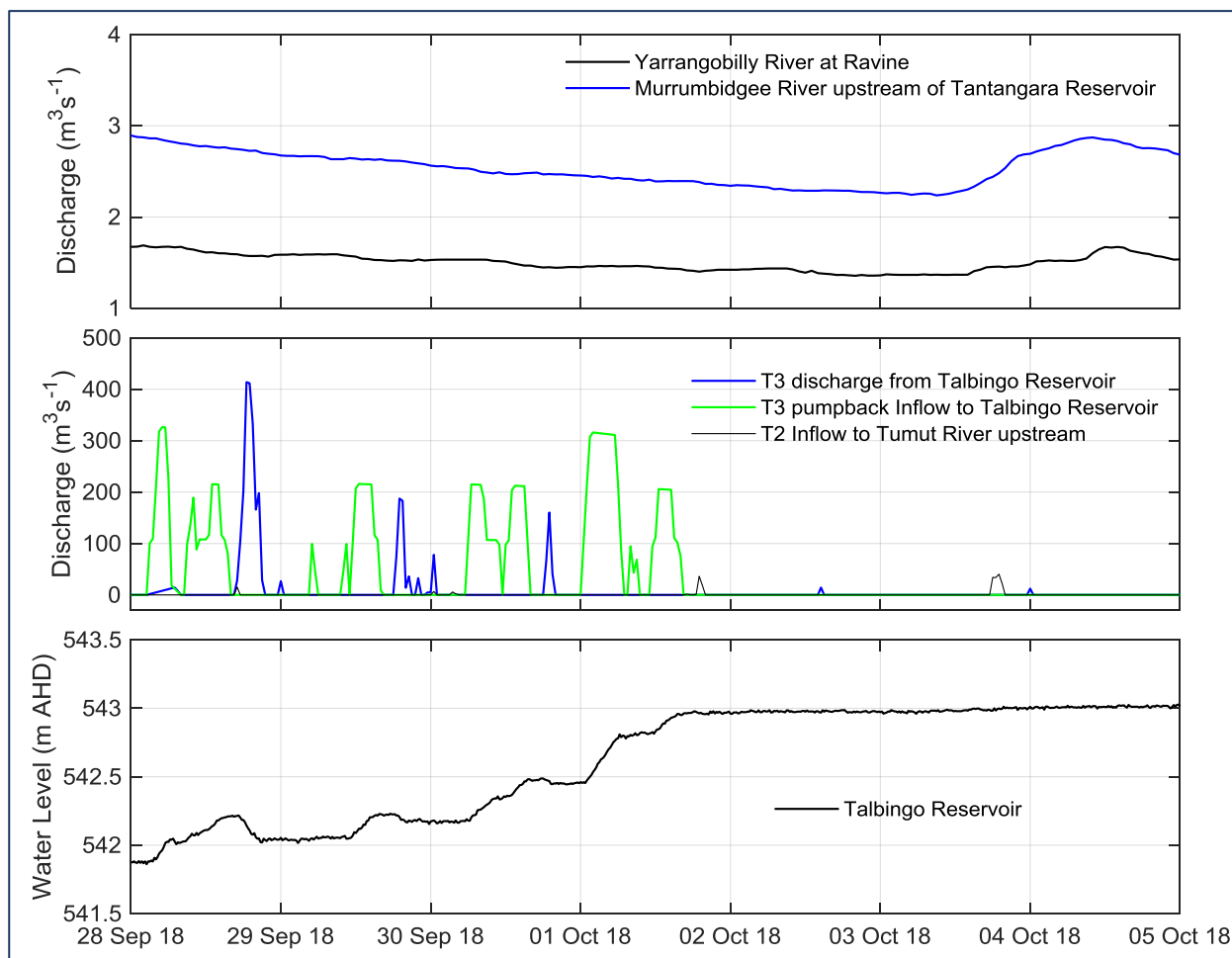


Figure 5-9 Thermal Structure - Temporal a) Yarrangobilly River stream discharge (top), b) T3 extraction and pumpback and T2 inflow (middle), and c) Talbingo Reservoir water level (bottom)

Correlations between the winds, thermal structure and currents data for the period 28 September 2018 to 5 October 2018 are presented in **Figure 5-10**. The wind northerly wind vector (red line in the top frame) shows:

- > An initial period of southerly wind from 00:00 to 06:00 on 28 September 2018 then a reasonably strong northerly from 06:00 to 18:00;
- > Fairly calm (<2 m/s) period from 18:00 28 September to 06:00 29 September 2018 then swinging to the south to 06:00 30 September 2018;
- > 30 September to 3 October 2018 a strong diurnal cycle comprising 4 m/s northerly winds between 06:00 and about 16:00 then swinging to stronger southerly 8 m/s overnight;
- > On 4 October 2018 the winds persist from the south;
- > The T3 discharge from near the Dam wall and T3 pumpback flows (**Figure 5-9**) also show a diurnal cycle (compare blue green sequence) on 28 and 29 September 2018, and only pumpback flows contributing to the rising water level on 1 and 2 October 2018;
- > The alignment between rising water level as the T3 pumpback flows (green line) and then falling water level during T3 discharge (blue line) is clearly visible in **Figure 5-9**; and
- > Only small flows were released into the Tumut River from the T2 Power Station.

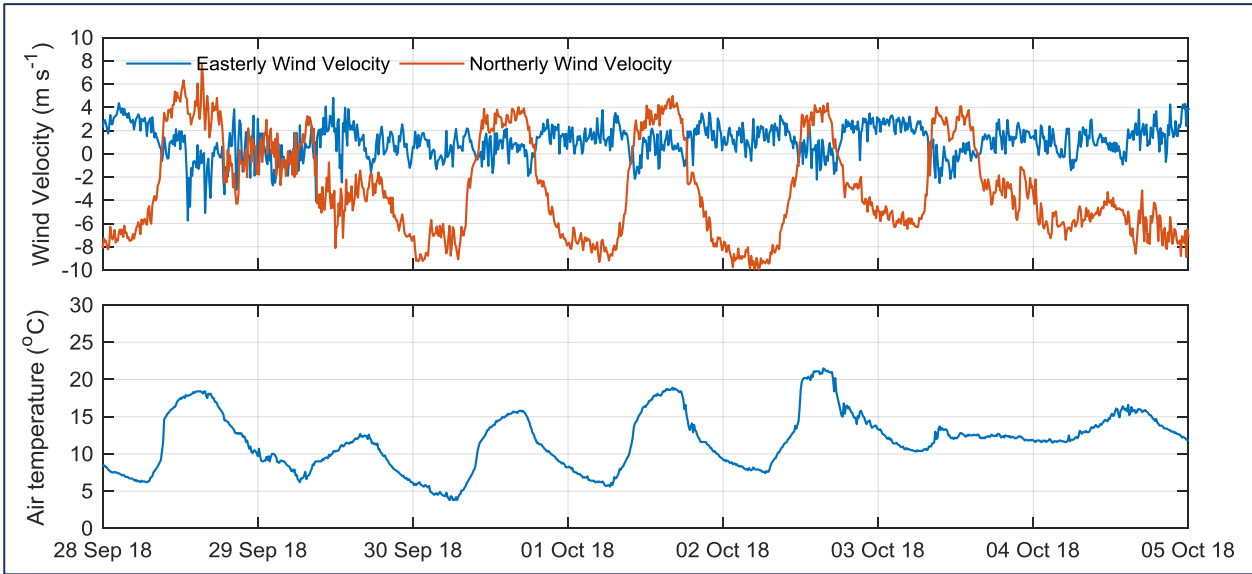


Figure 5-10 Easterly and northerly wind speeds (top) and air temperature (bottom) at Talbingo Reservoir (TAL_01) near the dam wall

The 8°C and 9°C isotherm depths shown in **Figure 5-11** indicate that near the dam wall the internal seiche motions respond to the strong diurnal surface winds and the diurnal pattern of T3 discharge and pumpback. The daytime northerly wind blows surface waters upstream causing the water column to rise and then the strong overnight southerly forces surface waters toward the dam, depressing the isotherms. At the shallower upstream locations TAL_02 and TAL_03 the response of these isotherms shows very small diurnal vertical oscillations and longer periods over a few days are more prevalent.

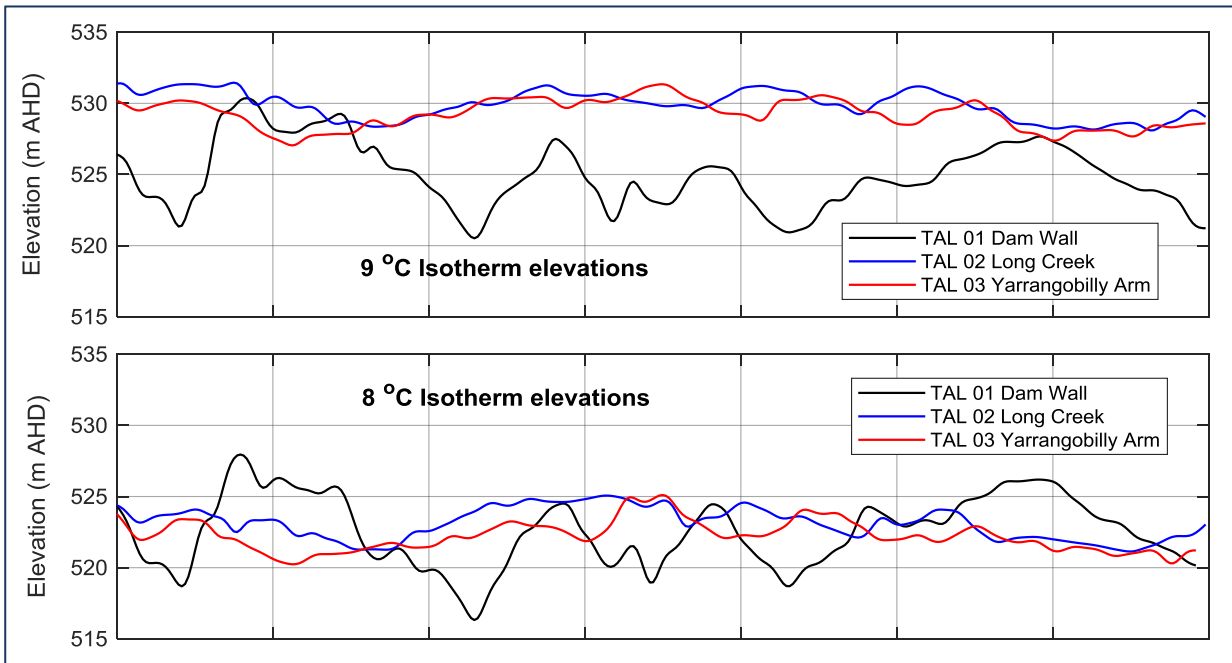


Figure 5-11 Isotherm depths, 8°C and 9°C at Tal_01 near the dam wall Tal_02 near Long Creek and Tal_03 in the Yarrangobilly arm

The longitudinal currents derived from the ADCP time series measurements at the site TAL_ADCP_02 in Yarrangobilly arm, just upstream of the confluence with the Tumut River arm are shown in **Figure 5-12**. The yellow to red colours indicate flow upstream and the green to blue colours indicate downstream flow. Note the diurnal wind-forced motions, vertical shear of the horizontal currents, and upstream flow near the bed between 1 and 5 October 2018. While the current magnitudes are quite low, the persistent shear and direction changes indicates a dispersive system with strong mixing and advective flows. Daily averaged current vectors at each depth for both the upstream ADCP sites are shown in **Figure 5-13**. Arrows to the

right indicate upstream flow. This figure again shows the complexity of the vertical structure with strong currents near the surface and bed, and flow reversals on a daily basis.

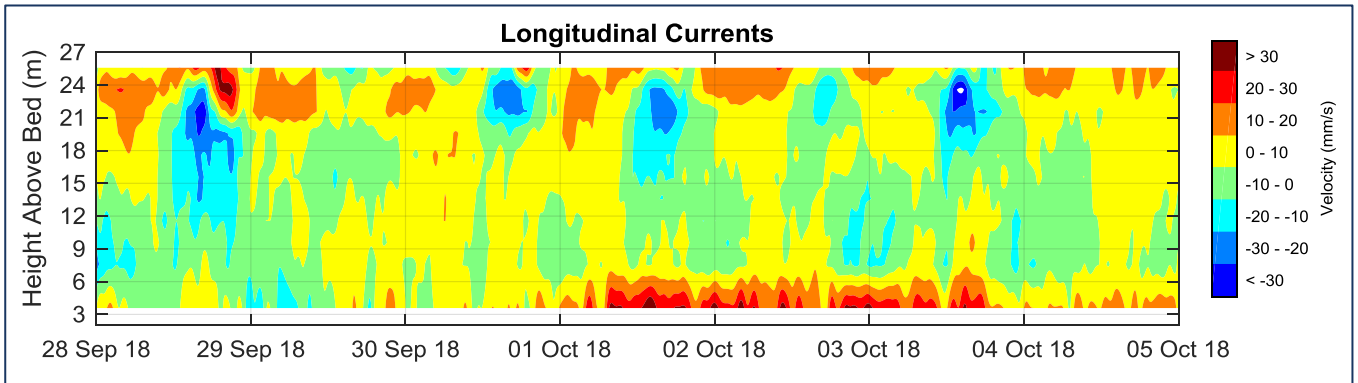


Figure 5-12 Longitudinal currents at ADCP site TAL_01 in the Yarrangobilly arm

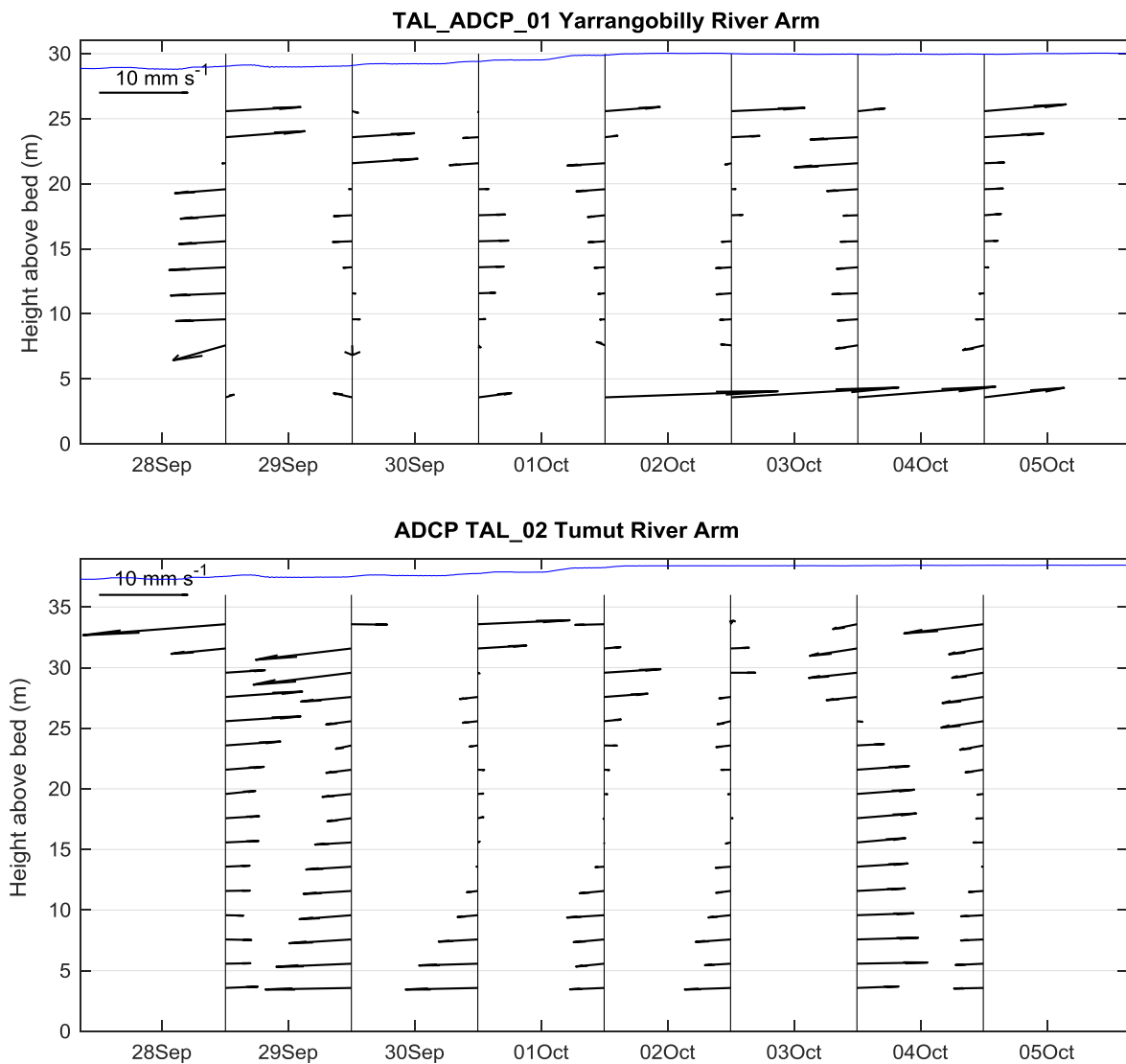


Figure 5-13 Daily averaged current vectors at each depth at the two ADCP sites

5.3.4 Spatial Structure (CTD Surveys)

The vertical profiles (**Appendix F**) collected along the reservoir on 2 October 2018 have been compiled into a longitudinal section (**Appendix G**) and are presented in **Figure 5-14** including an expanded view of

the top 50 m in lower frame. These profiles indicate the sloping isotherms at this time reflecting a range of mechanisms including:

- > Surface winds blowing the warmer surface waters upstream;
- > Broader temperature profile at the dam wall potentially reflecting the withdrawal of water from the T3 inlet and subsequent mixing induced by the T3 pumpback flows;
- > At the upstream extent in the Tumut arm the effect of the T2 releases of generally colder water leading to mixing of waters in the Tumut arm and its subsequent propagation downstream; and
- > Tilting of isotherms most likely due to internal seiche response to the diurnal wind forcing. This may include the vertical 2nd or higher order vertical modes.

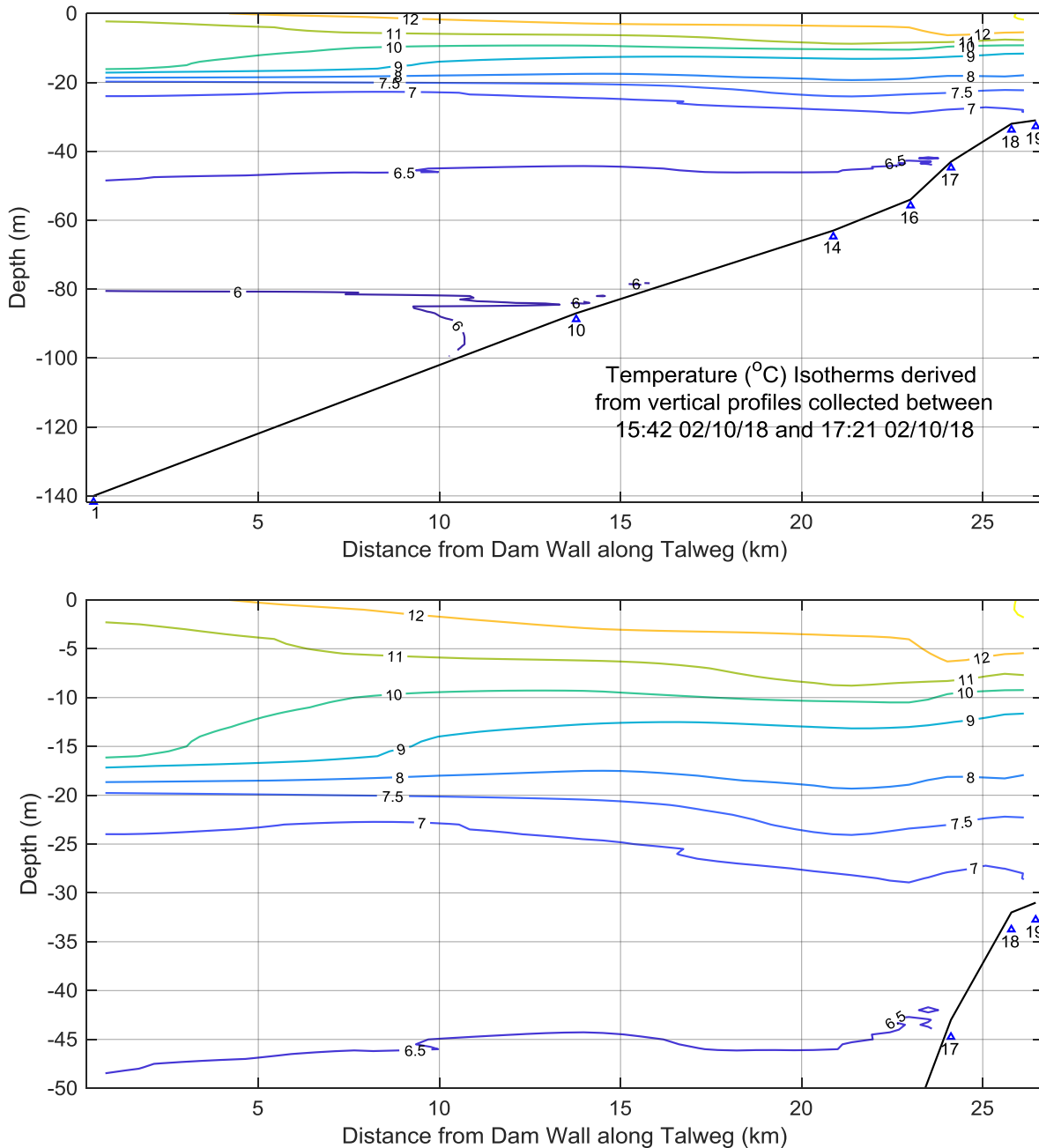


Figure 5-14 Longitudinal/depth contours on 2 October 2018 derived from vertical profiles (sites indicated). Lower panel zoomed in to 50 m depth. Triangles and numbers indicate the profiles sampling locations.

5.3.5 Water Density and Intrusions

The near bed specific conductivity data at site TAL_03 (**Appendix H, Figure H-3**) shows a series of fluctuations that are most likely due to the river inflow and/or T2 discharge events entering the reservoir from the Tumut River and plunging down the bed. The data at the deeper TAL_02 site suggest that these bed flows have been diluted by mixing with the surrounding waters prior to reaching this site. The actual TAL_03 thermistor string site is located above the deepest point in the bed profile and hence the bottom intrusions may not necessarily influence the bottom sensor at TAL_03. Another possibility is that the T2 discharge has flowed down the Tumut Arm of the reservoir and not penetrated upstream into the Yarrangobilly arm to the location of the TAL_03 thermistor string.

Appendix F shows the vertical profiles collected during the sampling program. Near the Talbingo dam wall in the late afternoon at 17:21 on 2 October 2018 (CTD profiling site TAL_01, **Figure F-17**), the temperature profile shows a surface stratified layer down to about 4 m depth and then a well-mixed layer between 4 and 17 m of temperature 10.5°C. The temperature decreases from 10.5°C to 7.5°C at 20 m with the thermocline (the depth of maximum buoyancy frequency, $N_{max} = 0.003 \text{ Hz}$) occurring at 18 m. The T3 inlet/outlet channel is shown in **Figure 5-15** that highlights the channel is about 1 km long, is generally about 20 m deep (below dam crest level) but has a sill of about 12 m depth at its southern end near the entrance to reservoir. To operate the T3 power station water is withdrawn from the reservoir via this channel and the depth of the sill is likely to act as a control on the withdrawal layer thickness within the main reservoir. Likewise during pumpback operation mixing within the channel and the sill depth are likely to influence the depth of intrusion of the Jounama Pondage inflow into the main reservoir.

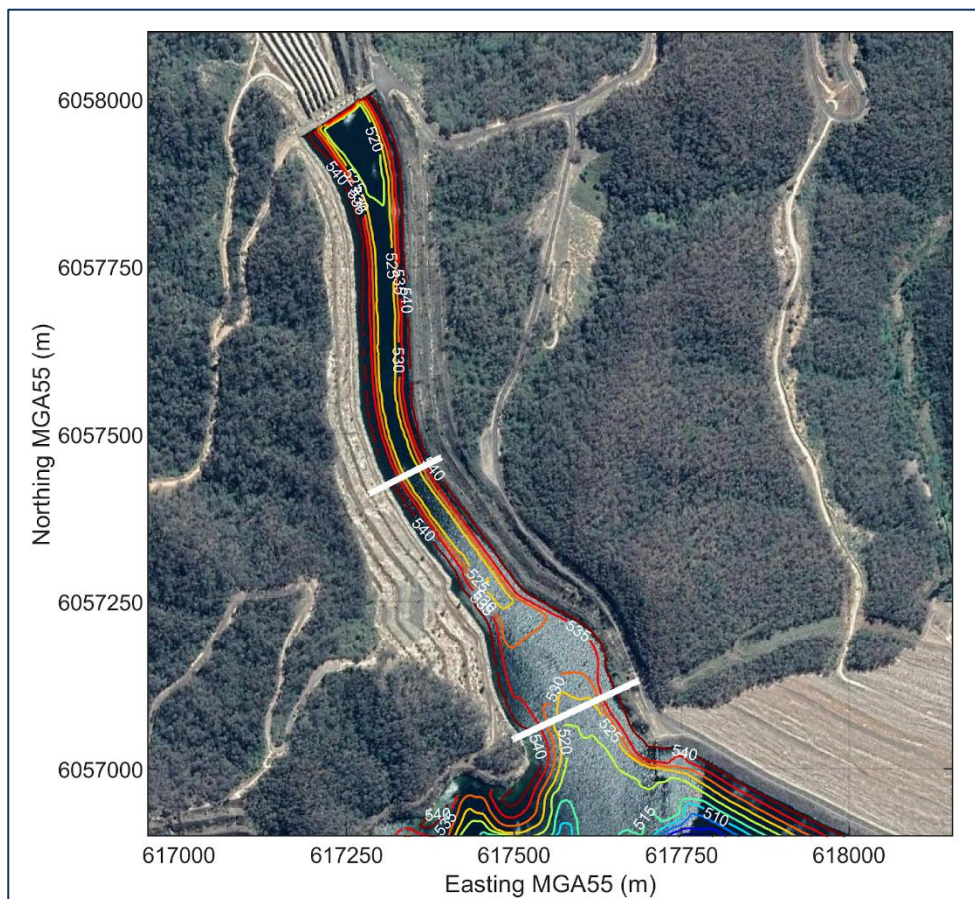


Figure 5-15 T3 inlet/outlet channel and transects

Withdrawal Layer Thickness

For the typical flow rates of the T3 intake (100 to 500 m³/s) the withdrawal layer thickness, using the point sink **Equation 6**, is estimated as $\delta \sim 46$ to 78 m. The dissolved oxygen (DO) profile on 22 March, 2019 at CTD profiling site TAL_01 (**Figure F-1**) indicates that below the thermocline there is a notable sag in DO concentration between 20 and 70 m depth. Profiling sites further upstream (CTD profiling site TAL_14 in **Figure F-10**) indicate the DO sag in waters between 20 and 70 m depth diminishes around the middle of the reservoir. The water between these depths is expected to reside there for some time, possibly greater than nine months, through the stratified period. DO depletion may be due to in-situ oxygen consumption,

or pumpback flows of lower DO and temperature intruding into the mid-depth of the reservoir. The intrusion depth will depend upon the temperature difference between the inflowing Jounama Pondage pumpback water and the water temperature within Talbingo Reservoir.

5.3.6 Seiches and Mixing

For an assumed reservoir length scale of 15 km (approximate length between dam wall and significant reflective boundary due to a sharp bend in the alignment) and depth 40 m the surface seiche period (**Equation 3**) is estimated as 25 minutes. It is expected that changes in wind speed and direction, larger river inflows and the impulse associated with the T3 and T2 flows will likely generate these surface seiches that affect the currents at a period of around 25 minutes. In general, the complex topography leads to rapid dissipation of the seiche energy and the seiche waves diminish within a few oscillations (see ADCP data in **Appendix I**).

For internal seiches the period of a first vertical mode seiche is given by **Equation 4** that is effectively the surface seiche equation (**3**) modified by the stratification or density gradient. In the case of Talbingo Reservoir, the diurnal wind and the combination of T3 discharges and pumpback flows creates significant internal seiches that propagate up the reservoir at the forced diurnal frequency and at the longer periods of a few days depending upon intensity of the stratification.

These motions then cascade energy from the longer periods to shorter period internal waves that in turn dissipate the energy into turbulent mixing and ultimately heat energy. The mixing of waters in the shallow parts of the reservoir leads to longitudinal density gradients resulting in intrusions of the mixed waters into the adjacent stratified waters at the level of neutral buoyancy. These processes lead to rapid horizontal mixing across the density stratified system. In summary, the mixing regime of Talbingo Reservoir is driven by a combination of energy sources including:

- > Natural heating cooling cycles leading to spring-summer evolution of thermal stratification and autumn/winter cooling leading to surface layer deepening and homogenisation of the lakes;
- > River inflows that intrude into the reservoir into their level of neutral buoyancy that varies from warm inflows along the surface to colder winter inflows along the bottom of the reservoir;
- > Transfers of water via the T2 Power Station from the Tumut 2 pondage are generally colder than waters in the Talbingo reservoir and flow down the Tumut arm and into the main part of the reservoir at the level of neutral buoyancy (after separating from the bed), these flows lead to significant mixing in the Tumut arm of the upper reservoir;
- > T3 pumpback flows from Jounama Pondage entering near the Talbingo Dam wall that lead to significant mixing within the inlet channel and intrusions in to the below the thermocline of the reservoir; and
- > T3 discharges (power generation) flows withdrawing water from a selective withdrawal layer within the reservoir and the thickness of this layer that depends on the intensity of the stratification. The short duration, typically six hours, followed by pumpback flows leads to significant mixing and withdrawal of water in a diurnal pattern that drives internal seiches in the deeper waters during the stratified conditions.

The relative contributions of these water and energy sources and the combination of the processes described above leads to a system that is rapidly mixed horizontally and develops a deep stratified surface layer. Through summer, autumn and winter the warm surface layers limit vertical mixing and the deep hypolimnion waters are gradually warmed by molecular diffusion of heat. In late winter-spring the deep hypolimnion waters are generally displaced upwards by cold density current intrusions from the upstream sources (T2 flows and Yarrangobilly River) and possibly the T3 pumpback flows.

5.4 Tantangara Reservoir 2018-19

5.4.1 Weather and Surface Heat Fluxes

Meteorological measurements were recorded at TAN_M02, adjacent the thermistor string mooring and data was available from 25 October 2018. The meteorological data are presented in **Appendix D** and for shorter snapshot periods in **Appendix J**. The strong diurnal signal in the winds is prevalent but the wind direction more variable than recorded at Talbingo Reservoir where the river valley tends to channel the winds along the valley axis. Note the cold, windy days and rain events in early and late November that influence the vertical mixing as discussed below in **Section 5.4.2**.

The monthly surface heat fluxes estimated from the meteorological data are presented in **Figure 5-16** and in **Table 5-5**. These indicate the seasonal nature - summer heating, winter cooling and transition in spring and autumn - of the surface flux variability with net heat gain intensifying the stratification during summer and the surface losses (negative net heat flux from the surface) during winter causing vertical mixing and homogenisation of the water column.

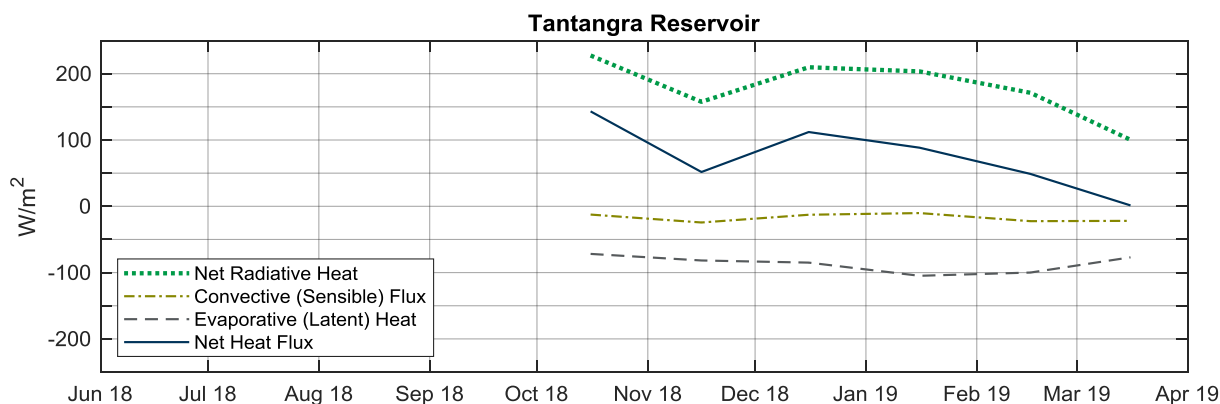


Figure 5-16 Monthly heat flux components and the net heat flux for Tantangara Reservoir

Table 5-5 Monthly heat flux components (see Section 4.3.3 for definitions) and the total heat flux in Tantangara Reservoir

Month	Q _{sn}	Q _{an}	Q _{br}	Q _{ev}	Q _{co}	Q _{tot}
November	259	277	379	82	24	52
December	314	291	396	85	13	112
January	317	305	418	105	10	88
February	294	284	406	100	22	49
March	211	285	394	77	22	1

5.4.2 Thermal Structure

The thermal structure of Tantangara Reservoir over the period June 2018 to March 2019 is shown in **Figure 5-17**. In the shallower (20-25 m deep) Tantangara Reservoir, the water column was vertically well-mixed when the thermistor strings were deployed on 6 June 2018 and the whole water column continued to cool and mix vertically through to late-August 2018 when the first signs of spring surface warming occur. The strong diurnal fluctuations are also present in Tantangara Reservoir but there is some confounding of surface cooling and seiche motions.

The two cold, wet and windy snaps in early and late November result in complete homogenisation of the water column at these times and in between the warmer days lead to development warm surface layers.

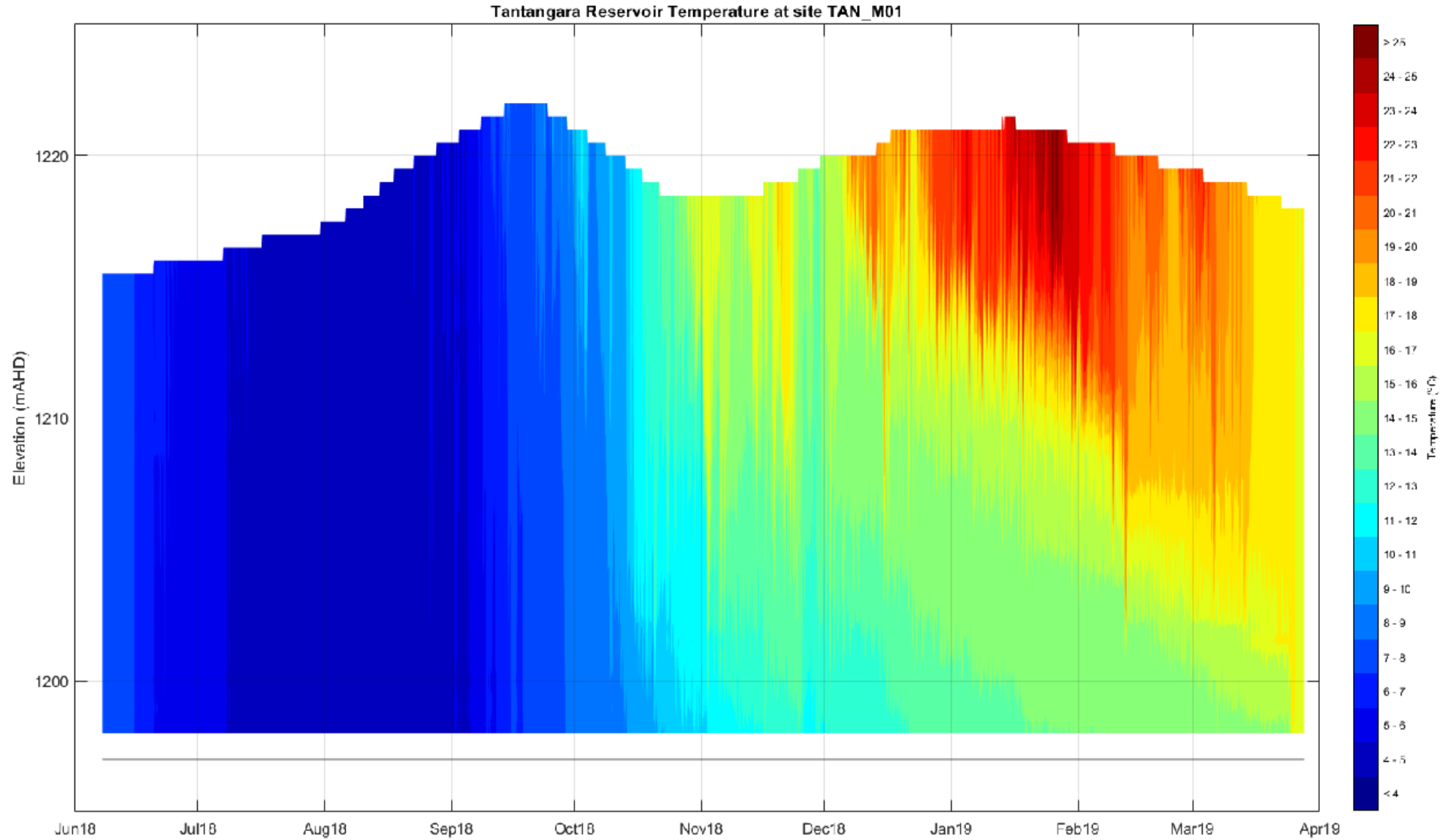


Figure 5-17 Temperature isotherms derived from 10 min samples at 30 thermistors deployed over the total depth near the dam wall at Tintangara Reservoir

Correlations between the winds, thermal structure and currents data for the weakly stratified period between 28 September 2018 and 5 October 2018 are discussed below. Isotherm depths at the two thermistor string sites, TAN_01 located 500 m upstream of the dam wall, and TAN_02 located 5 km upstream of the dam wall, are presented in **Figure 5-18**. The water level was gradually dropping through the period as releases to the Eucumbene Tunnel were discharged via the Dam wall inlet structure.

Similar to Talbingo Reservoir the complex nature of the internal seiche motions driven by the shifting winds leads to oscillations several metres in the deeper 8.5°C isotherm. The warming of the surface layer is observed from 1 to 4 October 2018 as the 9 and 10°C isotherms generally get deeper in the water column.

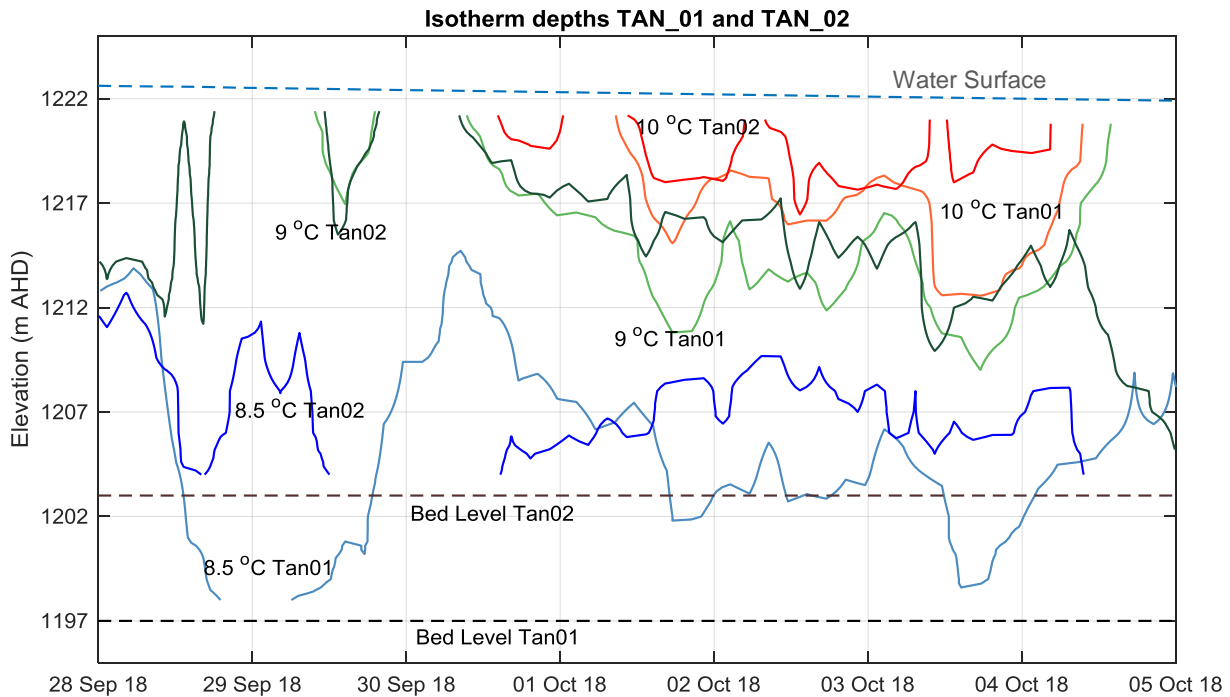


Figure 5-18 Isotherm depths at the two thermistor sites in Tantangara Reservoir

The currents at the ADCP site in the middle of the reservoir, some 3.5 km upstream of the dam wall (**Figure 5-19**) show complex vertical structure and a variable direction, as might be expected in the broader water body of Tantangara Reservoir. Periods of significant vertical shear and reversing directions are evident. Near bed flows in excess of 4 cm/s occur in both directions as indicated by the blue colour on 28 September 2018 and red colour on 4 October 2018.

The continuous extraction of water from the Murrumbidgee to Eucumbene inlet located near the dam wall at about 10 m above the bottom is likely to withdraw water from the hypolimnion during stratified periods with high reservoir water levels. There is some evidence to suggest the DO depletion within the hypolimnion waters by microbial processes leads to low DO concentrations after prolonged periods of stratified conditions. The volume of the hypolimnion varies with the water level in Tantangara Reservoir and hence the complex interaction between DO depletion rate and extraction of hypolimnic water is confounds the pattern of DO concentration variability.

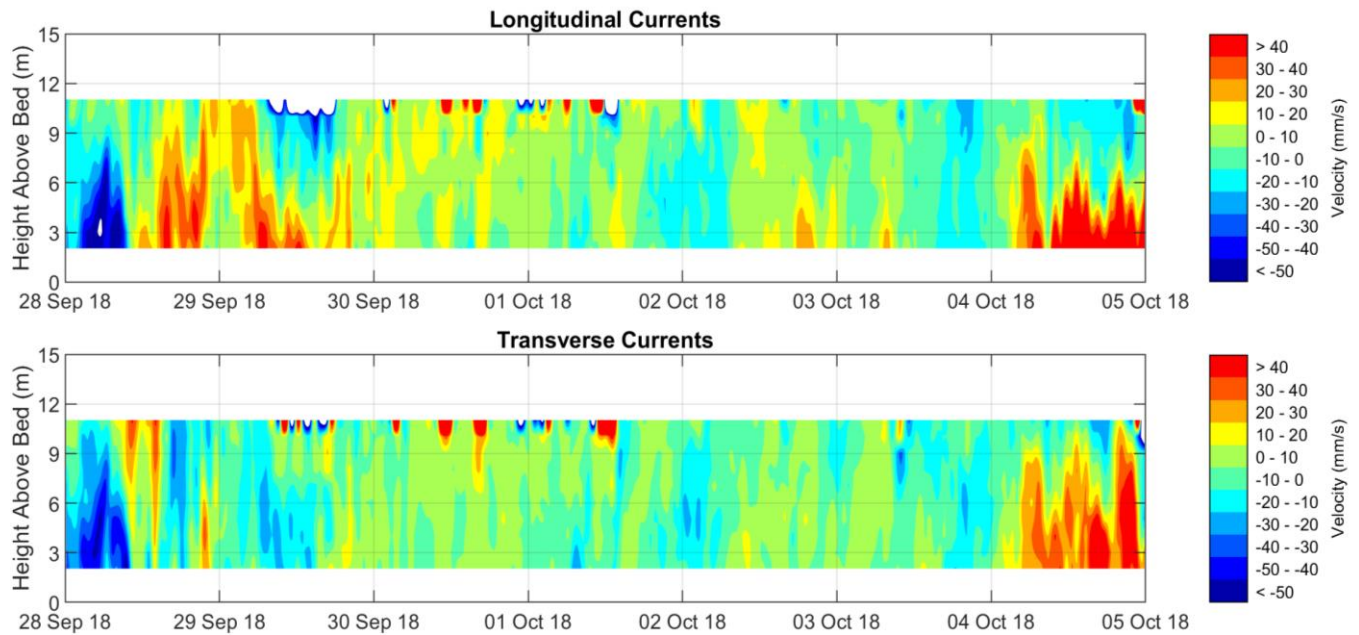


Figure 5-19 Longitudinal currents at ADCP site TAL_ADCP_01 in Tantangara Reservoir

The vertical CTD profiles collected on 4 October 2018 between 10:45 and 11:53 am at five sites along the reservoir (see sites in **Figure 4-2**) from the dam wall to the Murrumbidgee arm (**Figure 5-20**) show what appears to be a 2nd spatial mode seiche with the largest horizontal displacement occurring in the middle of the dam (Site 4). These motions lead to rapid mixing within the reservoir.

The CTD profiles indicate that in both reservoirs the DO concentrations remain at high levels for most of the year. It was anticipated that in the shallower Tantangara Reservoir, near-bottom DO would be depleted in late summer following the extended stratified period (DIPNR, 2003). The CTD profiling conducted in autumn on 20 March 2018 indicated that the water column was already well mixed vertically and hence any previous late summer low DO concentrations had likely been replenished by the vertical mixing events that preceded the sampling on 20 March.

In summary, the mixing regime of Tantangara Reservoir appears to be driven primarily by the wind and surface heat fluxes:

- > Natural heating cooling cycles leading to spring-summer evolution of thermal stratification and autumn/winter cooling leading to surface layer deepening and homogenisation of the reservoir;
- > River inflows that intrude into the reservoir into their level of neutral buoyancy that varies from warm inflows along the surface to colder winter inflows along the bottom of the reservoir;
- > Transfers of water to Lake Eucumbene are highly regulated and in combination with evaporation from the water surface lead to the gradual decline in the water level;
- > The selective withdrawal of water from the Eucumbene inlet structure is likely to extract hypolimnetic water from below the thermocline in summer stratified period;
- > Inflows from Goodradigbee transfer and natural flows from the upper Murrumbidgee River and smaller tributary inputs lead to increasing water level. These inflows and transfers are at generally low flow rates and the water surface elevations change fairly gradually and over a larger operational range than in the Talbingo Reservoir; and
- > The relative contributions of these processes leads to a system that is rapidly mixed horizontally and develops a stratified layer system that penetrates to the bed at 25 m deep.

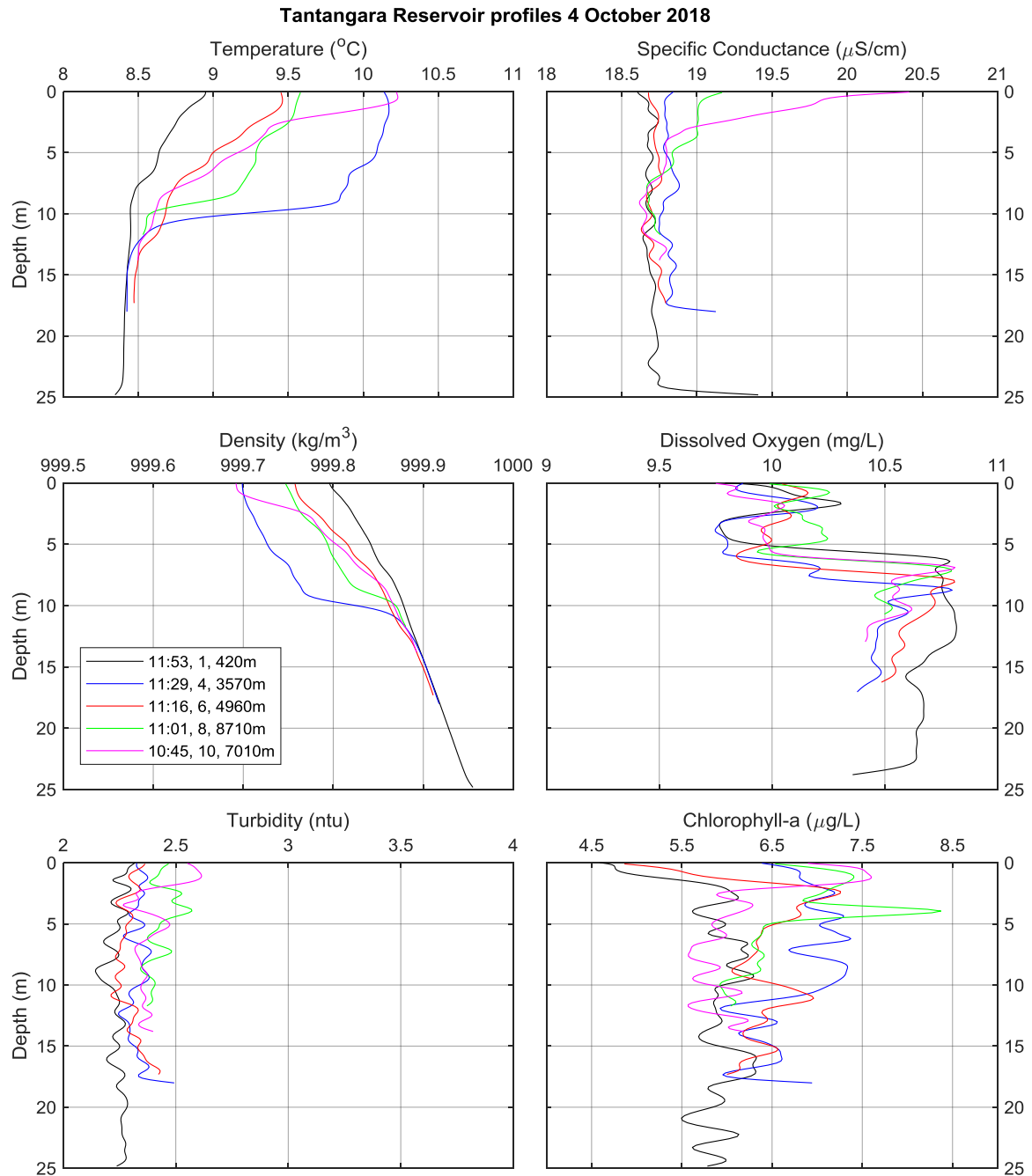


Figure 5-20 Vertical profiles collected on 4 October 2018 in Tantangara Reservoir at CTD profiling sites 1, 4, 6, 8 and 10

5.4.3 Underwater Light and Extinction Coefficient

The light extinction coefficient was determined from each of the vertical light profiles as discussed in **Section 4.3.6**. Turbidity and chlorophyll-a were then averaged over the photic depth, Z_p . The chlorophyll-a data collected at Tantangara Reservoir on 20 March 2018 comprised uncharacteristically constant values and were considered unreliable. These data were excluded from the linear regression analysis. A different CTD instrument was used on 20 and 22 March 2018 as compared to the 2 to 4 October 2018 field exercise. Turbidity is a relative measure and each instrument measures turbidity slightly differently and hence it is unclear how the turbidity measured by each different instrument compares in terms of absolute values, particularly in the low range turbidity signals measured in both reservoirs.

The linear regression algorithm (Matlab™) was applied to these data to determine the coefficients for the light extinction relationship, **Equation 10**. Results are presented in **Figure 5-21** and **Table 5-6**.

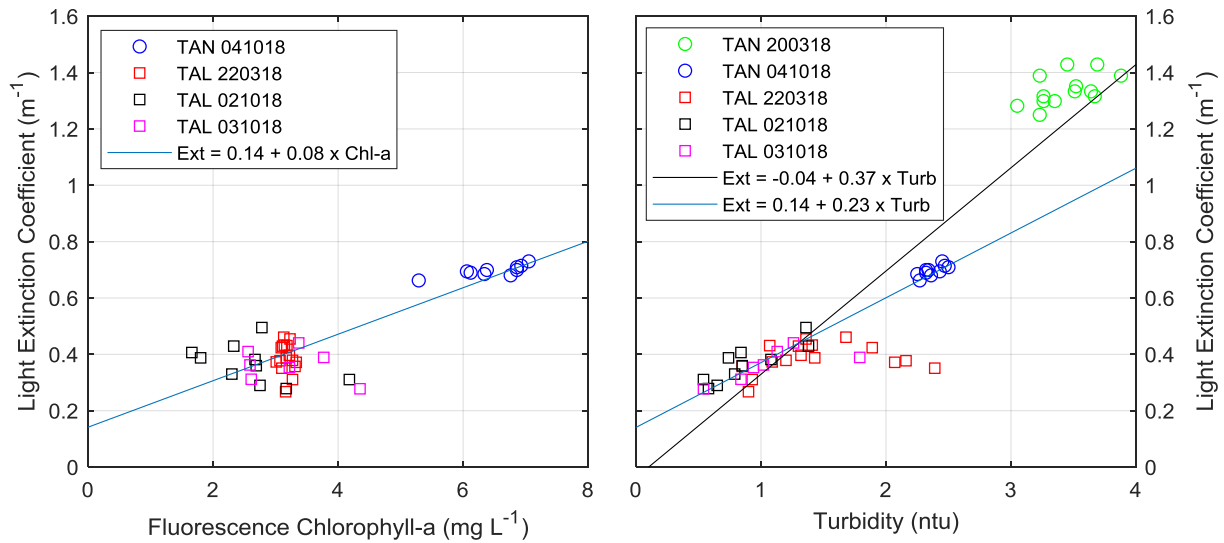


Figure 5-21 Light Extinction coefficient versus chlorophyll-a and Turbidity derived from CTD profiles in both Reservoirs

Table 5-6 Coefficients relating extinction coefficients to chlorophyll-a and turbidity using reliable data (44 points)

Coefficient	Symbol	Estimate	Standard Error	Student's t-Statistic	pValue
Intercept	a	0.122	0.017	7.3	0.000
Chl-a	b	0.015	0.006	2.5	0.017
Turbidity	c	0.200	0.014	13.8	0.000
Linear regression k versus Turbidity only					
Intercept	a	0.14	0.02	8.3	0.00
Turbidity	b	0.23	0.01	21.6	0.00

Using the reliable data (derived from 44 profiles) for the four days of sampling in both reservoirs the following relationship was derived

$$k = 0.122 + 0.20 \times \text{Turbidity (NTU)} + 0.015 \times \text{Chl-a (mg/L)},$$

Which shows the extinction coefficient is only weakly dependent upon chlorophyll-a concentrations, although it must be recognised that only very low values of chlorophyll-a were observed during the field sampling days.

An approximate fit to the turbidity data aggregated from all 44 CTD profiles from both reservoirs on five days:

$$k \approx 0.14 + 0.23 \text{ Turbidity (NTU)} \tag{Equation (11)}$$

Applying the above relationship to the typical range of turbidity values in the reservoirs, the estimates of extinction coefficient and photic depth are shown in the **Table 5-7**.

Table 5-7 Light Extinction, Photic Depth versus Turbidity

Turbidity (NTU)	Extinction Coefficient <i>k</i>	Photic Depth <i>Z_p</i>
1	0.4	12.4
2	0.6	7.7
5	1.3	3.6
10	2.4	1.9

The results presented in **Table 5-7** indicate that for an increase in turbidity from 2 to 10 NTU leads to a significant decrease in photic depth from around 8 m down to around 2 m. This light reduction would have

implications for primary producers such as phytoplankton within the water body as well as benthic plants that might survive in the reservoir photic zone. The implications of these aspects of the physical limnology for aquatic ecology of the reservoirs is discussed in the Aquatic Ecology report (Cardno, 2019).

6 Discussion

6.1 Temperature Comparison – Talbingo and Tantangara Reservoirs

Comparing the temperatures at different depths from the thermistor strings in both reservoirs highlights their different altitudes, thermal mass and mixing regimes (**Figure 6-1**). The black line from 30 m depth in Talbingo Reservoir shows the water beneath the thermocline remains cold at between 7 and 8°C for most of the year. The temperature in the deepest waters of Talbingo Reservoir near the dam wall (~130 m deep) remains reasonably constant between 6 and 6.3°C over the year while the shallower upstream sites (55 and 35 m deep) show a period in August with bottom water declining to 5.5°C (**Figure 5-6**). As the shallower (and considerably smaller volume) Tantangara Reservoir is generally less than 25 m deep the water temperature is more responsive to the surface heat fluxes and mixing events. Tantangara Reservoir waters mix earlier in the year and cool down to the lowest winter temperature of about 4.5°C in August.

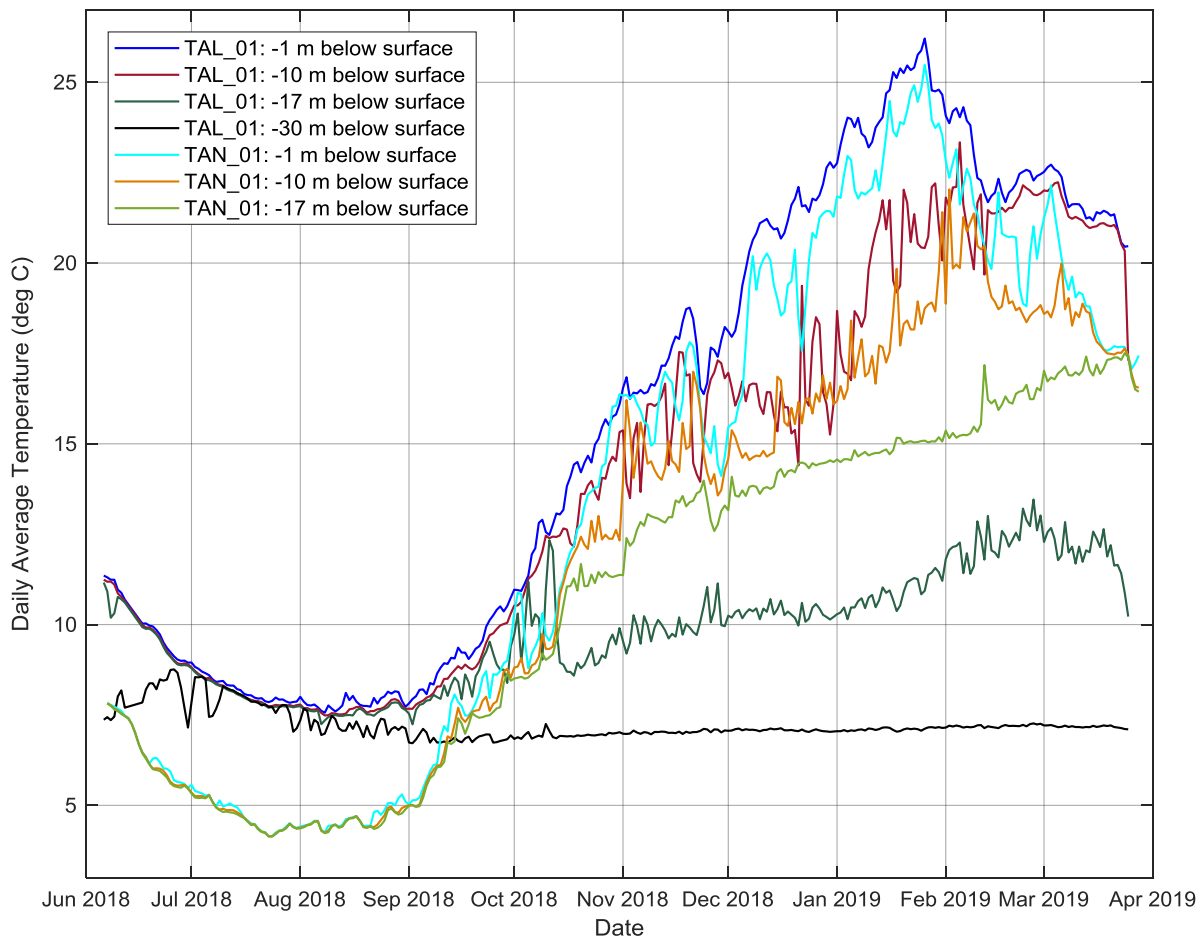


Figure 6-1 Temperature at different depths near the dam walls in Tantangara and Talbingo reservoirs

Moving up the water column, the temperature signals at 17 m depth are presented in green dark green for Talbingo Reservoir and light green for Tantangara Reservoir (refer **Figure 6-1**). The Talbingo Reservoir temperature at 17 m remains about 3°C warmer in winter (from July to mid-September) and 3 to 4°C colder in spring, summer and autumn (from late October to May) than in Talbingo Reservoir. Again this reflects the lower thermal mass and higher altitude of Tantangara Reservoir where the waters equilibrate to the surface heat fluxes more rapidly than the larger volume of Talbingo Reservoir water. The colder winter temperatures and stronger solar radiation (at altitude) in summer are key factors driving this difference.

For 10 m depth, compare orange line for Tantangara Reservoir and the red line for the Talbingo Reservoir (refer **Figure 6-1**). Again in winter (from July to mid-September) the Tantangara waters are around 3°C colder than in Talbingo Reservoir. For the rest of the year, the Tantangara water at 10 m depth remains only slightly cooler (<1 °C) than the Talbingo Reservoir waters. A similar pattern emerges

for the near surface water comparison at 1 m depth (compare dark blue, Talbingo and light blue, Tantangara lines).

6.2 Summary of Key Processes

As outlined in **Section 1.4**, the aim of this report is to collate, analyse and interpret available reservoir and meteorological data to describe the physical limnology of the existing Talbingo and Tantangara Reservoirs. The findings of this work are summarised in terms of the scope of works items below:

1. Describe the general long-term weather and rainfall patterns that affect reservoir dynamics:
 - > The weather patterns are a key driver of the surface heat fluxes at the daily (day-night), seasonal and inter-annual time scales. Rainfall patterns at the seasonal and inter-annual (drought-wet cycles) are a key driver of the water budget. SHL operational transfers, electricity generating and pump-back discharges also form a significant contribution to the water budget in both Talbingo and Tantangara Reservoirs;
 - > The surface wind patterns are characterized by strong diurnal variations, propagation of frontal systems lasting a few days and a weaker seasonal overlay. The surface winds make a significant contribution to the surface heat fluxes. Winds enhance the evaporative cooling of the surface waters and more importantly transfer energy to the reservoir. This energy leads to mixing of the surface layers and excites internal seiches that distribute energy to the deeper waters;
 - > Winds, surface cooling (negative heat flux) and water transfers input kinetic energy that affects the movement of water and more importantly provides the sources of energy for turbulent mixing;
 - > Turbulence kinetic energy is redistributed around the reservoir by internal waves that interact with the topography enhancing mixing in the bottom boundary layer and internally within the reservoir waters;
 - > In Talbingo Reservoir vertical mixing and surface layer deepening in autumn and winter does not penetrate to the deepest waters (>70m deep). Deep water renewal proceeds in late winter and spring with cold inflows from the T2 Power Station and natural catchment flows displacing the deep waters;
 - > In the shallower Tantangara Reservoir the vertical mixing of the surface layer leads to surface layer deepening through the whole water column homogenising the reservoir waters over the whole depth by mid-autumn; and
 - > Transfers and natural inflows enter the reservoirs as density current intrusions with seasonal patterns:
 - Warm inflows intrude at surface in summer,
 - Mid-temp inflows intrude at level of neutral buoyancy – spring, summer and autumn, and
 - Cold inflows – flow along the bed as bottom density currents in late winter and early spring.
2. Analyse data from the intensive field exercises carried out by Cardno between April 2018 and March 2019 to quantify internal seiche variability and the conditions that drive this variability:
 - > Internal seiches are key to distributing near surface energy inputs from wind and transfer flows to the deeper waters of the reservoirs;
 - > The strong diurnal wind patterns, typical of alpine areas, are a strong driver of the forced (24 hr) internal seiche in both reservoirs and surface seiches of ~25 minutes in Talbingo Reservoir and ~10 minutes in Tantangara Reservoir. Longer period (a few days) internal seiches are prevalent in the weaker stratified periods of autumn and spring; and
 - > The roughly diurnal pattern of release and pump flows to/from the T3 Power Station also contribute to forcing the diurnal internal seiche response.
3. Characterise the existing system surface mixed layer depth, metalimnion and hypolimnion thickness variability:
 - > The surface mixed layer depth varies on a daily basis with sunny days in summer leading to warming of the surface waters down to the photic depth and overnight cooling leading to surface layer deepening. The regular winds impart significant energy for mixing and the collapse of localised mixing events leads horizontal intrusive flows. In Talbingo Reservoir the T2 Power Station discharge to the upper Tumut arm and the T3 Power Station pumpback discharge into the inlet

channel near the dam wall lead to significant mixing within these areas that then propagate into the main waters of the reservoir from their respective directions;

- > The metalimnion, or main thermocline zone is typically 5 to 20 m deep and is generally deeper than the photic depth in Talbingo Reservoir. In Tantangara Reservoir the metalimnion extends to the total depth of the reservoir under the normal water level operation regime of the past 10 years; and
 - > In Talbingo Reservoir the hypolimnion extends from about 50-60 m depth down to the bottom and as discussed above (Point 1) waters are displaced vertically by cold oxygen rich bottom density currents generated by the T2 transfers and natural flows from Yarrangobilly River and other smaller tributaries. The hypolimnion thickness is more variable in Tantangara as the shallower reservoir undergoes more rapid vertical mixing than the deeper Talbingo Reservoir.
4. Discuss temporal variability in the vertical level of inflow intrusions (surface, mid-depth or bottom) under different seasonal conditions:
- > The seasonal temperature variations of the inflows and their relative difference to the reservoir waters are a key determinant of the depth of the intrusive flows. Spring snowmelt and cold water runoff is particularly key to drive deep density currents down the bed to the dam wall in Talbingo Reservoir;
 - > The shallower Tantangara Reservoir is regularly affected by the surface cooling periods can lead to complete mixing of the reservoir to the deepest waters (20 m depth), particularly when water levels are low;
 - > Regular diurnal wind forcing leads to internal seiches and benthic boundary mixing events. The level of intrusions of the Murrumbidgee River waters into Tantangara Reservoir depends upon the relative difference of water temperature in the river and reservoir;
 - > In Talbingo Reservoir the very deep waters (>70 m deep) near the dam wall are not normally affected by the surface cooling effects. Gradual warming of the deeper waters by molecular diffusion through the summer, autumn and winter followed by springtime bottom flowing density currents of colder water from T2 Power Station transfers and natural flows through the Yarrangobilly arm (snow melt) leads to upward displacement of these deeper waters. The withdrawal of water during T3 releases and pump-back of Jounama Pond waters appears to impact the stratification down to about 60 m depth in the main reservoir; and
 - > There is limited supply of fines from the catchment to the Talbingo Reservoir and the waters remain generally clear with low turbidity <4 NTU. Turbidity in Tantangara Reservoir is higher but generally <8 NTU.
5. Discuss the selective withdrawal process at intakes and its effects on reservoir stratification:
- > The transfer flows from Tantangara Reservoir to Lake Eucumbene in combination with the stratification in summer lead to the formation of a withdrawal layer;
 - > The large generating discharges from Talbingo Reservoir via the T3 Power Station inlet channel lead to a selective withdrawal layer estimated at about 60 m in the weaker stratified periods within the main part of the reservoir. CTD profiles suggest that near the Talbingo Dam wall in spring the withdrawal layer is shallower than 60 m depth and it is likely that at low release flows a narrow layer would form from the surface down to the thermocline at around 20 m depth; and
 - > In Tantangara Reservoir the primary discharge is the Murrumbidgee to Eucumbene inlet near the dam wall and located about 10 m above the deepest part of the reservoir. This position suggests that the selective withdrawal of water from Tantangara will primarily extract hypolimnetic waters.
6. Characterise the turbidity, extinction coefficient, light penetration:
- > The relationship between light penetration, turbidity and chlorophyll-a concentrations has been determined from the available CTD profiles collected on two field campaigns in autumn and spring. The light penetration and photic depth are relatively shallow, generally less than 8 m deep, for such low turbidity and low chlorophyll-a concentrations. Anecdotal evidence during the field campaigns suggests the relatively high colour content of the waters forms a significant contribution to low light penetration.
7. Summarise the key mixing and stratification regimes in the existing Talbingo and Tantangara Reservoirs to inform the modelling and aquatic ecology impact assessments:

- > In addition to the seasonal variations in surface heat fluxes and the strong diurnal wind forcing typical of alpine regions, the transfer of water between reservoirs and discharges for hydroelectric power generation creates an important source of energy for mixing and dispersion within the reservoirs;
- > Although the turbidity and chlorophyll-a concentrations are very low, light penetration is impeded by water colour such that the photic depth is generally less than 8 m depth, which is less than anticipated for similar low turbidity systems; and
- > In Talbingo Reservoir, the Tumut arm is subject to regular mixing by the discharges from the T2 Power Station. These flows are significantly greater than the natural flows and in the arm and generally introduce colder waters from the T2 Pondage some 300 m higher in altitude. Similarly, the T3 pump-back flows are introduced near the dam wall. Both these discharges contribute to the mixing and thermal structure in the main part of the reservoir.

7 References

- Anohin, V.V., J. Imberger, J.R. Romero and G.N. Ivey. 2006. Effect of long internal waves on the quality of water withdrawn from a stratified reservoir. *Journal of Hydraulic Engineering - ASCE*. 132(11): 1134-1145.
- Cardno, 2019. Aquatic Ecology Assessment. Snowy 2.0 Main Works. Prepared for EMM Consulting, in draft.
- Deltares, 2019. Delft3d-FLOW - Simulation of multi-dimensional hydrodynamic flows and transport phenomena, including sediments: User Manual. Deltares.
- DIPNR, 2003. Review of Water Quality in Reservoirs Operated by Snowy Hydro Limited 1989 to June 2003. DIPNR.
- Jamali, M. and Aghsaee, P. 2007. Effect of a contraction on selective withdrawal of a linearly stratified fluid from a line sink, *Physics of Fluids* 19, 106602, pp11.
- Snowy Hydro, 2017. Snowy 2.0 Study Report Chapter Eight Meteorology and hydrology, Snowy Hydro Limited (Commercial in Confidence).
- Transgrid (2018), Final Decision, TransGrid transmission determination 2018 to 2023, Overview, May 2018
- Wuest, A., Piepke, G. and van Senden, D.C. 2000. Turbulent kinetic energy balance as a tool for estimating vertical diffusivity in wind-forced stratified waters, *Limnol. Oceanogr.*, 45(6), 2000, 1388–1400.

APPENDIX

A

MONITORING PROGRAM

Appendix A: Snowy 2.0 - Reservoir Monitoring Program Methodology

Snowy Hydro 2.0

59918111

Prepared for
EMM Consulting Pty Ltd

29 August 2019



Contact Information

Cardno (NSW/ACT) Pty Ltd

ABN 95 001 145 035

Level 9 - The Forum
 203 Pacific Highway
 St Leonards NSW 2065
 Australia

www.cardno.com

Phone +61 2 9496 7700

Fax +61 2 9496 7748

Author(s):

Phebe Bicknell
 Senior Engineer

Matthew Smith
 Environmental Scientist

Approved By:



Andrew Bradford
 Principal Engineer

Document Information

Prepared for	EMM Consulting Pty Ltd
Project Name	Snowy Hydro 2.0
File Reference	59918111_R004_ReservoirSampling_RevE.docx
Job Reference	59918111
Date	29 August 2019
Version Number	RevE

Effective Date	23/08/2019
----------------	------------

Date Approved	29/08/2019
---------------	------------

Document History

Version	Effective Date	Description of Revision	Prepared by	Reviewed by
A	5/09/2018	Preliminary draft issued to client	Phebe Bicknell Matthew Smith	Andrew Bradford
B	13/09/2018	Final draft issued to client	Matthew Smith Andrew Bradford	Andrew Bradford
C	21/02/2019	Amended to cover progress and additional monitoring	Matthew Smith	Andrew Bradford
D	27/02/2019	Amended following client review	Andrew Bradford	Andrew Bradford
E	29/08/2019	Amended at completion of monitoring program	Matthew Smith Andrew Bradford	Andrew Bradford

Table of Contents

1	Introduction	1
2	Fieldwork Summary	1
3	CTD Profiling	3
	3.1 Instrumentation	3
	3.2 Locations	3
	3.3 Profiling Methodology	5
4	Water Sampling	6
	4.1 Sampling Equipment	6
	4.2 Analysis Suite	6
	4.3 Locations	9
	4.4 Sampling Methodology	11
	4.5 Phytoplankton Sampling Methodology	12
	4.6 Sample Preservation and Handling	13
	4.7 Corrective Actions	13
5	Sediment Sampling	13
	5.1 Sampling Equipment	13
	5.2 Analysis Suite	14
	5.3 Locations	14
	5.4 Sediment Sampling Methodology	16
	5.5 Benthic Infauna Sample Handling	17
6	Mooring Deployments	17
	6.1 Instrumentation	17
	6.2 Locations	18
	6.3 Mooring Arrangement	18
	6.4 Data Return	20
7	ADCP Deployments	20
	7.1 Instrumentation	20
	7.2 Locations	20
	7.3 Mooring Arrangement	21
	7.4 Data Return	22
8	Inflow Monitoring Deployments	22
	8.1 Instrumentation	22
	8.2 Locations	22
	8.3 Deployment Arrangement	23

Appendices

Appendix A Instrument specifications

Appendix B Instrument Data Return

Appendix C Location Maps

Tables

Table 2-1	Fieldwork Summary	1
Table 3-1	CTD Sensor Details	3
Table 3-2	Talbingo Reservoir CTD Profile Summary - Summer	3
Table 3-3	Tantangara Reservoir CTD Profile Summary - Summer	4
Table 3-4	Talbingo Reservoir CTD Profile Summary - Winter	4
Table 3-5	Tantangara Reservoir CTD Profile Summary - Winter	5
Table 4-1	Water Laboratory Analysis Suite - Summer	6
Table 4-2	Water Laboratory Analysis Suite - Winter	7
Table 4-3	Water Laboratory Analysis Suite – Additional Program	8
Table 4-4	Talbingo Reservoir WQ Sample Summary - Summer	9
Table 4-5	Talbingo Reservoir WQ Sample Summary - Winter	9
Table 4-6	Tantangara Reservoir WQ Sample Summary - Summer	10
Table 4-7	Tantangara Reservoir WQ Sample Summary - Winter	10
Table 4-8	Additional WQ Program Sample Summary	11
Table 5-1	Sediment Laboratory Analysis Suite	14
Table 5-2	Talbingo Reservoir Sediment Sampling Summary	14
Table 5-3	Talbingo Reservoir (Middle Bay) Sediment Sampling Summary	15
Table 5-4	Tantangara Reservoir Sediment Sampling Summary	15
Table 6-1	Moored Instrumentation	17
Table 6-2	Mooring Deployment Locations	18
Table 6-3	Thermistor Arrangement	20
Table 7-1	ADCP Configuration	20
Table 7-2	ADCP Deployment Locations	21
Table 8-1	Inflow Instrumentation	22
Table 8-2	Inflow Deployment Locations	23

Figures

Figure 6-1	General mooring arrangement	19
Figure 6-2	Instrument line arrangement	19
Figure 7-1	Bed Mounted ADCP Mooring arrangement	21
Figure 7-2	Moored ADCP Mooring arrangement	22
Figure B.1	- Talbingo Reservoir Data Return Summary	B
Figure B.2	- Tantangara Reservoir Data Return Summary	C

1 Introduction

Snowy Hydro Limited (Snowy Hydro) proposes to expand the generating capacity of the existing Snowy Mountains Hydro-electric Scheme (Snowy Scheme) by up to 50%. Snowy 2.0 will involve pumping water from Talbingo Reservoir to Tantangara Reservoir during times of low energy demand and releasing it back to Talbingo Reservoir during periods of high demand (via an underground power station).

The majority of the Scheme's expansion will be underground involving the construction of large pipelines, exploration tunnels and a power station located approximately 800m below the surface. Other ancillary structures e.g. on ground staging areas, construction camps, underground pipeline access points, inlets and outlets will also be required.

A key aspect of the project is the assessment of impacts associated with the sub-aqueous placement of spoil within Talbingo Reservoir and Tantangara Reservoir. In support of this assessment a data collection program has been undertaken by Cardno, comprising:

- > CTD (Conductivity Temperature Depth) profiling of the water column structure
- > Collection of water quality samples
- > Collection of sediment samples
- > Collection of aquatic ecology samples (benthic infauna and phytoplankton)
- > Deployment of moored instrumentation
- > Deployment of ADCP (Acoustic Doppler Current Profiler) instruments
- > Monitoring of reservoir inflows

This report outlines the scope and methodology for the delivery of these works.

2 Fieldwork Summary

Field activities were performed by at least two field personnel with all works performed using Cardno's 5m Webster Twinfisher vessel. This vessel is of sufficient size to handle the equipment used for these activities, while also being small enough to be launched at the available boat ramps. The vessel is fitted with a capstan winch allowing handling of the instrumentation and mooring hardware required.

All works were conducted under Cardno's HSE management system, with additional requirements such as communications and inductions conducted according to Snowy Hydro requirements.

A summary of fieldwork trips is presented in Table 2-1.

Table 2-1 Fieldwork Summary

#	Start Date	End Date	Field Personnel	Activities
1	19/03/2018	23/03/2018	Andrew Bradford Yesmin Chikani Chloe Vandervord	CTD Profiling Water Sampling
2	25/03/2018	29/03/2018	Daniel Strickland Ben Withnall Chloe Vandervord	Sediment Sampling Water Sampling
3	9/04/2018	12/04/2018	Andrew Bradford Matthew Smith	ADCP deployment (aborted due to vessel outboard motor damage)
4	17/04/2018	20/04/2018	Matthew Smith Ben Withnall	ADCP deployments Water Sampling (Phytoplankton only)
5	14/05/2018	18/05/2018	Andrew Bradford Matthew Smith	Mooring deployments (CTDs only due to thermistor manufacturing delays) Sediment Sampling

#	Start Date	End Date	Field Personnel	Activities
				Water Sampling (Phytoplankton only)
6	4/06/2018	8/06/2018	Andrew Bradford Matthew Smith	Mooring Deployments Water Sampling (Phytoplankton only)
7	2/07/2018	6/07/2018	Craig Blount Ben Withnall Jake Ludlow	Bulk Sediment Sampling Bulk Water Sampling
8	9/07/2018	13/07/2018	Matthew Smith Joel Griffiths	ADCP Servicing Inflow Deployments
9	30/07/2018	3/08/2018	Matthew Smith Andrew Bradford	Mooring servicing
10	3/09/2018	6/09/2018	Matthew Smith Joel Griffiths	ADCP servicing Mooring servicing Deployment of Yarrangobilly NTU (in reservoir) WQ sampling (UVT only)
11	19/09/2018	21/09/2018	Andrew Bradford Marcus Lincoln-Smith	ADCP servicing – Tantangara only
12	2/10/2018	5/10/2018	Matthew Smith Chris Roberts Andres Grigaliunas	CTD profiling WQ sampling
13	22/10/2018	26/10/2018	Matthew Smith Andrew Bradford	Mooring servicing WQ sampling (UVT only)
14	1/11/2018	2/11/2018	Matthew Smith Andrew Bradford	T2 temperature logger deployment WQ sampling (additional program)
15	19/11/2018	22/11/2018	Matthew Smith Andrew Bradford James Mason	ADCP servicing Mooring servicing WQ sampling (UVT & additional program)
16	3/12/2018	7/12/2018	Matthew Smith Chris Roberts	Mooring servicing WQ sampling (UVT & additional program)
17	14/01/2019	18/01/2019	Matthew Smith Chris Roberts	ADCP servicing Mooring servicing WQ sampling (UVT & additional program)
18	25/02/2019	1/03/2019	Matthew Smith Chris Roberts	Installation of Middle Creek inflow site ADCP redeployment (Tantangara) Mooring servicing WQ sampling (UVT & additional program)
19	25/03/2019	29/03/2019	Matthew Smith Joel Griffiths	Mooring servicing
20	16/04/2019	18/04/2019	Matthew Smith Ben Withnall	ADCP recovery
21	29/04/2019	3/05/2019	Matthew Smith Joel Griffiths	Mooring servicing
22	3/06/2019	7/06/2019	Matthew Smith Joel Griffiths	Mooring servicing
23	29/07/2019	2/08/2019	Matthew Smith Chris Roberts	Mooring recovery

Details of each of the monitoring components are presented in the following sections.

3 CTD Profiling

3.1 Instrumentation

The profiling instrument used was a Seabird SBE19plusV2 profiler fitted with conductivity, temperature, depth, dissolved oxygen (DO), pH, Nephelometric Turbidity Units (NTU), photosynthetically active radiation (PAR) and fluorescence sensors. All sensors are in calibration, with recent calibration certificates issued by NATA accredited laboratories on file. Sensor details are outlined in Table 3-1 and sensor specifications are included in Appendix A.

Table 3-1 CTD Sensor Details

Sensor	Parameter	Range (units)
Seabird SBE 3F	Temperature	-5 to 35°C
Seabird SBE 4C	Conductivity	0 to 9 µS/m
Diquartz	Pressure	0 to 200 psia
WET Labs EcoFLNTURT	Turbidity	0 to 200 NTU
Satlantic PAR	PAR	0 to 4500 µmol photons m ⁻² s ⁻¹
WET Labs EcoFLNTURT	Fluorescence (Chl-a)	0 to 75 µg/L
Seabird SBE 18	pH	0 to 14
Seabird SBE 43	DO	120% of surface saturation
Turner Cyclops-7*	Fluorescence (Oil in Water)	0 to 1,500 ppb

*Note: summer round only

3.2 Locations

In Talbingo Reservoir, twenty target locations were selected, and for Tantangara Reservoir ten target locations were selected. Locations are presented in Appendix C, Figure 1 and Figure 2.

3.2.1 Summer Sampling

The summer round of CTD profiling was conducted on 20 and 22 March 2018. Due to weather delays, not all locations were profiled in Talbingo Reservoir. Details of completed casts are outlined in Table 3-2 and Table 3-3.

Table 3-2 Talbingo Reservoir CTD Profile Summary - Summer

Cast	Location	Coordinates	Depth (m)	Date	Cast Start Time (UTC+10)	Cast End Time (UTC+10)
TAL01	TAL01	617775 6056539	137	22/03/2018	7:13	7:39
TAL05	TAL05	619706 6052838	84	22/03/2018	11:29	11:36
TAL07	TAL07	619713 6051010	105	22/03/2018	11:16	11:23
TAL08	TAL08	618412 6050603	64	22/03/2018	11:05	11:12
TAL09	TAL09	619523 6048919	96	22/03/2018	10:49	10:56
TAL10	TAL10	619977 6048126	89	22/03/2018	10:36	10:45
TAL11	TAL11	621040 6046999	60	22/03/2018	10:25	10:31
TAL12	TAL12	619716 6046197	83	22/03/2018	10:10	10:20
TAL13	TAL13	621230 6045474	70	22/03/2018	9:58	10:05
TAL14	TAL14	620758 6043961	64	22/03/2018	9:33	9:39

Cast	Location	Coordinates	Depth (m)	Date	Cast Start Time (UTC+10)	Cast End Time (UTC+10)
TAL15	TAL15	620056 6044027	36	22/03/2018	9:42	9:46
TAL16	TAL16	621343 6042725	56	22/03/2018	9:23	9:29
TAL17	TAL17	622360 6042530	44	22/03/2018	9:14	9:19
TAL18	TAL18	622741 6041725	34	22/03/2018	9:06	9:10
TAL19	TAL19	623113 6041797	32	22/03/2018	8:40	8:45
TAL20	TAL20	622600 6040832	34	22/03/2018	8:54	8:59

Table 3-3 Tantangara Reservoir CTD Profile Summary - Summer

Cast	Location	Coordinates	Depth (m)	Date	Cast Start Time (UTC+10)	Cast End Time (UTC+10)
TAN01	TAN01	650104 6037734	21	20/03/2018	9:40	9:47
TAN02	TAN02	649686 6038515	19	20/03/2018	9:54	9:59
TAN03	TAN03	649335 6038910	13	20/03/2018	10:02	10:05
TAN04	TAN04	649344 6040253	15	20/03/2018	10:26	10:31
TAN05	TAN05	649615 6040877	11	20/03/2018	10:38	10:43
TAN06	TAN06	650286 6041012	14	20/03/2018	10:48	10:51
TAN07	TAN07	649720 6042047	8	20/03/2018	11:01	11:04
TAN08	TAN08	649156 6042432	8	20/03/2018	11:10	11:13
TAN09	TAN09	649681 6043155	9	20/03/2018	11:23	11:26
TAN10	TAN10	650095 6042540	10	20/03/2018	11:31	11:34
TAN01b	TAN01	650104 6037734	21	20/03/2018	17:20	17:24
TAN06b	TAN06	650286 6041012	14	20/03/2018	17:09	17:12
TAN09b	TAN09	649681 6043155	8	20/03/2018	16:59	17:01

3.2.2 Winter Sampling

The summer round of CTD profiling was conducted on 2-4 October 2018. Due to time constraints, not all locations were profiled in Talbingo Reservoir. Details of completed casts are outlined in Table 3-4 and Table 3-5.

Table 3-4 Talbingo Reservoir CTD Profile Summary - Winter

Cast	Location	Coordinates	Depth (m)	Date	Cast Start Time (UTC+10)	Cast End Time (UTC+10)
2	TAL20	622600 6040832	37	2/10/2018	15:31	15:35
3	TAL19	623113 6041797	31	2/10/2018	15:42	15:45
4	TAL18	622741 6041725	32	2/10/2018	15:50	15:54
5	TAL17	622360 6042530	43	2/10/2018	15:58	16:03
6	TAL16	621343 6042725	54	2/10/2018	16:07	16:13
7	TAL15	620056 6044027	34	2/10/2018	16:19	16:23
8	TAL14	620758 6043961	63	2/10/2018	16:28	16:35
9	TAL10	619977 6048126	87	2/10/2018	16:45	16:55
10	TAL06	619706 6052838	107	2/10/2018	17:02	17:15
11	TAL01	617775 6056539	140	2/10/2018	17:21	17:38
12	TAL20	622600 6040832	37	3/10/2018	10:59	11:03

Cast	Location	Coordinates	Depth (m)	Date	Cast Start Time (UTC+10)	Cast End Time (UTC+10)
13	TAL19	623113 6041797	32	3/10/2018	11:12	11:16
14	TAL18	622741 6041725	33	3/10/2018	11:21	11:25
15	TAL17	622360 6042530	45	3/10/2018	11:31	11:36
16	TAL15	620056 6044027	35	3/10/2018	13:04	13:08
17	TAL14	620758 6043961	52	3/10/2018	13:12	13:18
18	TAL01	617775 6056539	140	3/10/2018	15:45	16:02

Table 3-5 Tantangara Reservoir CTD Profile Summary - Winter

Cast	Location	Coordinates	Depth (m)	Date	Cast Start Time (UTC+10)	Cast End Time (UTC+10)
1	TAN10	650095 6042540	16	4/10/2018	10:45	10:47
2	TAN09	649681 6043155	15	4/10/2018	10:53	10:55
3	TAN08	649156 6042432	14	4/10/2018	11:01	11:03
4	TAN07	649720 6042047	13	4/10/2018	11:08	11:10
5	TAN06	650286 6041012	20	4/10/2018	11:16	11:19
6	TAN05	649615 6040877	16	4/10/2018	11:23	11:25
7	TAN04	649344 6040253	20	4/10/2018	11:29	11:32
8	TAN03	649335 6038910	19	4/10/2018	11:38	11:41
9	TAN02	649686 6038515	25	4/10/2018	11:45	11:49
10	TAN01	650104 6037734	27	4/10/2018	11:53	11:57

3.3 Profiling Methodology

In preparation for the first profile of the day, the listed procedure was followed:

1. Profiler details were entered onto daily log sheet.
2. The mooring/instrumentation apparatus was checked for secure fastening.
The clear Tygon tubing connecting the conductivity and DO sensors to the 5P pump was removed.
3. The conductivity and DO cells were flushed with a 0.1% Triton solution using the supplied syringe/hose. The solution was drawn over and back through the DO/conductivity sensors several times.

At each monitoring location the listed procedure was followed:

1. On arrival at the site, the vessel skipper signaled the arrival at the monitoring site and confirmed orientation of vessel was suitable (taking into account sun angle and anticipated vessel windage, reservoir conditions and/or currents).
2. All equipment was checked as securely attached to the frame and frame to deployment line, and the depth recorded using the depth sounder.
3. Sensors were prepared for sampling: removed PAR sensor cap, EcoFLNTURT sensor cover, the pH sensor buffer bottle and the Tygon tubing joining the pump outlet and the conductivity cell inlet.
4. The CTD was switched on, with operator saying clearly 'Seabird ON', and then seconded by the skipper.
5. CTD was placed into the water and held 1 m below the surface for 1 minute to stabilise.
6. After 1 minute the CTD operation was confirmed by observing that the EcoFLNTURT blue flashing light was illuminated.

7. The time was recorded on the Daily Log Sheet and the frame assembly was lowered down through the water column at a maximum rate of 0.25 m/sec.
8. When the assembly touched the bottom, the CTD was lifted approximately 1 metre above the bed and held for approximately ten seconds.
9. The sampling apparatus was then retrieved using the capstan winch.
10. The CTD was carefully lifted on board, set down and secured.
11. The CTD magnetic switch was turned off and operator stated 'Seabird Off', then seconded by the skipper.
12. When a long transit was required to the next site, the 3 sensor caps were replaced and the syringe/hose was refilled with DI water and placed over conductivity cell inlet to fill to above the DO sensor plenum. Syringe handle was fitted and looped into frame.
13. When a long transit to the next site was required, all rope, cable and hose was coiled or hung neatly to avoid trip hazards before making way to the next site.

At end of day, all data files were uploaded from the CTD and backed up to a USB drive. As soon as possible the files were uploaded to the project directory on Cardno's servers.

4 Water Sampling

The scope of the water sampling component originally included two rounds of sampling during the nominal summer and winter field campaigns conducted alongside CTD profiling as described in Section 3. In November 2018 an additional campaign including monthly sampling at eight locations (four in each reservoir) of near surface samples was commenced to better capture temporal variability of water quality.

4.1 Sampling Equipment

Water sampling was conducted using Niskin 10 L external spring, Teflon coated sample bottles. Near surface and phytoplankton samples were collected using a 12 V submersible pump and food-grade PVC tubing.

All sample containers were prepared by the analysis laboratory with appropriate preservations.

4.2 Analysis Suite

The suite of analysed parameters selected for this sampling campaign is listed in Table 4-1 and Table 4-2 for the summer and winter rounds respectively. Table 4-3 outlines the suite of analysed parameters for the additional sampling program. Parameters are listed along with laboratory analysis methods and Limits of Reporting (LOR).

Table 4-1 Water Laboratory Analysis Suite - Summer

Parameter	LOR	Method Reference	Notes
Total Suspended Solids	1 mg/L	LTM-INO-4070	
Particle Size Distribution	-	Laser diffraction	Not for mid-level samples
Total Dissolved Solids	10 mg/L	4110	
Electrical Conductivity	1 µS/cm	LTM-INO-4030	
pH	0.1	LTM-GEN-7090	
Chlorophyll-a	5 µg/L	LTM-INO-4340	Not near-bed samples
Total Organic Carbon	5 mg/L	APHA 5310B	
Dissolved Organic Carbon	5 mg/L	APHA 5310B	
Reactive Silica (as SiO ₂)	3 mg/L	APHA 4500	
Anion Suite Chloride	1 mg/L	LTM-INO-4090	

Parameter	LOR	Method Reference	Notes
Sulphate (as SO ₄)	5 mg/L	LTM-INO-4110	
Fluoride	0.5 mg/L	APHA-F-C	
Bicarbonate Alkalinity (as CaCO ₃)	10 mg/L	APHA 2320	
Carbonate Alkalinity (as CaCO ₃)	20 mg/L	APHA 2320	
Hydroxide Alkalinity (as CaCO ₃)	10 mg/L	APHA 2320	
Total Alkalinity (as CaCO ₃)	20 mg/L	APHA 2320	
Cation Suite			
Alkali Metals (Ca, Mg, K, Na)	0.5 mg/L	USEPA 6010	
Hardness mg equivalent CaCO ₃ /L	5 mg/L	APHA 2340B	
Nutrients			
Total Nitrogen (as N)	0.2 mg/L	APHA 4500	
Total Kjeldahl Nitrogen (as N)	0.2 mg/L	LTM-INO-4310	
Nitrate & Nitrite (as N)	0.05 mg/L	APHA 4500	
Nitrate (as N)	0.02 mg/L	APHA 4500	
Nitrite (as N)	0.02 mg/L	APHA 4500	
Phosphate total (as P)	0.05 mg/L	APHA 4500	
Phosphorus reactive (as P)	0.05 mg/L	APHA 4500	
Ammonia (as N)	0.01 mg/L	APHA 4500	
Ammonium Ion (as N)	0.01 mg/L	APHA 4500	
Heavy Metals (Total and Filtered for all)		LTM-MET-3040	
Al, B, Fe	0.05 mg/L		
Ba	0.02 mg/L		
Mn, Mo, Ag, V, Zn	0.05 mg/L		
As, Be, Ch, Co, Cu, Pb, Ni, Se	0.001 mg/L		
Cd	0.0002 mg/L		
Hg	0.0001 mg/L	USEPA 7470/1	

Table 4-2 Water Laboratory Analysis Suite - Winter

Parameter	LOR	Method Reference	Notes
Total Suspended Solids	1 mg/L	APHA 2540 D	
Total Dissolved Solids	1 mg/L	Calculation	
Electrical Conductivity	1 µS/cm	APHA 2510 B	
pH	0.01	APHA 4500-H+B	
Turbidity	0.1 NTU	APHA 2130 B	
Chlorophyll-a	1 mg/m ³ ¹	APHA 10200 H (modified)	Not near-bed samples
Total Organic Carbon	1 mg/L	APHA 5310 B	
Dissolved Organic Carbon	1 mg/L	APHA 5310 B	
Anion Suite			
Chloride	1 mg/L	APHA 4500 CI – G	
Sulphate (as SO ₄)	1 mg/L	APHA 4500-SO ₄	
Bicarbonate Alkalinity (as CaCO ₃)	1 mg/L	APHA 2320 B	

Parameter	LOR	Method Reference	Notes
Carbonate Alkalinity (as CaCO ₃)	1 mg/L	APHA 2320 B	
Hydroxide Alkalinity (as CaCO ₃)	1 mg/L	APHA 2320 B	
Total Alkalinity (as CaCO ₃)	1 mg/L	APHA 2320 B	
Cation Suite	Alkali Metals (Ca, Mg, K, Na)	1 mg/L	APHA 3120 and 3125; USEPA SW 846 - 6010 and 6020
	Hardness mg equivalent CaCO ₃ /L	1 mg/L	APHA 2340 B
Nutrients	Total Nitrogen (as N)	0.05 mg/L	APHA 4500-P J
	Total Kjeldahl Nitrogen (as N)	0.05 mg/L	APHA 4500-P J & 4500-NO ₃ - I
	Nitrate & Nitrite (as N)	0.002 mg/L	APHA 4500-NO ₃ I
	Nitrate (as N)	0.002 mg/L	APHA 4500-NO ₃ I
	Nitrite (as N)	0.002 mg/L	APHA 4500-NO ₂ B
	Phosphorus total (as P)	0.01 mg/L	APHA 4500-P J
	Phosphorus reactive (as P)	0.002 mg/L	APHA 4500-P E
	Ammonia (as N)	0.002 mg/L	APHA 4500-NH ₃ H
Heavy Metals (Total and Filtered for all)			USEPA 6020
	Al, Se, V	0.01 mg/L	
	B, Fe	0.05 mg/L	
	As, Ba, Be, Ch, Co, Cu, Mn, Pb, Ni, Mb, Ag	0.001 mg/L	
	Cd	0.0001 mg/L	
	Hg	0.0001 mg/L	APHA 3112- Hg B

¹ – LOR is dependent on volume of sample able to be filtered. The actual LOR achieved is reported with the laboratory results.

Table 4-3 Water Laboratory Analysis Suite – Additional Program

Parameter	LOR	Method Reference	Notes
Total Suspended Solids	1 mg/L	APHA 2540 D	
pH	0.01	APHA 4500-H+B	
Turbidity	0.1 NTU	APHA 2130 B	
Nutrients	Total Nitrogen (as N)	0.05 mg/L	APHA 4500-P J
	Total Kjeldahl Nitrogen (as N)	0.05 mg/L	APHA 4500-P J & 4500-NO ₃ - I
	Nitrate & Nitrite (as N)	0.002 mg/L	APHA 4500-NO ₃ I
	Nitrate (as N)	0.002 mg/L	APHA 4500-NO ₃ I
	Nitrite (as N)	0.002 mg/L	APHA 4500-NO ₂ B
	Phosphorus total (as P)	0.01 mg/L	APHA 4500-P J
	Phosphorus reactive (as P)	0.002 mg/L	APHA 4500-P E
	Ammonia (as N)	0.002 mg/L	APHA 4500-NH ₃ H
Heavy Metals (Total and Filtered for all)			USEPA 6020
	Al, Se, V	0.01 mg/L	
	B, Fe	0.05 mg/L	

Parameter	LOR	Method Reference	Notes
As, Ba, Be, Ch, Co, Cu, Mn, Pb, Ni, Mb, Ag	0.001 mg/L		
Cd	0.0001 mg/L		
Hg	0.0001 mg/L	APHA 3112- Hg B	

4.3 Locations

Water sample locations are a subset of the CTD profile locations. Details of collected water samples in Talbingo Reservoir are outlined in Table 4-4 and Table 4-5 for the summer round and winter round of sampling respectively. Details of collected water samples in Tantangara Reservoir are outlined in Table 4-6 and Table 4-7 for the summer round and winter round of sampling respectively. Table 4-8 outlines the samples collected during the additional program of sampling. Locations are presented in Appendix C, Figure 3 and Figure 4.

Table 4-4 Talbingo Reservoir WQ Sample Summary - Summer

Sample ID	Coordinates	Date/Time of Sampling (UTC+10)	Depth of Sample (m)
TAL01-B	617775 6056539	21/03/2018 14:35	130
TAL01-M		21/03/2018 14:45	16
TAL01-S		21/03/2018 14:50	2
TAL09-B	619523 6048919	21/03/2018 15:40	85
TAL09-M		21/03/2018 15:45	16
TAL09-S		21/03/2018 15:50	2
TAL15B-B	620056 6044027	21/03/2018 17:00	28
TAL15B-M		21/03/2018 17:05	16
TAL15B-S		21/03/2018 17:10	2
TAL15-M		28/03/2018 11:25	14
TAL15-S		28/03/2018 11:20	2
TAL19-M	623113 6041797	27/03/2018 9:05	14
TAL19-S		27/03/2018 9:00	2
TAL20-M	622600 6040832	27/03/2018 10:15	14
TAL20-S		27/03/2018 10:10	2

Table 4-5 Talbingo Reservoir WQ Sample Summary - Winter

Sample ID	Coordinates	Date/Time of Sampling (UTC+10)	Depth of Sample (m)
TAL01-B	617775 6056539	3/10/2018 15:26	115
TAL01-M		3/10/2018 15:09	70
TAL01-S		3/10/2018 14:51	2
TAL09-B	619523 6048919	3/10/2018 16:45	90
TAL09-M		3/10/2018 16:35	50
TAL09-S		3/10/2018 16:15	2
TAL13-B	621230 6045474	3/10/2018 13:56	65
TAL13-M		3/10/2018 13:42	35

Sample ID	Coordinates		Date/Time of Sampling (UTC+10)	Depth of Sample (m)
TAL13-S			3/10/2018 13:30	2
TAL14-B	620758	6043961	3/10/2018 12:30	57
TAL14-M			3/10/2018 12:10	30
TAL14-S			3/10/2018 11:52	2
TAL15-B	620056	6044027	3/10/2018 12:57	30
TAL15-M			3/10/2018 12:46	15
TAL15-S			3/10/2018 12:37	2
TAL18-B	622741	6041725	3/10/2018 10:44	25
TAL18-M			3/10/2018 10:30	15
TAL18-S			3/10/2018 10:10	2
TAL19-B	623113	6041797	3/10/2018 9:58	25
TAL19-M			3/10/2018 9:40	15
TAL19-S			3/10/2018 9:36	2
TAL20-B	622600	6040832	3/10/2018 9:21	30
TAL20-M			3/10/2018 9:10	15
TAL20-S			3/10/2018 9:00	2

Table 4-6 Tantangara Reservoir WQ Sample Summary - Summer

Sample ID	Coordinates		Date/Time of Sampling (UTC+10)	Depth of Sample (m)
TAN01-B	650104	6037734	20/03/2018 14:50	19
TAN01-M			20/03/2018 14:55	10
TAN01-S			20/03/2018 15:00	1
TAN04-B	649344	6040253	20/03/2018 15:20	13
TAN04-M			20/03/2018 15:25	6
TAN04-S			20/03/2018 15:30	1
TAN06-B	650286	6041012	20/03/2018 15:40	12
TAN06-M			20/03/2018 15:45	6
TAN06-S			20/03/2018 15:50	1
TAN08-B	649156	6042432	20/03/2018 16:10	12
TAN08-M			20/03/2018 16:15	6
TAN08-S			20/03/2018 16:20	1
TAN09-B	649681	6043155	20/03/2018 16:40	11
TAN09-M			20/03/2018 16:45	5
TAN09-S			20/03/2018 16:50	1

Table 4-7 Tantangara Reservoir WQ Sample Summary - Winter

Sample ID	Coordinates		Date/Time of Sampling (UTC+10)	Depth of Sample (m)
TAN01-B	650104	6037734	4/10/2018 12:52	25
TAN01-M			4/10/2018 12:40	12
TAN01-S			4/10/2018 12:21	2

TAN04-B	649344	6040253	4/10/2018 13:33	18
TAN04-M			4/10/2018 13:20	10
TAN04-S			4/10/2018 13:10	2
TAN06-B	650286	6041012	4/10/2018 15:53	18
TAN06-M			4/10/2018 15:44	10
TAN06-S			4/10/2018 15:30	2
TAN08-B	649156	6042432	4/10/2018 15:16	12
TAN08-M			4/10/2018 15:06	7
TAN08-S			4/10/2018 14:56	2
TAN09-B	649681	6043155	4/10/2018 14:20	12
TAN09-M			4/10/2018 14:08	7
TAN09-S			4/10/2018 13:48	2

Table 4-8 Additional WQ Program Sample Summary

Sample ID	Coordinates		Date/Time of Sampling (UTC+10)				
			Round 1	Round 2	Round 3	Round 4	Round 5
TAL15	620056	6044027	1/11/2018 15:52	20/11/2018 16:30	5/12/2018 13:00	16/01/2019 14:27	27/02/2019 14:49
TAL18	622741	6041725	1/11/2018 16:28	20/11/2018 16:10	5/12/2018 13:45	16/01/2019 13:56	27/02/2019 13:47
TAL21	621516	6042297	1/11/2018 16:05	20/11/2018 16:20	5/12/2018 13:31	16/01/2019 14:10	27/02/2019 14:05
TAL22	624522	6040401	1/11/2018 16:17	20/11/2018 16:00	5/12/2018 13:15	16/01/2019 11:50	27/02/2019 13:34
TAN_M01	650029	6038067	1/11/2018 13:55	21/11/2018 8:35	6/12/2018 9:24	17/01/2019 8:23	28/02/2019 8:40
TAN_M02	650229	6041165	1/11/2018 10:05	21/11/2018 8:10	6/12/2018 8:49	17/01/2019 7:53	28/02/2019 8:15
TAN_ADCP_01	649796	6040378	1/11/2018 10:30	21/11/2018 8:20	6/12/2018 9:01	17/01/2019 8:05	28/02/2019 8:23
TAN11	649886	6039137	1/11/2018 13:40	21/11/2018 8:30	6/12/2018 9:14	17/01/2019 8:14	28/02/2019 8:33

4.4 Sampling Methodology

The following methodology was used for the collection of water quality grab samples. The method design was prepared to conform to AS/NZS 5667.1:1998 and with reference to published sample collection procedures such as the Queensland Government Monitoring and Sampling Manual 2018.

1. Sample containers were labelled and stored in a clean tub ready for filling away from the sampler preparation and winch area.
2. In situ water quality measurements were collected using the CTD before collecting water samples – data was then reviewed to determine the thermocline location.
3. Vessel was oriented to allow sampling from windward side of vessel and ensuring that water flow was towards the boat to limit vessel contamination.
4. One operator handled the water sampler external mechanism, deployment line, winch, and messenger weight – taking care not to come into contact with the internal surface of the sampler bottle. The other operator put on un-powdered nitrile gloves and was the designated sample handler – taking care to only handle sample bottles.

5. The internal surfaces of the water sampler were inspected, ensuring it was clean.
6. The water sampler was cocked and lowered into the water.
7. The sampler was then pulled out of the water, allowed to fully drain. This was repeated three times.
8. The water sampler was lowered to the required depth.
9. The water sampler was then triggered by dropping the messenger weight along the deployment line, then the sampler was retrieved from the water.
10. The labelled sample containers were then filled. This was done quickly to avoid sediment particles from settling to the bottom of the water sampler. Sample containers were then recapped.

For filtered samples:

1. Sample handler put on a new set of gloves immediately prior to the commencement of filtering.
2. The new filter and syringe were removed from their packaging and filter attached to syringe.
3. The interim water sample was shaken gently to resuspend particulate matter.
4. The syringe was then filled with sample water.
5. A couple of millilitres of sample were pushed through the filter to rinse, and rinsate discarded.
6. The syringe was refilled with sample water.
7. The lid of the 'filtered' sample container was removed and the required sample volume was filtered into the sample container.
8. Sample container was then recapped.
9. A final check was completed to ensure that details on the sample containers were correct.
10. Sample container was then stored in a chilled cooler (with ice or ice bricks). Samples double bagged if using ice.
11. Sampler then thoroughly rinsed three times with high quality deionised water, allow to dry and stored in a clean location prior to reuse at further sampling sites.
12. Chain of custody form completed.

For Chlorophyll-a analysis during summer sampling, in order to meet holding time limitations additional sample filtering was conducted at the end of day using a vacuum pump filter set. Samples were filtered on 0.45 µm filter paper until the 1 L sample was filtered, or until the rate of filtering dropped to near zero. The volume of sample filtered was recorded and the filter with residue stored in double wrapped aluminium foil and kept frozen until submission to the laboratory for analysis. During winter sampling, the samples were submitted for laboratory analysis within holding times and so no additional filtering of Chlorophyll-a samples was required.

4.5 Phytoplankton Sampling Methodology

Water samples for phytoplankton were collected from three depths at each location: immediately below water surface; 1 metre below surface and; 3 metres below water surface. The listed procedure was followed for each sample.

1. The required sample was extracted (500 mL) from water body, as per standard water sampling procedure using submersible pump.
2. A small amount of water was poured out of the bottle to leave headspace.
3. An initial dose of Lugol's iodine was added with a disposable transfer pipette, 1.25 – 1.5 mL/L. The sample then resembled the colour of weak tea.
4. The sample was stored in opaque plastic tub, with lid in place and in shade. Once preserved, samples remain stable but were kept out of direct sunlight and extreme heat to prevent the Lugol's iodine decomposing.
5. Sample labels were completed and details of the samples copied to the sample submission form for each sample collected.
6. Before transport to laboratory, Lugol's staining was confirmed as still adequate and additional Lugol's iodine was added if colour had lightened.

4.6 Sample Preservation and Handling

All samples were collected in laboratory supplied sample containers with preservation solutions provided as required according to AS/NZ 5667.1:1998. All samples were kept chilled in coolers during field activities until refrigeration on arrival at accommodation at the end of day.

Samples were packed in coolers with padding to ensure protection from damage (especially for glass bottles) and were either transported directly to the laboratory in Sydney or Canberra for submission depending on field schedules for each sampling round, thus ensuring samples were kept chilled for the duration of transit.

Samples were delivered to the laboratory with sufficient time for analysis to be conducted within recommended holding times for the winter round of sampling. During the summer round of sampling some nutrient parameters exceeded the recommended holding times, namely Nitrate (as N), Nitrite (as N) and, Reactive Phosphorus (as P). For these parameters the site location and available courier/freight services did not allow options for submission and analysis within the recommended holding times according to AS/NZS 5667.1:1998 (24 hours) or the laboratory recommended holding time (48 hours). Due to the expected combination of low nutrient load and low biological activity in the samples, a holding time of seven days was deemed acceptable. Comparison of results of Nitrate & Nitrite (as N) (Holding Time 28 days) with Nitrite (as N) and Nitrate (as N) and also comparison of Total Phosphorus (as P) (Holding Time 28 days) with Reactive Phosphorus (as P) provided support for this assumption.

4.7 Corrective Actions

Laboratory results for some dissolved metals exceeded results for the corresponding total metals for some samples during the summer round of sampling (all included in report 591008-W). This anomaly was flagged by the laboratory prior to issue of results, and full metals reanalysis was conducted for these samples by the laboratory. All results were confirmed by the reanalysis. As a result, Cardno reviewed field procedures with the sampling team and identified the following factors as potentially leading to sample contamination in the field during sample handling:

- The 0.45 micron filters packed for that field trip were not the recommended syringe filters, but 0.45 micron inline flow filters more suitable for use with peristaltic pump lines.
- These filters are able to be used with syringes, but require the sampler to use two hands to hold the syringe tip in the filter intake making the procedure more awkward.
- Moderate prevailing winds during sampling caused wind waves and associated vessel motion which may have led to the sampler contaminating their gloved hands on boat surfaces during sample filtering.

While the field review did not identify a definite cause of the anomalous dissolved metals results, the potential for contamination from the boat is consistent with the metals results affected.

The following corrective actions were implemented for the winter round of water quality sampling:

- Use of correct syringe type filter units to enable easy handling
- Particular care was taken to ensure that wind and vessel motion was acceptable before conducting sampling and associated field filtering activities

An additional modification to the water sampling procedure was made for the winter round and additional program of sampling. Following the summer round of sampling the analysis suite was amended and this modified suite required sample submission within 24 hours, particularly due to the inclusion of ultra-trace nutrient analysis. As a result, sampling was carefully scheduled to ensure that either Cardno or a Snowy Hydro representative could deliver samples to the Canberra laboratory for expedited analysis within the 24 hour timeframe.

5 Sediment Sampling

5.1 Sampling Equipment

All sediment sampling was performed using a stainless steel Van Veen type grab. A Ponar type grab was also mobilised, but the Van Veen performed well in the sediment experienced in both reservoirs. The sediment grab was lowered by hand and recovered using the vessel's capstan winch.

5.2 Analysis Suite

The suite of analysed parameters selected for this sampling campaign is listed in Table 5-1. Parameters are listed along with laboratory analysis methods and Limits of Reporting (LOR).

Table 5-1 Sediment Laboratory Analysis Suite

Parameter	LOR	Method Reference
Particle Size Distribution	-	Sieve and Hydrometer
Moisture Content	1%	LTM-GEN-7080
Total Phosphorus	5 mg/kg	USEPA 6010
Total Nitrogen (as N)	10 mg/kg	APHA 4500-N
Total Kjeldahl Nitrogen (as N)	10 mg/kg	LTM-INO-4310
Nitrate & Nitrite (as N)	5 mg/kg	APHA 4500
Total Organic Carbon	0.1%	APHA 5310B
Total Inorganic Carbon	0.1%	APHA 5310B
Heavy Metals		
Fe	20 mg/kg	LTM-MET-3030
Al, Ba, B, V	10 mg/kg	
Ch, Co, Cu, Pb, Mn, Mo, Ni, Zn	5 mg/kg	
As, Be, Se	2 mg/kg	
Cd	0.4 mg/kg	
Ag	0.2 mg/kg	
Hg	0.1 mg/kg	USEPA 7470/1
Total Recoverable Hydrocarbons	20-100 mg/kg	TRH C6-C40 - LTM-ORG-2010
Benzene, Toluene, Ethylbenzene, and Xylenes (BTEX)	0.1-0.3 mg/kg	TRH C6-C40 - LTM-ORG-2010
Polycyclic Aromatic Hydrocarbons	0.5 mg/kg	LTM-ORG-2130
Organochlorine Pesticides	0.05-1 mg/kg	LTM-ORG-2220
Organophosphorus Pesticides	0.2-2 mg/kg	LTM-ORG-2200
Volatile Organic Compounds	0.5 mg/kg	LTM-ORG-2150

5.3 Locations

Details of collected sediment samples in Talbingo Reservoir during the summer round of sampling are outlined in Table 5-2. Table 5-3 outlines the samples collected during the additional round of sampling in Talbingo Reservoir. Details of collected sediment samples in Tantangara Reservoir during the summer round of sampling are outlined in Table 5-4. Locations are presented in Appendix C, Figure 5 and Figure 6.

Table 5-2 Talbingo Reservoir Sediment Sampling Summary

Sample ID	Coordinates	Sampling Date/Time (UTC+10)	Sample Depth (m)
TALN_SQ_03a1	617922 6055287	26/03/2018 14:00	138
TALN_SQ_03a2	617908 6055290	26/03/2018 14:30	137
TALN_SQ_03d1	618706 6055429	26/03/2018 15:49	15
TALN_SQ_03d2	618717 6055433	26/03/2018 16:20	16
TALN_SQ_AS1	617088 6056444	27/03/2018 16:40	16
TALN_SQ_AS2	617087 6056453	27/03/2018 17:00	16
TALS_SQ_01a1	619311 6049142	27/03/2018 14:30	53
TALS_SQ_01a2	619322 6049137	27/03/2018 15:05	32

TALS_SQ_07a1	622675	6041714	26/03/2018 9:00	38
TALS_SQ_07a2	622664	6041723	26/03/2018 9:50	37
TALS_SQ_07b1	622555	6041746	26/03/2018 10:38	33
TALS_SQ_07b2	622543	6041736	26/03/2018 10:59	28
TALS_SQ_07c1	622268	6041638	26/03/2018 11:56	8
TALS_SQ_07c2	622271	6041641	26/03/2018 12:10	9
TALS_SQ_07d1	622333	6041551	26/03/2018 11:17	20
TALS_SQ_07d2	622324	6041556	26/03/2018 11:40	19
TALS_SQ_11a1	620107	6044113	27/03/2018 10:30	39
TALS_SQ_11a2	620109	6044112	27/03/2018 10:45	37
TALS_SQ_11b1	619837	6043951	27/03/2018 11:16	28
TALS_SQ_11b2	619860	6043932	27/03/2018 11:34	29
TALS_SQ_11c1	620220	6044277	27/03/2018 11:50	25
TALS_SQ_11c2	620140	6044263	27/03/2018 12:04	34
TALS_SQ_11d1	620232	6044041	27/03/2018 12:34	27
TALS_SQ_11d2	620231	6044021	27/03/2018 12:53	25

Table 5-3 Talbingo Reservoir (Middle Bay) Sediment Sampling Summary

Sample ID	Coordinates		Sampling Date/Time (UTC+10)	Sample Depth (m)
MBSQ01	624326	6040416	16/05/2018 13:13	10
MBSQ02	624376	6040401	16/05/2018 13:02	12
MBSQ03	624436	6040424	16/05/2018 12:49	10
MBSQ04	624478	6040407	16/05/2018 12:37	9
MBSQ05	624516	6040370	16/05/2018 12:24	8
MBSQ06	624563	6040353	16/05/2018 12:12	9
MBSQ07	624600	6040349	16/05/2018 12:00	10
MBSQ08	624641	6040353	16/05/2018 11:47	10
MBSQ09	624675	6040371	16/05/2018 11:36	7
MBSQ10	624709	6040381	16/05/2018 11:25	7
MBSQ11	624731	6040384	16/05/2018 11:05	7

Table 5-4 Tantangara Reservoir Sediment Sampling Summary

Sample ID	Coordinates		Sampling Date/Time (UTC+10)	Sample Depth (m)
TANN_SQ_07a1	649419	6040129	28/03/2018 11:46	17
TANN_SQ_07a2	649442	6040120	28/03/2018 11:57	15
TANN_SQ_07b1	649754	6040113	28/03/2018 12:14	14
TANN_SQ_07b2	649757	6040114	28/03/2018 12:30	14
TANN_SQ_07c1	649986	6040006	28/03/2018 12:40	8
TANN_SQ_07c2	649969	6040003	28/03/2018 12:50	8
TANN_SQ_07d1	650102	6039890	28/03/2018 13:00	4
TANN_SQ_07d2	650096	6039895	28/03/2018 13:10	5

Sample ID	Coordinates	Sampling Date/Time (UTC+10)	Sample Depth (m)
TANN_SQ_09a1	649187 6042412	28/03/2018 9:40	7
TANN_SQ_09a2	649185 6042411	28/03/2018 10:00	6
TANN_SQ_09b1	649242 6042344	28/03/2018 10:15	16
TANN_SQ_09b2	649237 6042342	28/03/2018 10:30	16
TANN_SQ_09c1	649103 6042666	28/03/2018 10:40	15
TANN_SQ_09c2	649122 6042662	28/03/2018 10:55	15
TANN_SQ_09d1	649016 6042575	28/03/2018 11:16	6
TANN_SQ_09d2	649040 6042555	28/03/2018 11:20	6
TANS_SQ_05a1	649326 6038878	28/03/2018 14:00	13
TANS_SQ_05a2	649328 6038878	28/03/2018 14:20	13
TANS_SQ_05b1	649785 6038826	28/03/2018 14:30	17
TANS_SQ_05b2	649780 6038835	28/03/2018 14:45	18
TANS_SQ_05c1	649913 6038866	28/03/2018 14:55	9
TANS_SQ_05c2	649912 6038870	28/03/2018 15:05	10
TANS_SQ_05d1	649923 6038930	28/03/2018 15:15	6
TANS_SQ_05d2	649916 6038943	28/03/2018 15:25	6

5.4 Sediment Sampling Methodology

1. The vessel skipper located the target site to be sampled using the hand held GPS and assessed the location for exposed portions of submerged trees, and evidence of submerged trees on the vessel echo sounder.
2. Depending on the conditions, the skipper would then drop an anchor to maintain position if required.
3. The sample handling tub was rinsed and cleaned following any previous sampling.
4. Once the vessel was in position and the vessel skipper provided approval for deployment of the grab, the rope attached to the grab was loaded into the capstan arm.
5. The grab hook was armed to keep the grab in the open position.
6. The grab was raised from the resting frame/tub to a height such that it cleared the gunnel. The grab was positioned away from the boat and over the water then lowered into the water.
7. The grab was lowered through the water column at approximately 1 ms^{-1} to the seabed to keep the grab stable and facing downward.
8. Once the grab settled on the seabed, the lifting line became slack.
9. After pausing for 5 seconds, a mark was taken on the GPS, and then the grab was lifted slowly to bite into the sediment.
10. The grab was then raised by hand slowly at first, to allow complete closure of the grab and to ensure a good sample, then raised quickly on the capstan winch.
11. When the grab reached the surface it was stabilised and swung on board as soon as possible.
12. The grab was lowered into a large rectangular sample handling tub.
13. Sample handler put on new non-powdered nitrile gloves and assisted scraping sample from grab into sample handling tub while grab handler held grab arms open, ensuring no contact with the sample.
14. A sample was collected for laboratory analysis in a pre-labelled glass jar (laboratory provided) ensuring that the sample was taken from the top of the sediment (not scraping from base of tub).
15. A sample for PSD analysis was collected in a 500 g ziplock bag.
16. The remaining sample was collected for the benthic infauna sample.

17. Sample containers were stored in chilled coolers (jars and PSD bags) or opaque plastic tubs (benthic infauna).
18. All equipment was rinsed thoroughly between grab deployments in surface water over side of boat, ensuring all sediment was washed off sides of grab and sample handling tub.
19. GPS coordinates were recorded on the daily log sheet.

5.5 Benthic Infauna Sample Handling

Additional sample handling procedures were conducted in the field to preserve the samples for benthic infauna analysis. These procedures are presented in a memorandum describing the benthic infauna methodology and results.

6 Mooring Deployments

6.1 Instrumentation

Each mooring consisted of a moored surface buoy, with a range of instruments deployed either on the ballast cage secured beneath the buoy or on a line suspended below the buoy. On select sites a weather station was also mounted on a short pole on the top of the surface buoy. The instrumentation deployed is listed in Table 6-1. The depth at which each instrument's sensor was located is listed with reference either to the water surface or the bed below the mooring.

Table 6-1 Moored Instrumentation

Sensor	Parameter	Range	Sample Interval (minutes)	Sensor Depth (m)
WET Labs MicroCAT SBE37	Conductivity	0 to 70 mS/cm	15	0.6 below surface
(Top Instrument)	Temperature	-5 to 35°C	15	0.6 below surface
	Depth (pressure)	0 to 45 psia	15	0.6 below surface
WET Labs EcoFLNTUSB	Turbidity	0 to 200 NTU	15	1.0 below surface
	Chl-a	0 to 75 µg/L	15	1.0 below surface
OnSet HOBO U26	DO	0 – 20 mg/L	15	1.0 below surface
WET Labs MicroCAT SBE37	Conductivity	0 to 70 mS/cm	15	4.5 above bed
(Bottom Instrument)	Temperature	-5 to 35°C	15	4.5 above bed
	Depth (pressure)	0 to 45 psia	15	4.5 above bed
	DO	0 to 120% surface saturation	15	4.5 above bed
NexSens TS210	Temperature	0 – 45 deg C	10	Multiple depths
Lufft WS502	Air Temperature	-50 to 60 deg C	10	1.5m above water
	Relative Humidity	0 to 100% RH	10	1.5m above water
	Air Pressure	300 to 1200 hPa	10	1.5m above water
	Wind Speed	0 to 75 m/sec	10	1.5m above water
	Wind Direction	0 to 359.9 deg	10	1.5m above water
	Solar Radiation	0 to 1400 W/m2	10	1.5m above water

6.2 Locations

Three mooring locations were selected in Talbingo Reservoir and two mooring locations in Tantangara Reservoir. For both reservoirs, one location is located in deep water near the respective dam walls (M01 for both reservoirs). In Talbingo Reservoir, the other two locations are in Cascade Bay (M02) and near the confluence of the Tumut and Yarrangobilly arms (M03). For Tantangara Reservoir the second location is in the northern end of the main reservoir arm. Details of these deployment locations are provided in Table 6-2. Locations are presented in Appendix C, Figure 7 and Figure 8.

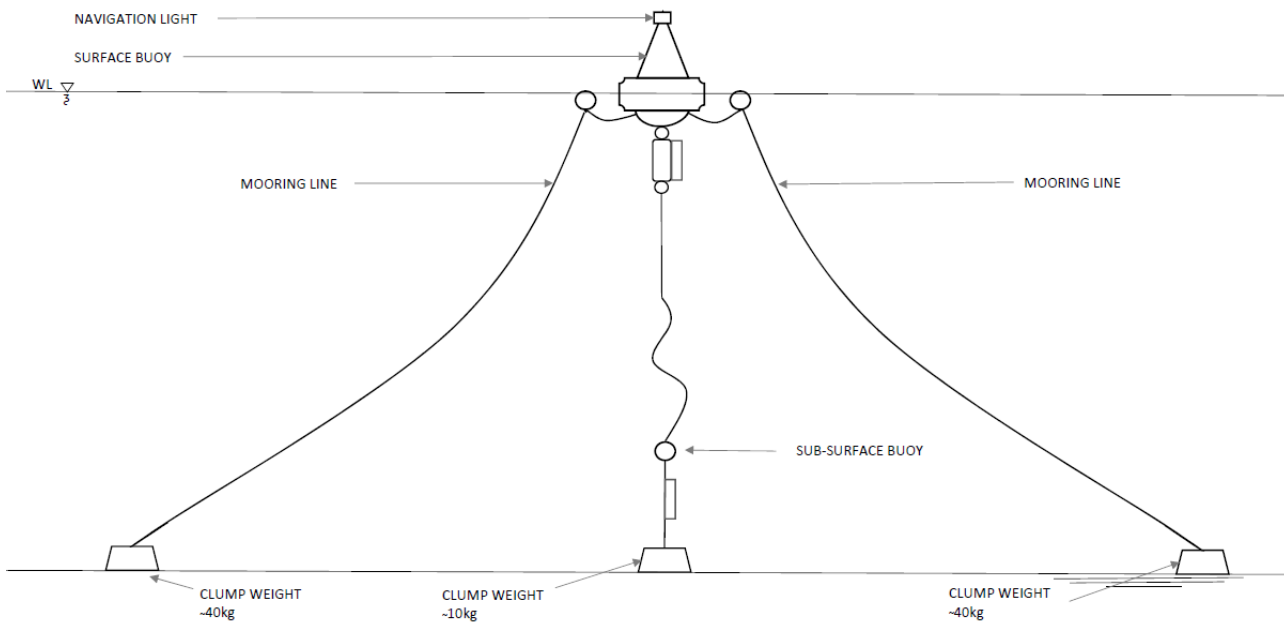
Table 6-2 Mooring Deployment Locations

Location	Coordinates	Deployment/Recovery Dates	Notes
TAL_M01	55 H 617842 6056463	17/05/2018 (CTDs only)	Lufft weather included
		6/06/2018 (Full instrumentation)	
		29/07/2019	
TAL_M02	55 H 620643 6044228	5/06/2018	Lufft weather included
		27/02/2019 (Addition of Lufft weather)	
		30/07/2019	
TAL_M03	55 H 622801 6041757	17/05/2018 (CTDs only)	
		6/06/2018 (Full instrumentation)	
		30/07/2019	
TAN_M01	55 H 650029 6038067	7/06/2018	
		1/08/2019	
TAN_M02	55 H 650229 6041165	15/05/2018 (CTDs only)	Lufft weather included
		7/06/2018 (Full instrumentation)	
		1/08/2019	

6.3 Mooring Arrangement

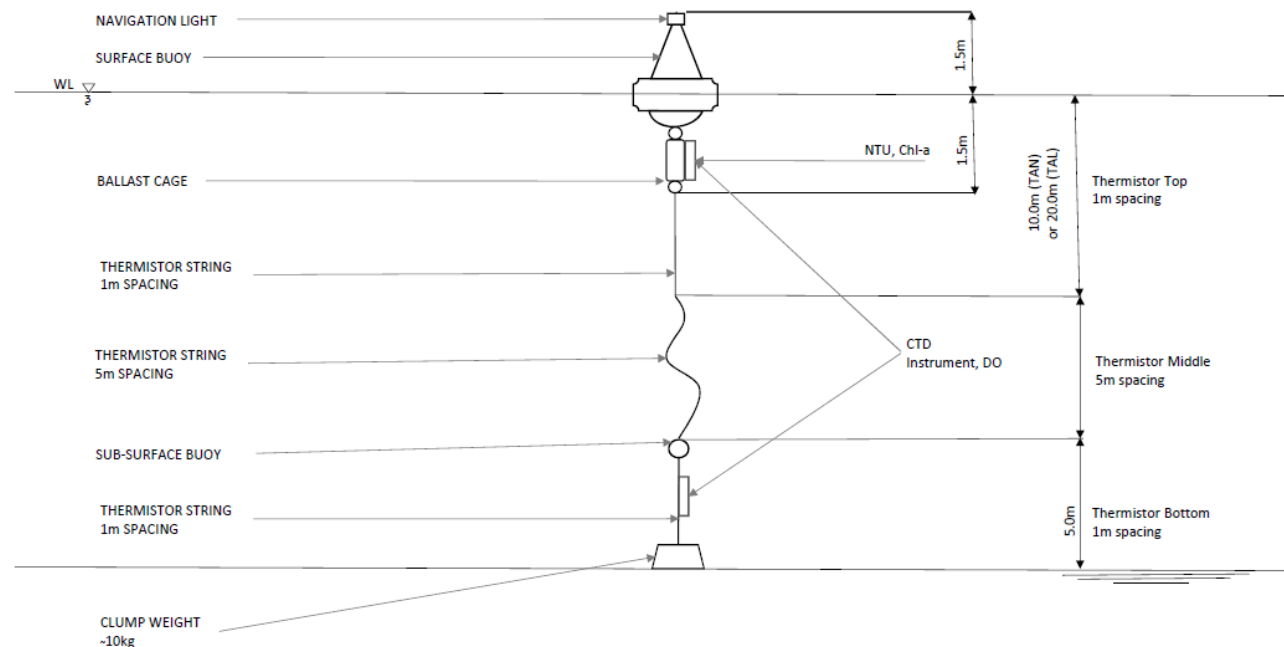
The general mooring arrangement of the moored instrumentation is shown on Figure 6-1. The instrument string was lowered beneath the buoy, with two additional mooring lines securing the surface buoy in a two-point arrangement. This provided a fixed orientation to the buoy and avoided twisting of the instrument line, and also confined the surface buoy within a limited excursion radius. The instrument line was able to be retrieved during servicing works without recovery of the mooring lines.

Figure 6-1 General mooring arrangement



The general arrangement of the instrument line is shown on Figure 6-2. The mooring lines are not shown for clarity. Secured to the instrument cage below the buoy were the CTD, DO and FLNTU instruments. The thermistor string was secured to a suspended line secured to the bed with a mooring weight. A subsurface buoy held the lower 5 metres of the thermistor string and bottom CTD instrument above the bed. Due to the depth rating of the CTD instruments (100 m depth) the bottom CTD at TAL_M01 was suspended 100 m below the surface buoy, rather than being suspended 5 m above the bed by the sub-surface float.

Figure 6-2 Instrument line arrangement



Thermistor strings consisted of 1 m spaced sections and 5 m spaced sections. The upper 10 m and 20 m for Tantangara Reservoir and Talbingo Reservoir deployments respectively consisted of 1-m spaced thermistors. The bottom 5 m consisted of 1-m spaced thermistors for all sites and this bottom section was suspended at fixed distance above the bed by a sub-surface float. The middle sections for all sites consisted of 5 m spaced thermistors. The total thermistor length at all sites was greater than the maximum expected

depth (Tantangara moorings deployed with sufficient length for approximately 60% gross storage). As a result, the lower portion of the 5-m spaced middle section under lower water levels was partially hanging alongside the suspended bottom 5 m length. As a result, care must be taken in determining the depth of the lower thermistors, and the possibility that at low water these may even be resting on the bed. The thermistors are unaffected should they have reached the bed as the sensors are contained in a moulded plastic body. In the event that sediment did attach to the sensor, some reduction in the response time of the thermistor may have been experienced, although no occurrence of sediment build-up was observed during servicing works. The thermistor arrangement is summarised in Table 6-3.

Table 6-3 Thermistor Arrangement

Location	Top (1m spacing)	Middle (5 m spacing)	Bottom (1 m spacing)	Total Sensors / Length
TAL_M01	20 sensors	20 sensors (23 m – 118 m depth)	5 sensors	45 / 125 m
TAL_M02	20 sensors	6 sensors (23 m – 48 m depth)	5 sensors	31 / 85 m
TAL_M03	20 sensors	2 sensors (23 and 28 m depth)	5 sensors	27 / 35 m
TAN_M01	10 sensors	2 sensors (13 and 18 m depth)	5 sensors	17 / 25 m
TAN_M02	10 sensors	2 sensors (13 and 18 m depth)	5 sensors	17 / 25 m

6.4 Data Return

A summary of data recovery is presented in Appendix B.

7 ADCP Deployments

7.1 Instrumentation

All ADCP deployments consisted of a Teledyne RDI Workhorse Sentinel ADCP. For the shallower locations in Tantangara Reservoir, 1200kHz instruments were deployed, while the deeper deployments in Talbingo Reservoir used 600kHz instruments.

Instrument configuration details are presented in Table 7-1.

Table 7-1 ADCP Configuration

Setup Parameter	Talbingo/Tantangara
Ensemble Interval (logging interval)	10 minutes
Pings / Ensemble	140 / 110
# Depth Cells	25
Cell Length	2.0 / 1.0 m
First Cell range (from instrument)	3.08 / 1.54 m
Last Cell range (from instrument)	51.08 / 25.54 m
Velocity Standard Deviation (per bin ensemble measurement)	0.34 / 0.3 cm/sec

7.2 Locations

Two locations were chosen for both Talbingo Reservoir and Tantangara Reservoir. In Talbingo Reservoir, TAL_ADCP_01 was deployed in the Yarrangobilly arm and TAL_ADCP_02 was deployed in the Tumut arm of the reservoir. Both locations were near the confluence of the two arms. For Tantangara Reservoir, TAN_ADCP_01 was deployed in the main arm of the reservoir, while TAN_ADCP_02 was deployed in the

lower Murrumbidgee arm of the reservoir. TAL_ADCP_02 was relocated to Plain Creek Bay in November 2018. Details of these deployments are presented in Table 7-2. Locations are presented in Appendix C, Figure 7 and Figure 8.

Table 7-2 ADCP Deployment Locations

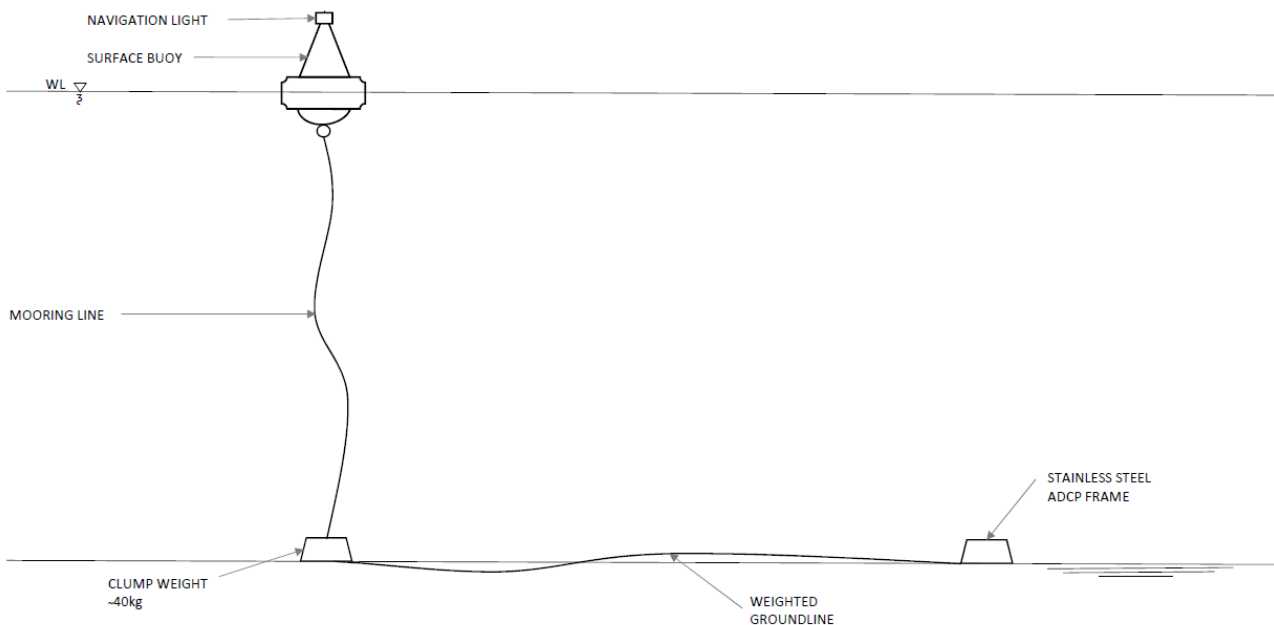
Location	Coordinates	ADCP Frequency (kHz)	Deployment/Recovery Dates	Depth at Deployment (m)
TAL_ADCP_01	55H 623261 6041754	600	18/04/2018 20/11/2018 (servicing)	26
TAL_ADCP_02	55H 622556 6041216	600	18/04/2018 20/11/2018 (relocation)	36
TAL_ADCP_PCB ¹	55H 621516 6042297	600	20/11/2018 16/04/2019	32
TAN_ADCP_01	55H 649796 6040378	1200	19/04/2018 17/04/2019	15
TAN_ADCP_02	55H 649215 6042553	1200	19/04/2018 17/04/2019	9

¹ – relocation of TAL_ADCP_02

7.3 Mooring Arrangement

Generally (with the exception of TAL_ADCP_PCB, see below) instruments were deployed fixed to bed-mounted stainless steel frames (instruments upwards facing), with a ground-line to a clump weight and surface buoy with navigational marker light. This L-shaped mooring arrangement ensured that the mooring lines did not interfere with the instruments measurement beams. The general arrangement is presented in Figure 7-1.

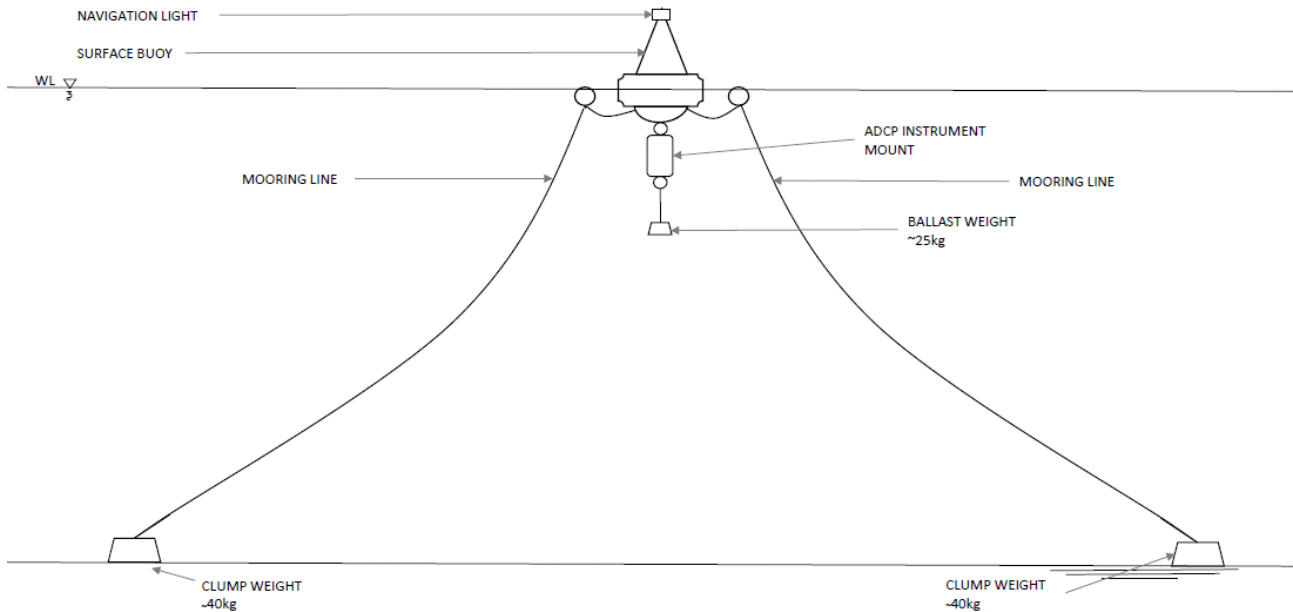
Figure 7-1 Bed Mounted ADCP Mooring arrangement



The mooring used for TAL_ADCP_PCB was a buoy-mounted downward facing arrangement rather than the bed-mounted arrangement used for all other locations. This was due to the presence of submerged trees in Plain Creek Bay precluding the use of the L-type mooring due to the risk of entanglement and the impact of the trees on the instrument operation. Note that trees can still affect the measurements in this orientation, although the upper water column is clear of interference. The ballast weight providing stability to the

instrument mount and buoy was clear of the instrument’s acoustic beams. The general mooring arrangement is presented in Figure 7-2.

Figure 7-2 Moored ADCP Mooring arrangement



7.4 Data Return

A summary of data recovery is presented in Appendix B.

8 Inflow Monitoring Deployments

8.1 Instrumentation

Instrumentation consisted of self-contained logging Onset HOBO U24-001 instruments for temperature and conductivity, and an Onset HOBO U20-001-01 Water Level logger for depth. At selected sites, a WET Labs ECO FLNTUSB was also deployed to measure turbidity and fluorescence (Chl-a).

Table 8-1 Inflow Instrumentation

Sensor	Parameter	Range	Sampling Interval (minutes)
OnSet HOBO U24-001	Conductivity	0 to 1000 uS/cm	10
OnSet HOBO U20-001-01	Temperature	0 to 36°C	10
	Depth (pressure)	0 to 9 m	10
WET Labs EcoFLNTUSB	Turbidity	0 to 200 NTU	15
	Chl-a	0 to 75 µg/L	15

8.2 Locations

Three deployment locations were selected for Talbingo Reservoir inflows, and one location for Tantangara Reservoir inflows. For Talbingo, these were the primary inflow sources, Yarrangobilly and T2 outlet tailbay and also Long Creek due to its proximity to Cascade Bay. At the Yarrangobilly River and Middle Creek sites a WET-Labs ECO FLNTUSB instrument was also deployed for turbidity (NTU) and Chl-a (fluorescence) measurements. Due to site access constraints to a suitable Yarrangobilly River in-stream location, a WET-Labs ECO FLNTUSB instrument was deployed at an in-reservoir location in the upper Yarrangobilly River arm to capture turbidity measurements during elevated flows. This instrument was relocated to the Yarrangobilly River in-stream site once access was possible during high reservoir levels.

For Tantangara Reservoir, the primary inflow of the Murrumbidgee River was selected for inflow monitoring. The deployment location selected was upstream of expected reservoir extents but not above the full reservoir level due to the distance from the reservoir and boat access requirements. Locations are presented in Appendix C, Figure 7 and Figure 8.

Table 8-2 Inflow Deployment Locations

Location	Coordinates	Deployment/Recovery Dates	Notes
Yarrangobilly River (in upper reservoir)	55 H 624862 6039986	5/09/2018 4/12/2018 (relocation)	Turbidity only
Yarrangobilly River	55 H 625321 6039359	4/12/2018 30/07/2019	Included turbidity
T2 Tailrace Outlet	55 H 623336 6034774	1/11/2018 31/07/2019	Temperature and pressure (depth) only
Long Creek	55 H 619114 6043696	17/05/2018 31/07/2019	
Middle Creek	55 H 624462 6042123	26/02/2019 30/07/2019	Included turbidity
Murrumbidgee River	55 H 644836 6041127	4/09/2018 1/08/2019	

8.3 Deployment Arrangement

Instruments were deployed approximately 20cm above bed mounted to a fixed steel stake or weighted stainless steel frame near the stream bank. Locations were selected to ensure that the instruments were in streamflow and not in still or stagnant pools. Consideration was also made to assess whether sensors would still be submerged during periods of low stream flow. The instruments were housed in PVC canisters for impact protection with ample openings for flushing to ensure that measurements were representative of streamflow. Where available, the stakes or frames were located behind large tree trunks or significant boulders for protection from impact during flood flows. Additional stakes were added as increased support where deemed necessary.

The upper reservoir Yarrangobilly River instrument was deployed immediately below a 30cm plastic surface float secured with a mooring line and clump weight. The T2 instrument was mounted to a weighted stainless steel frame approximately 15cm above the bed. The frame was connected to an L-mooring, similar to the arrangement used for the ADCP deployments and described in Section 7. Sufficient weight was used for the frame and clump weight to ensure that the mooring hardware did not move during high flows from T2 operations.

APPENDIX

A

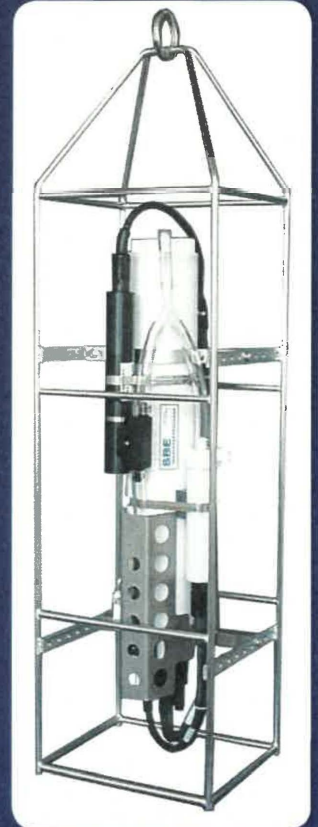
INSTRUMENT SPECIFICATIONS

SBE 19plus V2 SeaCAT Profiler CTD

The SBE 19plus V2 SeaCAT measures conductivity, temperature, and pressure at 4 scans/sec (4 Hz) and provides high accuracy and resolution, reliability, and ease-of-use for a wide range of research, monitoring, and engineering applications. Pump-controlled, T-C ducted flow minimizes salinity spiking caused by ship heave and allows for slow descent rates without slowing sensor responses, improving dynamic accuracy and resolving small scale structure in the water column. The 19plus V2 supports numerous auxiliary sensors (dissolved oxygen, pH, turbidity, fluorescence, oil, PAR, nitrates, altimeter, etc.) with six A/D channels and one RS-232 data channel. Data is recorded in memory and can also be output in real-time in engineering units or raw HEX. Nine alkaline D-cells provide power for up to 60 hours of profiling.

The 19plus V2 is commonly used autonomously, recording data internally. It can also provide real-time acquisition and display over short cables via the RS-232 interface; a load-bearing cable for hand-hauled, real-time profiling is available. External power and communication over 10,000 m of single-core, armored cable can be provided with the SBE 36 Deck Unit and PDIM. The 19plus V2 is easily integrated with a Sea-Bird Water Sampler; both real-time and autonomous auto-fire operations are possible.

In moored mode, the 19plus V2 records data at user-programmable intervals. This is easily configured with setup commands and by removing the profiling T-C Duct and installing optional anti-foulant devices.



Shown with optional cage,
SBE 5P pump, &
SBE 43 DO sensor

Features

- Conductivity, Temperature, Pressure, and up to seven auxiliary sensors.
- User-programmable mode: profiling at 4 Hz, or moored sampling at user-programmable intervals.
- RS-232 interface, internal memory, and internal alkaline batteries (can be powered externally).
- Pump-controlled, T-C ducted flow to minimize salinity spiking.
- Depths to 600, 7000, or 10,500 m.
- Seasoft® V2 Windows software package (setup, data upload, real-time data acquisition, and data processing).
- Next generation of the SeaCAT family, field-proven since 1987.
- Five-year limited warranty.

Components

- Unique internal-field conductivity cell permits use of T-C Duct, minimizing salinity spiking.
- Aged and pressure-protected thermistor has a long history of exceptional accuracy and stability.
- Pressure sensor with temperature compensation is available in eight strain-gauge ranges (to 7000 m) and eleven Digiquartz® ranges (to 10,500 m). *Note: Sampling rate 2 Hz when Digiquartz installed.*
- Pump runs continuously (profiling mode), providing correlation of CTD and plumbed auxiliary sensor measurements.

Options

- Plastic (600 m) or titanium (7000 or 10,500 m) housing; XSG/AG or wet-pluggable MCBH connectors.
- SBE 5M pump for pumped conductivity; or SBE 5P or 5T pump for pumped conductivity and auxiliary sensor(s).
- Sea-Bird Scientific auxiliary sensors — dissolved oxygen, pH, fluorescence, oil, radiance (PAR), light transmission, turbidity, nitrates (profiling only), etc.
- Auxiliary sensors from other manufacturers.
- Stainless steel protection cage.
- Rechargeable Nickel Metal Hydride (NiMH) batteries and charger.
- Moored mode conversion kit with anti-foulant device fittings.
- Load-bearing underwater cable for hand-hauled, real-time profiling.
- SBE 36 CTD Deck Unit & PDIM or SBE 33 Deck Unit & Sea-Bird water sampler (real-time operation on single-core armored cable to 10,000 m).
- Plastic shipping case.

Measurement Range

Conductivity	0 to 9 S/m
Temperature	-5 to +35 °C
Pressure	Strain-gauge 0 to 20/100/350/600/1000/2000/3500/7000 m; Quartz 20/60/130/200/270/680/1400/2000/4200/7000/10,500 m

Initial Accuracy

Conductivity	± 0.0005 S/m
Temperature	± 0.005 °C
Pressure	Strain-gauge ± 0.1% of full scale range; Quartz ± 0.02% of full scale range

Typical Stability

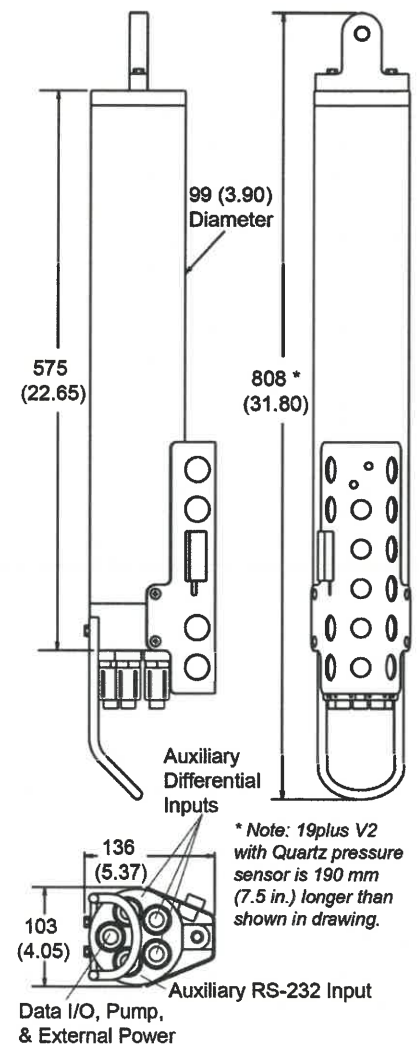
Conductivity	0.0003 S/m per month
Temperature	0.0002 °C per month
Pressure	Strain-gauge ± 0.1% of full scale range per year; Quartz ± 0.02% of full scale range per year

Resolution

Conductivity	0.00005 S/m typical
Temperature	0.0001 °C
Pressure	Strain-gauge 0.002% of full scale range; Quartz 0.0025% of full scale range

Sampling Speed	Profiling: 4 Hz (strain-gauge pressure) or 2 Hz (Quartz pressure)
Memory & Data Storage	64 Mbyte non-volatile FLASH Bytes/sample: 6 T&C; 5 pressure; 2 each external voltage; 4 date & time (RS-232 sensor is sensor dependent)
Power Supply & Consumption	9 alkaline D-cell batteries, 60 hours CTD profiling (see manual)
Optional External Power	9 - 28 VDC; consult factory for required current
Auxiliary Sensors	Power out up to 500 mA at 10.5 - 11 VDC; Voltage sensor A/D resolution 14 bits & input range 0-5 VDC
Housing, Depth Rating, & Weight (add 0.3 to 0.7 kg [in air] for pump, depending on model)	Acetal Copolymer Plastic, 600 m, in air 7.3 kg, in water 2.3 kg 3AL-2.5V Titanium, 7000 m, in air 13.7 kg, in water 8.6 kg 6AL-4V Titanium, 10,500 m
Optional Cage (weight in air)	(strain-gauge pressure version) 1016 x 241 x 279 mm, 6.3 kg

Dimensions in millimeters (inches)



Specifications subject to change without notice. ©2014 Sea-Bird Scientific. All rights reserved. Rev. June 2016

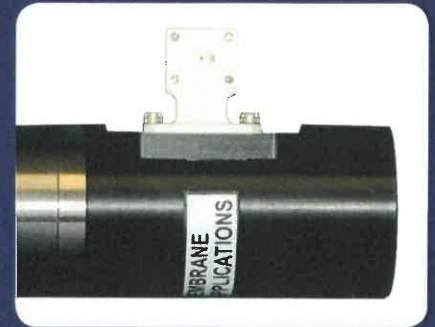


Sea-Bird Electronics
+1 425-643-9866
sales@seabird.com
www.seabird.com

SBE 43 Dissolved Oxygen Sensor

The SBE 43 is an individually calibrated, high-accuracy oxygen sensor to assist in critical hypoxia and ocean stoichiometric oxygen chemistry research on a variety of profiling and moored platforms. Careful choices of materials, geometry, and sensor chemistry are combined with superior electronics and calibration methodology to yield significant gains in performance.

The SBE 43 is designed for use in a CTD's pumped flow path, providing optimal correlation with CTD measurements. Elapsed time between the CTD and associated oxygen measurement is easily quantified, and corrected for, in post-processing. The black plenum and plumbing's black tubing blocks light, reducing in-situ algal growth. Plumbing isolates the SBE 43 from continuous exposure to the external environment, allowing trapped water to go anoxic and minimizing electrolyte consumption between samples for moored deployments.



Features

- Voltage or frequency output.
- Fully and individually calibrated; calibration drift rates of less than 0.5% over 1000 hours of operation (*on time*).
- For use in CTD pumped flow path, optimizing correlation with CTD measurements.
- Oxygen measurement dramatically improved because of improved temperature response.
- Signal resolution increased by on-board temperature compensation.
- Continuous polarization eliminates stabilization wait-time after power-up.
- Hysteresis largely eliminated in upper ocean (1000 m) due to improved temperature response. Hysteresis at greater depths predictable and correctable in post-processing.
- No degradation of signal or calibration when used for profiling in hydrogen sulfide environments.
- 600 or 7000 m housing.
- Five-year limited warranty (during warranty period, one sensor re-charge [electrolyte refill, membrane replacement, recalibration] performed free of charge).

Configuration Options

- SBE 43 voltage output sensor can be integrated with any Sea-Bird CTD that accepts 0-5 volt auxiliary sensor input. It is available with 600 m plastic or 7000 m titanium housing; XSG or wet-pluggable MCBH connector; 0.5-mil membrane (fast response, typically for profiling applications) or 1-mil membrane (slower response but more rugged for enhanced long-term stability, typically for moored applications).
- SBE 43F frequency output sensor can be integrated with SBE 52-MP or Glider Payload CTD, or used for OEM applications (requires OEM circuit board); it is available with 600 m plastic or 7000 m titanium housing. Another 43F version is used as an integral part in SBE 37-SIP-IDO MicroCATs.

Performance

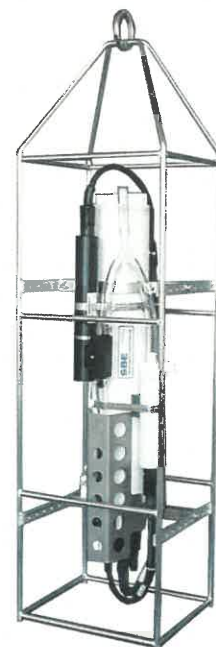
Measurement Range	120% of surface saturation in all natural waters (fresh and salt)
Initial Accuracy	± 2% of saturation
Typical Stability	0.5% per 1000 hours of deployed time (clean membrane)
Response Time Tau*	2 to 5 sec for 0.5-mil membrane, 8 to 20 sec for 1.0-mil membrane *Time to reach 63% of final value for a step change in oxygen; dependent on ambient water temperature and flow rate (see Application Note 64 for discussion)

Electrical

Input Power	6.5 - 24 VDC; 60 milliwatts (SBE 43) or 45 milliwatts (SBE 43F)
Output Signal	0 - 5 VDC (SBE 43), frequency (SBE 43F)

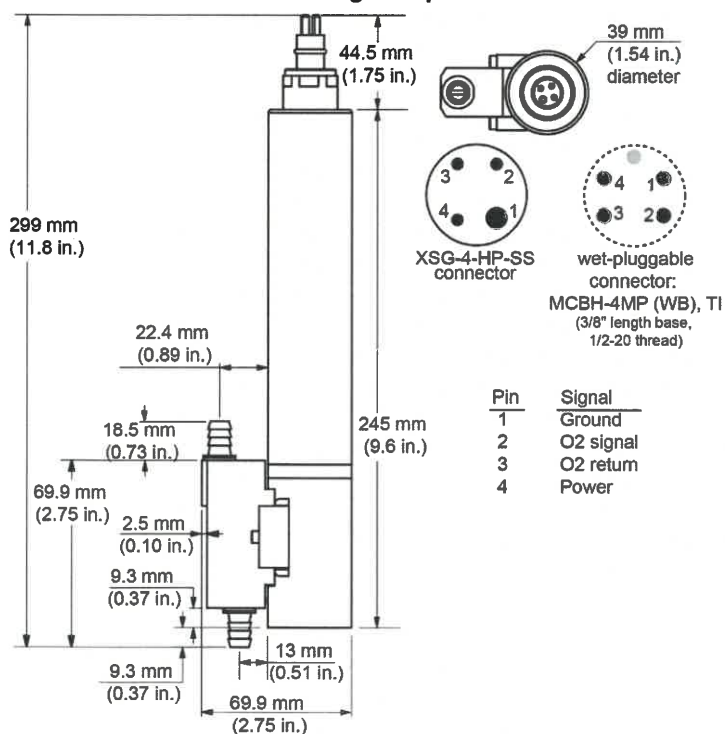
Mechanical

SBE 43 (voltage output)	600 m Plastic housing - 0.5 kg in air, 0.1 kg in water 7000 m Titanium housing - 0.7 kg in air, 0.4 kg in water
SBE 43F (frequency output)	600 m Plastic housing - 0.3 kg in air, 0.1 kg in water 7000 m Titanium housing - 0.4 kg in air, 0.2 kg in water

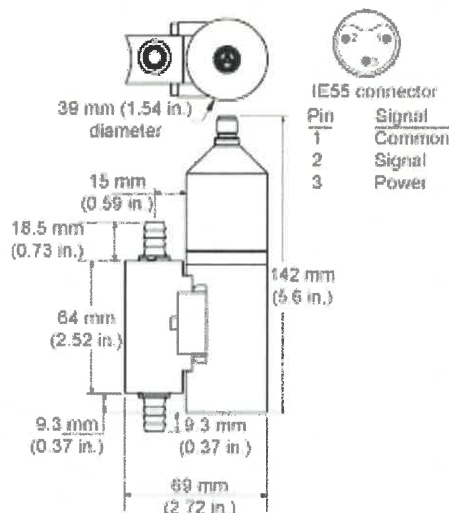


SBE 43 voltage output sensor integrated with SBE 19plus V2 CTD

SBE 43 Voltage Output Sensor



SBE 43F Frequency Output Sensor (for 52-MP, Glider Payload CTD, & OEM applications)



Specifications subject to change without notice. ©2016 Sea-Bird Scientific. All rights reserved. Rev. June 2016

SBE 18 pH Sensor

The SBE 18 pH Sensor uses a pressure-balanced glass-electrode, Ag/AgCl-reference pH probe to provide *in-situ* measurements at depths to 1200 m. The replaceable pH probe is permanently sealed and is supplied with a soaker bottle attachment that prevents the reference electrode from drying out during storage. The sensor is a modular, self-contained package that is easy to install, service, and calibrate.

The SBE 18 is intended for use as an add-on auxiliary sensor for profiling CTDs (SBE 9plus; SBE 19, 19plus, and 19plus V2 SeaCAT; and SBE 25 and 25plus Sealogger). Power / signal interface cables and mounting hardware are available separately.



Deploy with pH probe
in vertical orientation,
as shown

Features

- Voltage output; interface circuits buffer and offset the differential glass-electrode/reference potential to produce a high-level, pH-dependant, output voltage.
- Calibrated against precision buffer solutions (4, 7, and 10 pH \pm 0.02 pH); results tabulated on a certificate furnished with each sensor.
- 1200 m housing.
- Supplied with plastic soaker bottle and KCl soaker solution.
- Seasoft® V2 Windows software package (computation of pH in engineering units).
- Five-year limited warranty.

Options

- Straight endcap for vertical mounting, or right angle endcap for horizontal mounting (for example, in an extension stand below an SBE 32 Carousel Water Sampler).
- XSG or wet-pluggable MCBH connector.

Performance

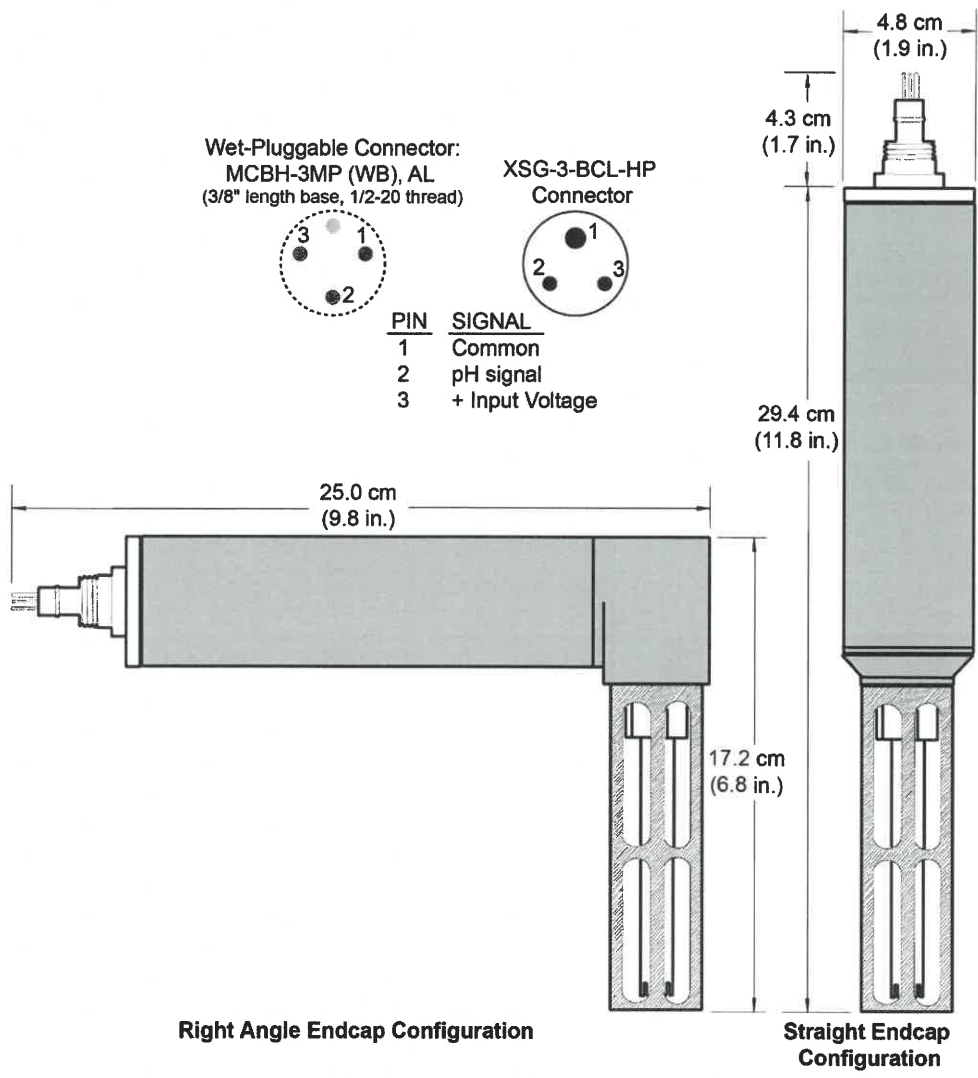
Measurement Range	0 to 14 pH
Accuracy	± 0.1 pH (stated accuracy achievable with frequent field calibrations)
Time Response	1 sec (time to reach 63% of final value for a step change in pH)

Electrical

Input Power	6 to 24 VDC, 15 mA
Output Signal	0 to +5 VDC

Mechanical

Housing, Depth rating, & Weight	Anodized aluminum (6061-T6), stainless steel 1200 m depth rating 0.7 kg in air, 0.4 kg in water
---------------------------------	-------------------------------------------------------------------------------------------------------



Note: SBE 18 must always be mounted with the pH probe in a vertical orientation, as shown in drawings at left. A right angle endcap configuration is typically required for applications where the CTD is mounted horizontally (for example, in an extension stand below an SBE 32 Carousel Water Sampler) and the SBE 18 is mounted to the CTD.

PAR Sensor

Photosynthetically Active Radiation Sensor



Applications

- Oceanographic and Freshwater Productivity Studies
- Vertical Profiling
- Laboratory Photosynthetic Physiology Studies
- Agronomic and Terrestrial Productivity Studies
- Meteorological Stations

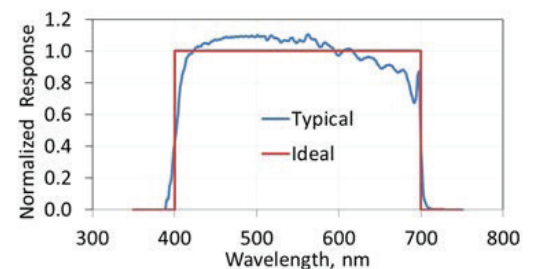
Options

- Integrated temperature and tilt sensors for serial option
- Optics: In Air | In Water
- Housing: 1000m Plastic | 7000m Titanium
- Data output: Serial ASCII | Linear Analog | Logarithmic Analog
- Easy integration with Sea-Bird Electronics CTD platforms

From limnologists and oceanographers to plant and crop physiologists, scientists trust Satlantic PAR sensors to provide superior data quality and rugged construction to withstand harsh field conditions.

Features

The ideal spectral response for a PAR sensor gives equal emphasis to all photons between 400 and 700 nm. Satlantic PAR sensors use a high quality filtered silicon photo diode to provide a near equal spectral response across the entire wavelength range of the measurement.



Tilt

- Tilt sensor reports two axis pitch and roll, to 0.1 degree resolution.
- Accuracy is approximately 1 degree

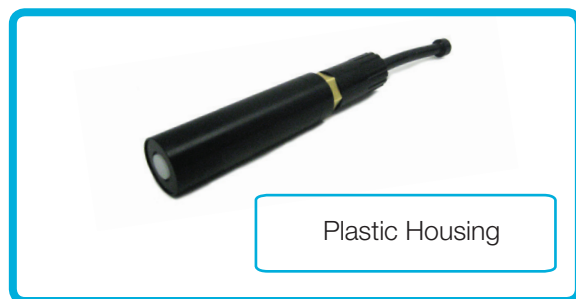
Optical

Spectrum:	400 – 700 nm
PAR Range:	0 - 5000 $\mu\text{mol photons m}^{-2} \text{s}^{-1}$
Spatial:	cosine response
Cosine error:	0° – 60° <3% 60° – 85° <10%
Collector area:	86 mm ²
Detector:	17 mm ² silicon photodiode



Electrical

Input Voltage:	6 – 28 VDC
Current Draw:	17 mA @ 12 VDC
Connector:	Subconn MCBH4M or MCBH8M (serial)
Auxiliary Sensors	Integrated temperature and tilt sensors for serial option



Telemetry

Sample Rate:	100 Hz maximum
Digital Output:	RS-232 ASCII, up to 100 Hz
Analog Signal Output:	0.125 - 4.0 V
Analog Signal Scaling:	linear or logarithmic



Physical

Weight (in air):	88g (plastic) or 182g (titanium)
Weight (in water):	39 g (plastic) or 133 g (titanium)
Depth Rating:	1000 m (plastic) or 7000 m (titanium)
Length:	139 mm (with connector) 89 mm (housing)
Diameter:	25 mm



ECO Triplet-w

Scattering/Fluorescence Combination

The ECO Triplet custom optical instrument is now available with active anti-biofouling. It features an evolutionary design that builds off the bio-wiper and faceplate available on the current ECO line. The optics of the ECO Triplet-w are arranged on a circumference on the face of the instrument. A copper faceplate covers all but the optics, and a central pivot three-armed copper and neoprene wiper clears the optics prior to sampling.



Features

- Addresses the need for multiple simultaneous scattering and fluorescence sensors for autonomous and unattended measurement platforms
- Performs a free space measurement and requires no pump. It accommodates a variety of deployment options
- Provides excellent precision, reliability, and overall performance at a fraction of the cost and size of similar instruments
- Ships with WET Labs' ECOView host software for communication and configuration
- Provides multiple measurements in a compact design, making the ECO Triplet unique among *in-situ* fluorometers

Options

Configuration options:

- Three scattering
- Two scattering, one fluorescence
- Three fluorescence
- One scattering, two fluorescence

Measurement options:

- Blue scattering
- Green scattering
- Red scattering
- Chlorophyll fluorescence
- CDOM fluorescence
- Phycocyanin fluorescence
- Phycoerythrin fluorescence
- Rhodamine fluorescence

Optical

Scattering wavelengths ¹ Sensitivity, all Range, typical	470, 532, 650, or 700 nm 0.003 m ⁻¹ 0–5 m ⁻¹
Chlorophyll EX/EM Sensitivity Range, typical	470/695 nm 0.025 µg/l 0–50 µg/l
CDOM EX/EM Sensitivity Range, typical	370/460 nm 0.28 ppb 0–375 ppb
Uranine EX/EM Sensitivity Range, typical	470/530 nm 0.15 ppb 0–300 ppb
Rhodamine EX/EM	518/595 nm
Phycocyanin EX/EM ²	630/680 nm
Phycoerythrin EX/EM ³ Sensitivity Range Linearity	518/595 nm 0.09 ppb 0–175 ppb 99% R2

Mechanical

Diameter	8.08 cm
Length	Triplet-w: 22.1 cm Triplet-wB: 33.34 cm
Weight in air	Triplet-w: 1.25 kg Triplet-wB: 2.1 kg
Weight in water*	Triplet-w: 0.29 kg Triplet-wB: 0.43 kg
Materials	Acetal co-polymer

- ECO Triplet w—Ships with wiper for long term operation
- ECO Triplet wB—Ships with wiper and internal batteries for long term autonomous operation

Electrical

Digital output resolution	12 bit
Internal data logging	Yes
Internal batteries	Triplet-w: No Triplet-wB: Yes
Connector	Triplet-w: MCBH6MP Triplet-wB: MCBH6MP & MCBH3FS
Input	7–15 VDC
Current, non-wiping	60 mA
Current, wiper active	200 mA
Current, sleep	140 µA
Data memory	67,000 samples
Sample rate	User selectable to 4 Hz
RS-232 output	19200 baud

Environmental

Operation Temperature Range	0 - 30 °C
Depth Rating	ECO-Triplet-W: 1500m ECO-Triplet-WB: 1000m

1. Backscattering specifications are given in beam cp (m⁻¹) based on the regression of the response of the instrument relative to the beam c_p measured at the coincident wavelength using an ac-s spectrophotometer. Scale factors for backscattering incorporate the target weighting function and the solid angle subtended.
2. Measurement made with BB 3 dye.
3. Measurement made with Rhodamine WT dye.

Teledyne RD Instruments

Workhorse Sentinel

Self-Contained 1200, 600, 300kHz ADCP

The Industry Standard for High Accuracy Data Collection



The self-contained SENTINEL is Teledyne RD Instruments' most popular and versatile Acoustic Doppler Current Profiler (ADCP) configuration, boasting thousands of units in operation in over 50 countries around the world.

By providing profiling ranges from 1 to 154m, the high-frequency Sentinel ADCP is ideally suited for a wide variety of applications. Thanks to Teledyne RDI's Broadband signal processing, the Sentinel also offers unbeatable precision, with unmatched low power consumption, allowing you to collect more data over an extended period.

The lightweight and adaptable Sentinel is easily deployed on buoys, boats, or mounted on the seafloor. Real-time data can be transmitted to shore via a cable link or acoustic modem, or data can be stored internally for short or long-term deployments. The Sentinel is easily upgraded to include pressure, bottom tracking, and/or directional wave measurement—for the ultimate data collection solution.



PRODUCT FEATURES

- **Versatility:** Direct reading or self contained, moored or moving, the Sentinel provides precision current profiling data when and where you need it most.
- **A solid upgrade path:** The Sentinel has been designed to grow with your needs. Easy upgrades include pressure, bottom tracking, and directional wave measurement.
- **Precision data:** Teledyne RDI's BroadBand signal processing delivers very low-noise data, resulting in unparalleled data resolution and minimal power consumption.
- **A four-beam solution:** Teledyne RDI's 4-beam design improves data reliability by providing a redundant data source in the case of a blocked or damaged beam; improves data quality by delivering an independent measure known as error velocity; and improves data accuracy by reducing variance in your data.



Workhorse Sentinel

Self-Contained 1200, 600, 300 kHz ADCP



TECHNICAL SPECIFICATIONS

Water Profiling	Depth Cell Size ¹	Typical Range ² 12m 1200kHz		Typical Range ² 50m 600kHz		Typical Range ² 110m 300kHz	
		Vertical Resolution	Range ³	Std. Dev. ⁴	Range ³	Std. Dev. ⁴	Range ³
	0.25m	11m	14.0cm/s				
	0.5m	12m	7.0cm/s	38m	14.0cm/s	see note 1	
	1m	13m	3.6cm/s	42m	7.0cm/s	83m	14.0cm/s
	2m	15m ²	1.8cm/s	46m	3.6cm/s	93m	7.0cm/s
	4m	see note 1		51m ²	1.8cm/s	103m	3.6cm/s
	8m					116m ²	1.8cm/s
Long Range Mode	2m	19m	3.4m/s				
	4m			66m	3.6cm/s		
	8m					154m	3.7cm/s
Profile Parameters	Velocity accuracy	0.3% of the water velocity relative to ADCP ±0.3cm/s		0.3% of the water velocity relative to ADCP ±0.3cm/s		0.5% of the water velocity relative to ADCP ±0.5cm/s	
	Velocity resolution	0.1cm/s		0.1cm/s		0.1cm/s	
	Velocity range:	±5m/s (default) ±20m/s (max)		±5m/s (default) ±20m/s (max)		±5m/s (default) ±20m/s (max)	
	Number of depth cells	1–255		1–255		1–255	
	Ping rate	Up to 10Hz		Up to 10Hz		Up to 10Hz	
Echo Intensity Profile	Vertical resolution	Depth cell size, user configurable					
	Dynamic range	80dB					
	Precision	±1.5dB					
Transducer and Hardware	Beam angle	20°					
	Configuration	4-beam, convex					
	Internal memory	Two PCMCIA card slots; one memory card included					
	Communications	RS-232 or RS-422; ASCII or binary output at 1200-115,200 baud					
Power	DC input	20–50VDC.					
	Number of batteries	1 internal battery pack					
	Internal battery voltage	42VDC (new) 28VDC (depleted)					
	Battery capacity @ 0°C	450 watt hrs					
Standard Sensors	Temperature (mounted on transducer)	Range -5° to 45°C, Precision ±0.4°C, Resolution 0.01°					
	Tilt	Range ±15°, Accuracy ±0.5°, Precision ±0.5°, Resolution 0.01°					
	Compass (fluxgate type, includes built-in field calibration feature)	Accuracy ±2° ⁵ , Precision ±0.5° ⁵ , Resolution 0.01°, Maximum tilt ±15°					
Environmental	Standard depth rating	200m; optional to 500m, 1000m, 6000m					
	Operating temperature	-5° to 45°C					
	Storage temperature (without batteries)	-30° to 60°C					
	Weight in air	13.0kg					
	Weight in water	4.5kg					
Software	TRDI's Windows™-based software included: WinSC —Data Acquisition System; WinADCP —Data Display and Export						
Available Options	<ul style="list-style-type: none"> • Memory: 2 PCMCIA slots, total 4GB • Pressure sensor • External battery case • High-resolution water-profiling modes • Bottom tracking or surface referencing track • AC/DC power converter, 48VDC output • Pressure cases for depths up to 6000m • Directional Wave Array • Acoustic Modem • Inductive Modem • Velocity for advanced post processing 						
Dimensions	228.0mm wide x 405.5mm long (line drawings available upon request)						

1 User's choice of depth cell size is not limited to the typical values specified.

2 Longer ranges available.

3 Profiling range based on temperature values at 5°C and 20°C, salinity = 35ppt.

4 BroadBand mode single-ping standard deviation (Std. Dev.).

5 <±1.0° is commonly achieved after calibration.

SBE 37-SMP-ODO MicroCAT CT(D)-DO

The SBE 37-SMP-ODO pumped MicroCAT is a high-accuracy conductivity and temperature (pressure optional) recorder with Serial interface (RS-232 or RS-485), internal batteries, Memory, integral Pump, and Optical Dissolved Oxygen. The MicroCAT is designed for moorings or other long-duration, fixed-site deployments.

Data is recorded in memory and can be output in real-time. Measured data and derived variables (salinity, sound velocity, specific conductivity) are output in engineering units.

Memory capacity exceeds 380,000 samples. Battery endurance varies, depending on sampling scheme and deployment temperature and pressure. Sampling every 15 minutes (10 °C, 500 dbar), the MicroCAT can be deployed for almost 9 months (25,000 samples).

Features

- Moored Conductivity, Temperature, Pressure (optional), and Optical Dissolved Oxygen, at user-programmable 10-sec to 6-hour intervals.
- Integral pump.
- RS-232 or RS-485 interface.
- Internal memory and battery pack (can be powered externally).
- Expendable anti-foulant devices, unique flow path, and pumping regimen for bio-fouling protection.
- Adaptive Pump Control for high-accuracy oxygen data.
- 350 m plastic or 7000 m titanium housing.
- Seasoft® V2 Windows software package (setup, data upload, and data processing).
- Field-proven MicroCAT family, with more than 10,000 instruments deployed.
- Five-year limited warranty.

Components

- Unique internal-field conductivity cell permits use of expendable anti-foulant devices, for long-term bio-fouling protection.
- Aged and pressure-protected thermistor has a long history of exceptional accuracy and stability.
- Optional strain-gauge pressure sensor with temperature compensation is available in eight ranges (maximum depth 7000 m).
- Oxygen sensor is field-proven, individually calibrated SBE 63 Optical Dissolved Oxygen sensor.
- Pump runs for each sample, providing improved conductivity and oxygen response, bio-fouling protection, and correlation of CTD and oxygen measurements.



Deploy in
orientation shown
(connector end down)
for proper operation

Options

- Plastic (350 m) or titanium (7000 m) housing.
- RS-232 or RS-485 interface.
- No pressure, or strain-gauge pressure sensor in one of 8 ranges.
- XSG or wet-pluggable MCBH connector.
- Wire mounting clamp and guide or brackets for mounting to a flat surface.

Measurement Range

Conductivity	0 to 7 S/m (0 to 70 mS/cm)
Temperature	-5 to 45 °C
Optional Pressure	20 / 100 / 350 / 600 / 1000 / 2000 / 3500 / 7000 (meters of deployment depth capability)
Dissolved Oxygen	120% of surface saturation in all natural waters (fresh and salt)

Initial Accuracy

Conductivity	± 0.0003 S/m (0.003 mS/cm)
Temperature	± 0.002 °C (-5 to to 35 °C); ± 0.01 °C (35 °C to 45 °C)
Optional Pressure	± 0.1% of full scale range
Dissolved Oxygen	larger of ± 3 µmol/kg (0.07 ml/L, 0.1 mg/L) or ± 2%

Typical Stability

Conductivity	0.0003 S/m (0.003 mS/cm) per month
Temperature	0.0002 °C per month
Optional Pressure	0.05% of full scale range per year
Dissolved Oxygen	sample-based drift < 1 µmol/kg/100,000 samples (20 °C)

Resolution

Conductivity	0.00001 S/m (0.0001 mS/cm)
Temperature	0.0001 °C
Optional Pressure	0.002% of full scale range
Dissolved Oxygen	0.2 µmol/kg

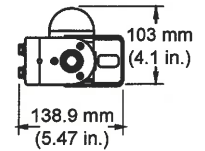
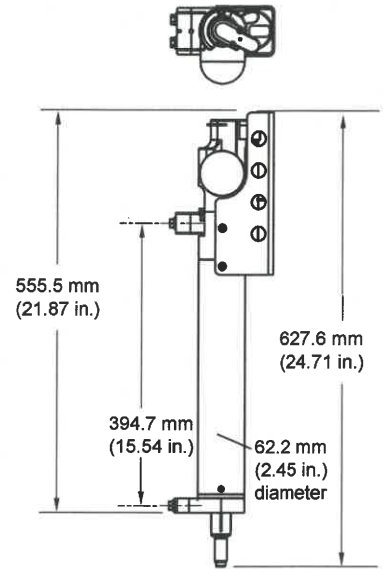
Acquisition Time 2.4 - 3.2 sec/sample (see manual)

Power Supply & Consumption 7.8 Amp-hour (nominal) battery pack (derated for calculations)
25,000 samples CTD-DO (see manual)

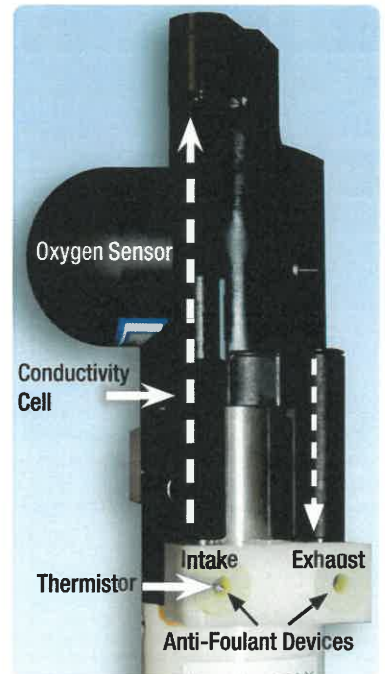
Optional External Power 0.25 Amps at 9-24 VDC

Memory Capacity 380,000 samples CTD-DO

Housing, Depth Rating, & Weight Plastic: 350 m, 3.4 kg in air, 1.5 kg in water
Titanium: 7000 m, 4.2 kg in air, 2.3 kg in water



Wire Mounting Clamp and Guide



Pumped flow through conductivity cell and oxygen sensor (conductivity cell guard removed)

Specifications subject to change without notice. ©2018 Sea-Bird Scientific. All rights reserved. Rev. July 2018



Sea-Bird Scientific
+1 425-643-9866
sales@seabird.com
www.seabird.com

TS210

THERMISTOR STRING

- Build multi-point temp strings
- ± 0.075 °C temperature accuracy
- Integral titanium thermistor
- Marine-grade cable with Kevlar core
- RS-485 Modbus RTU signal output

The NexSens **TS210** Thermistor String provides high accuracy temperature data for profiling in lakes, streams, and coastal waters. It features an integral titanium thermistor secured and epoxied in a protective housing for underwater deployments. A marine-grade cable with braided Kevlar core help ensure reliability in extreme environments.

Each sensor is accurate to ± 0.075 C for high-precision measurements. The exposed titanium thermistor makes direct contact with water, allowing readings to stabilize within 60 seconds. Temperature data is transmitted on a RS-485 Modbus RTU string bus for integration with data loggers and SCADA systems. The string is powered by 4-28 VDC for operation on a 12 or 24 VDC power supply.

TS210 strings are available standard with 1m spacing or at custom intervals to meet project requirements. Cable lengths are available up to 1,219 meters (4,000 feet) with a maximum 250 nodes. Strings terminate in a NexSens UW plug and receptacle connector, allowing additional sections or sensors to be added as required. Optional accessories include a bottom pressure sensor, cable clamps, stainless steel mooring line, and communication adapters.

TS210

THERMISTOR STRING

specifications

Sensor	Thermistor
Range	0 to 45°C (32 to 113°F)
Accuracy	±0.075°C
Resolution	0.01 C
T90 Response Time	60 seconds
Refresh Rate	2 seconds
Maximum Sensors	250
Maximum Length	1219m (4000 ft)
Communications	RS-485 Modbus RTU
Power Requirement	4 - 28 VDC
Current Draw Per Node	1.3mA active; 0.35mA sleep; 0.05mA deep sleep
Connector	8 pin, sensorBUS
Dimensions	7.62cm L x 3.3cm Dia. (3.0" L x 1.3" Dia.)



parts list

Part #	Description
TS210-1	TS210 thermistor string with 1m spacing, priced per meter
SS187-L	Custom built 3/16" vinyl coated SS mooring line, priced per meter
TS-Clamp	Mooring clamp kit for NexSens thermistor strings & 3/16" vinyl coated SS wire rope, pack of 2
UW-FL1R	UW receptacle to flying lead cable, 1m
RS485-RS232	RS-485 to RS-232 adapter



tel: **937.426.2703**
8am to 7pm EST, Monday-Friday

fax: **937.426.1125**

NexSens Technology, Inc.
2091 Exchange Court
Fairborn, OH 45324
info@nexsens.com

nexsens.com



HOBO® Dissolved Oxygen Logger

Affordable, high performance dissolved oxygen monitoring

The HOBO U26 Dissolved Oxygen Logger measures concentrations of dissolved oxygen in lakes, streams, rivers, estuaries, and coastal waters. Used by aquatic biologists, hydrologists, and other research professionals to monitor water quality, the U26 is ideal for climate change and environmental impact studies as well as ecological and oceanographic research.

The HOBO U26 combines the high-accuracy, robust performance of industry-leading RDO® Basic (Rugged Dissolved Oxygen) sensor technology with an easy-to-maintain design, all at a fraction of the cost of other monitoring options.

Supported Measurements: Dissolved Oxygen, Temperature



Key Advantages:

- Affordable, high performance DO monitoring with 0.2 mg/L accuracy
- Optical DO sensor technology for long-lasting calibration, less maintenance
- Software corrects for measurement drift from fouling; provides salinity-adjusted DO concentration and percent saturation (Salinity adjustment requires salinity meter reading or data logger file. Percent saturation requires barometric pressure data file.)
- Optic USB interface for high-speed, reliable data offload
- Easy-to-replace DO sensor cap lasts six months

Minimum System Requirements:



Software



Base Station*



Coupler¹

*HOBO Base Station or HOBO Waterproof Shuttle required.

¹Coupler included with HOBO Base Station or HOBO Waterproof Shuttle.

► For complete information and accessories, please visit: www.onsetcomp.com

Part number	U26-001
	Dissolved Oxygen
Sensor Type	Optical
Measurement Range	0 to 30 mg/L
Calibrated Range	0 to 20 mg/L; 0 to 35°C (32 to 95°F)
Accuracy	± 0.2 mg/L up to 8 mg/L; ± 0.5 mg/L from 8 to 20 mg/L
Resolution	0.02 mg/L
Response time	To 90% in less than 2 minutes
DO Sensor Cap Life	6 months (cap expires 7 months after initialization)
	Temperature
Operating Temperature and Measurement Range	-5 to 40°C (23 to 104°F), non-freezing
Temperature Accuracy	0.2°C (0.36°F)
Temperature Resolution	± 0.02°C (± 0.04°F)
Response Time	To 90% in less than 30 minutes
	Logger
Memory	21,700 sets of DO and temperature measurements
Logging Rate	1 minute to 18 hours
Time Accuracy	± 1 minute per month at 25°C (77°F)
Battery	3.6 V lithium battery; factory replaceable, life: 3 years (at 1 minute logging)
Maximum Depth	100 m (328 ft)
Dimensions	39.6 mm diameter x 266.7 mm (1.56 in diameter x 10.5 in)
CE Compliant	Yes

Contact Us

Sales (8am to 5pm ET, Monday through Friday)

- Email sales@onsetcomp.com
- Call 1-508-759-9500
- In U.S. toll free 1-800-564-4377
- Fax 1-508-759-9100

Technical Support (8am to 8pm ET, Monday through Friday)

- Contact Product Support onsetcomp.com/support/contact
- Call 1-508-759-9500
- In U.S. toll free 1-877-564-4377

Onset Computer Corporation
470 MacArthur Boulevard
Bourne, MA 02532

Lufft WS502-UMB – Temperature, Relative Humidity, Radiation, Air Pressure, Wind, Electronic Compass

From the WS product family of professional intelligent measurement transducers with digital interface for environmental applications.

Integrated design with ventilated radiation protection for measuring:

- Air temperature
- Relative humidity
- Air pressure
- Wind direction
- Wind speed
- Solar Radiation

Relative humidity is measured by means of a capacitive sensor element; a precision NTC measuring element is used to measure air temperature.

Ultrasonic sensor technology is used to take wind measurements.

Measurement output can be accessed by the following protocols:
UMB-Binary, UMB-ASCII, SDI-12, MODBUS

Lufft WS502-UMB Compact Weather Station			Order No.
WS502-UMB			8375.U10
Technical Data	Dimensions	Ø approx. 150mm, height 317mm	
	Weight	approx. 1.5 kg	
Temperature	Principle	NTC	
	Measuring range	-50 ... 60 °C	
	Accuracy	±0.2 °C (-20 °C ... +50 °C), otherwise ±0.5 °C (> -30 °C)	
Relative humidity	Principle	Capacitive	
	Measuring range	0 ... 100 % RH	
	Accuracy	±2 % RH	
Radiation	Response time (95%)	< 1s	
	Spectral range	300 to 1100 nm	
	Measuring range	1400 W/m ²	
Air pressure	Principle	MEMS capacitive	
	Measuring range	300 ... 1200 hPa	
	Accuracy	±1.5 hPa	
Wind direction	Principle	Ultrasonic	
	Measuring range	0 ... 359.9 °	
	Accuracy	±3 °	
Wind speed	Principle	Ultrasonic	
	Measuring range	0 ... 60 m/s	
	Accuracy	± 0.3 m/s or ±3 % (0 ... 35 m/s)	
General Information	Heating	20 VA at 24 VDC	
	Protection type housing	IP65	
	Interface	RS485, 2-wire, half-duplex	
	Operating power consumption	24 VDC +/- 10 %	
	Operating humidity range	0 ... 100 %	
Accessories	Operating temperature range	-50 ... 60 °C	
	Surge protection		8379.USP
	Power supply 24V/4A		8366.USV1
	UMB Interface converter ISOCON-UMB		8160.UISO
	Digital-analog-converter DACON8-UMB		8160.UDAC
	Temperature Sensor WT1		8160.WT1
	Surface Temperature Sensor WST1		8160.WST1
	Rain Sensor WTB100		8353.10



All in One

Aspirated temperature/humidity measurement

Open communication protocol:

- UMB-ASCII
- UMB-Binary
- SDI-12
- MODBUS
- Analogue outputs in combination with 8160.UDAC



HOBO® U20 Series Water Level Loggers

Accurate, affordable water level monitoring

HOBO Water Level data loggers offer high accuracy at an affordable price, with no cumbersome vent tubes or desiccants to maintain. These data loggers are ideal for recording water levels and temperatures in wells, streams, lakes, wetlands and tidal estuaries.

Supported Measurements: Water Level, Barometric Pressure, Pressure (Absolute), Temperature

Key Advantages:

- Available in 4 depth ranges
- No-vent-tube design for easy and reliable deployment
- Available in stainless steel and titanium* versions
- Durable ceramic pressure sensor for reliable performance
- Calibration certificate included



Minimum System Requirements:



Software



Base Station¹



Coupler²

Water Level Logger Kits:

Deluxe Kit includes a carrying case, two HOBO Water Level Loggers (one 13 foot for barometric pressure and one 13 foot, 30 foot, or 100 foot), HOBOWare Pro software, and a HOBO Waterproof Data Shuttle with coupler. The Starter Kit includes a HOBO Water Level Logger, HOBOWare Pro Software, and an Optic USB Base Station. Available in 13 foot, 30 foot, and 100 foot depths.



Deluxe Kit



Starter Kit

*Titanium version recommended for saltwater deployment.

¹HOBO Base Station or HOBO Waterproof Shuttle required.

²Coupler included with HOBO Base Station or HOBO Waterproof Shuttle.

► For complete information and accessories, please visit: www.onsetcomp.com

Part number	U20-001-04/ U20-001-04-Ti	U20-001-01/ U20-001-01-Ti	U20-001-02/ U20-001-02-Ti	U20-001-03/ U20-001-03-Ti
HOBO Water Level Specifications				
Range	0-4 m (0-13 ft) 0-145 kPa (0-21 psia)	0-9 m (0-30 ft) 0-207 kPa (0-30 psia)	0-30 m (0-100 ft) 0-400 kPa (0-58 psia)	0-76 m (0-250 ft) 0-850 kPa (0-123 psia)
Factory Calibrated Range (0° to 40°C; 32° to 104°F)	69 to 145 kPa (10-21 psia)	69 to 207 kPa (10-30 psia)	69 to 400 kPa (10-58 psia)	69 to 850 kPa (10-123 psia)
Water Level Accuracy (Typical Error)	± 0.3 cm (0.01 ft) (± 0.075% FS)	± 0.5 cm (0.015 ft) (± 0.05% FS)	± 1.5 cm (0.05 ft) (± 0.05% FS)	± 3.8 cm (0.125 ft) (± 0.05% FS)
Resolution	0.14 cm (0.005 ft)	0.21 cm (0.007 ft)	0.41 cm (0.013 ft)	0.87 cm (0.028 ft)
Burst Pressure	310 kPa (45 psia) 18 m (60 ft) depth		500 kPa (72.5 psia) 40.8 m (134 ft) depth	1200 kPa (174 psia) 112 m (368 ft) depth
Temperature Specifications (all models)				
Range	-20° to 50°C (-4° to 122°F)			
Accuracy	± 0.37° @ 20°C (± 0.67° @ 68°F) ± 0.44° from 0° to 50°C (± 0.79° from 32° to 122°F)			
Resolution (10 bit)	0.1° @ 20°C (0.18° @ 68°F)			
Response time	5 minutes (to 90% in water)			
Dimensions	2.46 cm diameter x 15 cm (0.97 x 5.9 in) hole in mounting bail 6.3 mm (0.25 in)			
CE compliant	Yes			

Contact Us

Sales (8am to 5pm ET, Monday through Friday)

- Email sales@onsetcomp.com
- Call 1-508-759-9500
- In U.S. toll free 1-800-564-4377
- Fax 1-508-759-9100

Technical Support (8am to 8pm ET, Monday through Friday)

- Contact Product Support onsetcomp.com/support/contact
- Call 1-508-759-9500
- In U.S. toll free 1-877-564-4377

Onset Computer Corporation
470 MacArthur Boulevard
Bourne, MA 02532



HOBO® Conductivity Loggers

Conductivity monitoring for freshwater and stable saltwater applications

HOBO Conductivity Loggers are convenient, rugged, and cost-effective data loggers for a variety of freshwater and saltwater monitoring applications.



The HOBO U24-001 model provides high-accuracy conductivity data in freshwater environments, for applications such as environmental impact monitoring, stormwater management, and water quality studies.

The HOBO U24-002-C model is for saltwater environments with relatively small changes in salinity ($\pm 5,000 \mu\text{S}/\text{cm}$) such as saltwater bays, or to detect salinity events such as upwelling, rainstorm, and discharge events. This logger can also be used to gather salinity data for salinity compensation of HOBO U26 Dissolved Oxygen logger data. **Note:** This logger is not intended for monitoring salinity levels in waters with widely changing salinities as it can have significant measurement error and drift in those environments.

Supported Measurements: Conductivity, Salinity, Temperature

Key Advantages:

- Non-contact capacitive sensor provides long life
- Easy access to sensor for cleaning and shedding air bubbles
- HOBOWare Pro software provides compensation for fouling using calibration points from the start and end of each deployment
- Optical interface provides high-speed, reliable data offload in wet environments
- Compatible with HOBO Waterproof Shuttle for easy and reliable data retrieval

Minimum System Requirements:



Software



Base Station*



Coupler¹

*HOBO Base Station or HOBO Waterproof Shuttle required.

¹Coupler included with HOBO Base Station or HOBO Waterproof Shuttle.

► For complete information and accessories, please visit: www.onsetcomp.com

Part number	U24-001 Conductivity	U24-002-C Conductivity/Salinity
Memory	18,500 temperature and conductivity measurements when using one conductivity range; 14,400 sets of measurements when using both conductivity ranges (64 kbytes)	
Conductivity Calibrated Measurement Ranges	Low Range: 0 to 1,000 $\mu\text{S/cm}$ Full Range: 0 to 10,000 $\mu\text{S/cm}$	Low Range: 100 to 10,000 $\mu\text{S/cm}$ High Range: 5,000 to 55,000 $\mu\text{S/cm}$
Conductivity Calibrated Range – Temperature Range	5° to 35°C (41° to 95°F)	
Specific Conductance Accuracy (in Calibrated Range using Conductivity Assistant and Calibration Measurements)	Low Range: 3% of reading, or 5 $\mu\text{S/cm}$ Full Range: 3% of reading, or 20 $\mu\text{S/cm}$, whichever is greater	Low Range: 3% of reading or 50 $\mu\text{S/cm}$, whichever is greater High Range: 5% of reading, in waters within a range of $\pm 3,000 \mu\text{S/cm}$; waters with greater variation can have substantially greater error
Conductivity Resolution (typical)	1 $\mu\text{S/cm}$	2 $\mu\text{S/cm}$
Conductivity Drift	Less than 3% sensor drift per year	Up to 12% sensor drift per month. Use monthly start & end-point calibration to compensate
Temperature Accuracy (in Calibrated Range)	0.1°C (0.2°F)	
Temperature Resolution	0.01°C (0.02°F)	
Response Time	1 second to 90% of change (in water)	
Measurement and Operating Range	0° to 36°C (32° to 97°F) -non-freezing	-2° to 36°C (28° to 97°F) -non-freezing
Sample rate	1 second to 18 hrs, fixed or multiple-rate sampling with up to 8 user-defined sampling intervals	
Time Accuracy	± 1 minute per month	
Battery	3.6 Volt lithium battery, life: 3 years (at 1 minute logging), typical	
Maximum Depth	70 m (225 ft)	
Dimensions	3.18 cm diameter x 16.5 cm, with 6.3 mm mounting hole (1.25 in diameter x 6.5", $\frac{1}{4}$ in hole)	
CE compliant	Yes	

Contact Us

Sales (8am to 5pm ET, Monday through Friday)

- Email sales@onsetcomp.com
- Call 1-508-759-9500
- In U.S. toll free 1-800-564-4377
- Fax 1-508-759-9100

Technical Support (8am to 8pm ET, Monday through Friday)

- Contact Product Support onsetcomp.com/support/contact
- Call 1-508-759-9500
- In U.S. toll free 1-877-564-4377

Onset Computer Corporation
470 MacArthur Boulevard
Bourne, MA 02532

APPENDIX

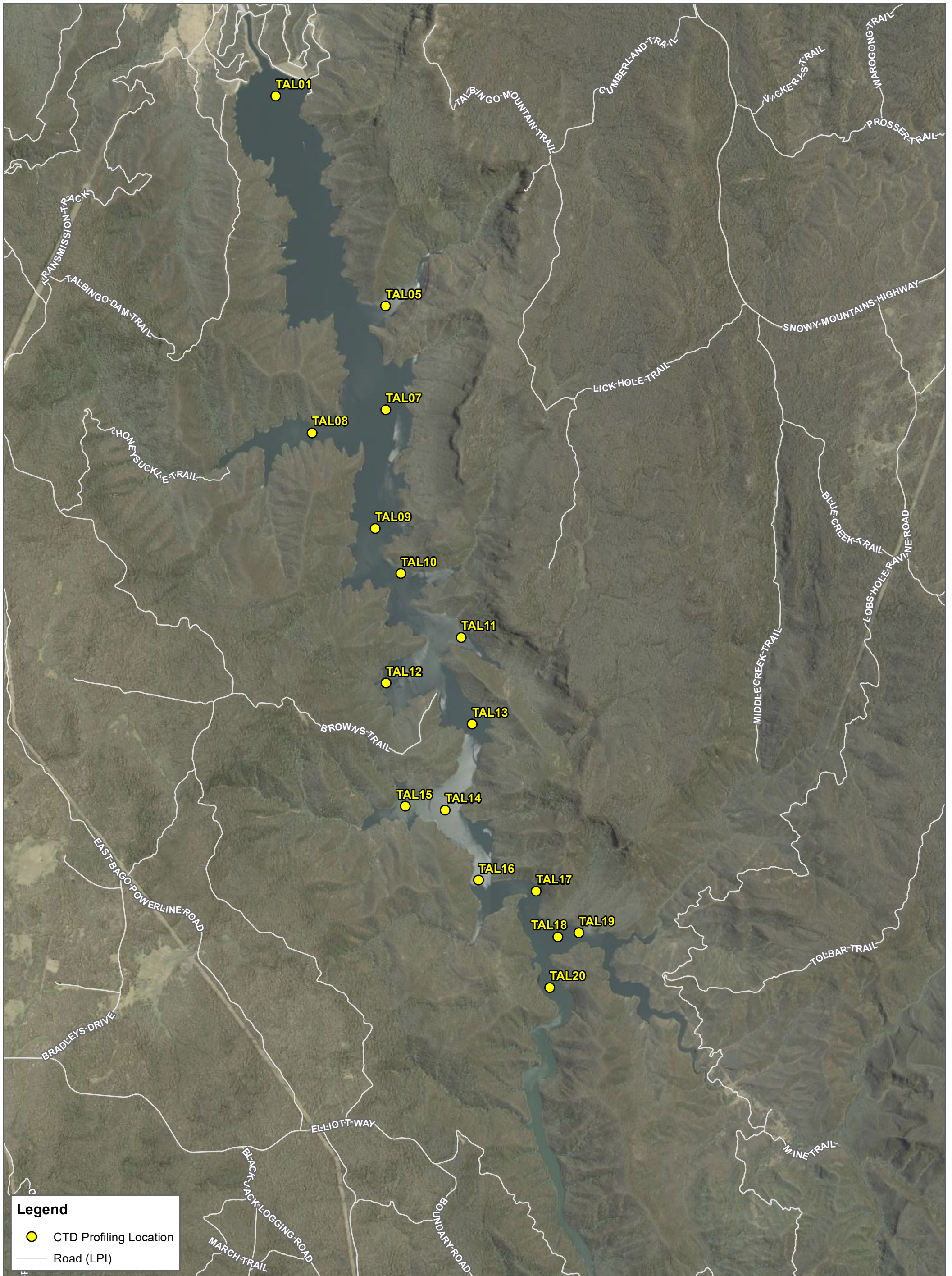
B

INSTRUMENT DATA RETURN

APPENDIX

C

LOCATION MAPS



Legend

- CTD Profiling Location
- Road (LPI)

FIGURE 1
 1:60,000 Scale at A3

km
 0 0.5 1 1.5 2

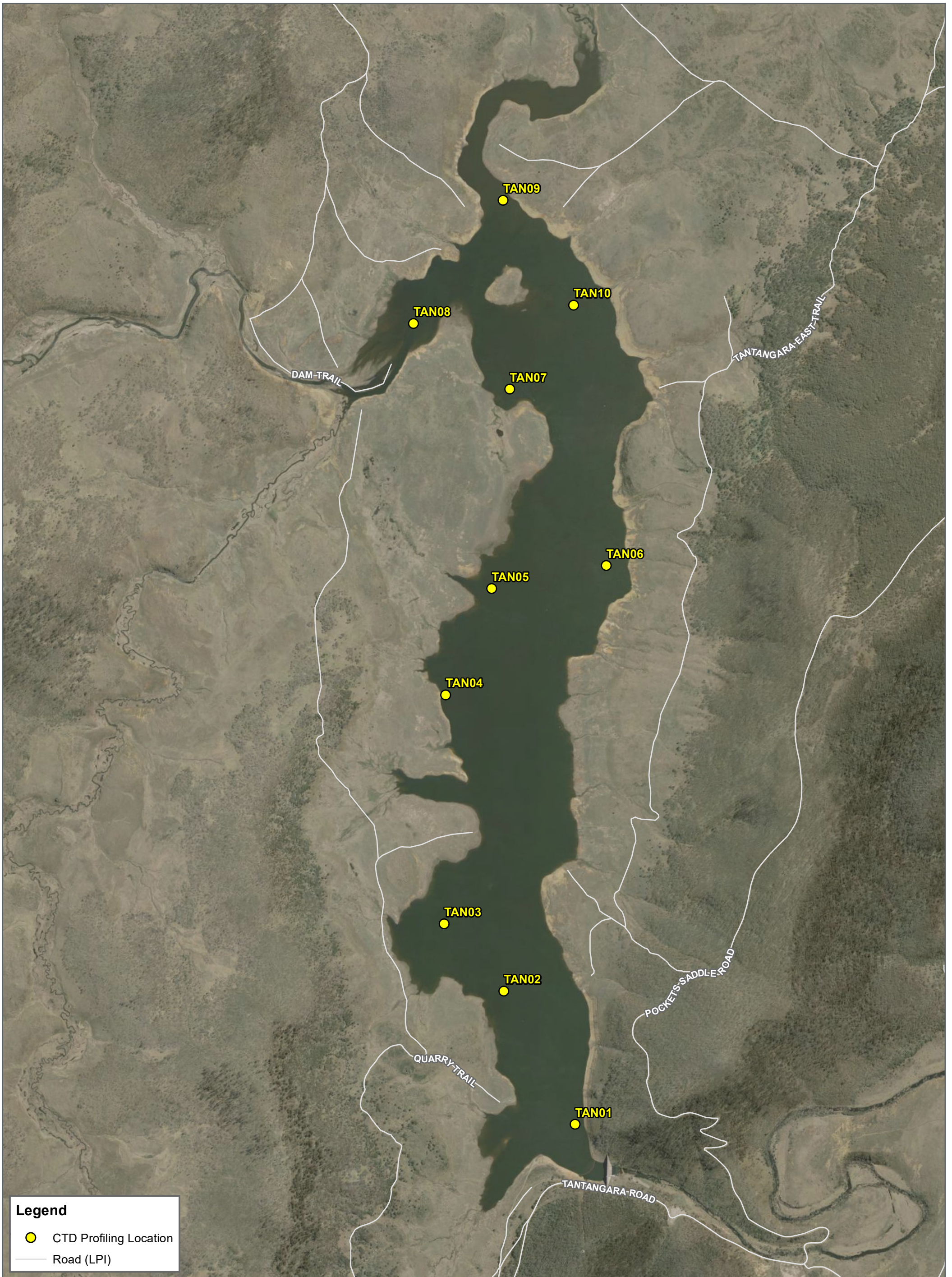
**CTD Profiling Locations
 Talbingo**

SNOWY HYDRO 2.0



Cardno

Map Produced by Cardno NSW/ACT Pty Ltd (WOL)
 Date: 2018-11-16 | Project: 59918111
 Coordinate System: GDA 1994 MGA Zone 55
 Map: 59918111_GS009_TALB_CTDProfiles.mxd 01
 Aerial imagery supplied by NSW LPI (2018)



Legend

- CTD Profiling Location
- Road (LPI)

FIGURE 2
1:20,000 Scale at A3

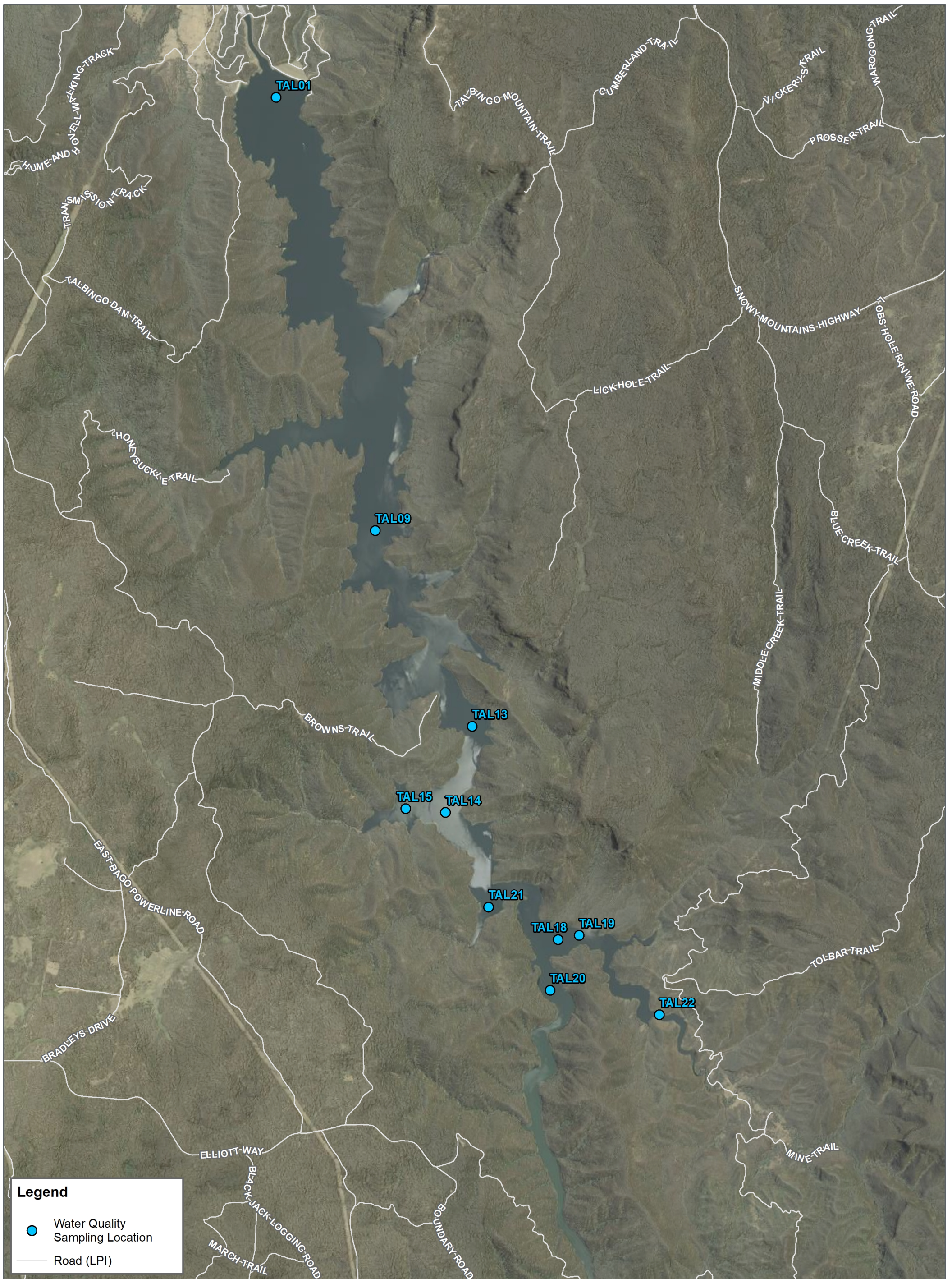


**CTD Profiling Locations
Tantangara**

SNOWY HYDRO 2.0



Map Produced by Cardno NSW/ACT Pty Ltd (WOL)
 Date: 2018-11-16 | Project: 59918111
 Coordinate System: GDA 1994 MGA Zone 55
 Map: 59918111_GS010_TANT_CTDProfiles.mxd 01
 Aerial imagery supplied by NSW LPI (2018)



Legend

- Water Quality Sampling Location
- Road (LPI)

FIGURE 3
 1:60,000 Scale at A3

km

0 0.5 1 1.5 2

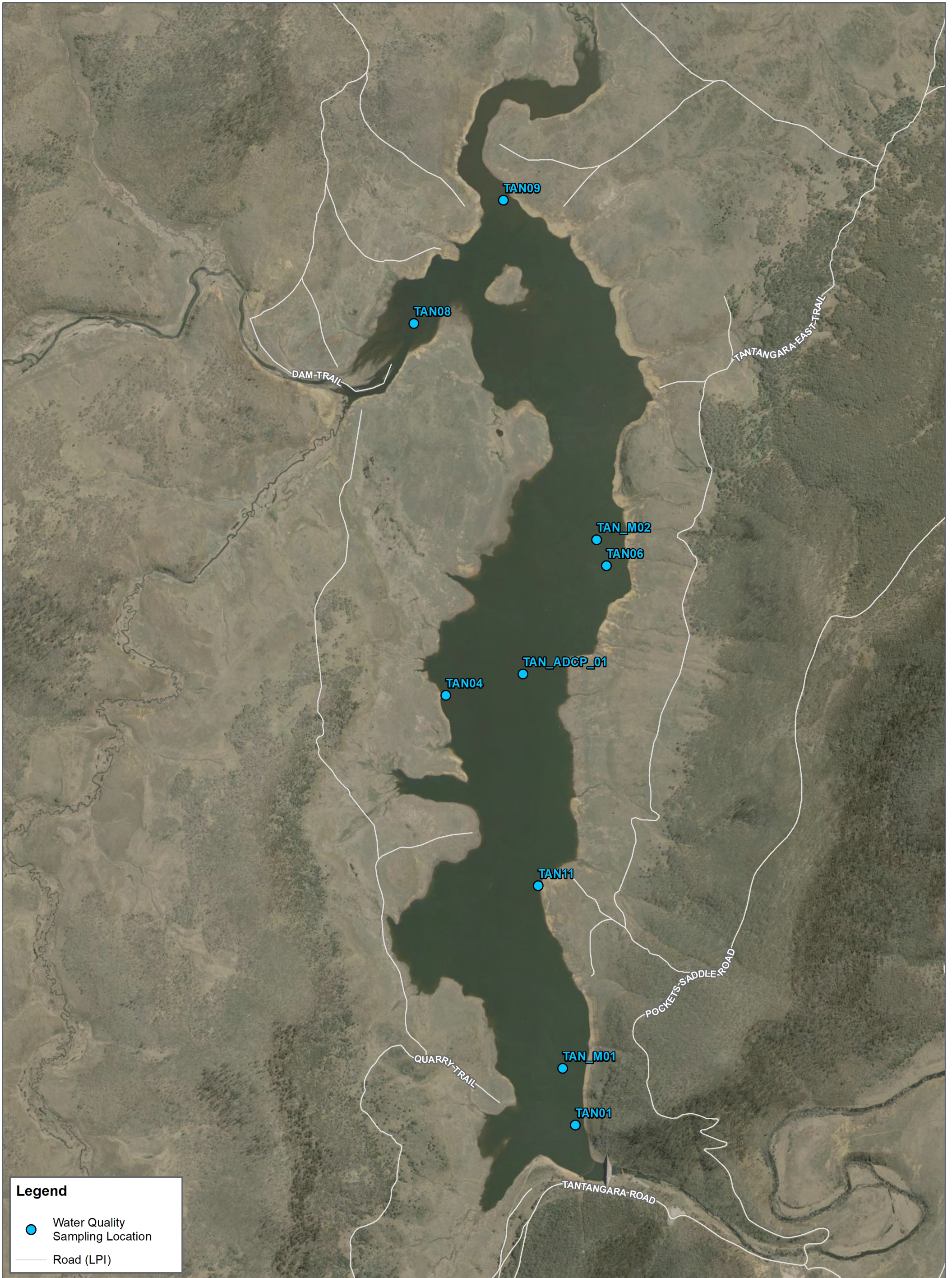
Water Quality Sampling Locations Talbingo

SNOWY HYDRO 2.0



Cardno

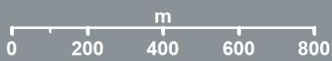
Map Produced by Cardno NSW/ACT Pty Ltd (WOL)
 Date: 2019-08-29 | Project: 59918111
 Coordinate System: GDA 1994 MGA Zone 55
 Map: 59918111_GS011_TALB_WQSamples.mxd 02
 Aerial imagery supplied by NSW LPI (2018)



Legend

- Water Quality Sampling Location
- Road (LPI)

FIGURE 4
1:20,000 Scale at A3

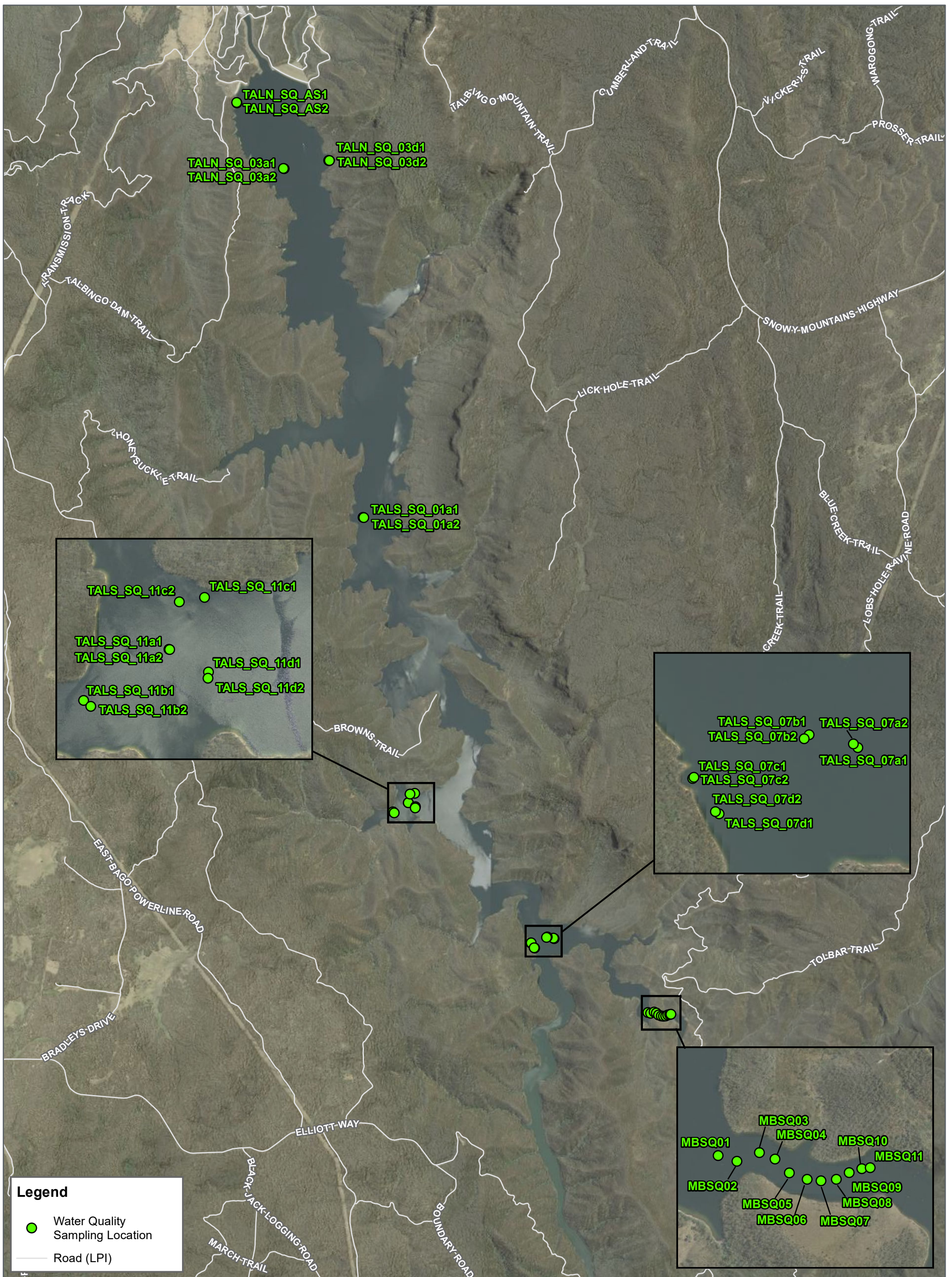


**Water Quality Sampling Locations
Tantangara**

SNOWY HYDRO 2.0

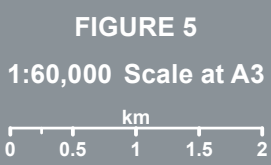


Map Produced by Cardno NSW/ACT Pty Ltd (WOL)
Date: 2019-08-29 | Project: 59918111
Coordinate System: GDA 1994 MGA Zone 55
Map: 59918111_GS012_TANT_WQSamples.mxd 02
Aerial imagery supplied by NSW LPI (2018)



Legend

- Water Quality Sampling Location
- Road (LPI)

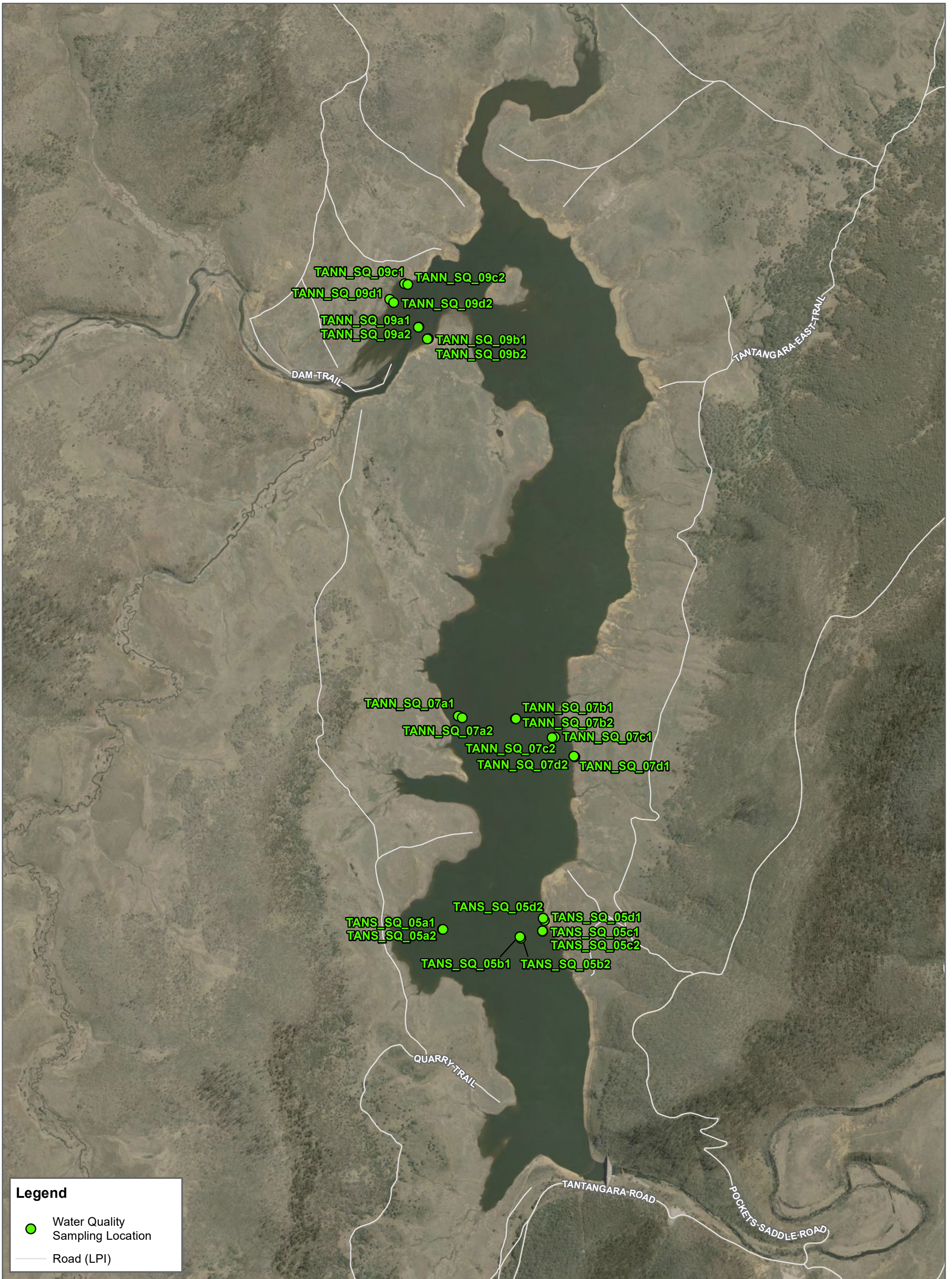


Sediment Sampling Locations Talbingo

SNOWY HYDRO 2.0



Cardno
Map Produced by Cardno NSW/ACT Pty Ltd (WOL)
Date: 2018-11-16 | Project: 59918111
Coordinate System: GDA 1994 MGA Zone 55
Map: 59918111_GS013_TALB_SedSamples.mxd 01
Aerial imagery supplied by NSW LPI (2018)



Legend

- Water Quality Sampling Location
- Road (LPI)

FIGURE 6
1:20,000 Scale at A3

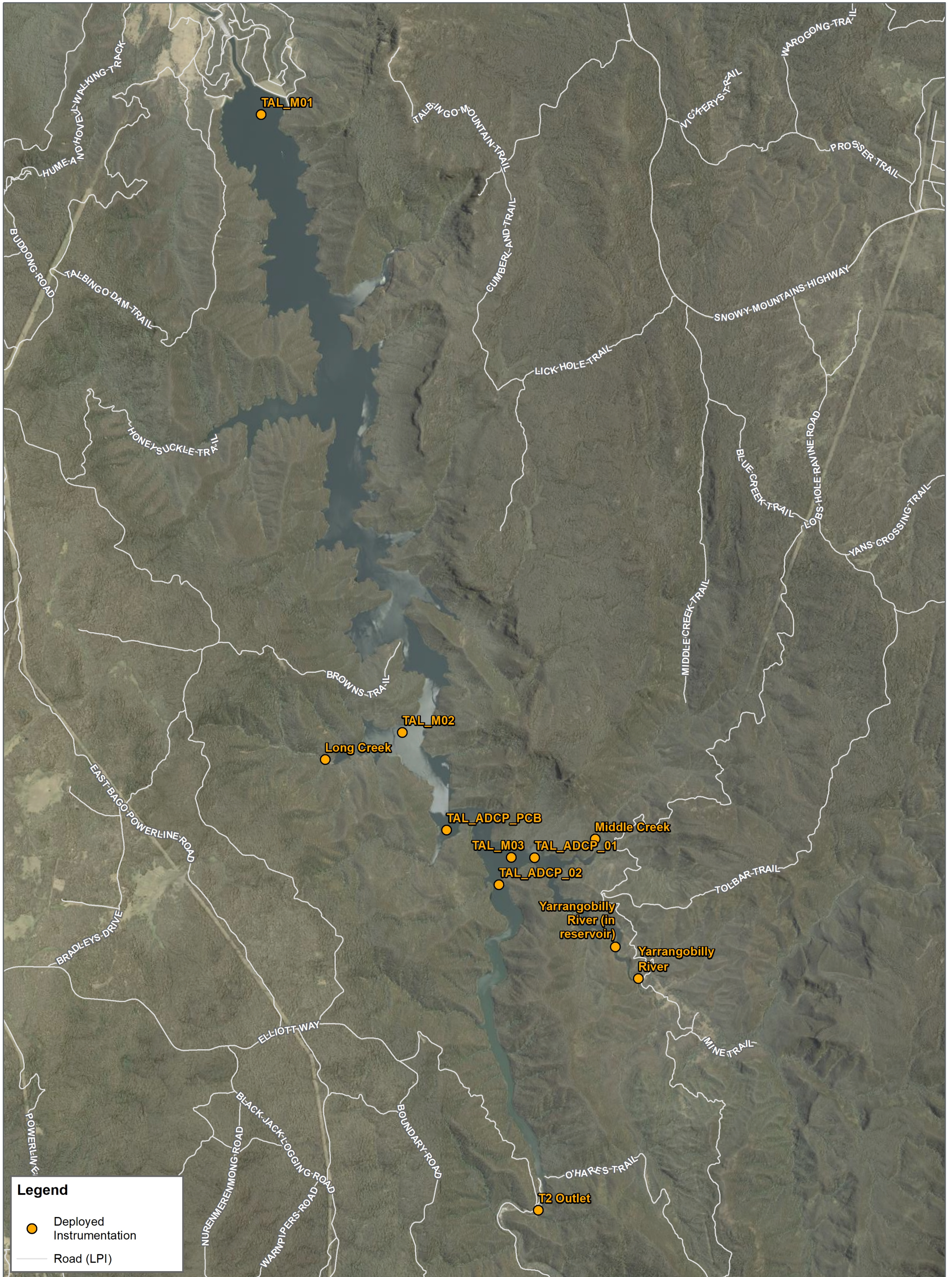


**Sediment Sampling Locations
Tantangara**

SNOWY HYDRO 2.0



Map Produced by Cardno NSW/ACT Pty Ltd (WOL)
Date: 2018-11-16 | Project: 59918111
Coordinate System: GDA 1994 MGA Zone 55
Map: 59918111_GS014_TANT_SedSamples.mxd 01
Aerial imagery supplied by NSW LPI (2018)



Legend

- Deployed Instrumentation
- Road (LPI)

FIGURE 7
 1:67,500 Scale at A3

km

0 0.5 1 1.5 2

Deployed Instrumentation Talbingo

SNOWY HYDRO 2.0





Legend

- Deployed Instrument
- Road (LPI)

FIGURE 8
 1:25,000 Scale at A3

m

0 200 400 600 800

**Deployed Instrumentation
 Tantangara**

SNOWY HYDRO 2.0



Cardno

Map Produced by Cardno NSW/ACT Pty Ltd (WOL)
 Date: 2019-08-29 | Project: 59918111
 Coordinate System: GDA 1994 MGA Zone 55
 Map: 59918111_GS016_TANT_DepInstruments.mxd 02
 Aerial imagery supplied by NSW LPI (2018)

APPENDIX

B

HEAT FLUX METHODS

1 Reservoir Heat Content

1.1 Background

$$\Delta HC = HC_{in} + HC_{SHF} - HC_{out} = c_E \rho \int T_{in} Q_{in} dt + \int Q_{net} A_s dt - c_E \rho \int T_{out} Q_{out} dt \quad (1)$$

The above equation can be used to determine the accuracy of meteorological data in estimating the change in heat content in a reservoir. Temperature profiles can be used to determine ΔHC .

The heat content (HC) of a reservoir is the potential energy stored in the water body, which can be determined in accordance with Eq. 2. HC, measured in Joules, defines the total heat content in a reservoir at any given time. Therefore, ΔHC can be calculated as the difference between HC at any two defined periods, e.g. two different days.

$$HC = \int_0^{z_s} \rho C_E (T) T(z) A(z) dz \approx \sum_{z=0}^{z_s} \rho c_E T_z A_z \Delta z \quad (2)$$

Where: HC = Heat Content of Reservoir Volume [J]

ρ = Water Density [kg/m³]

C_E = Specific Heat Capacity of Water [kJ/kgK]

T_z = Water Temperature at Layer z [°K]

A_z = Surface Area of Reservoir at Layer z [m²]

Δz = Height of Discrete Layer z [m]

The specific heat capacity, C_E and water density, ρ can be calculated as a function of temperature for fresh water, given as:

$$\rho = 1000 \left(1 - \frac{T+288.9414}{508,929.2(T+68.12963)} (T - 3.9863^2) \right) [1]$$

$$C_E = 4217.4 + T \times -3.720283 + 0.1412855T^2 - 2.654387 \times 10^{-3}T^2 + 2.093236 \times 10^{-5}T^4 [2]$$

As shown in Eqn. 1, the change in heat content is determined by a number of factors as described in **Table 1-1**.

Table 1-1 Reservoir heat content source and sinks

HC_{IN}		HC_{SURF}		HC_{OUT}	
Potential Energy added to the water body through inflows		Heat Energy gained or lost to the atmosphere through the water surface		Heat energy lost from the body through outflows	
$c_E \rho \int T_{in} Q_{in} dt$		$\int Q_{net} A_s dt$		$c_E \rho \int T_{out} Q_{out} dt$	
T_{in}	$Q_{in} dt$	Q_{net}	A_s	T_{out}	$Q_{out} dt$
Temperature of inflow (°K)	Volume of inflow over time period	Surface heat flux calc'd from Surface heat flux equations	Surface area	Temperature of outflow (°K)	Volume of outflow over time period

2 Surface Heat Flux

The heat radiation emitted by the sun reaches the earth in the form of electromagnetic waves with wavelengths in the range of 0.15 to 4 μm . In the atmosphere the radiation undergoes scattering, reflection and absorption by air, cloud, dust and particles. On average, neither the atmosphere nor the earth accumulates heat, which implies that the absorbed heat is emitted back again. The wavelengths of these emitted radiations are longer (between 4 and 50 μm) due to the lower prevailing temperature in the atmosphere and on Earth. Schematically, the radiation process, along with the heat flux mechanisms at the water surface are shown in **Figure 2-1**.

The various heat flux components are defined as:

- Q_{sc} Solar radiation for a clear day [$\text{J}/\text{m}^2\text{s}$]
- Q_{sn} Net incident solar radiation (short-wave) [$\text{J}/\text{m}^2\text{s}$] - $Q_s - Q_{sr}$
- Q_s Solar radiation (short-wave) [$\text{J}/\text{m}^2\text{s}$]
- Q_{sr} Reflected solar radiation (short-wave) [$\text{J}/\text{m}^2\text{s}$]
- Q_{an} Net incident atmospheric radiation (long-wave) [$\text{J}/\text{m}^2\text{s}$]
- Q_a Atmospheric radiation (long-wave) [$\text{J}/\text{m}^2\text{s}$]
- Q_{ar} Reflected atmospheric radiation (long-wave) [$\text{J}/\text{m}^2\text{s}$]
- Q_{br} Surface back radiation (long-wave) [$\text{J}/\text{m}^2\text{s}$]
- Q_{ev} Evaporative (latent) heat loss [$\text{J}/\text{m}^2\text{s}$]
- Q_{co} Convective (sensible) heat loss [$\text{J}/\text{m}^2\text{s}$]

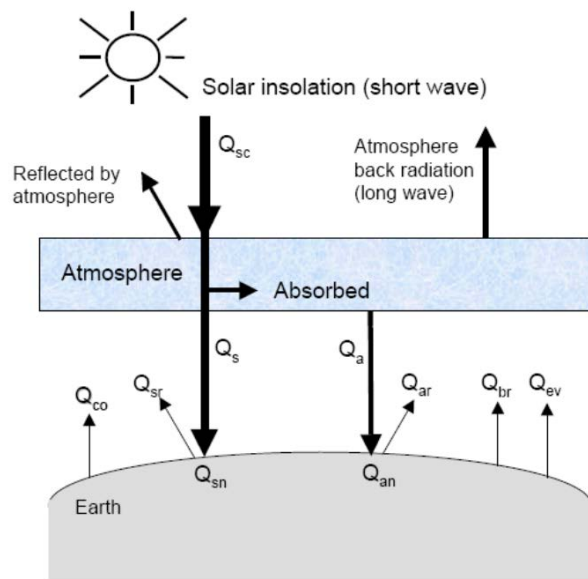


Figure 2-1 Overview of the heat exchange mechanisms at a water body surface [1]

There exists various models. Most formulations differ in the dependency of the exchange on the meteorological parameters such as wind speed, cloudiness and humidity.

The **Total Heat Flux**, Q_{tot} through the free surface reads:

$$Q_{tot} = Q_{sn} + Q_{an} - Q_{br} - Q_{ev} - Q_{cov}$$

The individual heat flux components are described in detail in the proceeding subsections. The required variable inputs are summarised in **Table 2-1**.

Table 2-1 Summary of variable inputs required to heat flux models

	Air Temperature		Fraction of Sky Covered by Cloud (%)	Water Surface Temperature		Wind Speed (m/s)	Relative Humidity (%)	Solar Radiation (W/m ²)
	T _a (°C)	T̄ _a (°K)	F _c	T _s (°C)	T̄ _s (°K)	U ₂	r _{hum}	
Q _{sn}								X
Q _{an}		X	X					
Q _{br}					X			
Q _{ev}		X			X	X	X	
Q _{co}		X			X	X	X	

2.2 Solar Radiation (Short-Wave Radiation)

Radiation from the sun consists of electromagnetic waves with wave lengths varying from 1,000 to 30,000 Å. Most of this is absorbed in the ozone layer, leaving only a fraction of the energy to reach the surface of the Earth. Furthermore, the spectrum changes when sunrays pass through the atmosphere. Most of the infrared and ultraviolet compound is absorbed such that the solar radiation on the Earth mainly consists of light with wave lengths between 4,000 and 9,000 Å. The intensity of the solar radiation depends on the distance to the sun, declination angle and latitude, extra-terrestrial radiation, the cloudiness and amount of water vapour in the atmosphere [2].

The net solar radiative flux, Q_{sn} is defined as:

$$Q_{sn} = (1 - \alpha)Q_s$$

Where:

Q_s = Short-Wave Solar Radiation (W/m² or J/s)

α = Albedo Constant [-]

Solar radiation that impinges on a water surface does not all penetrate the water surface. Parts are reflected back and are lost unless they are backscattered from the surrounding atmosphere. This reflection of solar energy is termed the albedo, α. The amount of energy, which is lost due to albedo, depends on the angle of incidence, i and angle of refraction, r. For a smooth sea the reflection can be expressed as:

$$\alpha = \left(\frac{\sin^2 i - r}{\sin^2 i + r} + \frac{\tan^2 i - r}{\tan^2 i + r} \right)$$

For altitudes exceeding 30°, the Albedo constant can be approximated as 0.05 [2]. Constant, values recommended by Deltares range between 0.06 and 0.09 [1].

It should be noted that solar radiative flux can therefore be approximated through the application of direct solar radiation measurements. The Luftt WS502 weather sensor, used as part of the Cardno measurement campaign measures solar radiation in the range of 300-11,000 Å, marginally extending into the long-wave bandwidth.

2.3 Atmospheric Radiation (Long-Wave Radiation)

A body or a surface emits electromagnetic energy at all wavelengths of the spectrum. The long wave radiation consists of waves with wavelengths between 9,000 and 25,000 Å. Atmospheric radiation is primarily due to emission of absorbed solar radiation by water vapour, carbon dioxide and ozone in the atmosphere. The emission spectrum of the atmosphere is highly irregular. The amount of atmospheric radiation that reaches the earth is determined by applying the Stefan-Boltzmann's law that includes the emissivity coefficient of the atmosphere ε. Taking into account the effect of reflection by the surface and reflection and absorption by clouds, the relation for the net atmospheric radiation Q_{an} reads [1]:

$$Q_{an} = (1 - r)\epsilon\sigma T_a^4 g(F_c)$$

Where:

ε = Emissivity Factor [-]

σ = Stefan-Boltzmann Constant (5.6703x10⁻⁸) [W/m²K⁴]

r = Reflection Coefficient (0.03) [-]

T_a = Air Temperature [K]

$g(F_c)$ = Cloud Cover Function [-]

The Cloud Coverage Function, $g(F_c)$ is given as:

$$g(F_c) = 1.0 + 0.17F_c^2$$

Where:

F_c = Percentage of Cloud Coverage

It should be noted that the emissivity of the atmosphere typically varies between 0.7 for clear sky and low temperatures and 1.0. A constant value of 0.7 for atmospheric emissivity has been adopted herein.

2.4 Back Radiation (Long-Wave Radiation)

Similar to the atmosphere (see Section 2.3), a water body also emits radiation in the long-wave frequency band. Water radiates as a near black body, so the heat radiated back by the water can be described by Stefan-Boltzmann's law of radiation, corrected by an emissivity factor $\varepsilon = 0.985$ for water (Sweers, 1976; Octavio et al., 1977) and a reflection coefficient for the air-water interface of $r = 0.03$ [3]:

$$Q_{br} = (1 - r)\varepsilon\sigma T_s^4$$

Where:

ε = Emissivity Factor (0.985) [-]

σ = Stefan-Boltzmann Constant (5.6703×10^{-8}) [W/m²K⁴]

r = Reflection Coefficient (0.03) [-]

T_s = Surface Temperature [K]

2.5 Convective (Sensible Heat) Flux

The convective (or "sensible") heat flux depends on the type of boundary layer between the water surface and the atmosphere. Generally this boundary layer is turbulent implying the following relationship to the evaporative heat flux through the Bowen Ratio [1]:

$$Q_{co} = R_b Q_{ev}$$
$$R_b = \gamma \frac{T_s - T_a}{e_s - e_a}$$

Where:

T_s = Water Surface Temperature [K]

T_a = Atmospheric Temperature [K]

e_s = Saturated Vapour Pressure

e_a = Actual Vapour Pressure

γ = Bowen's Constant (0.61) [-]

The vapour pressure components are defined as:

$$e_s = 23.38e^{\left(18.1 - \frac{5303.3}{T_s}\right)}$$
$$e_a = r_{hum} 23.38e^{\left(18.1 - \frac{5303.3}{T_a}\right)}$$

Where:

r_{hum} = Relative Humidity (%)

2.5.1 Evaporative (Latent Heat) Flux

Evaporation is an exchange process that takes place at the interface between water and air and depends on the conditions both in the water near the surface and the air above it. The phase change from liquid to vapour during evaporation, requires an input of energy, called the latent heat of evaporation. As a result, during evaporation, heat energy is removed from the water body to undertake this process.

The evaporative heat-flux, Q_{ev} can be defined as [2]:

$$Q_{ev} = L_v C_e (a_1 + b_2 W_{2m}) (Q_{water} - Q_{air})$$

Where:

L_v = Latent Heat of Vaporisation ($2.5 \times 10^6 - 2.3 \times 10^3 T_s$) [J/kg]

C_e = Moisture Transfer Coefficient (Dalton Number) (1.32×10^{-3}) [-]

a_1 = Coefficient (0.5) [-]

b_2 = Wind Coefficient (0.9) [-]

W_{2m} = Wind Speed referenced to 2 m above the reservoir surface [m/s]

Q_{water} = Vapour Density close to the Surface

Q_{air} = Vapour Density of Atmosphere

Measurements of Q_{air} and Q_{water} are not directly available, but the vapour density can be related to the vapour pressures as per:

$$Q_i = \frac{0.2167}{T_i} e_i$$

Where:

i = Subscript for both Air and Water

T_i = Water Surface or Atmospheric Temperature [°K]

e_i = Vapour Pressure [Pa]

The saturated vapour pressure close to the surface of reservoir, e_{water} can be expressed in terms of the water temperature, assuming that the air close to the surface is saturated and has the same temperature as the water:

$$e_s = 6.11 e^{5418 \left(\frac{1}{T_K} - \frac{1}{T_s} \right)}$$

Similarly, the actual vapour pressure of the air can be expressed in terms of the air temperature and the relative humidity, R

$$e_a = r_{hum} 6.11 e^{5418 \left(\frac{1}{T_K} - \frac{1}{T_a} \right)}$$

Where:

$T_K = 273.15$ [°K]

T_s = Water Surface Temperature [°K]

T_a = Atmospheric Temperature [°K]

r_{hum} = Relative Humidity (%)

It should be noted that the vapour pressures equations used for the determination of evaporative heat flux give marginally different results to those mentioned in Section 2.5 for the determination of the convective heat flux. These variations arise due to the differences between the two heat flux models and their empirical calibrations.

3 Surface Heat Flux Calculation Methodology

3.1 Inputs

The assumed input parameters and variables, required for the determination of surface heat flux are summarised in **Table 3-1**.

Table 3-1 Summary of surface heat flux inputs

Heat Flux Component	Variables/ Parameters	Description
Net Solar Radiation	Incident Solar Radiation, Q_s	Source: Direct Measurement (Cardno) Format: Varying in Time, Constant in Space [J/sm ²]
	Albedo Constant, α	Format: Constant Parameter Value: 0.06 [1]
Atmospheric Radiation (Long-Wave)	Emissivity Factor, ϵ	Format: Constant Parameter Value: 0.65
	Stefan-Boltzmann Constant, σ	Format: Constant Parameter Value: $5.6703 \times 10^{-8} \text{ W/m}^2\text{K}^4$
	Reflection Coefficient, r	Format: Constant Parameter Value: 0.03 [1]
	Air Temperature, T_a	Source Direct Measurement (Cardno) [K] Format: Varying in time, constant in space
	Cloud Coverage Factor, F_c	Source: NCEP CFSv2 Model [-] Format: Varying in time, constant in space
Back Radiation (Long-Wave)	Emissivity Factor, ϵ	Format: Constant Parameter Value: 0.985 [1]
	Stefan-Boltzmann Constant, σ	Format: Constant Parameter Value: $5.6703 \times 10^{-8} \text{ W/m}^2\text{K}^4$
	Reflection Coefficient, r	Format: Constant Parameter Value: 0.03 [1]
	Surface Temperature, T_a	Source Direct Measurement (Cardno) [K] Format: Varying in time, constant in space
Convective (Sensible Heat)	Surface Temperature, T_s	Source Direct Measurement (Cardno) [K] Format: Varying in time, constant in space
	Atmospheric Temperature, T_a	Source Direct Measurement (Cardno) [K] Format: Varying in time, constant in space
	Relative Humidity, R_{hum}	Source Direct Measurement (Cardno) [%] Format: Varying in time, constant in space
	Bowen's Constant, γ	Format: Constant Parameter Value: 0.61 [1]
	Saturated Vapour Pressure, e_s	Source: Empirical (Input of T_s) Format: Varying in time, constant in space
	Actual Vapour Pressure, e_a	Source: Empirical (Input of T_a and R_{hum}) Format: Varying in time, constant in space
Evaporative Heat	Atmospheric Temperature, T_a	Source: Direct Measurement (Cardno) Format: Varying in time, constant in space
	Surface Temperature, T_s	Source Direct Measurement (Cardno) Format: Varying in time, constant in space

Heat Flux Component	Variables/ Parameters	Description
	Latent Heat of Vaporisation, L_v	Source: Empirical (Input of T_s) Format: Varying in time, constant in space
	Saturated Vapour Pressure, e_s	Source: Empirical (Input of T_s) Format: Varying in time, constant in space
	Actual Vapour Pressure, e_a	Source: Empirical (Input of T_a) Format: Varying in time, constant in space
	Relative Humidity, R_{hum}	Source: Direct Measurement (Cardno) Format: Varying in time, constant in space
	Wind Speed 2 m above Surface, U_2	Source: Direct Measurement (Cardno) with Height Adjustment. Format: Varying in time, constant in space

3.2 Input Processing

3.2.1 Atmospheric Temperature

Atmospheric temperatures covering the period of the Cardno measurement campaign have been obtained from the buoy mounted weather stations, situated approximately 1.5 m above the free surface. Temperatures measurements have been converted from °C to °K for input to the heat flux algorithms.

3.2.2 Water Surface Temperature

Water surface temperatures covering the period of the Cardno measurement campaign have been obtained from the thermistor string deployments. Surface water temperature is approximated by the first thermistor located at 1 m below the free surface. Water surface temperatures have been converted from °C to °K for input to heat flux algorithms.

3.2.3 Wind Speed

Wind speeds measured as part of the Cardno campaign have been obtained from buoy mounted weather stations, situated approximately 1.5 m above the free surface. Measured $U_{1.5}$ wind speeds, are recorded as 4 minute averages, taken at the end of 10 minute reading interval.

The empirical equation for evaporative heat flux, described in **Section 2.5.1** has calibrated using the wind speed measured at 2 m above the surface, U_2 . Assuming a logarithmic velocity profile, U_2 can be estimated as:

$$U_2 = U_{1.5} \frac{\ln\left(\frac{2}{z_0}\right)}{\ln\left(\frac{1.5}{z_0}\right)}$$

Where, the roughness height, z_0 is taken as 0.0002 m, representative of open seas and lakes [3].

3.2.4 Incident Solar Radiation

Incident solar radiation, measured as part of the Cardno campaign have been obtained from buoy mounted weather stations, situated approximately 1.5 m above the free surface. The instrument specifications indicate that the incident solar radiation is measured from 300 to 11,000 Å, covering the entirety of the short-wave frequency band.

Incident solar radiation, measured in W/m^2 has been directly used as input for the estimation of net solar radiation, based on the assumption of an albedo reflection coefficient to account for surface reflection.

3.3 Total Heat Flux

The total heat flux has been calculated based on the summation of all time dependent source and sink terms. To establish a long-term time series of heat flux, a common time series among all datasets is required. Considering the available datasets, discussed in **Section 3.4**, the record frequency typically ranges between 5-15 minutes, although it should be noted that based on the instrumentation, the timestamps of individual records may differ between instrument loggers.

As such, a synthetic time series, spanning the period of available data and with a time-step of 30 minutes is established for the purpose of calculating total heat flux. For instances in which record time-steps do not coincide with the synthetic time series, linear interpolation of the datasets has been used.

3.4 Available Datasets

3.4.1 Talbingo

At the Talbingo Reservoir, surface heat fluxes have been estimated for the period spanning between the 1st August 2018 to the 25th of March 2019 using Cardno datasets. A summary of the adopted datasets, including details of the measurement site locations is presented in **Table 3-2** and **Table 3-3**. It should be noted that the percentage of cloud cover was required to supplement the Cardno dataset and has been obtained from the NCEP CFSv2 Atmospheric Model [6].

Table 3-2 Summary of Cardno Datasets (Talbingo)

Variable	Description	Units	Site	Coordinates (m MGA 55)		Data Period		Sensor Depth
				Easting	Northing	Start	End	
T _a	Air Temperature	°C	MET_CARD_TAL_01	617842	6056463	1 Aug 2018	25 Mar 2019	1.5 m above FS
Q _s	Incident Solar Radiation	J/sm ²	MET_CARD_TAL_01	617842	6056463	1 Aug 2018	25 Mar 2019	1.5 m above FS
T _s	Surface Temperature	°C	THERM_CARD_TAL_01	617842	6056463	6 Jun 2018	25 Mar 2019	1.0 m below FS
U	Wind Speed	m/s	MET_CARD_TAL_01	617842	6056463	1 Aug 2018	25 Mar 2019	1.5 m above FS
R _{hum}	Relative Humidity	%	MET_CARD_TAL_01	617842	6056463	1 Aug 2018	25 Mar 2019	1.5 m above FS
F _c	% of Cloud Cover	%	NCEP CFSv2 Model	617190	6051558	01 Apr 2011	Present	Total Cloud Cover

Table 3-3 Measurement Reading Frequencies (Talbingo)

Variable	Description	Units	Site	Reading Frequency
T _a	Air Temperature	K	MET_CARD_TAL_01	10 Minute
Q _s	Incident Solar Radiation	J/sm ²	MET_CARD_TAL_01	10 Minute
T _s	Surface Temperature	K	THERM_CARD_TAL_01	10 Minute
U	Wind Speed	m/s	MET_CARD_TAL_01	10 Minute
R _{hum}	Relative Humidity	%	MET_CARD_TAL_01	10 Minute
F _c	% of Cloud Cover	%	NCEP CFSv2 Model	60 Minute

3.4.2 Tantangara

At the Tantangara Reservoir, surface heat fluxes have been estimated for the period spanning between the 2nd August 2018 to the 28th of March 2019 using Cardno datasets. A summary of the adopted datasets, including details of the measurement site locations is presented in **Table 3-4** and **Table 3-5**. It should be noted that the percentage of cloud cover was required to supplement the Cardno dataset and has been obtained from the NCEP CFSv2 Atmospheric Model [6].

Table 3-4 Summary of Cardno Datasets (Tantangara)

Variable	Description	Units	Site	Coordinates (m MGA 55)		Data Period		Sensor Depth
				Easting	Northing	Start	End	
T _a	Air Temperature	K	MET_CARD_TAN_01	650229	6041165	2 Aug 2018	28 Mar 2019	1.5 m above FS
Q _s	Incident Solar Radiation	J/sm ²	MET_CARD_TAN_01	650229	6041165	2 Aug 2018	28 Mar 2019	1.5 m above FS
T _s	Surface Temperature	K	THERM_CARD_TAN_02	617842	6056463	7 Jun 2018	28 Mar 2019	1.0 m below FS
U	Wind Speed	m/s	MET_CARD_TAN_01	650229	6041165	2 Aug 2018	28 Mar 2019	1.5 m above FS
R _{hum}	Relative Humidity	%	MET_CARD_TAN_01	650229	6041165	2 Aug 2018	28 Mar 2019	1.5 m above FS
F _c	% of Cloud Cover	%	NCEP CFSv2 Model	617190	6050992	01 Apr 2011	Present	Total Cloud Cover

Table 3-5 Measurement Reading Frequencies (Talbingo)

Variable	Description	Units	Site	Reading Frequency
T _a	Air Temperature	K	MET_CARD_TAN_01	10 Minute
Q _s	Incident Solar Radiation	J/sm ²	MET_CARD_TAN_01	10 Minute
T _s	Surface Temperature	K	THERM_CARD_TAN_02	10 Minute
U	Wind Speed	m/s	MET_CARD_TAN_01	10 Minute
R _{hum}	Relative Humidity	%	MET_CARD_TAN_01	10 Minute
F _c	% of Cloud Cover	%	NCEP CFSv2 Model	60 Minute

The heat content, instantaneous heat fluxes and monthly average heat fluxes for Talbingo and Tantangara Reservoirs are shown in Figures B-1 to B-6.

4 References

- [1] J. L. Martin and S. C. McCutcheon, *Hydrodynamics and Transport for Water Quality Modelling*, Washington D.C.: Lewis Publishers, 1999.
- [2] A. E. Gill, *Atmosphere-Ocean Dynamics*, London: Academic Press, Inc (London) Ltd., 1982.
- [3] Deltares, "Delft3d-FLOW - Simulation of multi-dimensional hydrodynamic flows and transport phenomena, including sediments: User Manual," Deltares, 2019.
- [4] DHI, "MIKE 21 & MIKE 3 Flow Model FM - Hydrodynamic and Transport Module. Scientific Documentation," Danish Hydraulics Institute, 2017.
- [5] J. Wieringa, A. Daveport, C. Grimmon and T. Oke, "New revision of Davenport roughness classification," *Proceedings of the 3rd European and African Conference on Wind Engineering, Eindhoven*, 2001.
- [6] DOC/NOAA/NWS/NCEP, "Climate Forecast System Version 2 (CFSv2) Operational Analysis," ational Climatic Data Center, NESDIS, NOAA, U.S. Department of Commerce, 2019.

Talbingo Reservoir

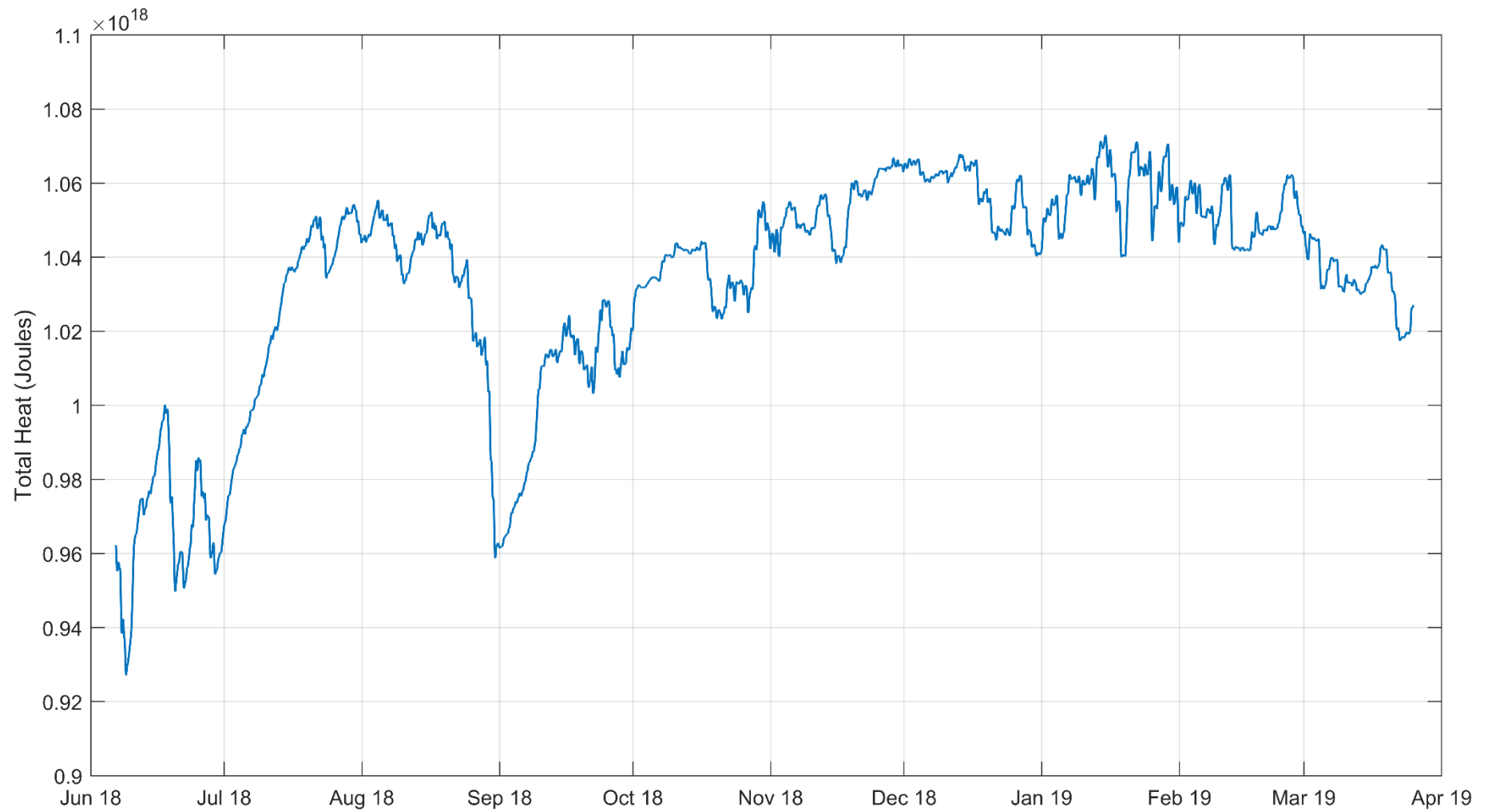
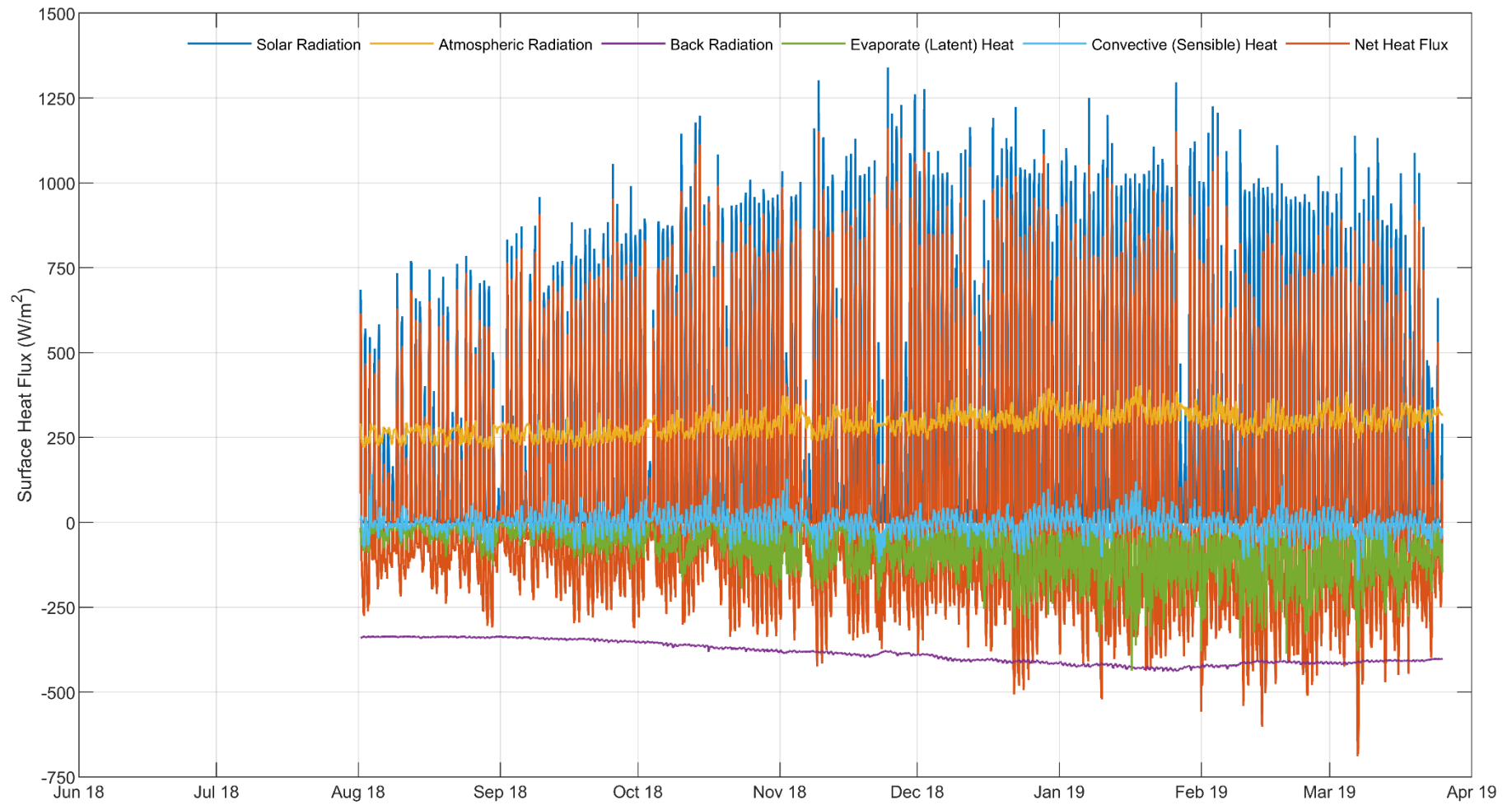


Figure B-1 Total heat content of Talbingo Reservoir (June 2018 to April 2019)



N:\Projects\599\FY18\111_EMMSnowyHydro\Phase 6 - Physical Limnology\Des_An\Matlab\Data Analysis\4. Heat Fluxes\talbingoHeatFlux.m

Figure B-2 Net surface heat flux and individual flux components at Talbingo Reservoir - +ve value indicates reservoir heat gain (June 2018 to April 2019)

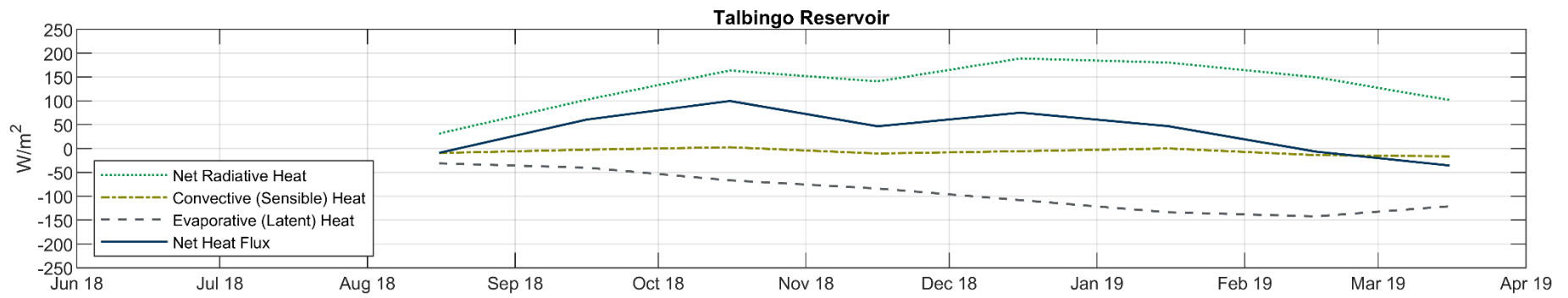


Figure B-3 Monthly averaged net surface heat flux and individual flux components at Talbingo Reservoir - +ve value indicates reservoir heat gain (June 2018 to April 2019)

Tantangra Reservoir

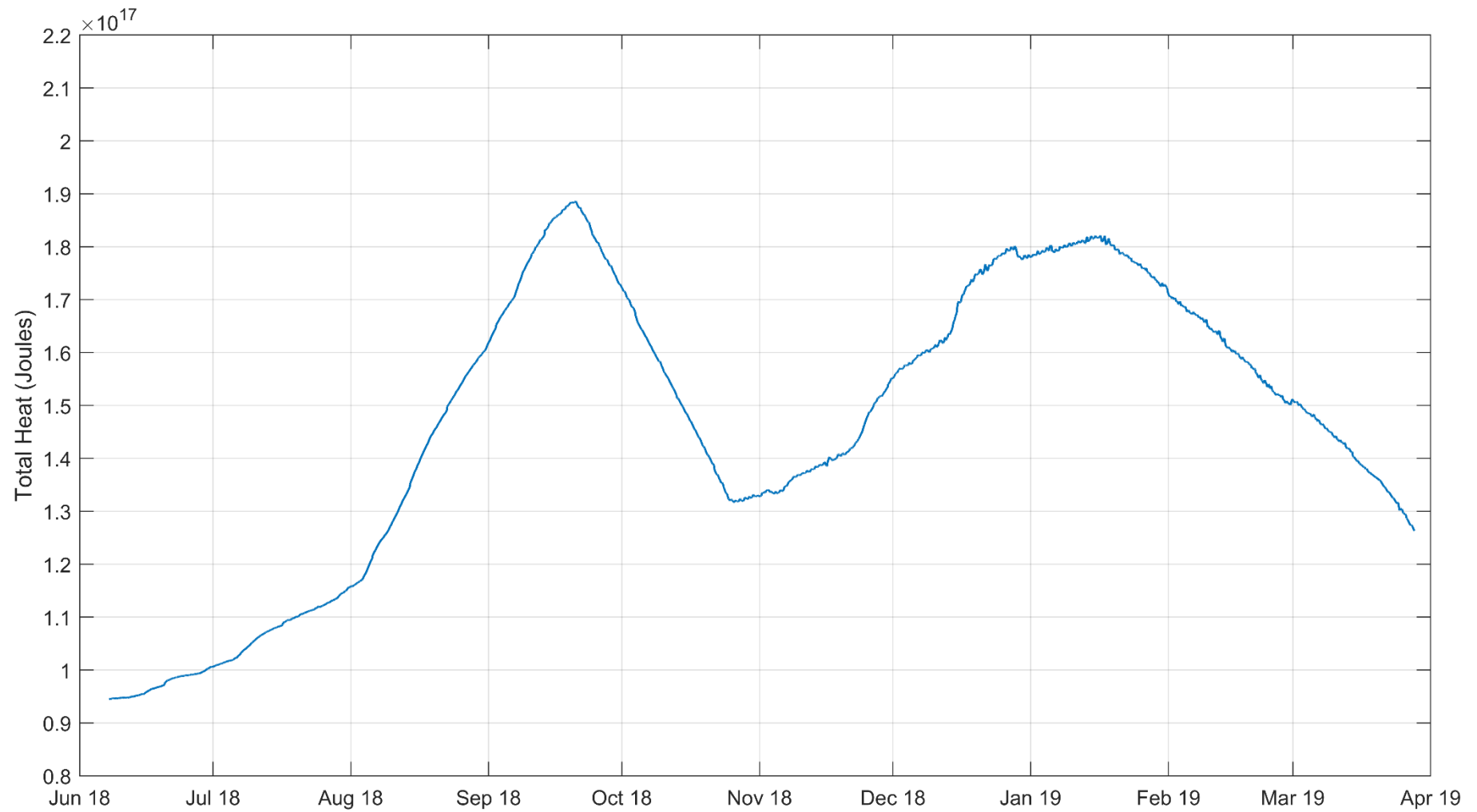


Figure B-4 Total heat content of Tantangra Reservoir (June 2018 to April 2019)

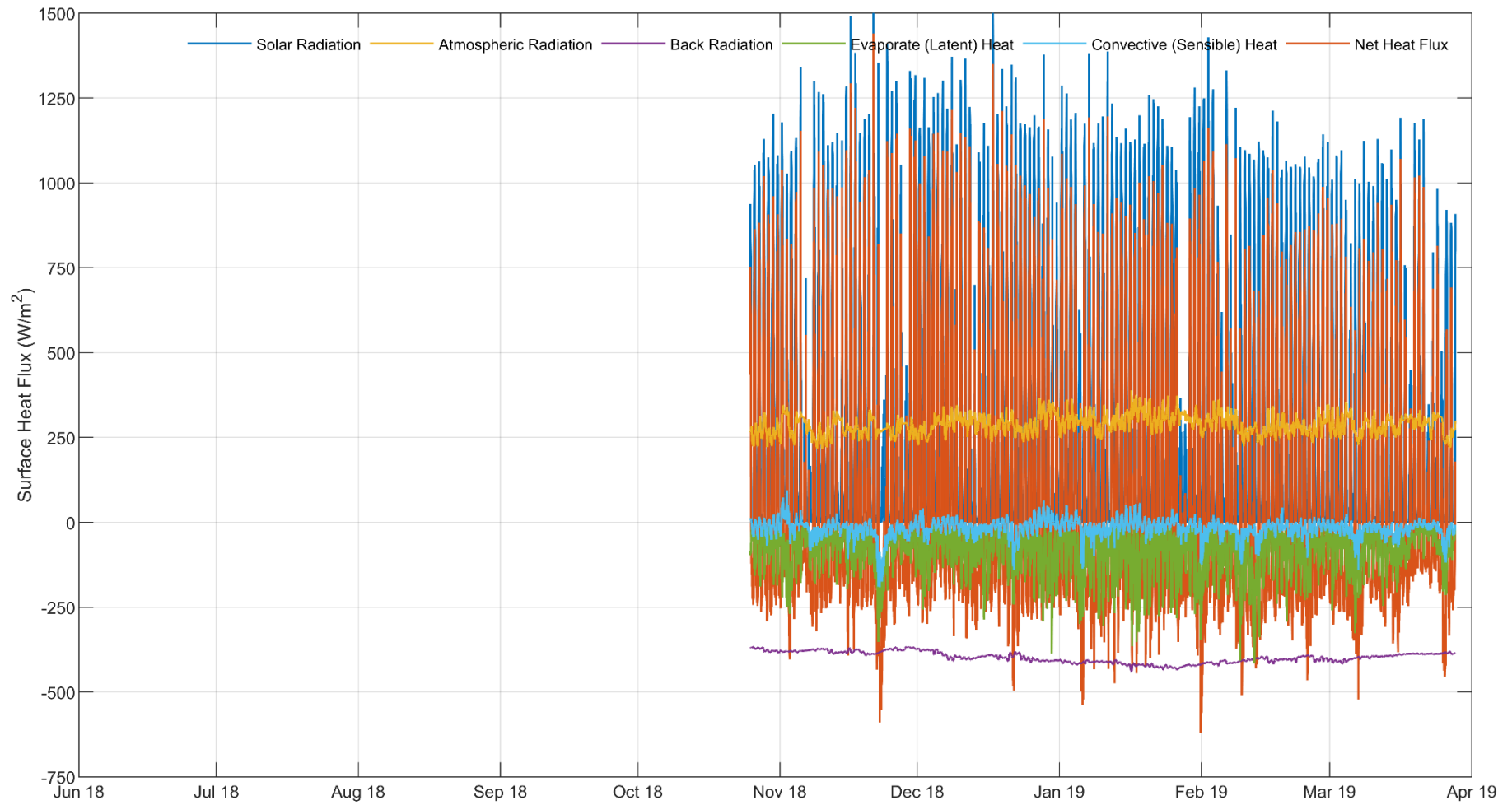


Figure B-5 Net surface heat flux and individual flux components at Tantangra Reservoir - +ve value indicates reservoir heat gain (June 2018 to April 2019)

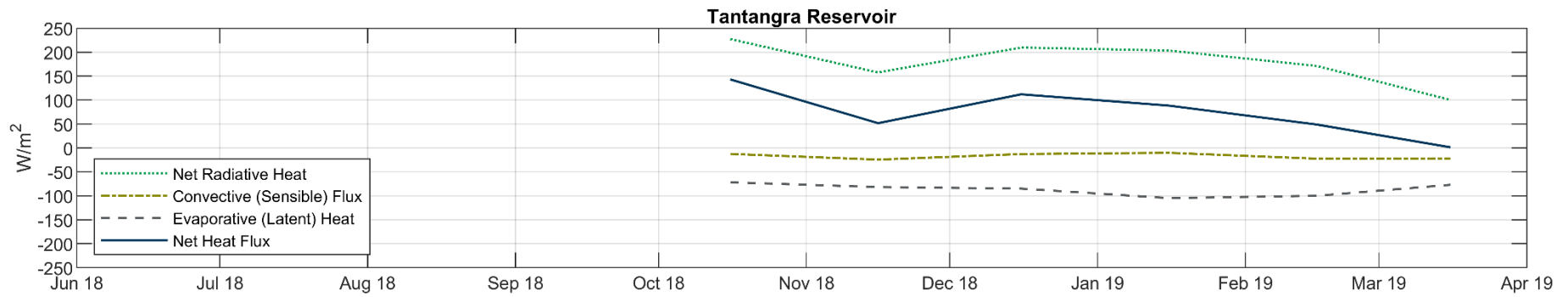


Figure B-6 Monthly averaged net surface heat flux and individual flux components at Tantangra Reservoir - +ve value indicates reservoir heat gain (June 2018 to April 2019)

APPENDIX

C

INFLOWS AND TRANSFERS

Reservoir Water Levels

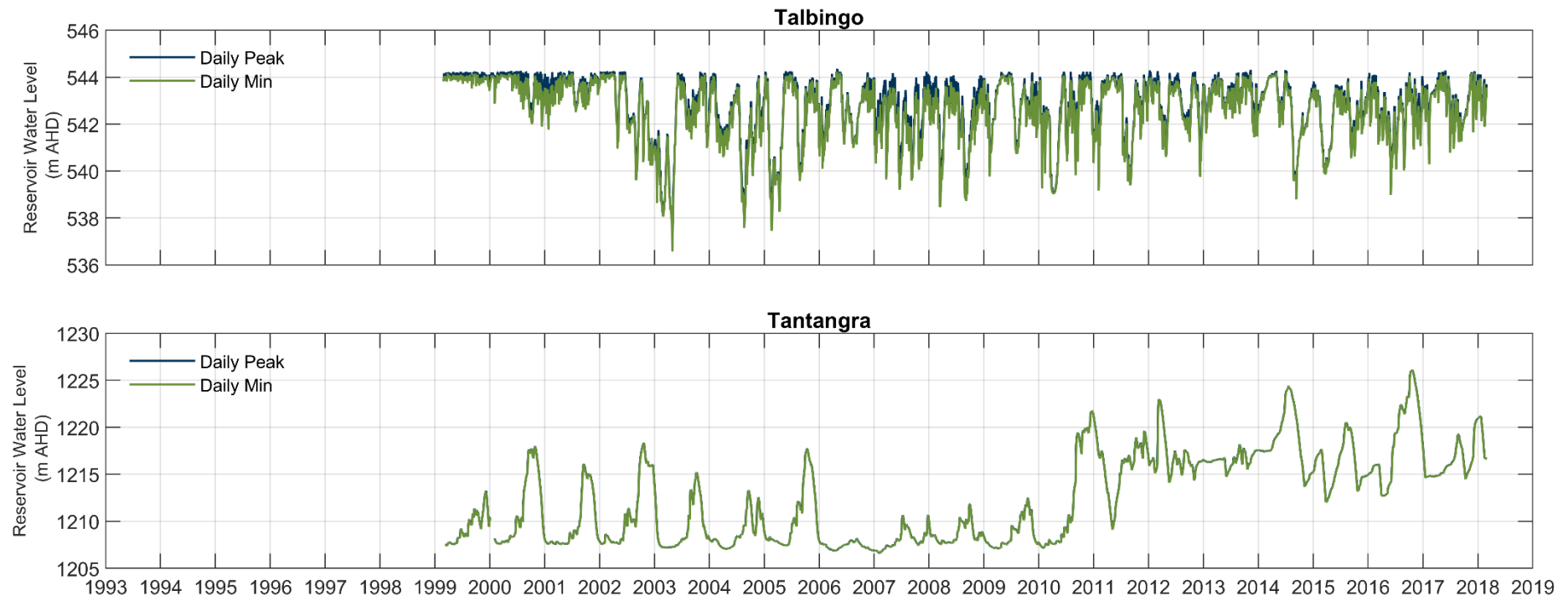


Figure C-1 Daily minimum and peak water levels at the Talbingo (top) and Tantangra (bottom) Reservoirs between 1993 and 2019

Reservoir Flows

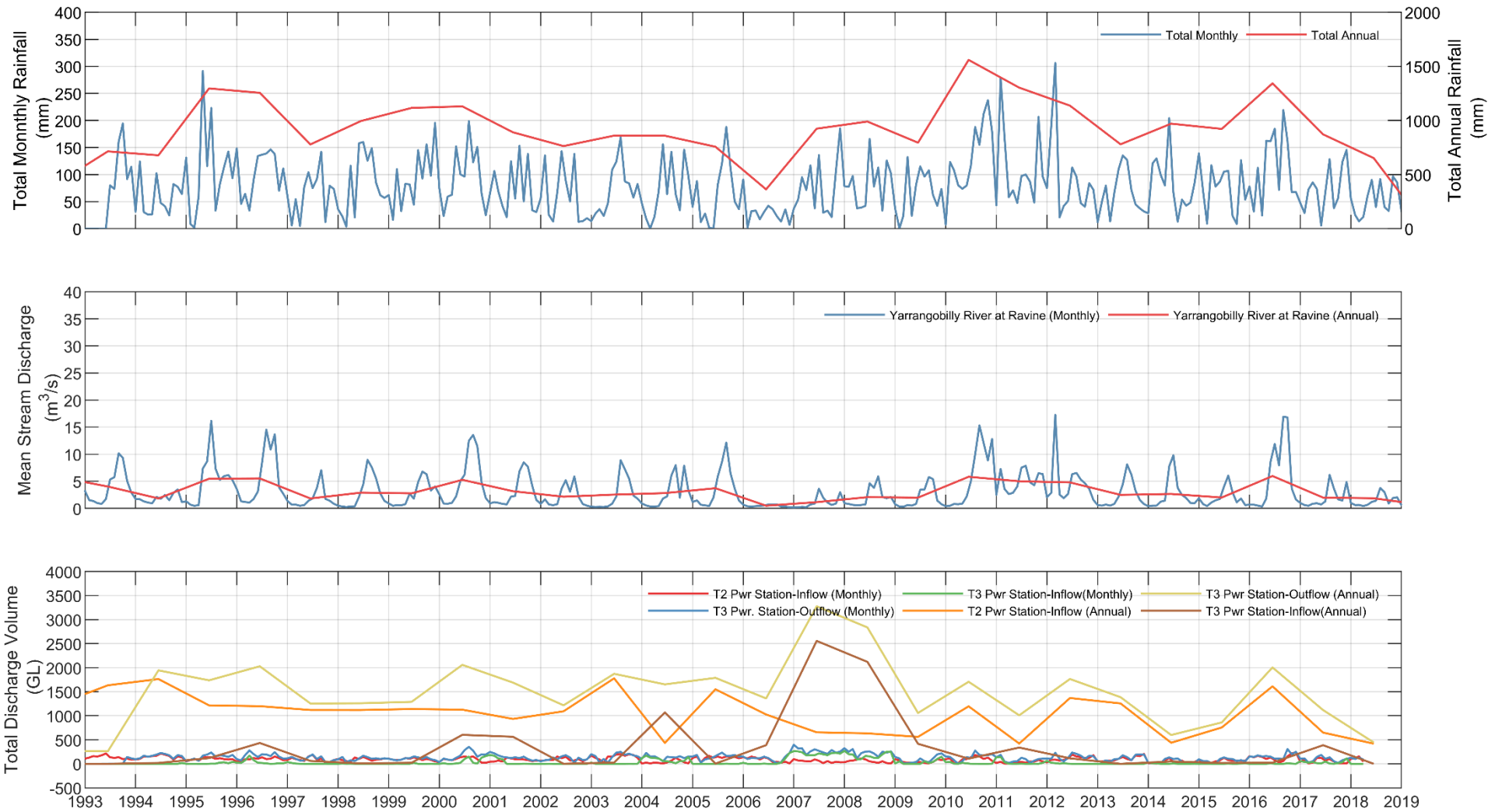


Figure C-2 Historical mean rainfall, stream discharges (inflows) and power station release (outflow)/ pumped storage (inflow) volumes at Talbingo Reservoir (1993 - 2019)

Table C-1 Total annual rainfall, mean stream flows and power station release (outflow)/ pumped storage (inflow) volumes at Talbingo Reservoir (1993-2019)

Year	Total Rainfall (mm)	Mean Flow Rate (m3/s) Yarrangobilly River at Ravine	Total Annual Power Station Flows (GL)			
			T3 Discharge (Outflow)	T3 Pumping (Inflow)	T2 discharge (Inflow)	Net Power Station Flows
1993	714	4.0	-	0.000	1,632.84	-
1994	677	1.8	1,943.48	18.06	1,762.97	-162.45
1995	1296	5.5	1,736.56	118.80	1,215.64	-402.12
1996	1255	5.5	2,028.65	433.23	1,198.69	-396.73
1997	778	1.8	1,254.75	60.30	1,119.38	-75.07
1998	995	2.9	1,259.43	8.10	1,118.77	-132.56
1999	1115	2.8	1,288.99	21.73	1,139.51	-127.76
2000	1130	5.3	2,057.87	602.46	1,126.33	-329.08
2001	890	3.2	1,689.35	562.93	933.63	-192.79
2002	763	2.1	1,216.82	1.33	1,092.47	-123.03
2003	859	2.5	1,872.06	27.01	1,777.62	-67.44
2004	858	2.8	1,652.11	1,068.40	434.68	-149.04
2005	757	3.7	1,788.06	4.50	1,549.55	-234.01
2006	363	0.5	1,360.13	387.90	1,026.49	54.26
2007	924	1.1	3,276.14	2,556.46	655.06	-64.63
2008	989	2.1	2,836.44	2,119.88	633.81	-82.75
2009	794	2.0	1,057.28	416.03	561.03	-80.22
2010	1559	5.8	1,706.37	107.40	1,195.91	-403.06
2011	1303	5.0	1,009.06	338.43	421.55	-249.08
2012	1136	4.8	1,763.95	114.86	1,368.43	-280.66
2013	779	2.5	1,385.73	0.13	1,255.96	-129.65
2014	970	2.7	599.06	48.65	437.91	-112.50
2015	921	2.0	860.76	17.69	755.92	-87.16
2016	1342	6.0	2,004.22	23.29	1,611.69	-369.24
2017	871	2.0	1,117.64	387.38	649.15	-81.11
2018	652	1.9	444.83	0.00	419.52	-25.30
2019	33	0.6	-	-	-	-

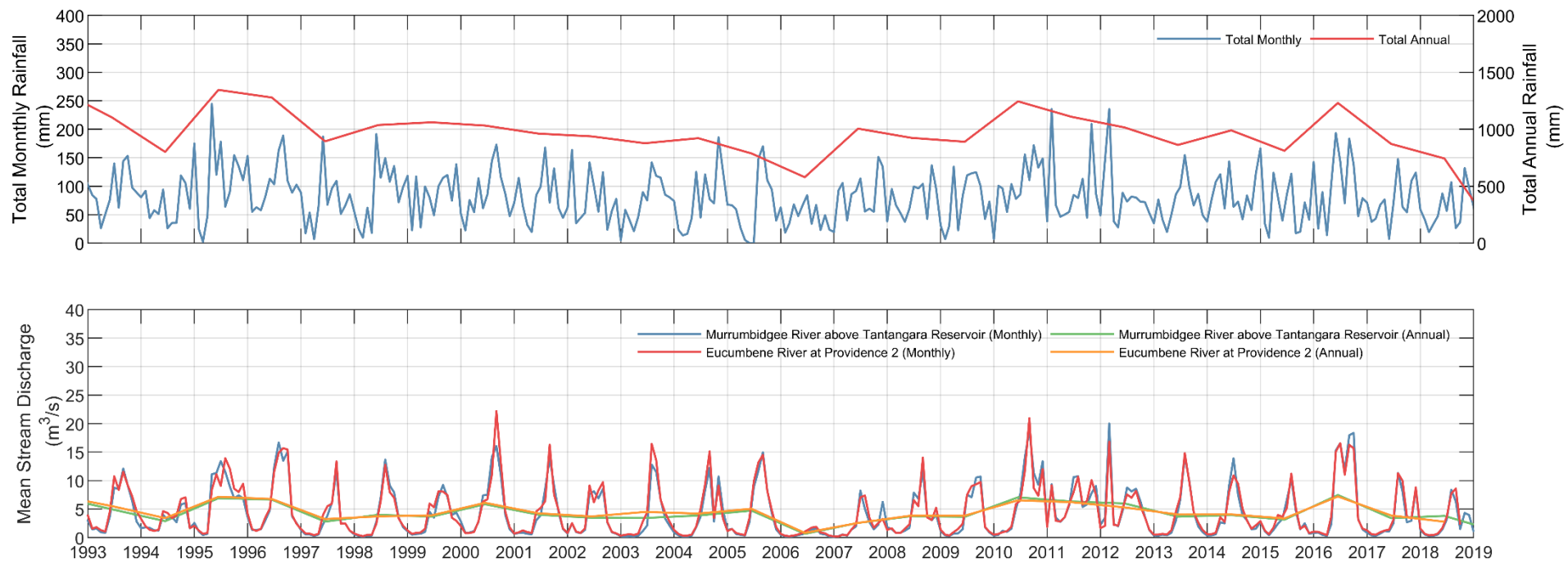


Figure C-3 Historical mean rainfall and stream discharges (inflows) at Tantangra Reservoir (1993 - 2019)

Table C-2

Total annual rainfall and mean stream flows at Tantangra Reservoir (1993-2019)

Year	Total Rainfall (mm)	Mean Flow Rate (m ³ /s)	
		Murrumbidgee River above Tantangara Reservoir	Eucumbene River at Providence 2
1993	1,104	5.0	5.5
1994	801	2.9	3.4
1995	1,345	6.9	7.2
1996	1,278	6.7	6.8
1997	894	2.8	3.2
1998	1,037	4.0	3.7
1999	1,061	3.7	3.9
2000	1,032	5.8	6.1
2001	962	4.0	4.3
2002	937	3.5	3.7
2003	877	3.4	4.5
2004	921	3.9	4.2
2005	787	4.7	5.1
2006	579	0.7	0.8
2007	1,005	2.6	2.6
2008	924	3.8	3.9
2009	890	3.6	3.8
2010	1,245	7.1	6.5
2011	1,109	6.3	6.2
2012	1,015	6.0	5.3
2013	862	3.7	4.0
2014	990	3.9	4.1
2015	810	3.1	3.4
2016	1,230	7.5	7.2
2017	871	3.4	3.9
2018	743	3.8	2.8
2019	64	1.0	-

APPENDIX

D

METEOROLOGICAL FIGURES

Talbingo Reservoir

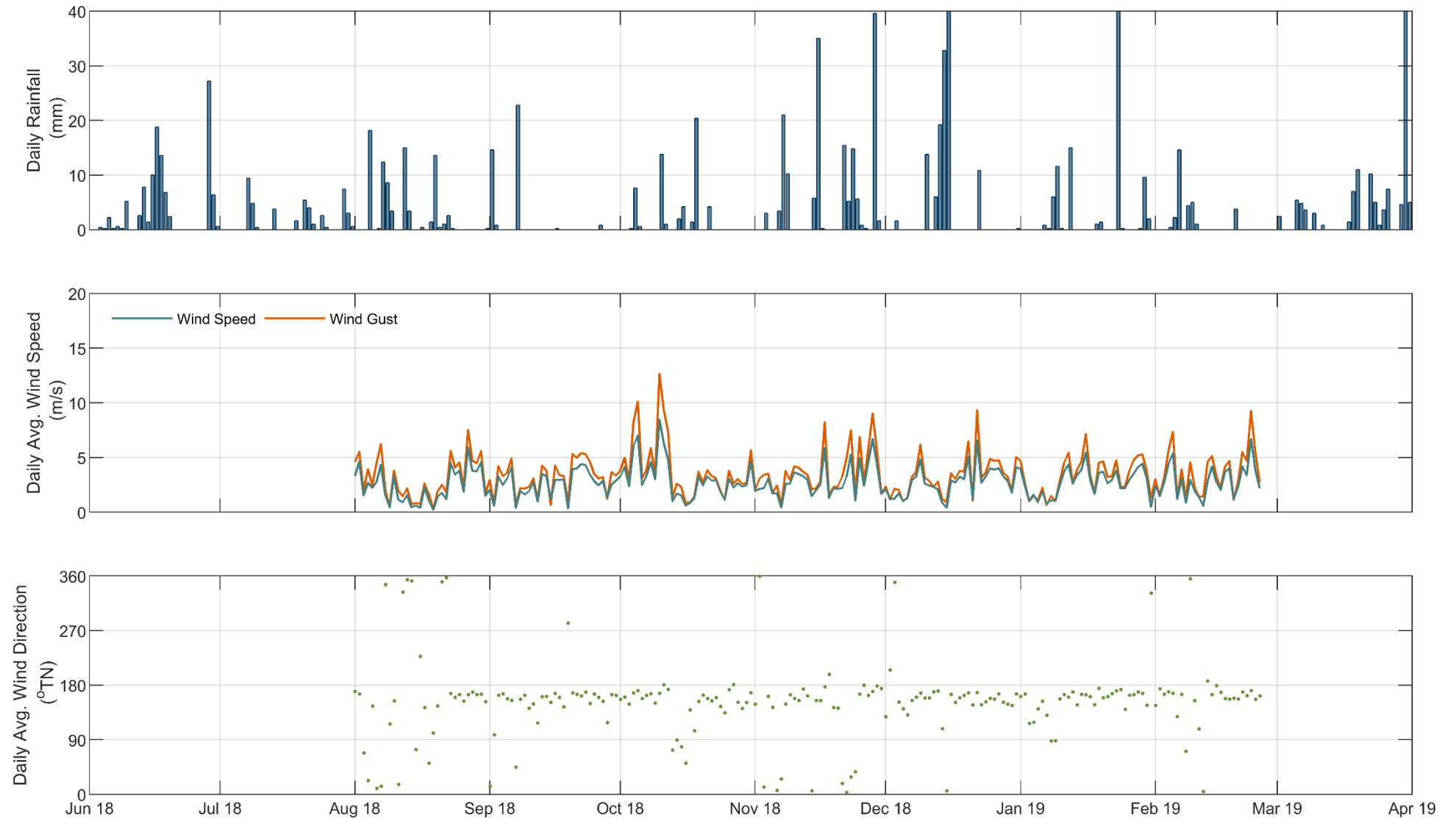


Figure D-1 Daily rainfall (top), wind speed (middle) and wind direction (bottom) time series at site TAL_01 near the dam wall

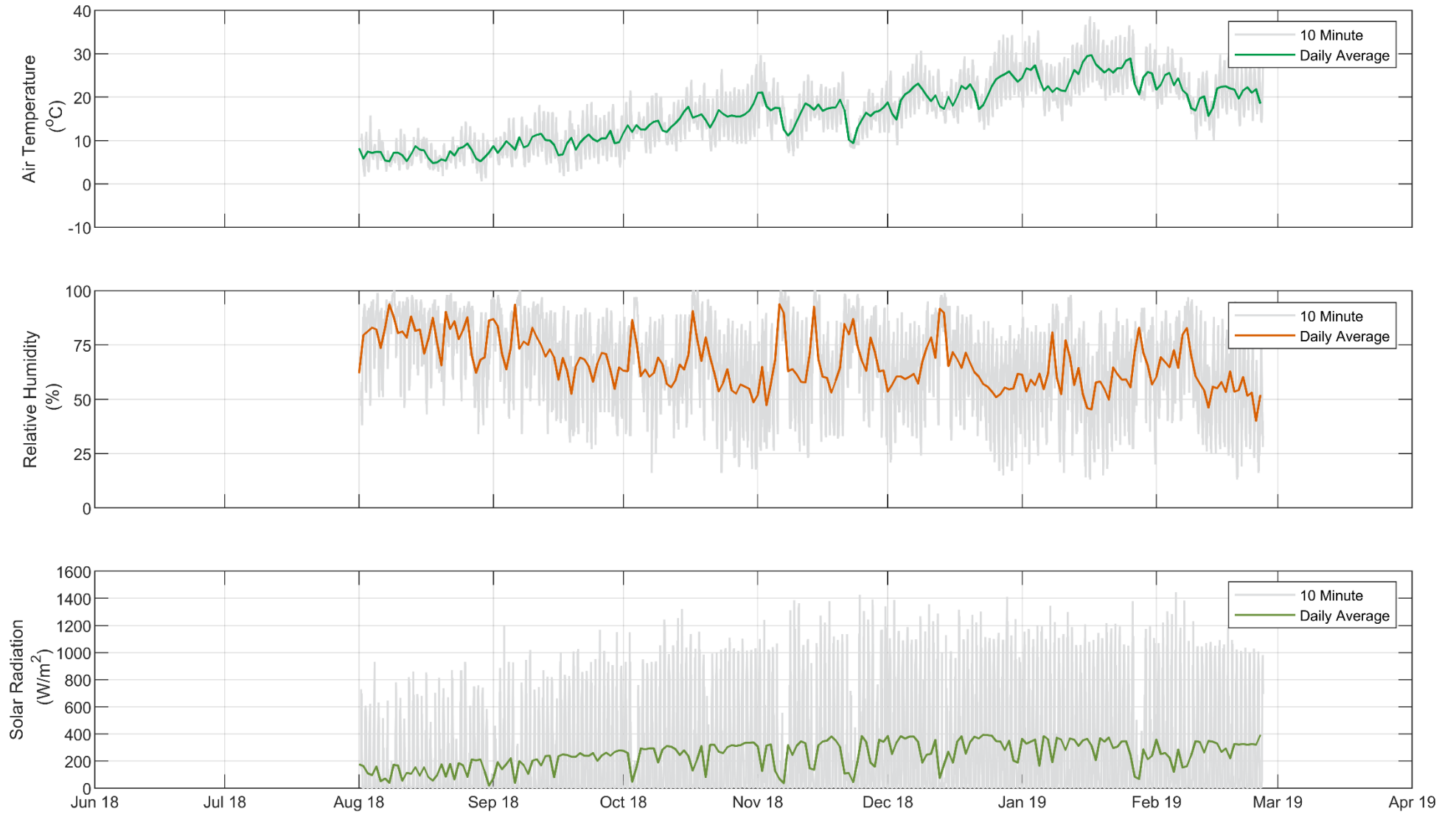


Figure D-2 Daily air temperature (top), relative humidity (middle) and solar radiation (bottom) time series at site TAL_01 near the dam wall

Tantangra Reservoir

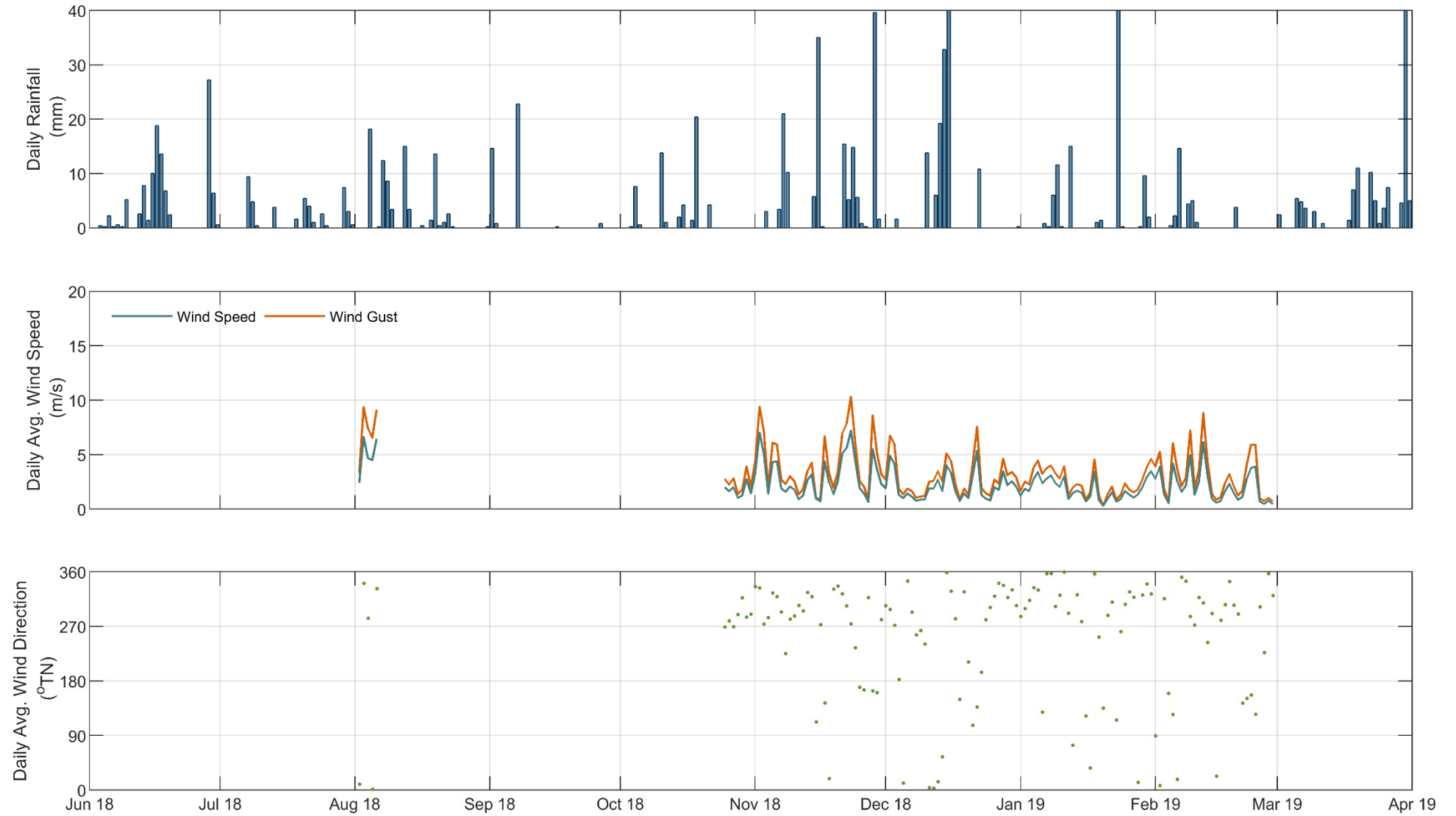


Figure D-3 Daily rainfall (top), wind speed (middle) and wind direction (bottom) time series at site TAN_02, 2 km upstream of the dam wall

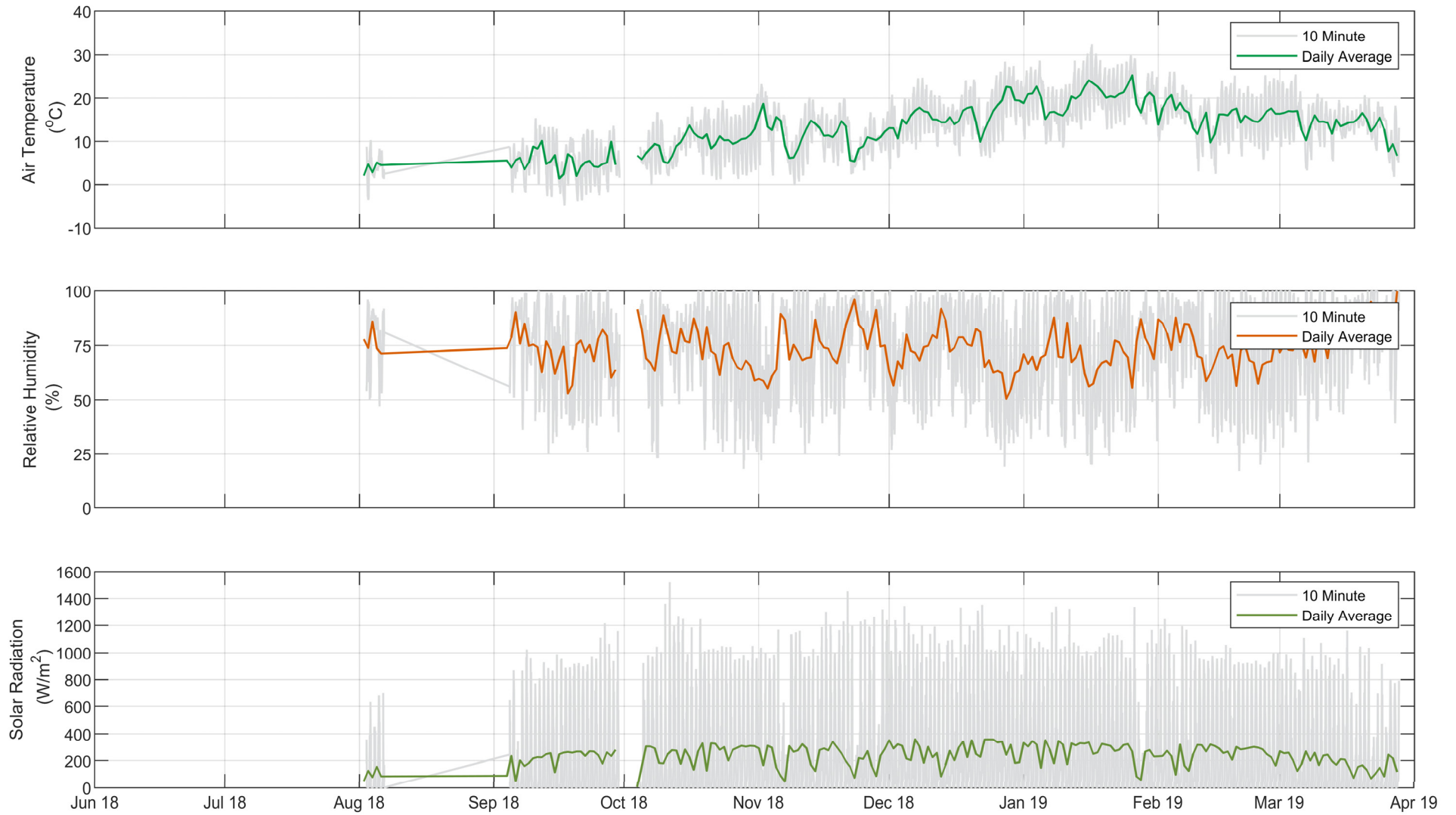


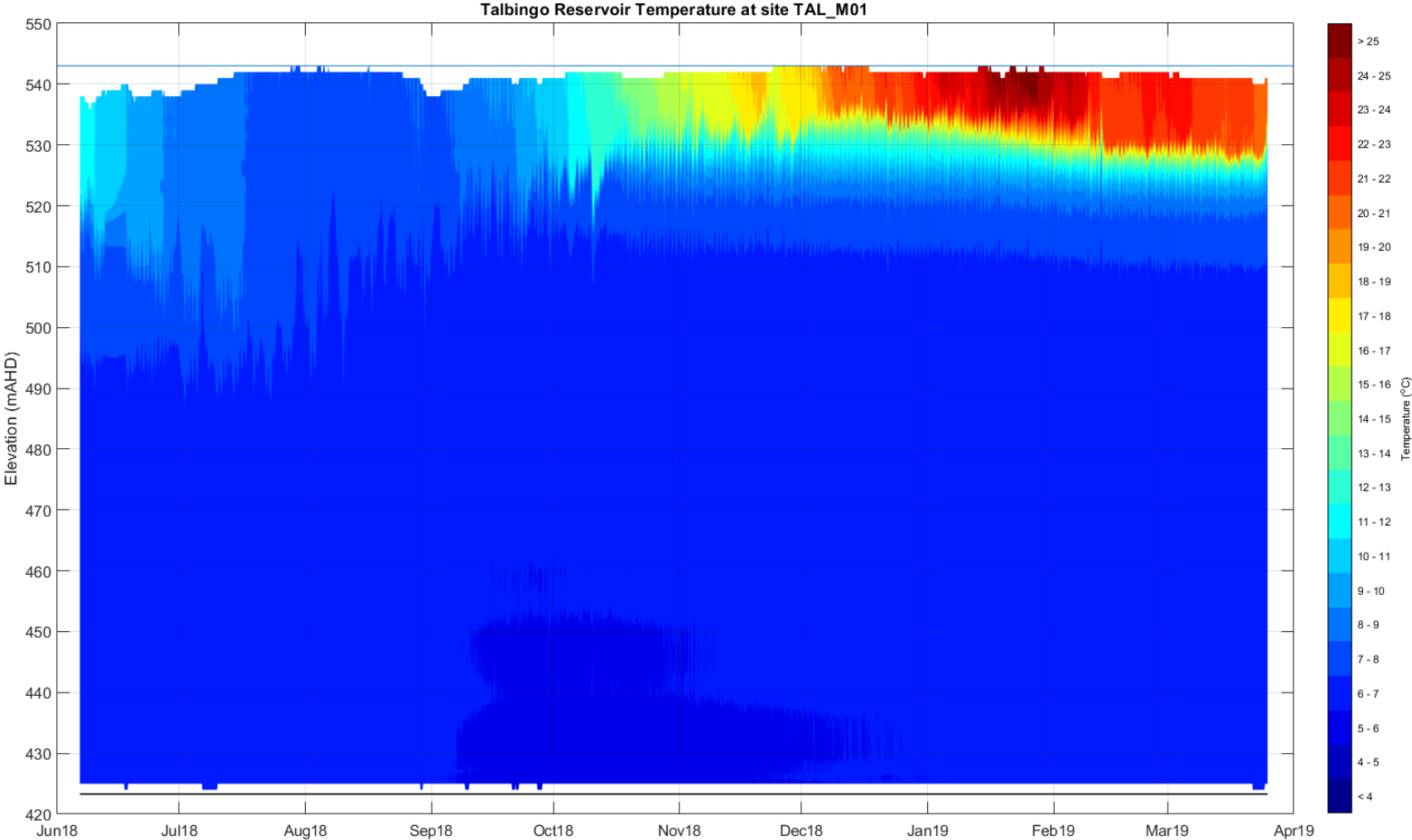
Figure D-4 Daily air temperature (top), relative humidity (middle) and solar radiation (bottom) time series at site TAN_02, 2 km upstream of the dam wall

APPENDIX

E

THERMISTOR STRING FIGURES

Figure E-1 Talbingo thermistor string temperature contours at site TAL_M01 near the dam wall. Water depth 129.7m below dam crest level (543 m AHD – blue line).



N:\Projects\599\FY18\111_EMMSnowHydroPhase 6 - Physical Limnology\Des_Ani\Matlab\Data Analysis\2. Thermistor's_plot_thermistor_data.m

Figure E-2 Talbingo thermistor string temperature contours at site TAL_M02 in the Yerrangobilly River arm. Water depth 51m below dam crest level (543 m AHD – blue line).

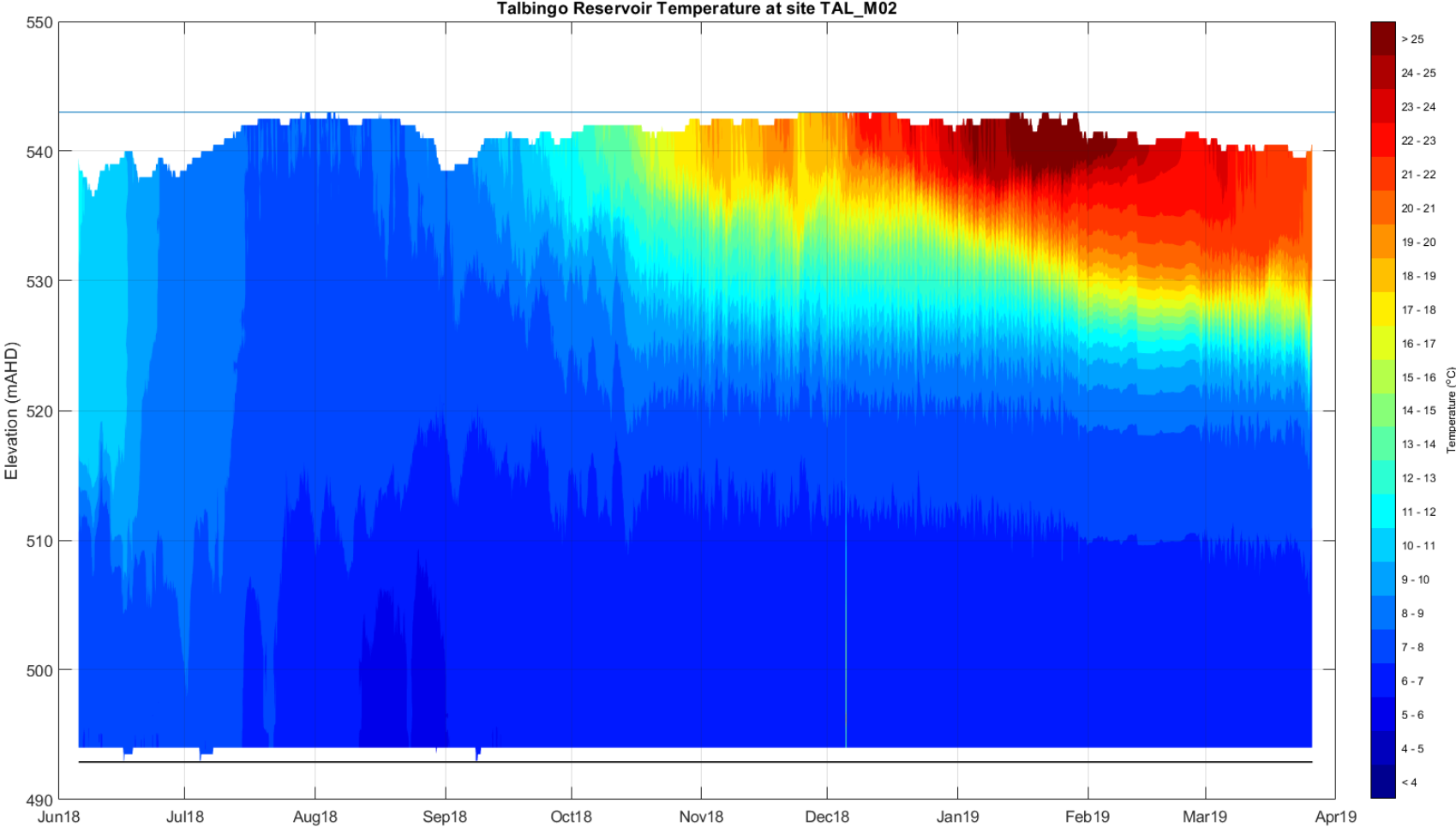
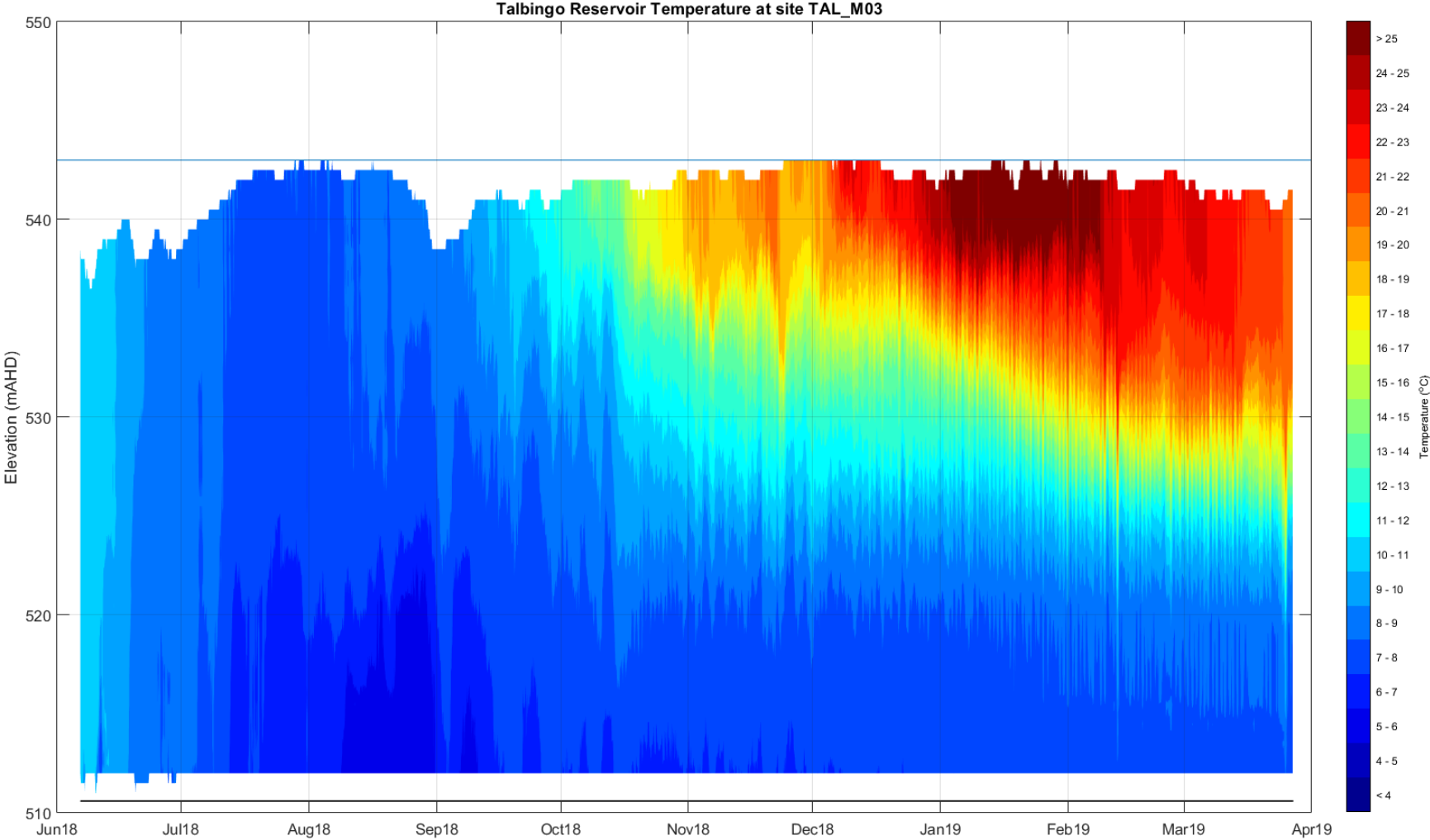
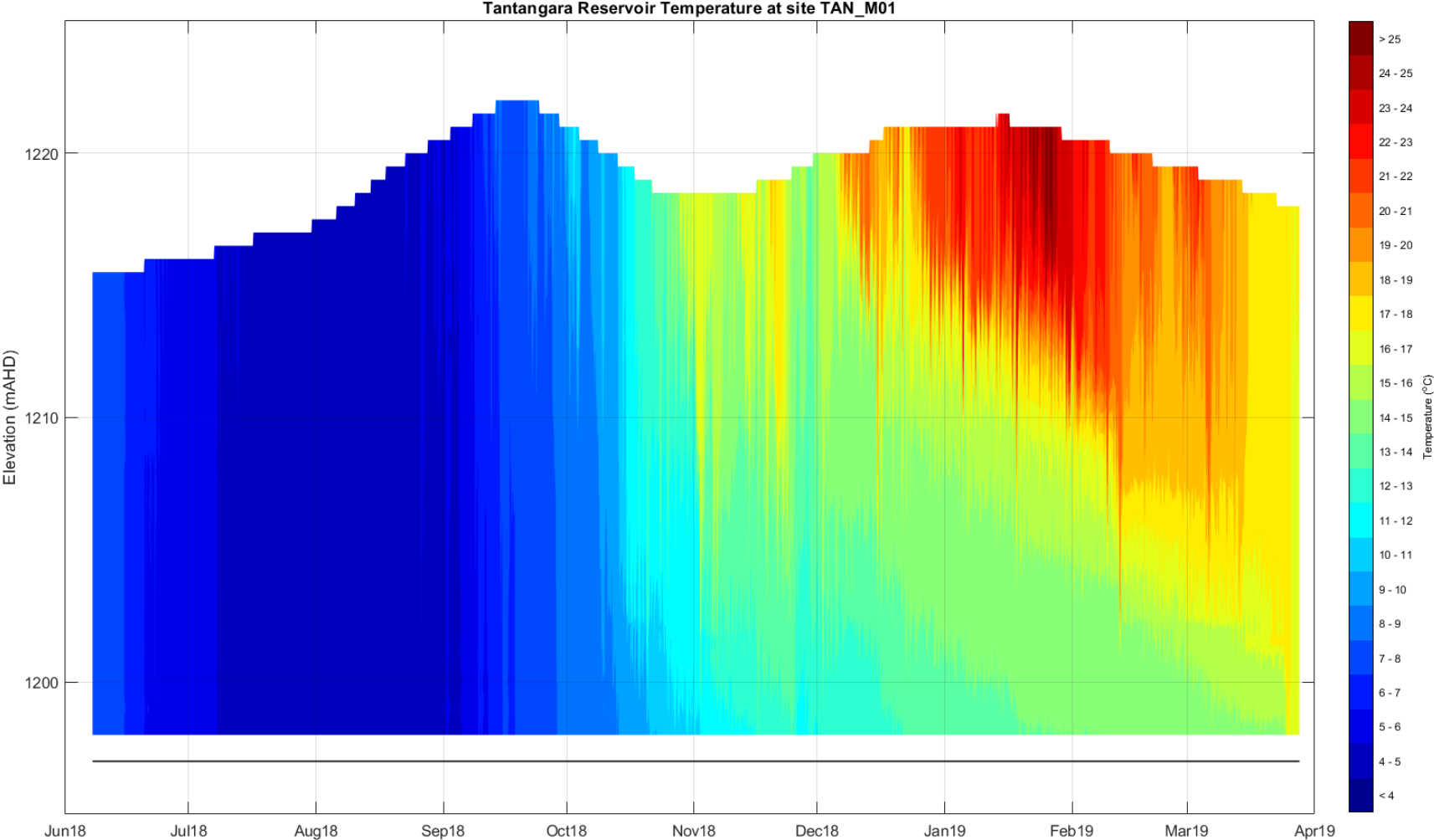


Figure E-3 Talbingo thermistor string temperature contours at site TAL_M03 in the Tumut River arm. Water depth 32.4m below dam crest level (543 m AHD – blue line).



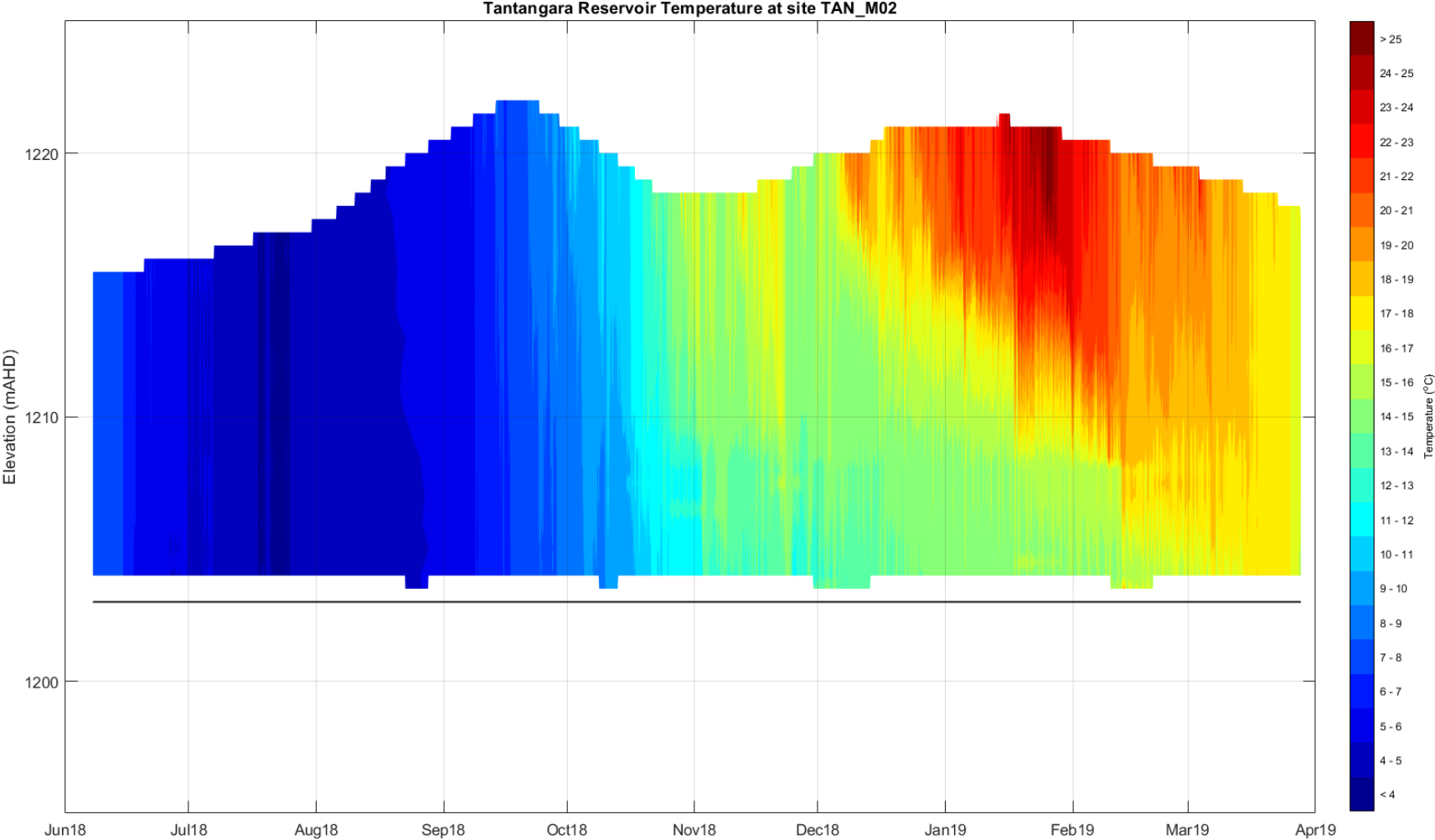
N:\Projects\599\FY18\111_EMMSnowHydroPhase 6 - Physical Limnology\Des_Ar\Matlab\Data Analysis\2. Thermistor's_plot_thermistor_data.m

Figure E-4 Tantangara thermistor string temperature contours at site TAN_M01 600m upstream of the dam wall. Water depth 33m below dam crest level (1230 m AHD).



N:\Projects\599\FY18\111_EMMSnowHydro\Phase 6 - Physical Limnology\Des_Ar\Matlab\Data Analysis\2. Thermistor\plot_thermistor_data.m

Figure E-5 Tantangara thermistor string temperature contours at site TAN_M02 2 km upstream of the dam wall. Water depth 27m below dam crest level (1230 m AHD).



N:\Projects\599\FY18\111_EMMSnowHydroPhase 6 - Physical Limnology\Des_Ar\Matlab\Data Analysis\2_Thermistor\plot_thermistor_data.m

APPENDIX

F

CTD PROFILES

Talbingo Reservoir – 22nd March 2018

Figure F-1 Talbingo Reservoir CTD Profile, site TAL_01 at 0713 on 22 March 2018

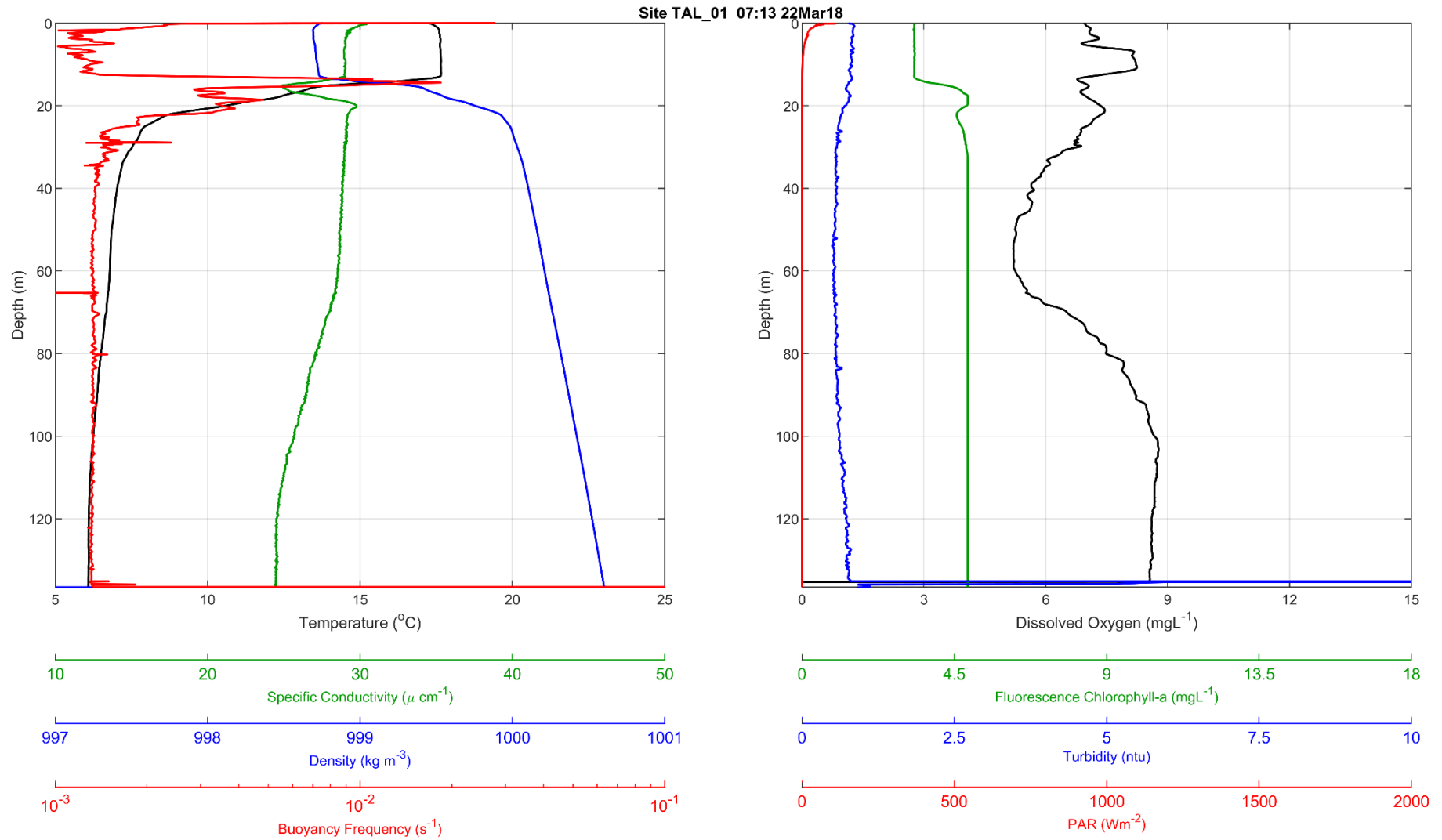


Figure F-2 Talbingo Reservoir CTD Profile, site TAL_05 at 1129 on 22 March 2018

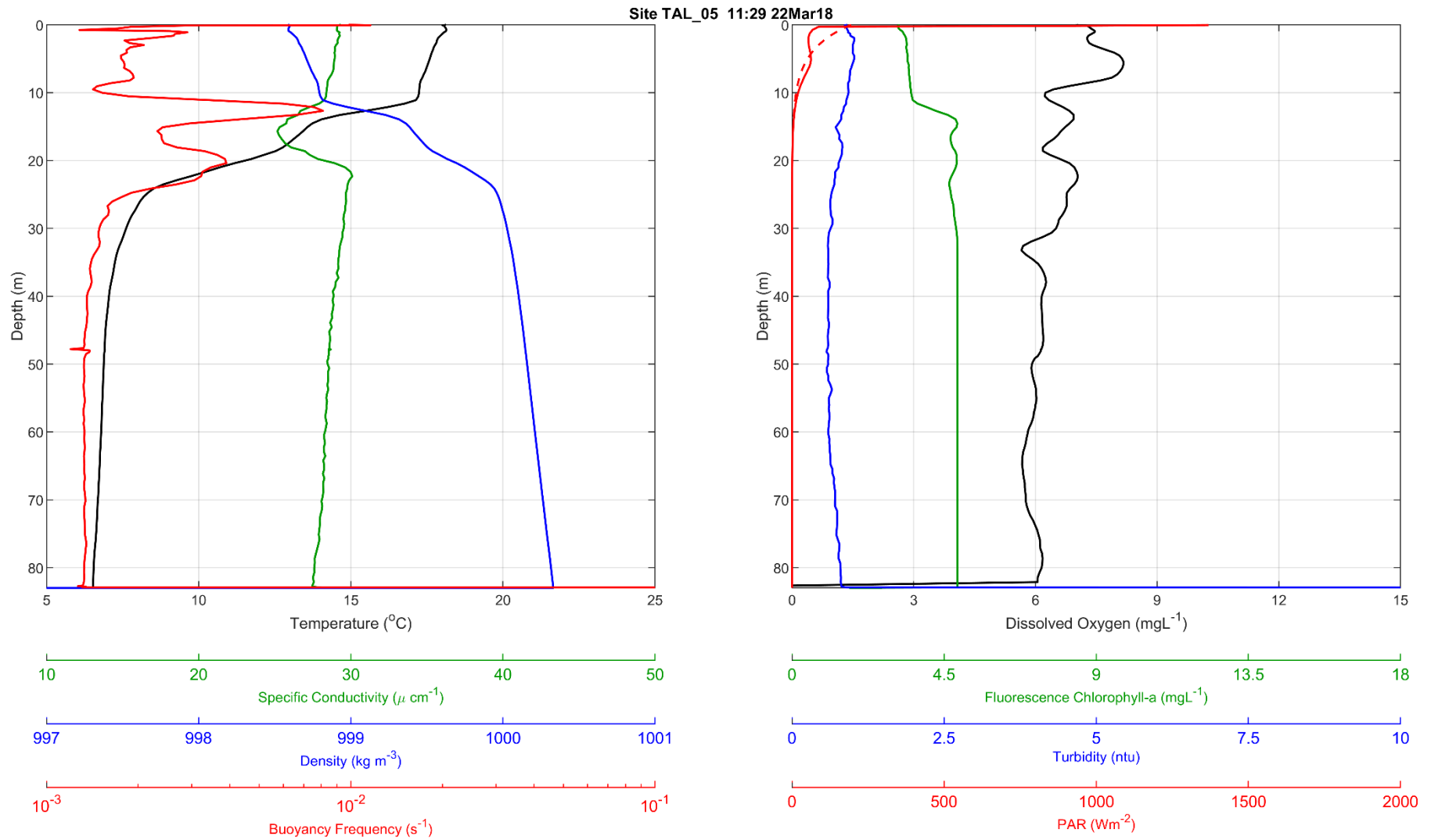


Figure F-3 Talbingo Reservoir CTD Profile, site TAL_07 at 1116 on 22 March 2018

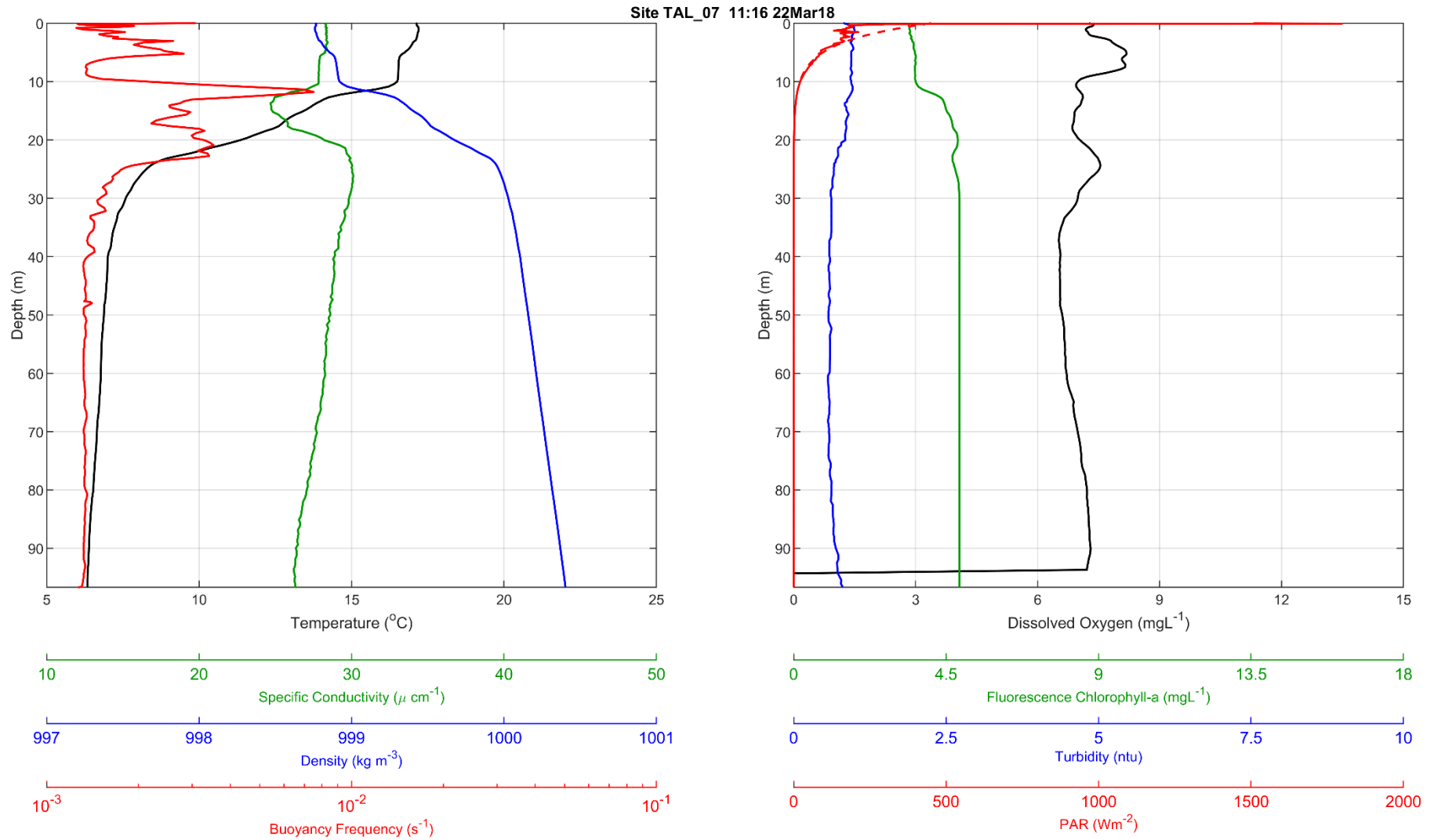


Figure F-4 Talbingo Reservoir CTD Profile, site TAL_08 at 1105 on 22 March 2018

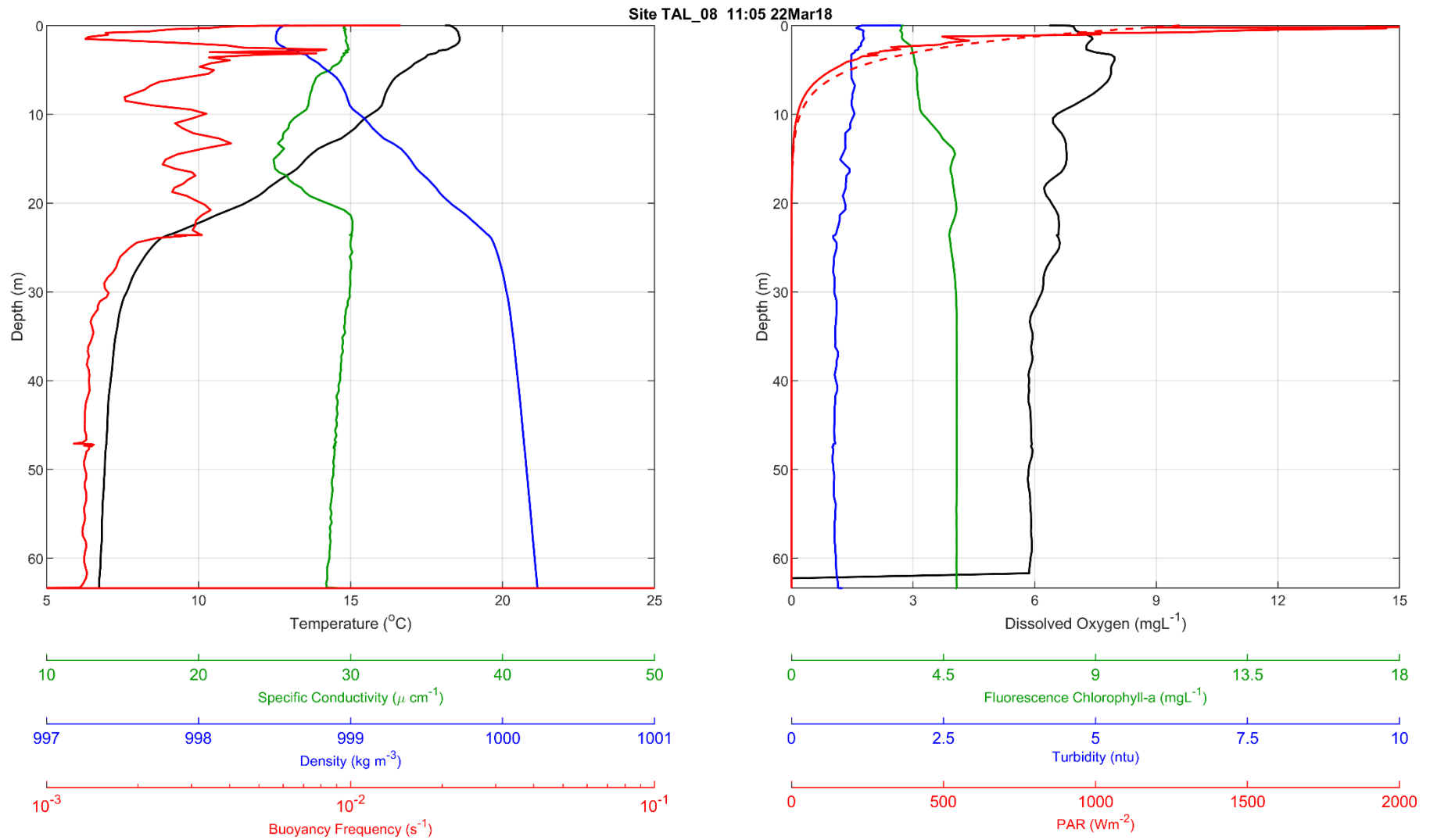


Figure F-5 Talbingo Reservoir CTD Profile, site TAL_09 at 1049 on 22 March 2018

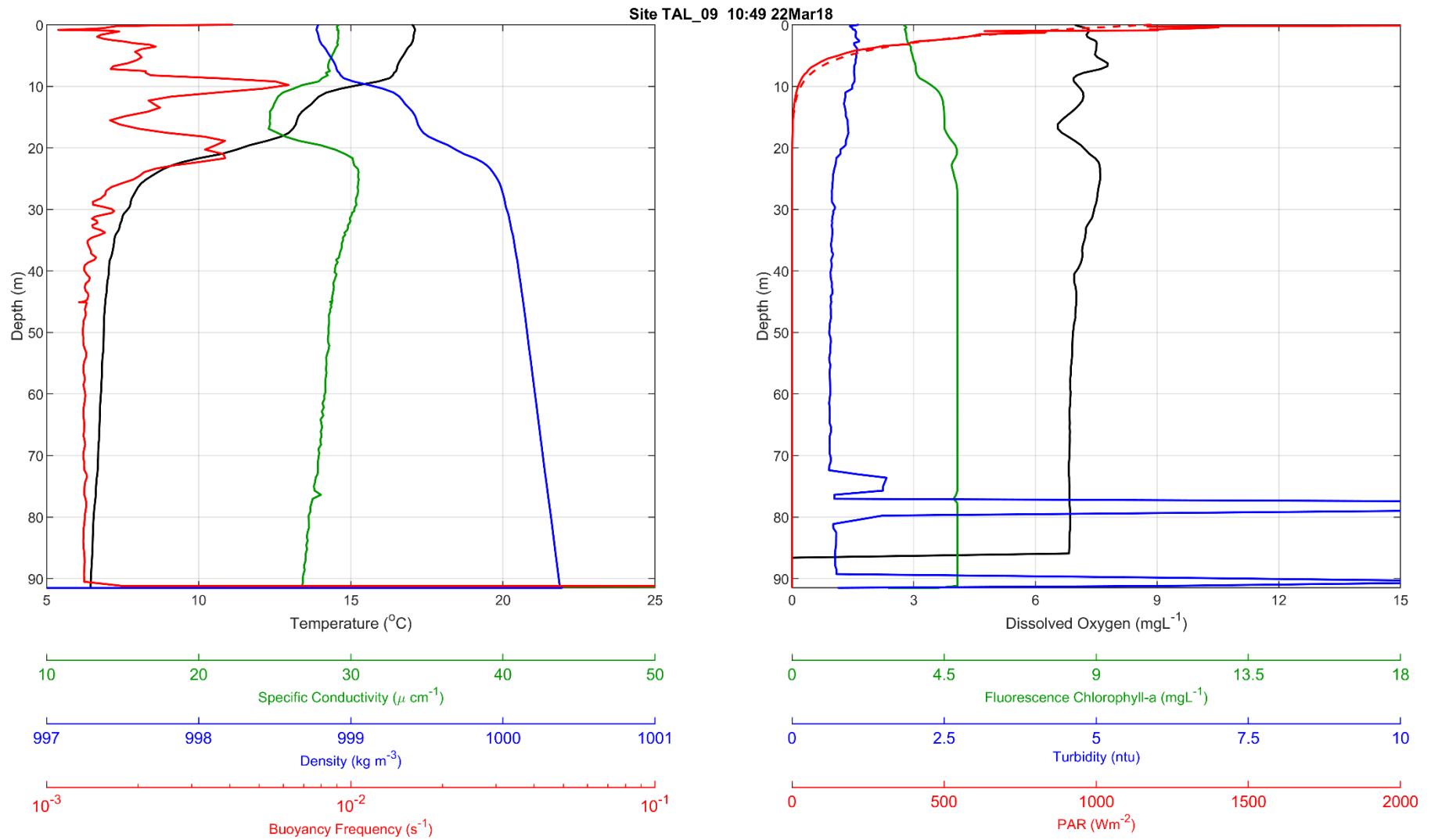


Figure F-6 Talbingo Reservoir CTD Profile, site TAL_10 at 1036 on 22 March 2018

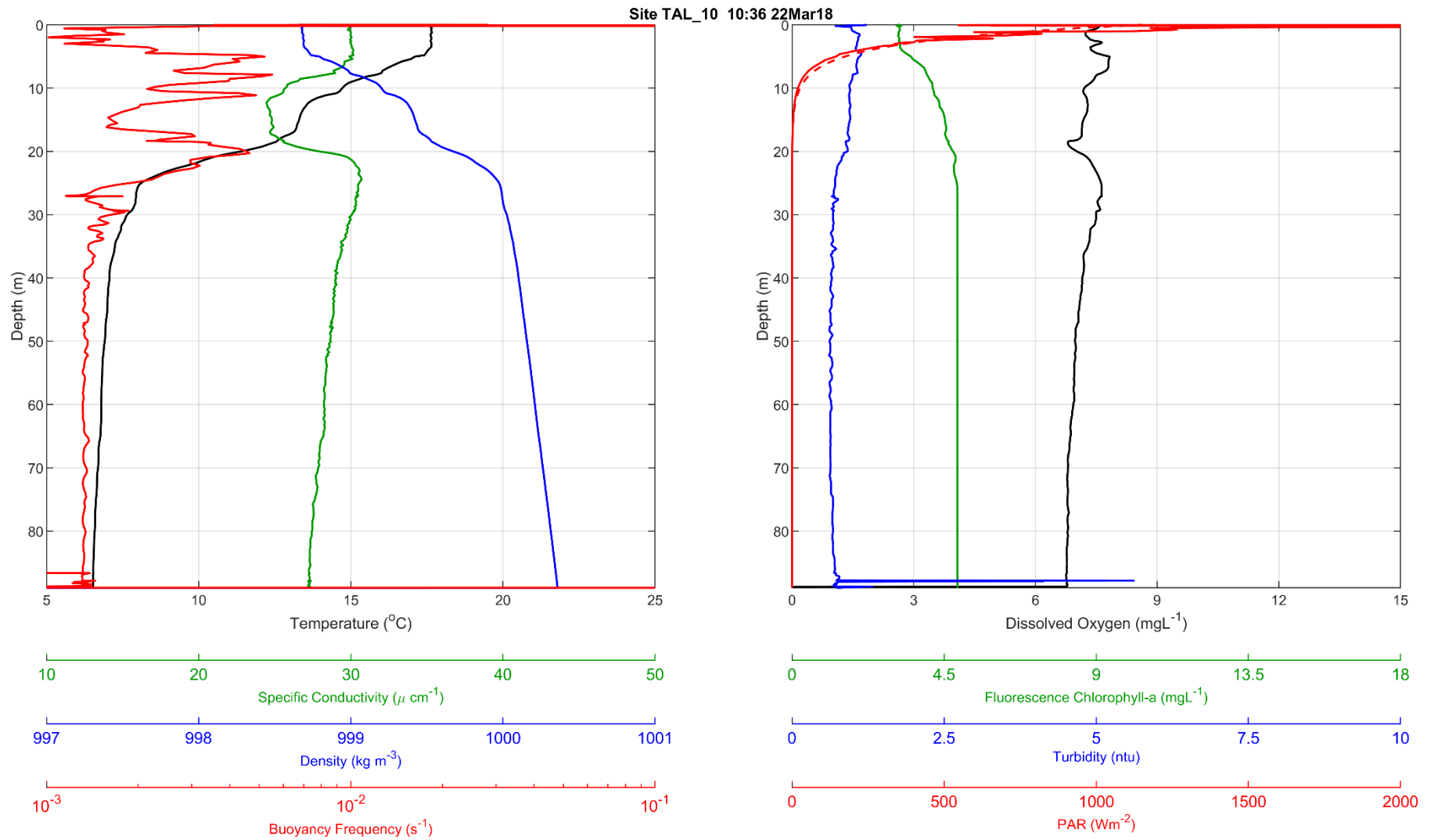


Figure F-7 Talbingo Reservoir CTD Profile, site TAL_11 at 1025 on 22 March 2018

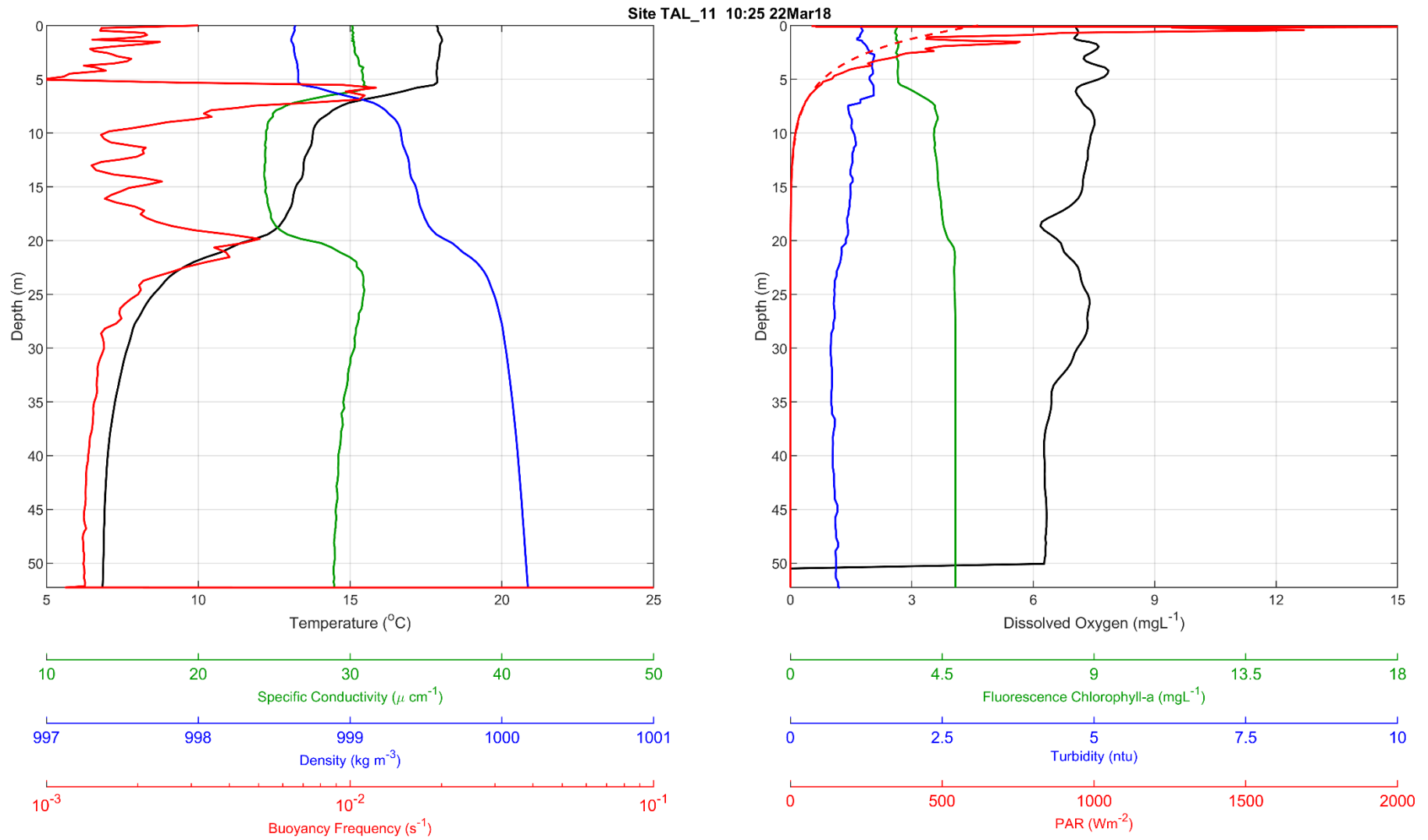


Figure F-8 Talbingo Reservoir CTD Profile, site TAL_12 at 1010 on 22 March 2018

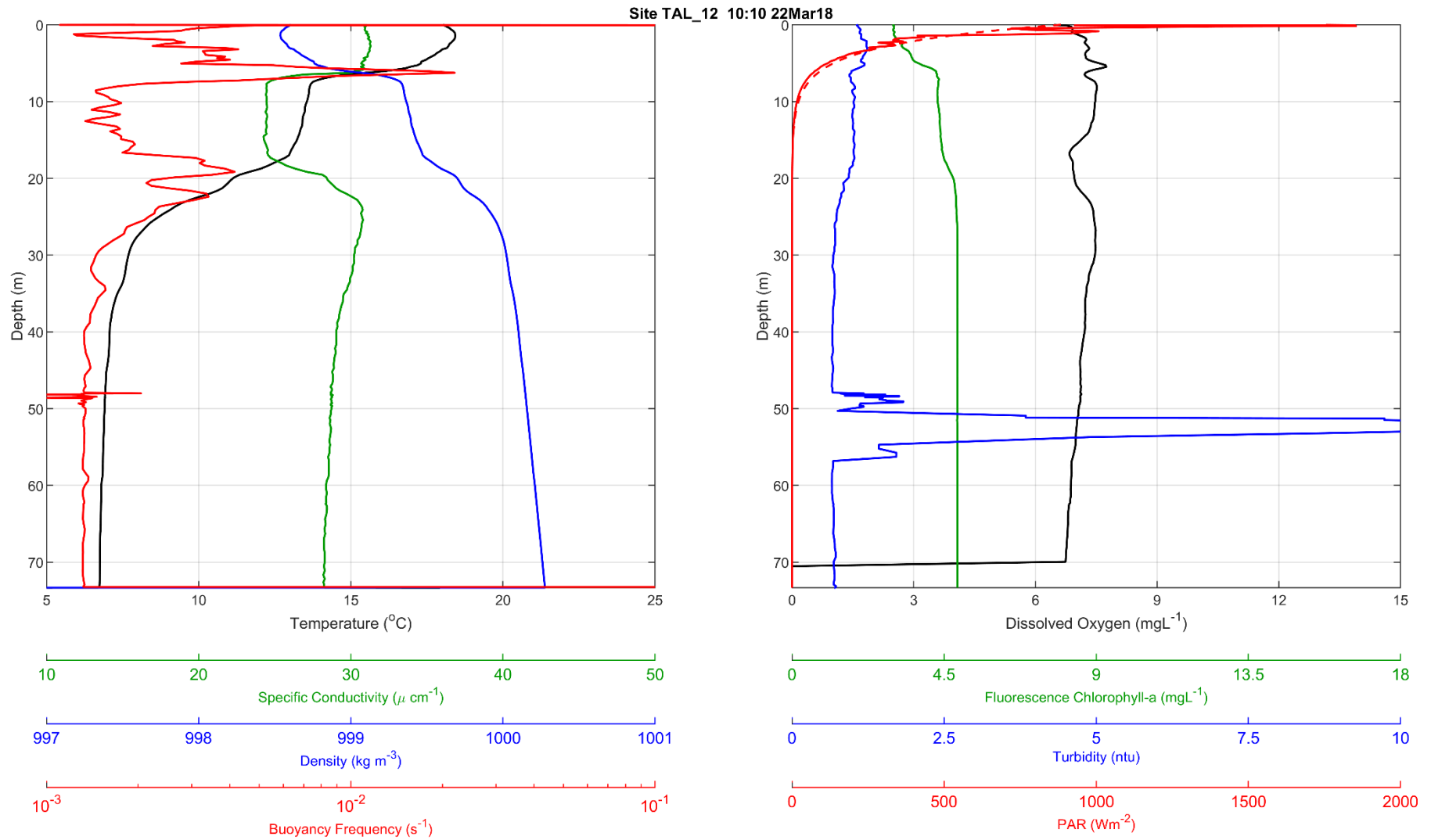


Figure F-9 Talbingo Reservoir CTD Profile, site TAL_13 at 0958 on 22 March 2018

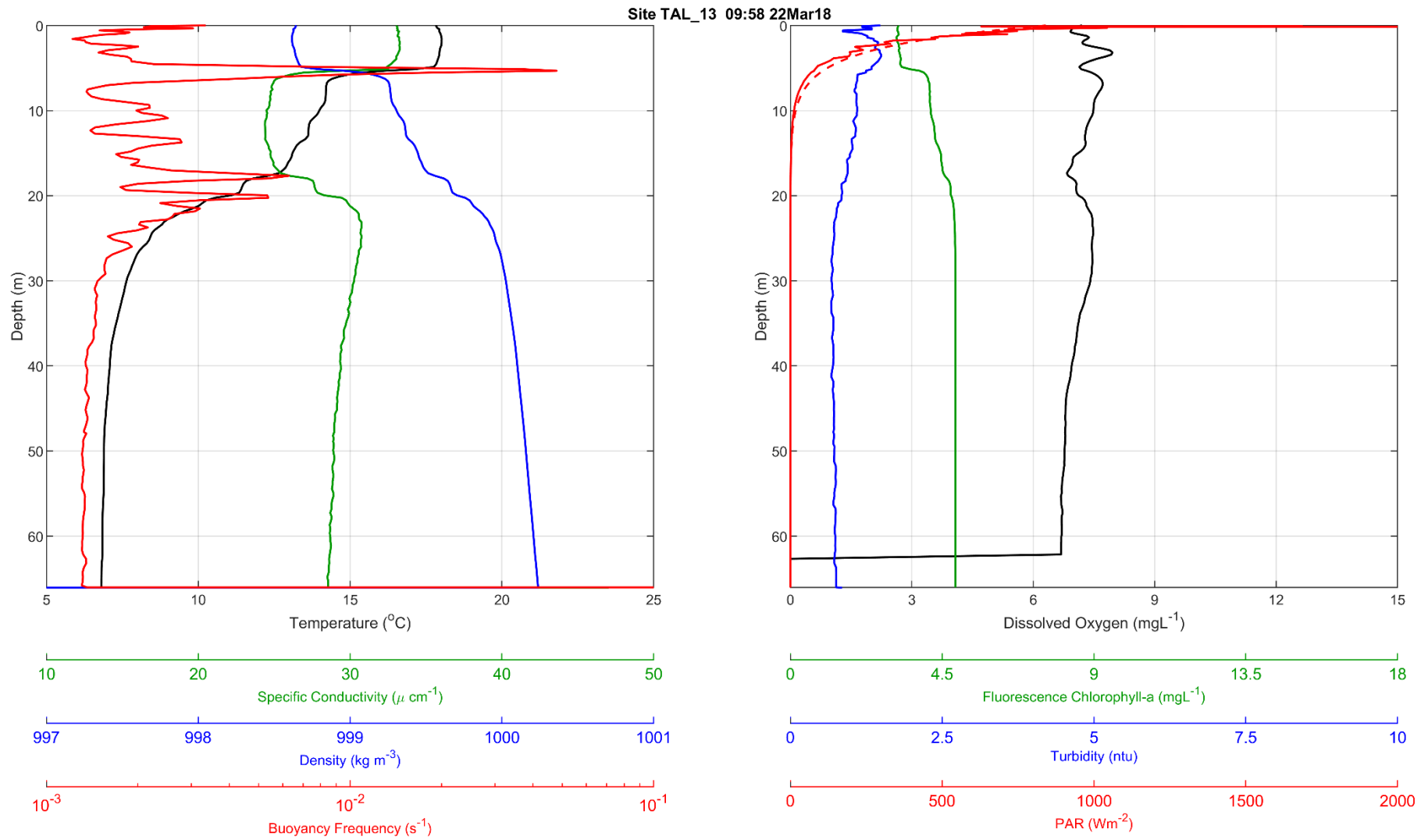


Figure F-10 Talbingo Reservoir CTD Profile, site TAL_14 at 0933 on 22 March 2018

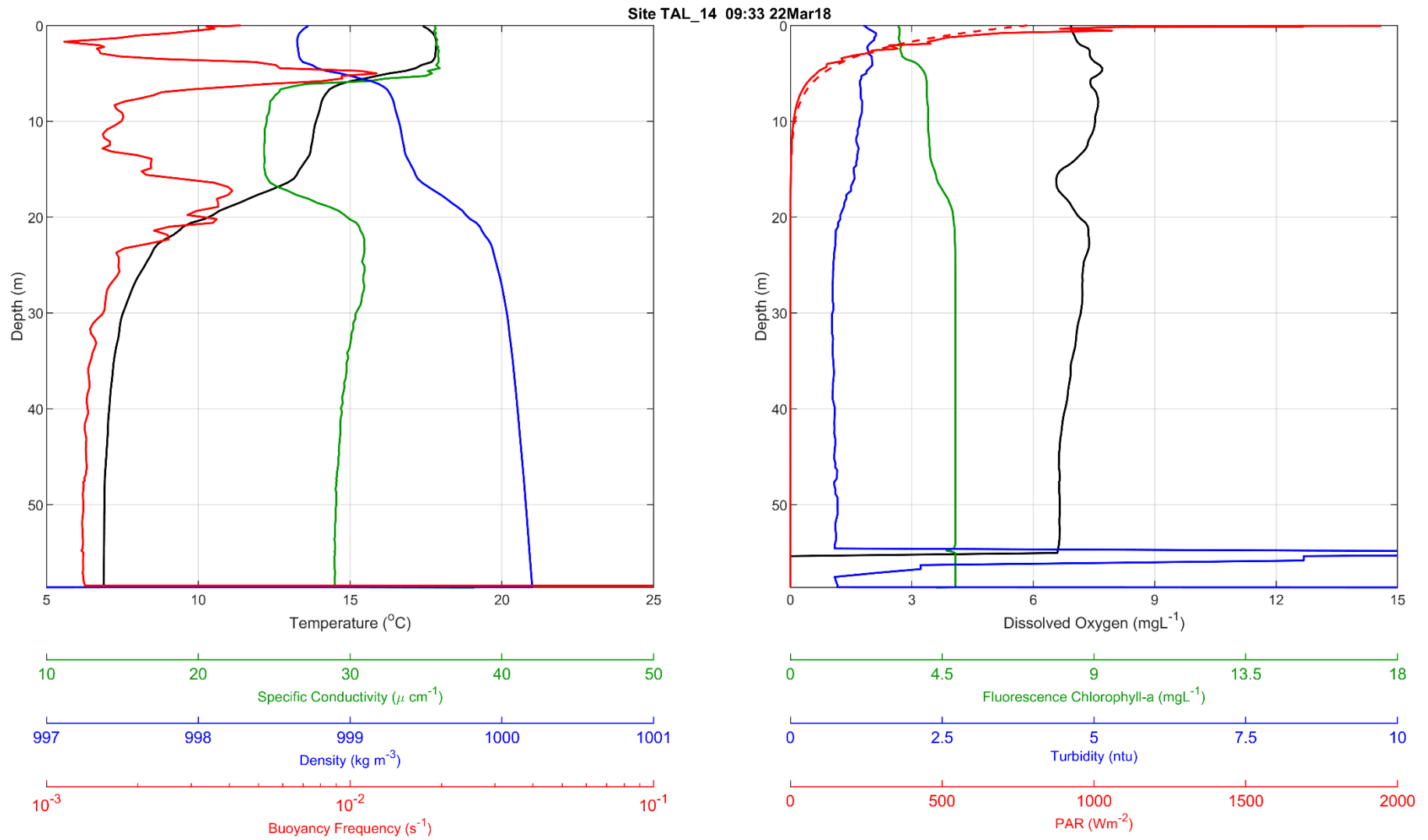


Figure F-11 Talbingo Reservoir CTD Profile, site TAL_15 at 0942 on 22 March 2018

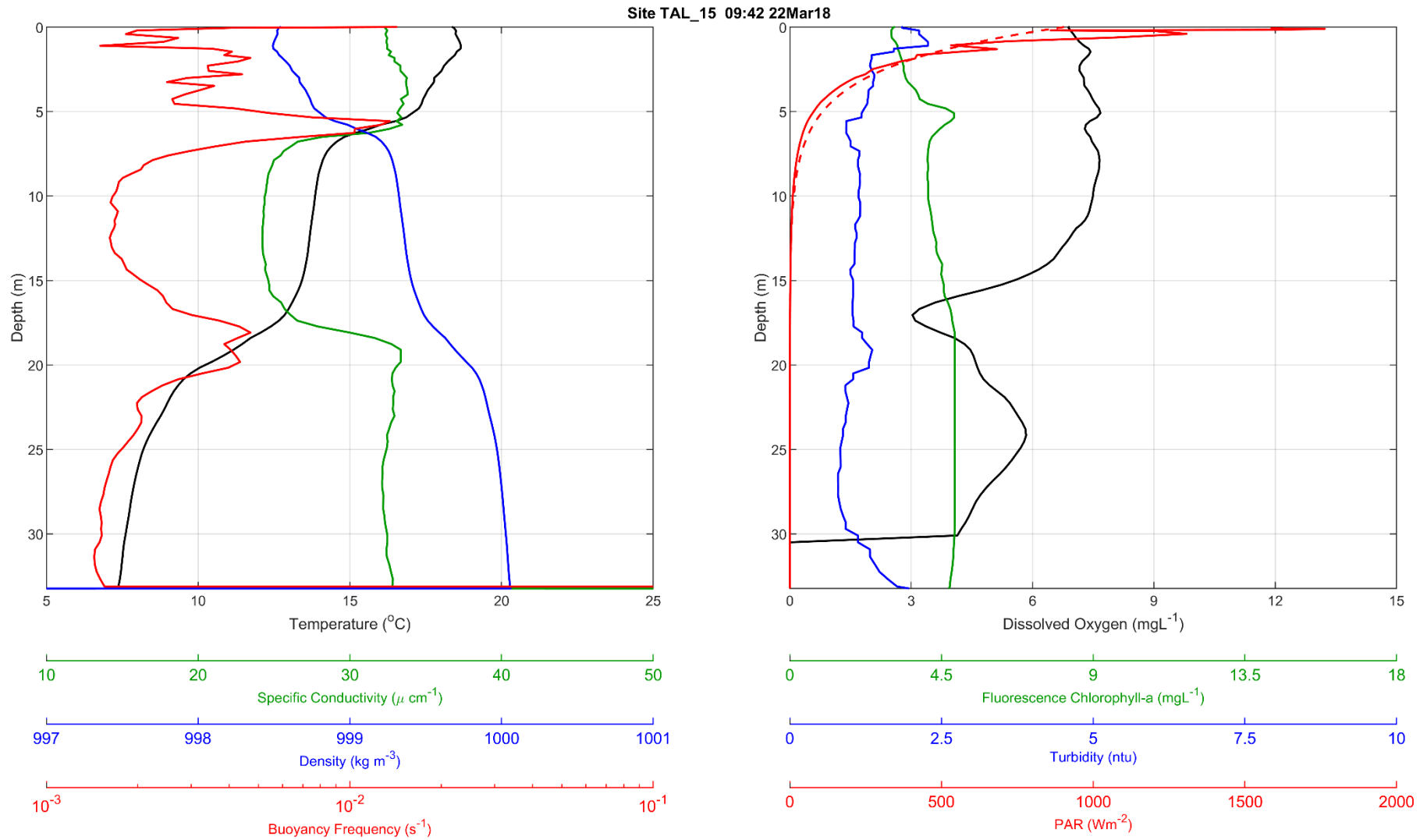


Figure F-12 Talbingo Reservoir CTD Profile, site TAL_16 at 0923 on 22 March 2018

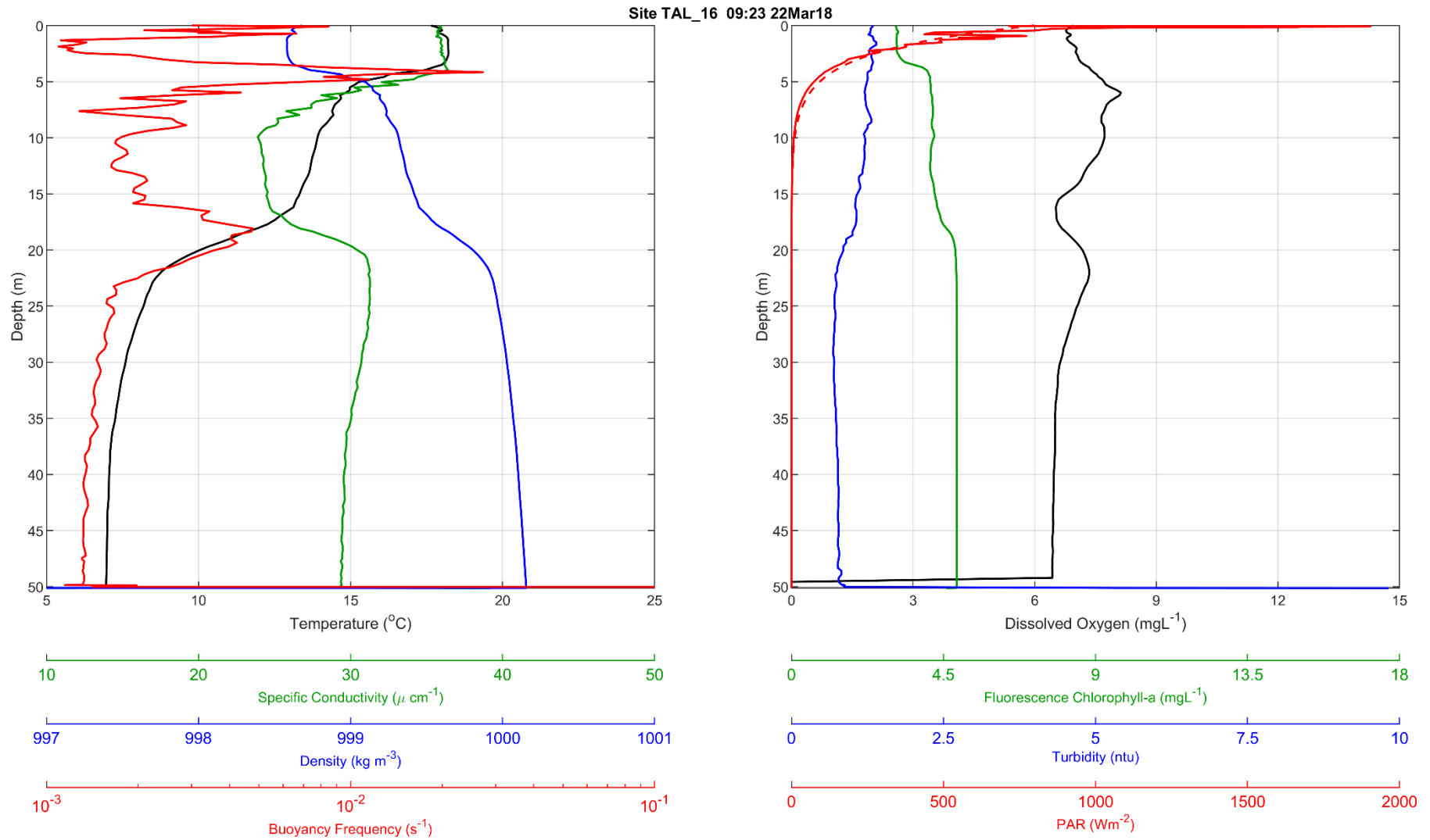


Figure F-13 Talbingo Reservoir CTD Profile, site TAL_17 at 0914 on 22 March 2018

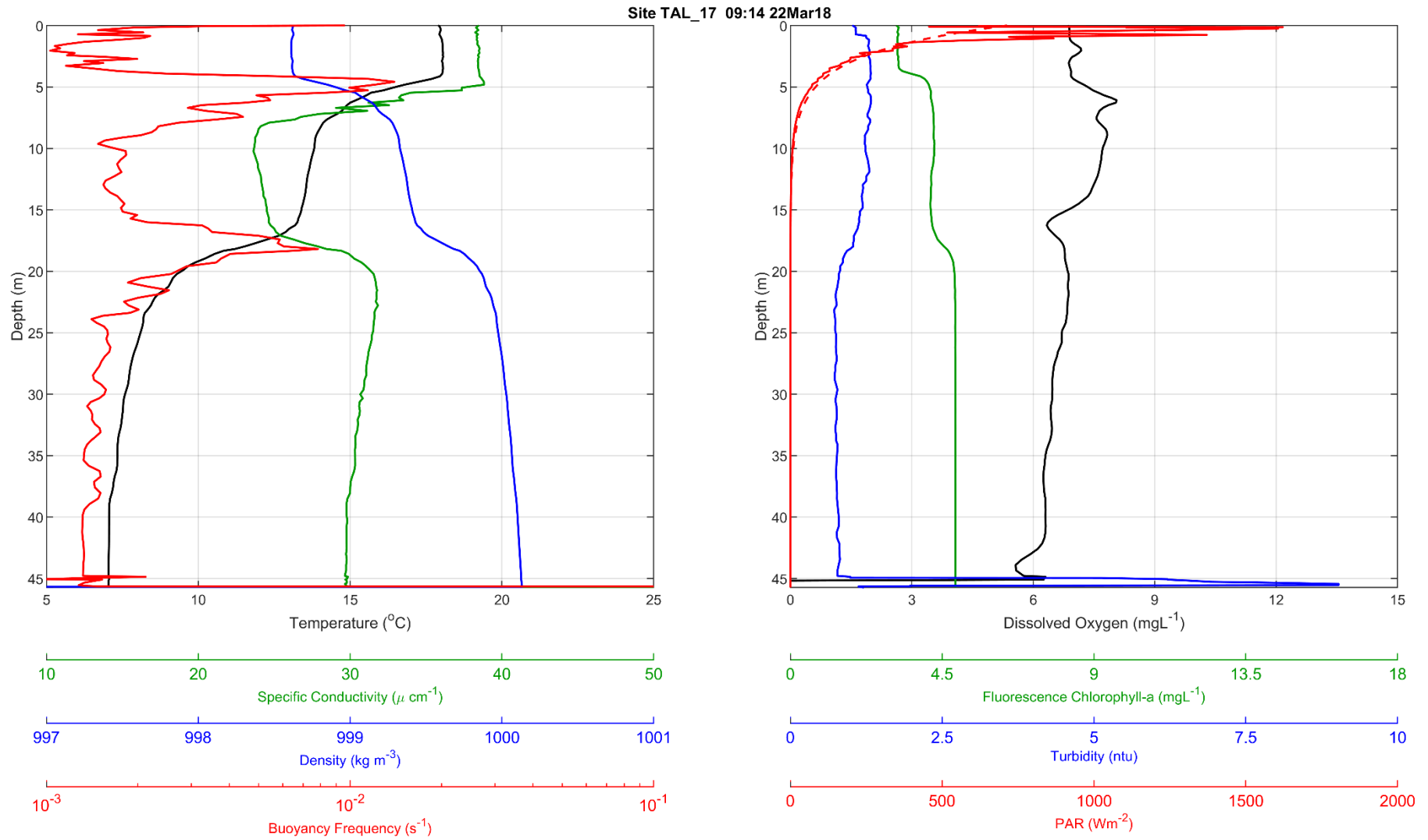


Figure F-14 Talbingo Reservoir CTD Profile, site TAL_18 at 0906 on 22 March 2018

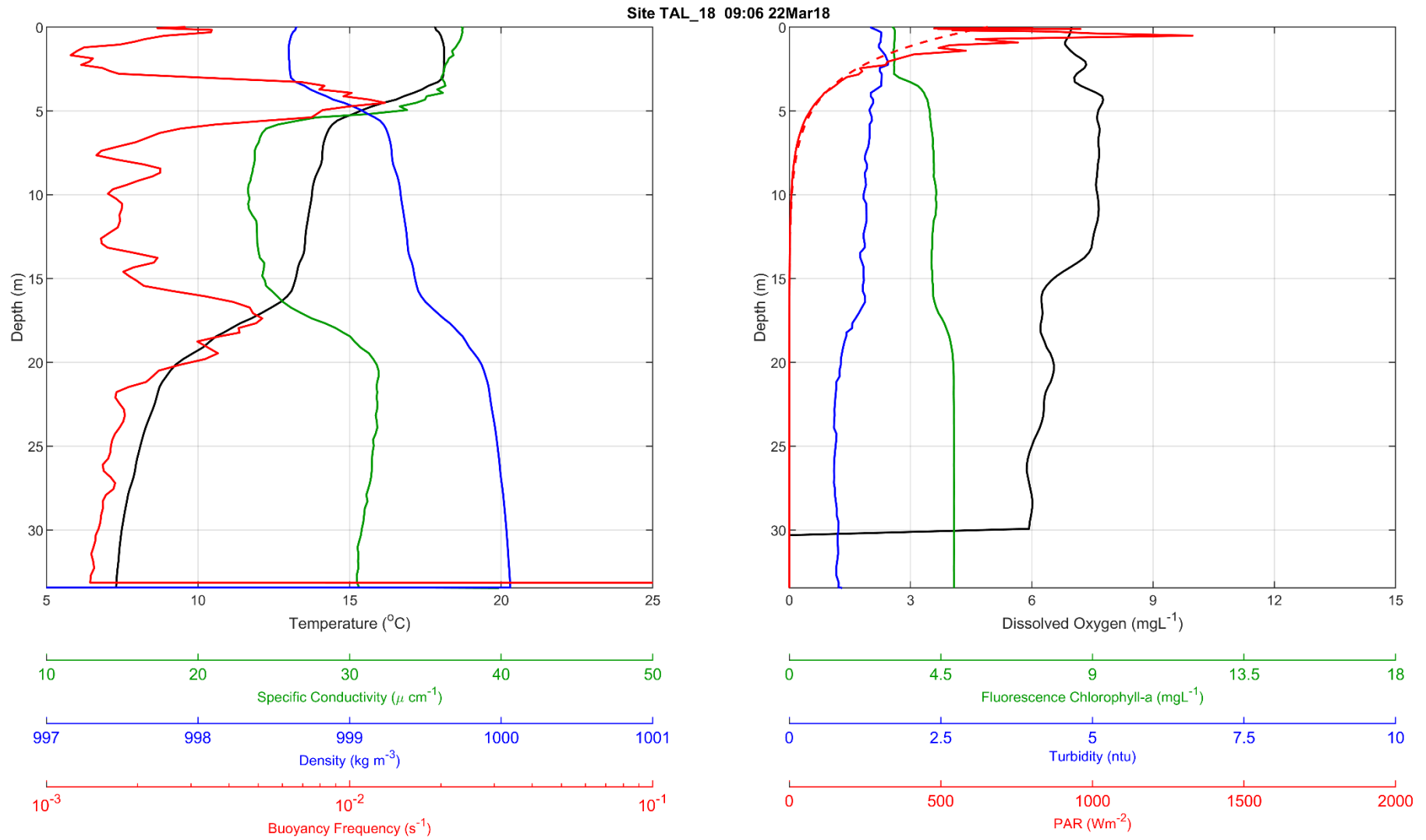


Figure F-15 Talbingo Reservoir CTD Profile, site TAL_19 at 0840 on 22 March 2018

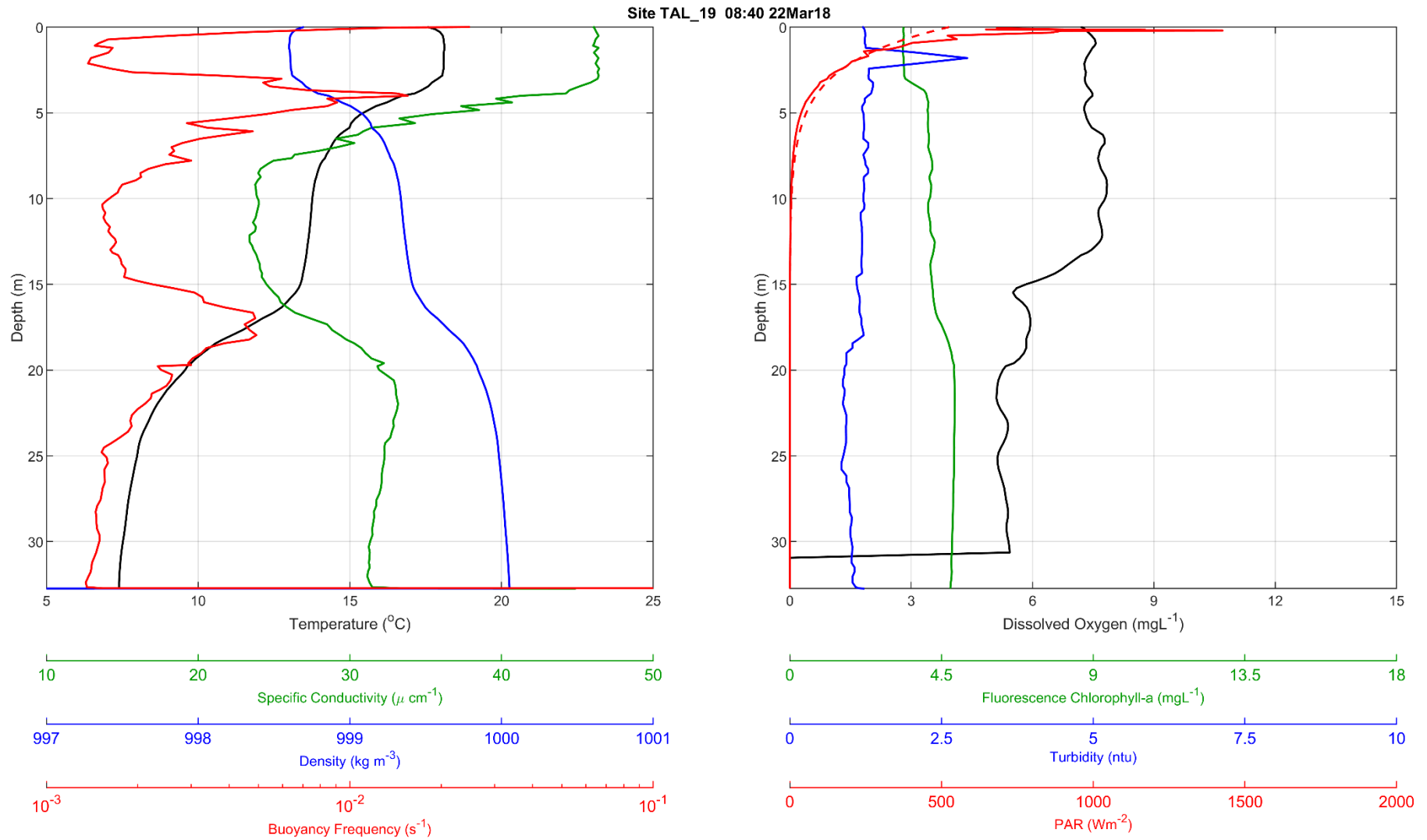
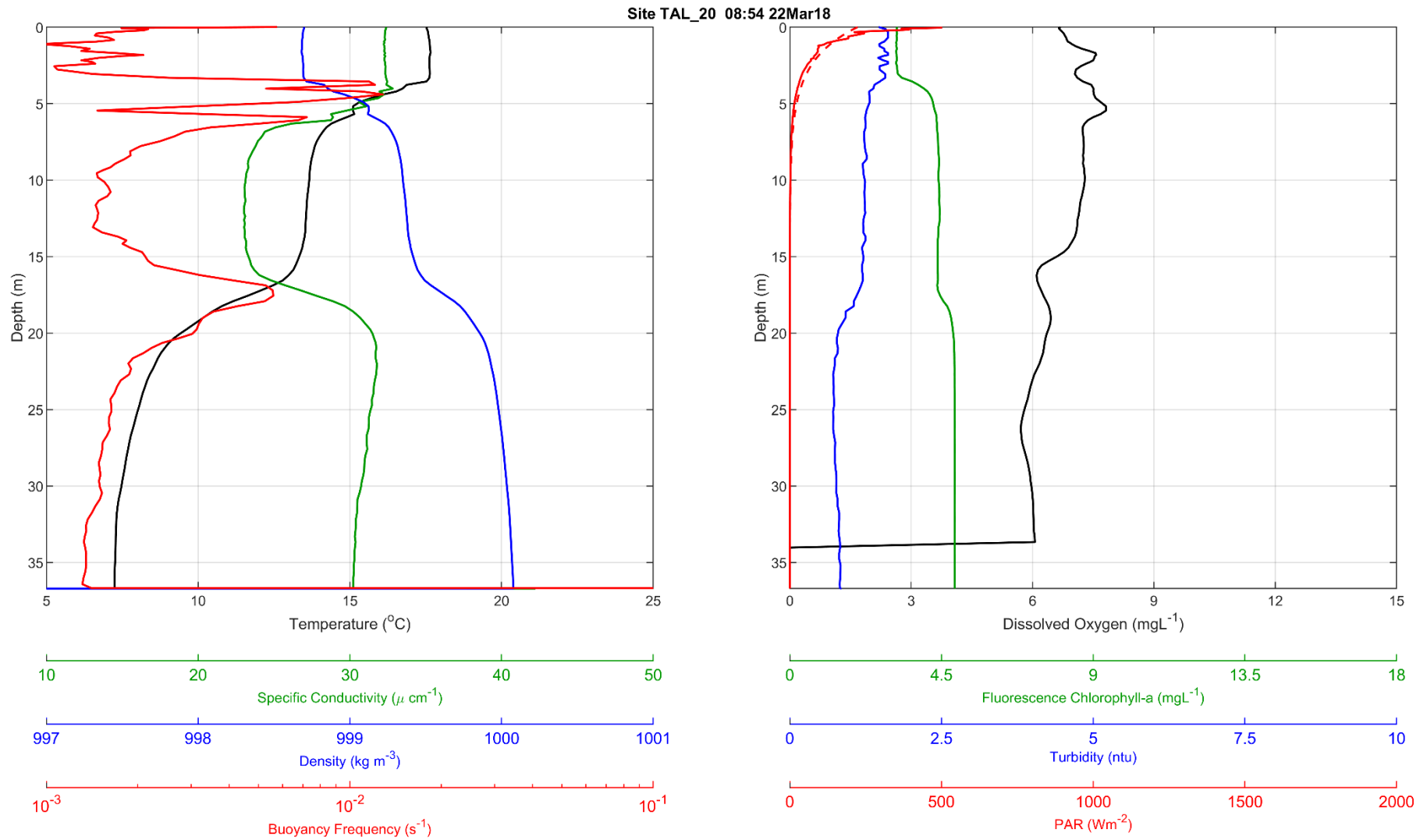


Figure F-16 Talbingo Reservoir CTD Profile, site TAL_20 at 0854 on 22 March 2018



Talbingo Reservoir – 2nd October 2018

Figure F-17 Talbingo Reservoir CTD Profile, site TAL_01 at 1721 on 2 October 2018

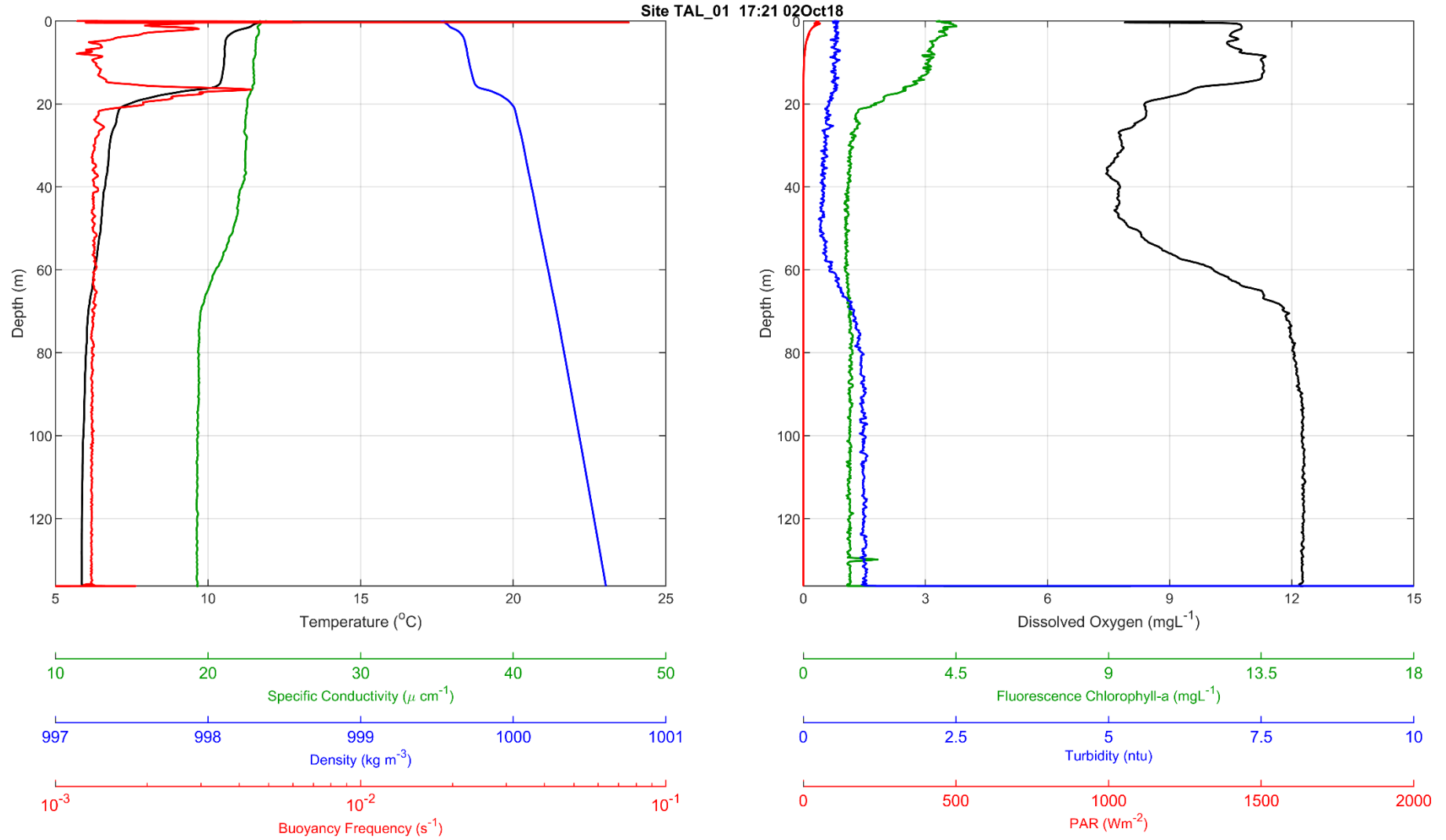


Figure F-18 Talbingo Reservoir CTD Profile, site TAL_06 at 1702 on 2 October 2018

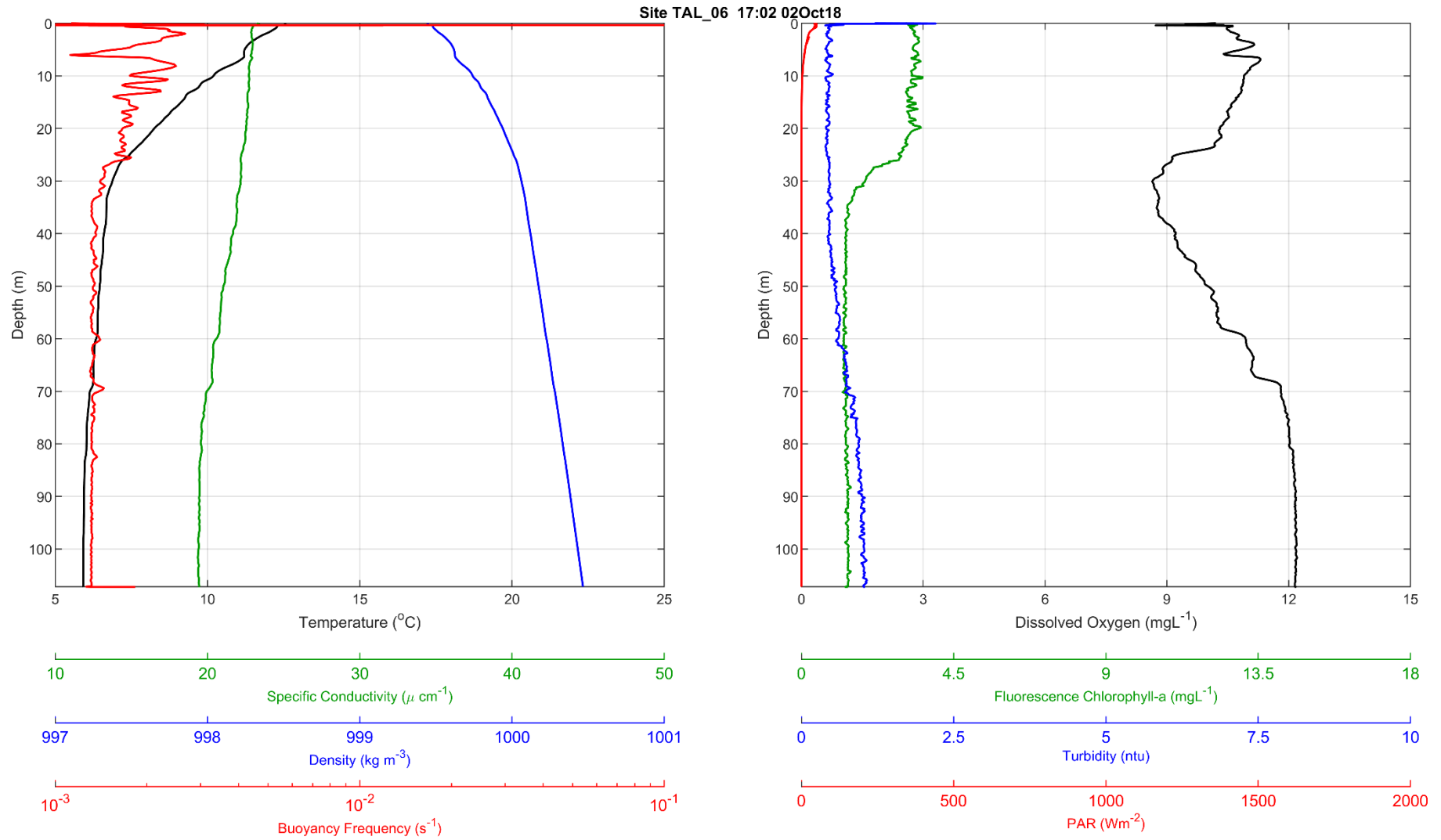


Figure F-19 Talbingo Reservoir CTD Profile, site TAL_10 at 1645 on 2 October 2018

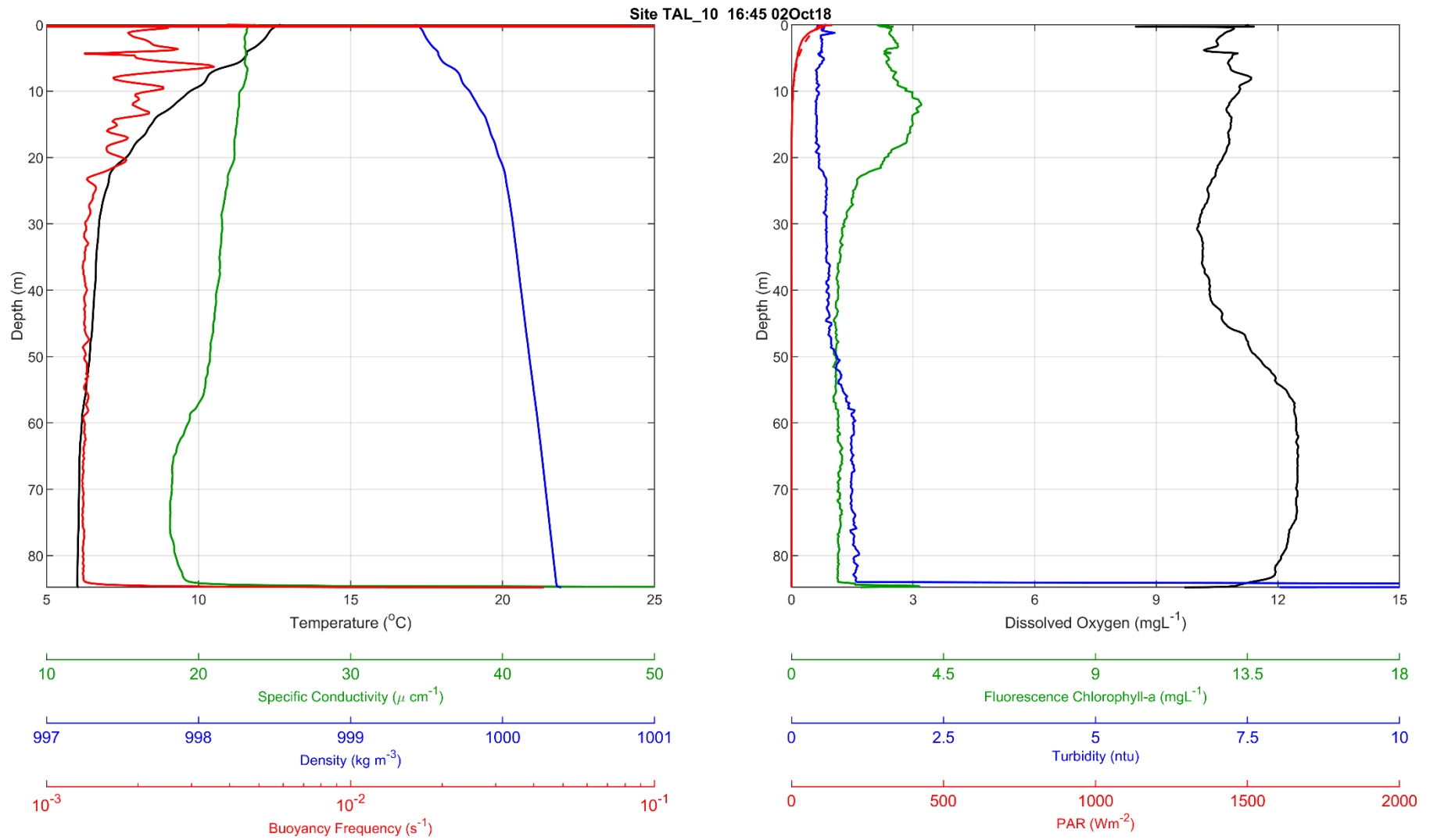


Figure F-20 Talbingo Reservoir CTD Profile, site TAL_14 at 1628 on 2 October 2018

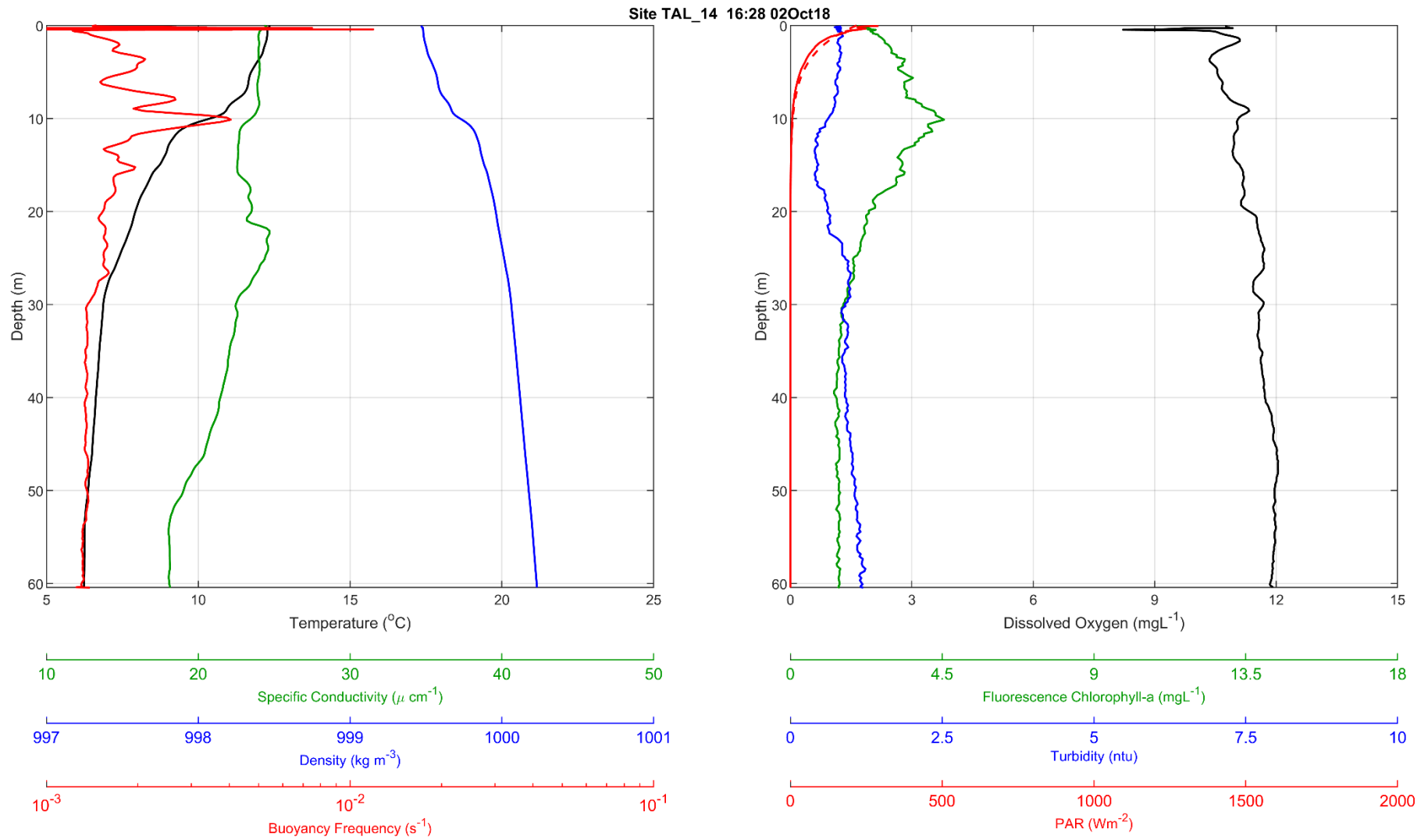


Figure F-21 Talbingo Reservoir CTD Profile, site TAL_15 at 1619 on 2 October 2018

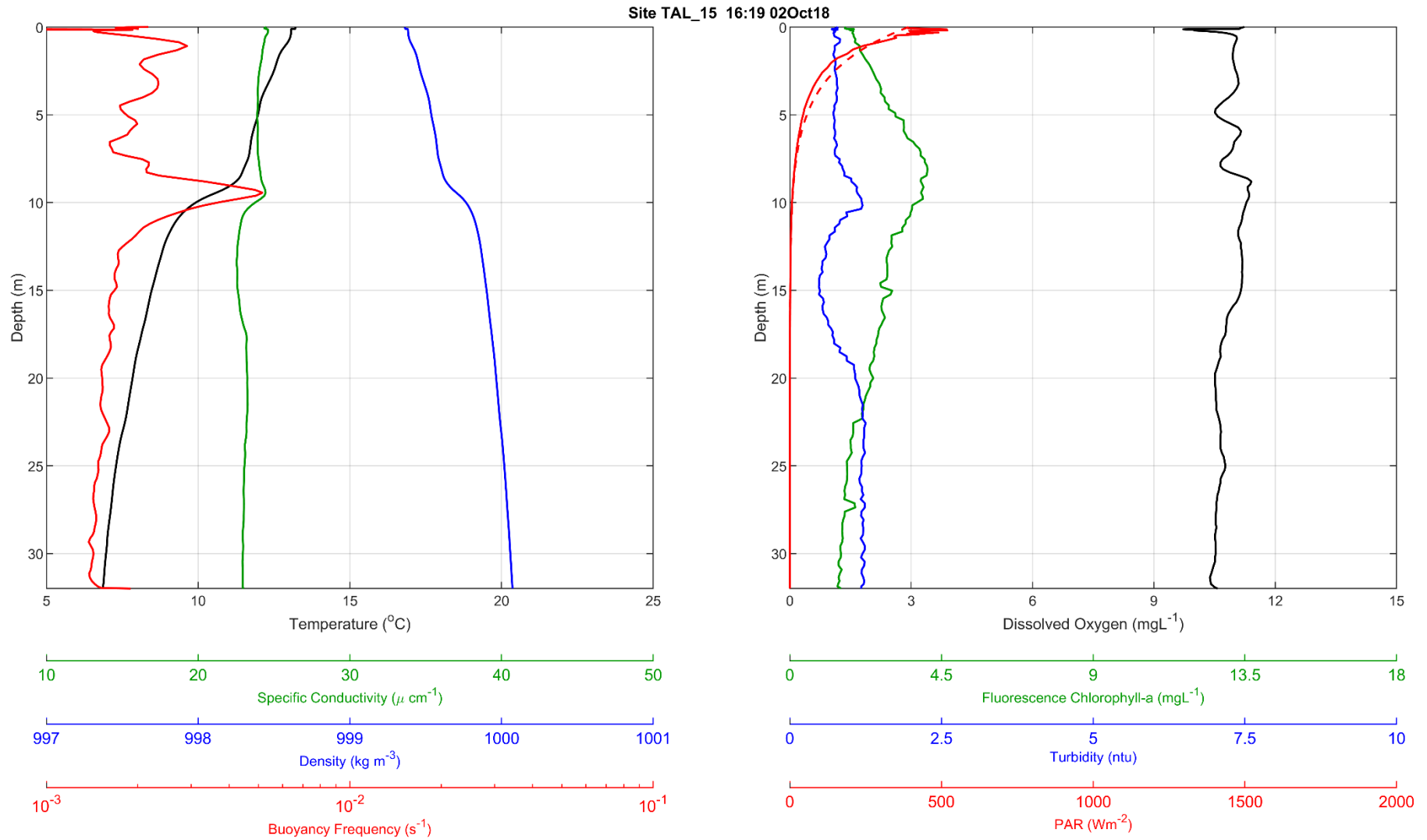


Figure F-22 Talbingo Reservoir CTD Profile, site TAL_16 at 1607 on 2 October 2018

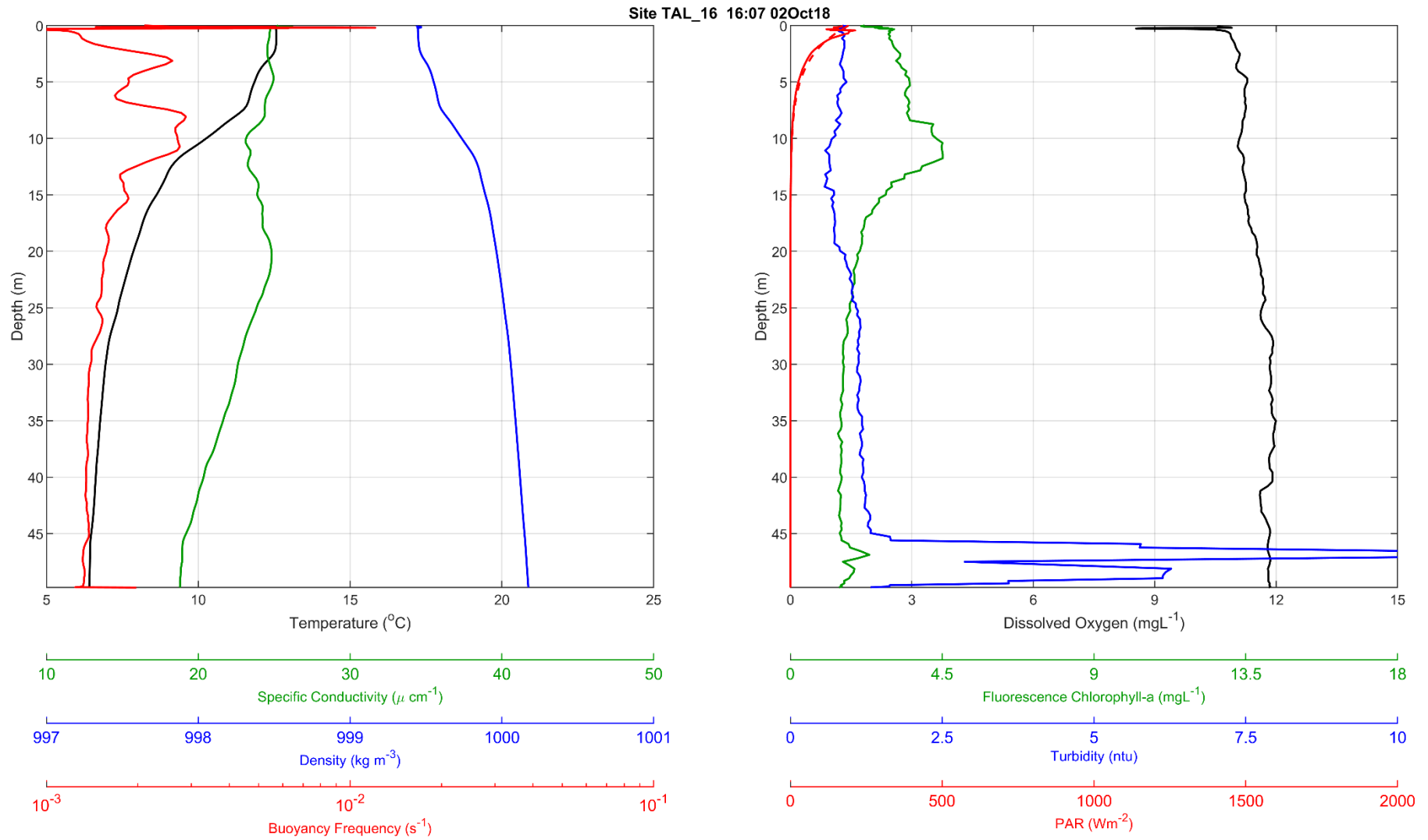


Figure F-23 Talbingo Reservoir CTD Profile, site TAL_17 at 1558 on 2 October 2018

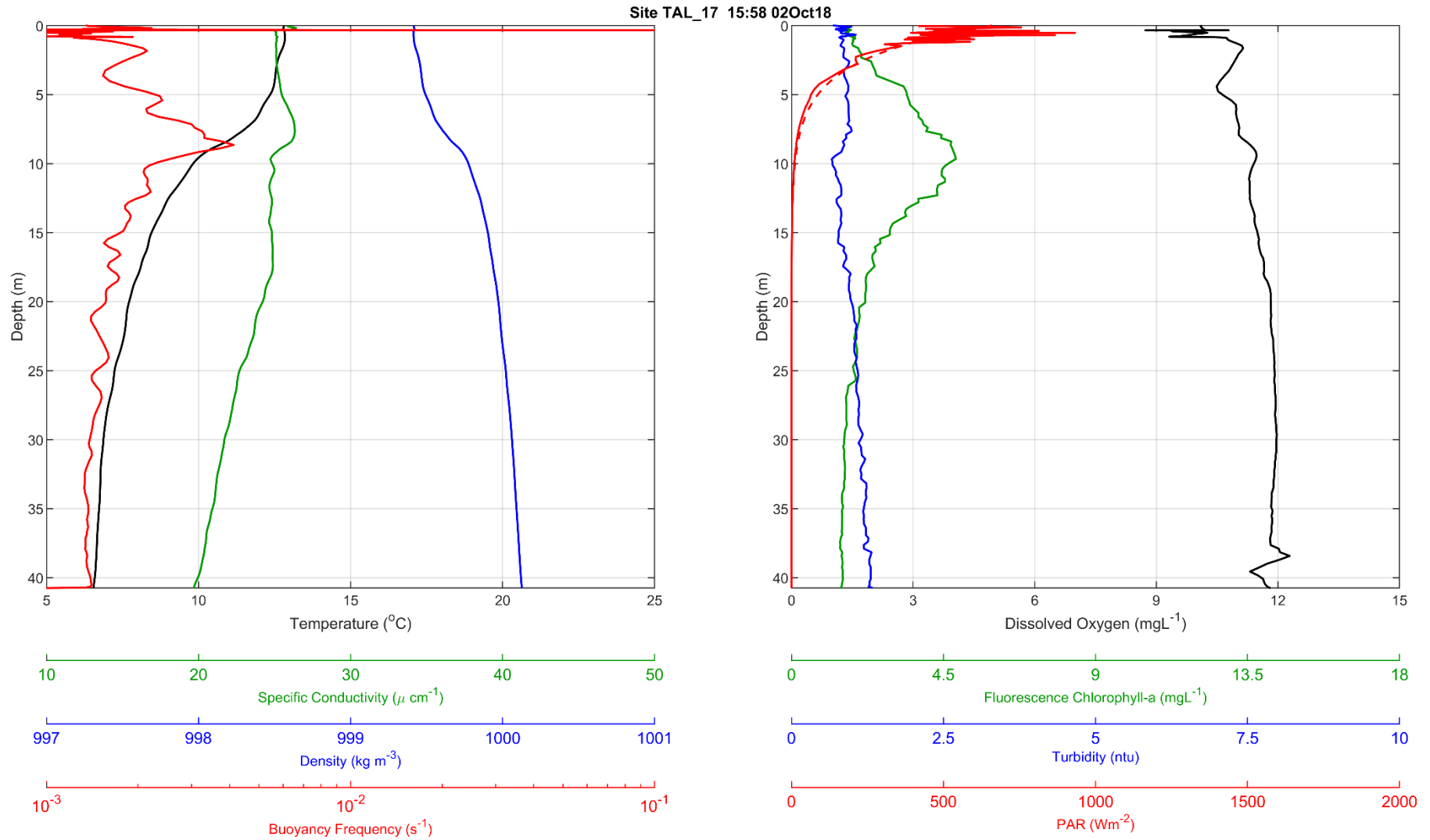


Figure F-24 Talbingo Reservoir CTD Profile, site TAL_18 at 1550 on 2 October 2018

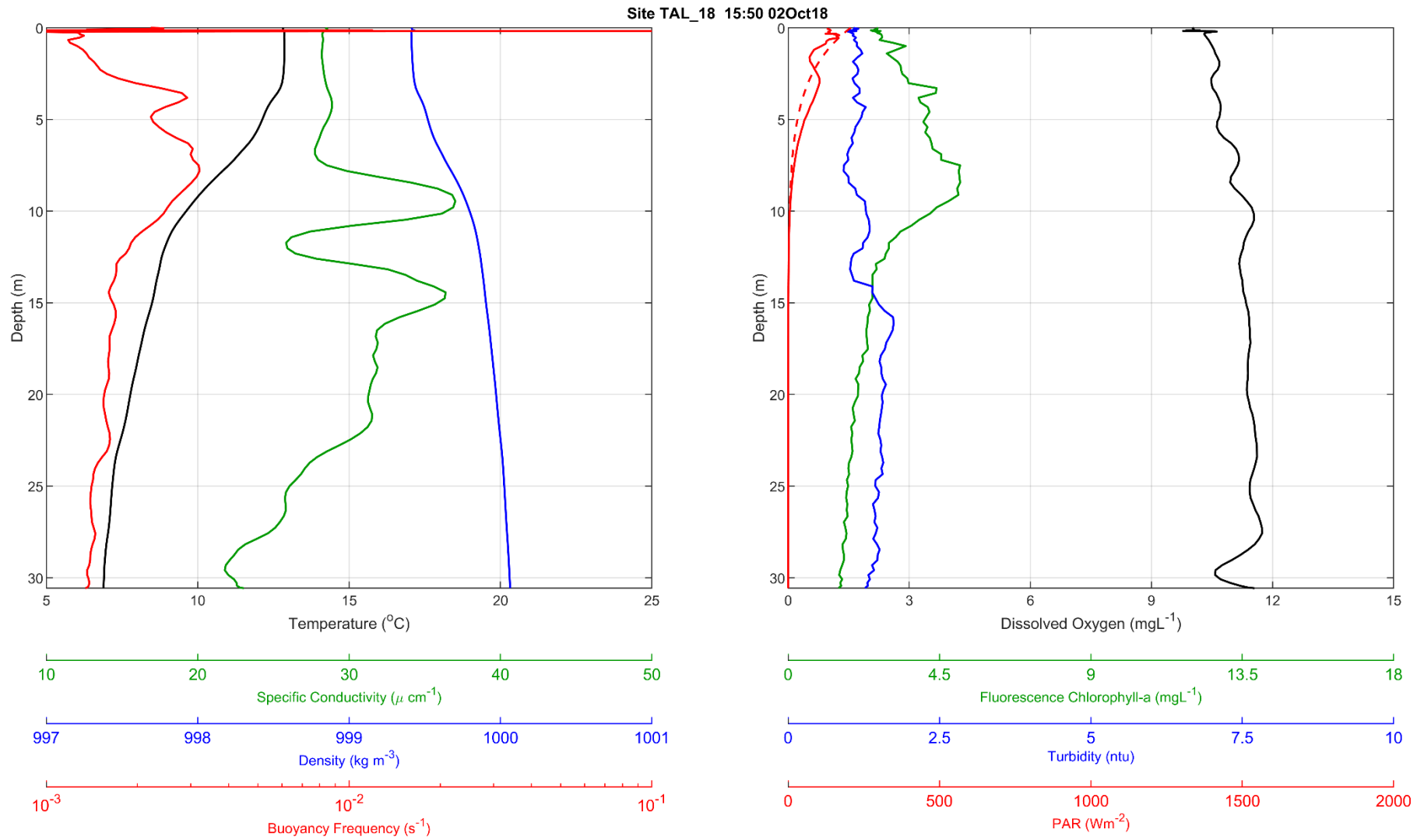


Figure F-25 Talbingo Reservoir CTD Profile, site TAL_19 at 1542 on 2 October 2018

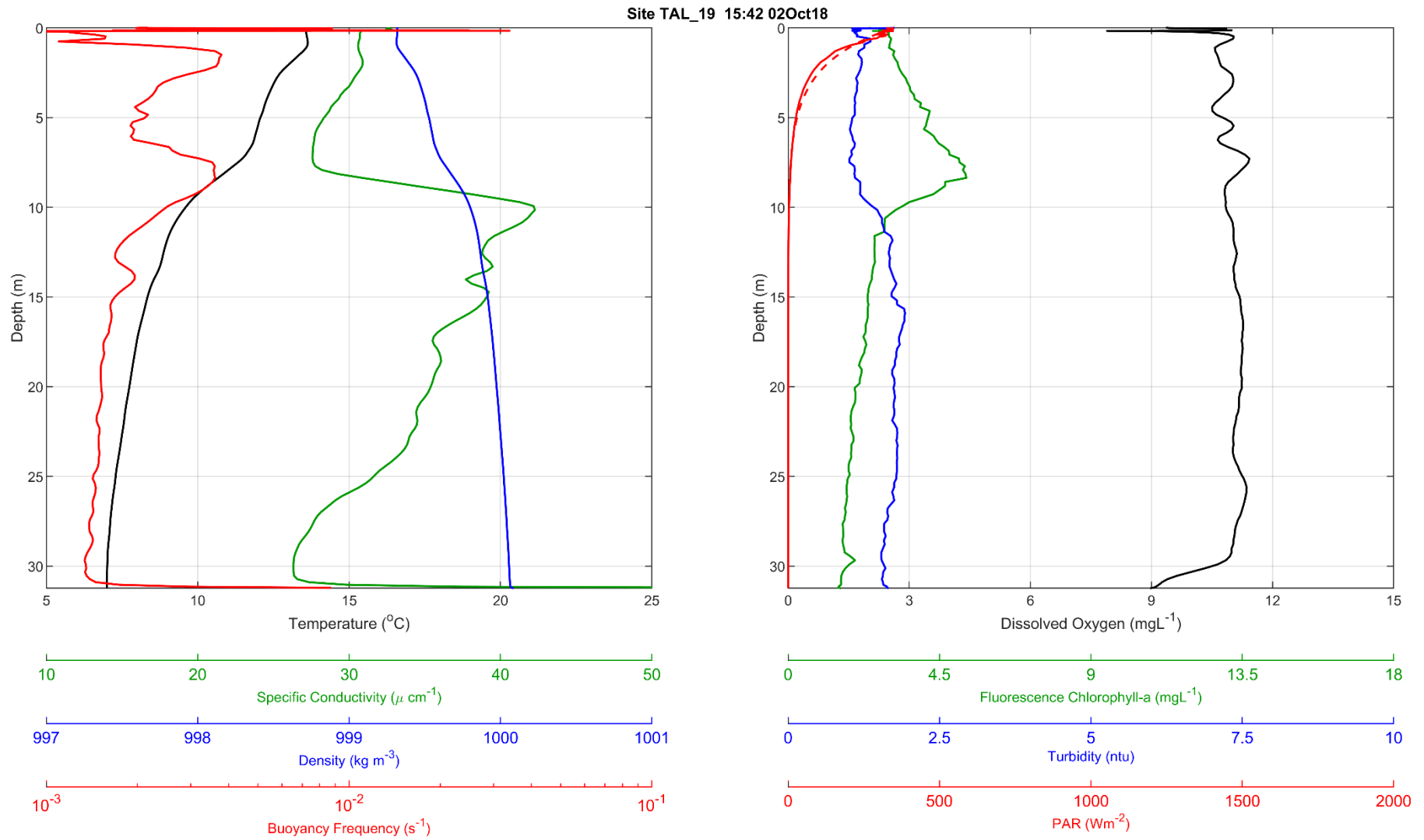
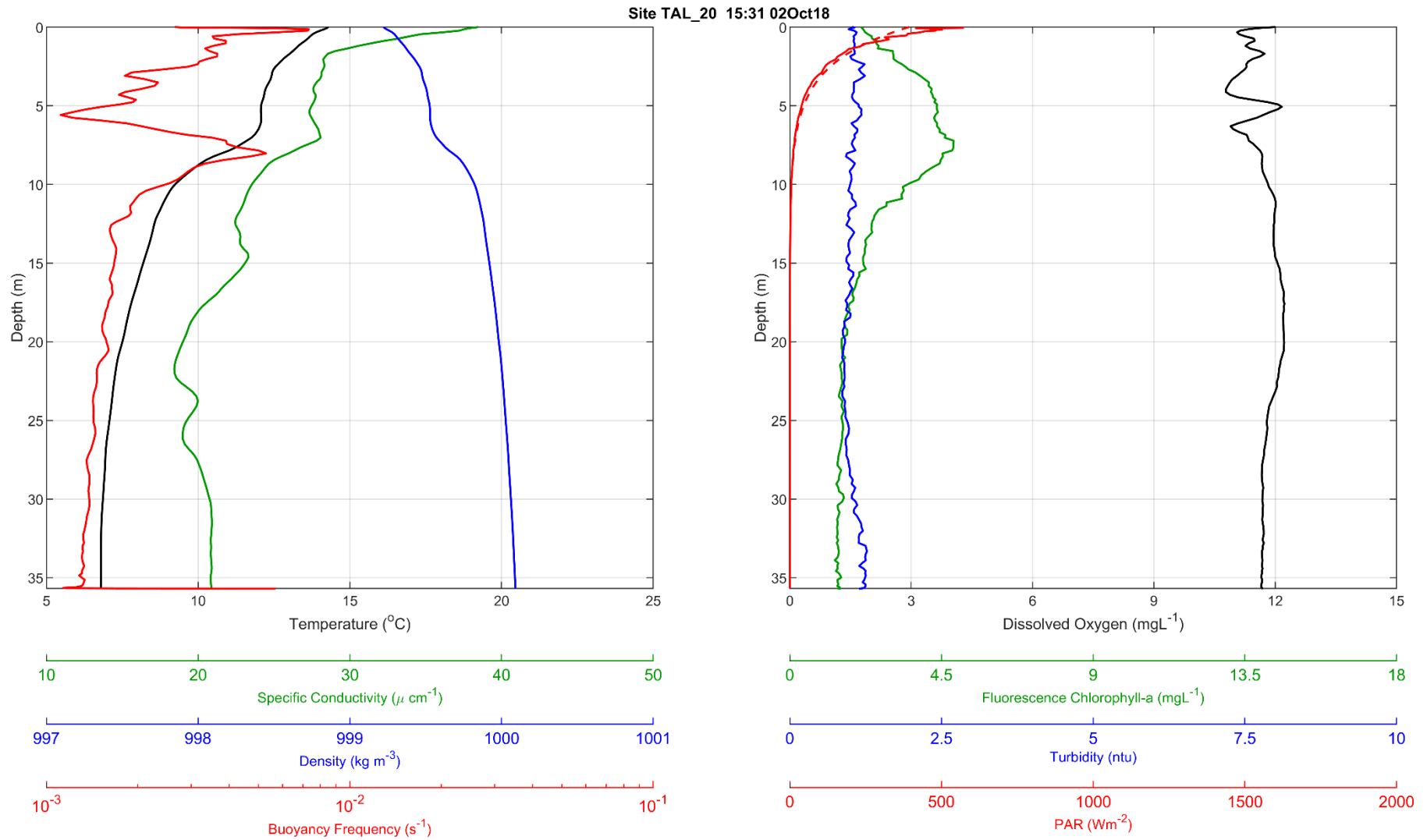


Figure F-26 Talbingo Reservoir CTD Profile, site TAL_20 at 1531 on 2 October 2018



Talbingo Reservoir – 3rd October 2018

Figure F-27 Talbingo Reservoir CTD Profile, site TAL_01 at 1545 on 3 October 2018

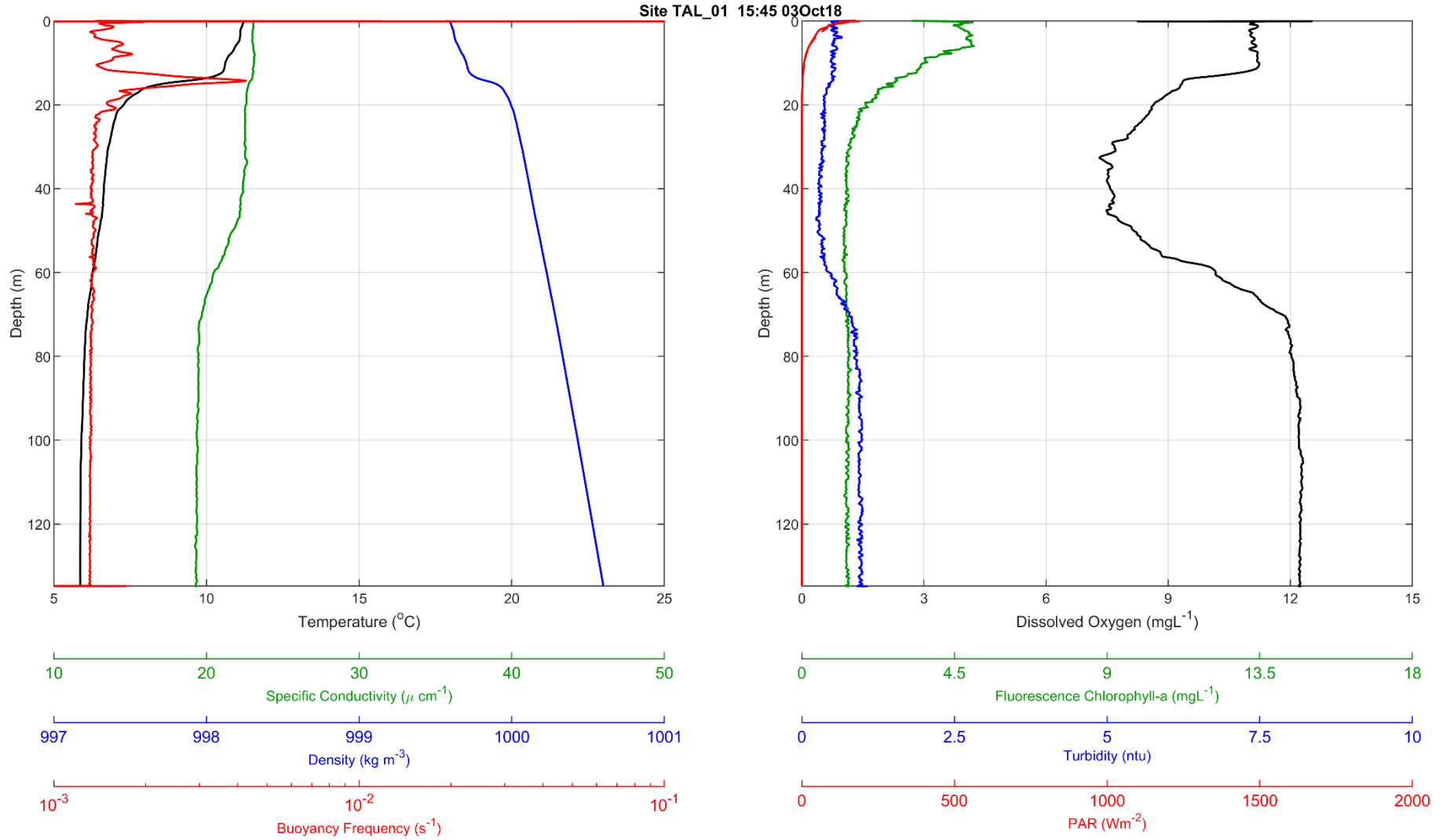


Figure F-28 Talbingo Reservoir CTD Profile, site TAL_14 at 1312 on 3 October 2018

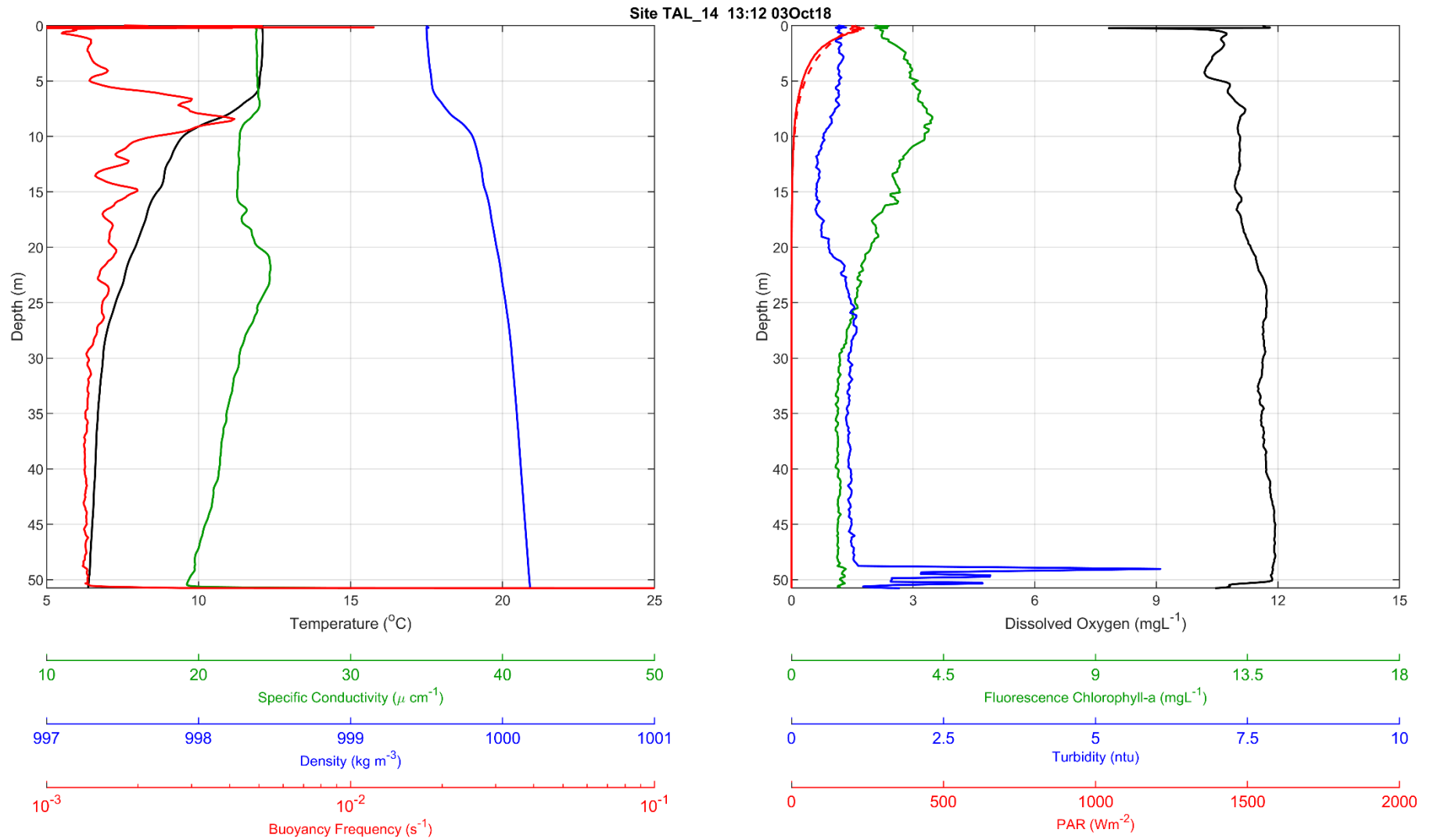


Figure F-29 Talbingo Reservoir CTD Profile, site TAL_15 at 1304 on 3 October 2018

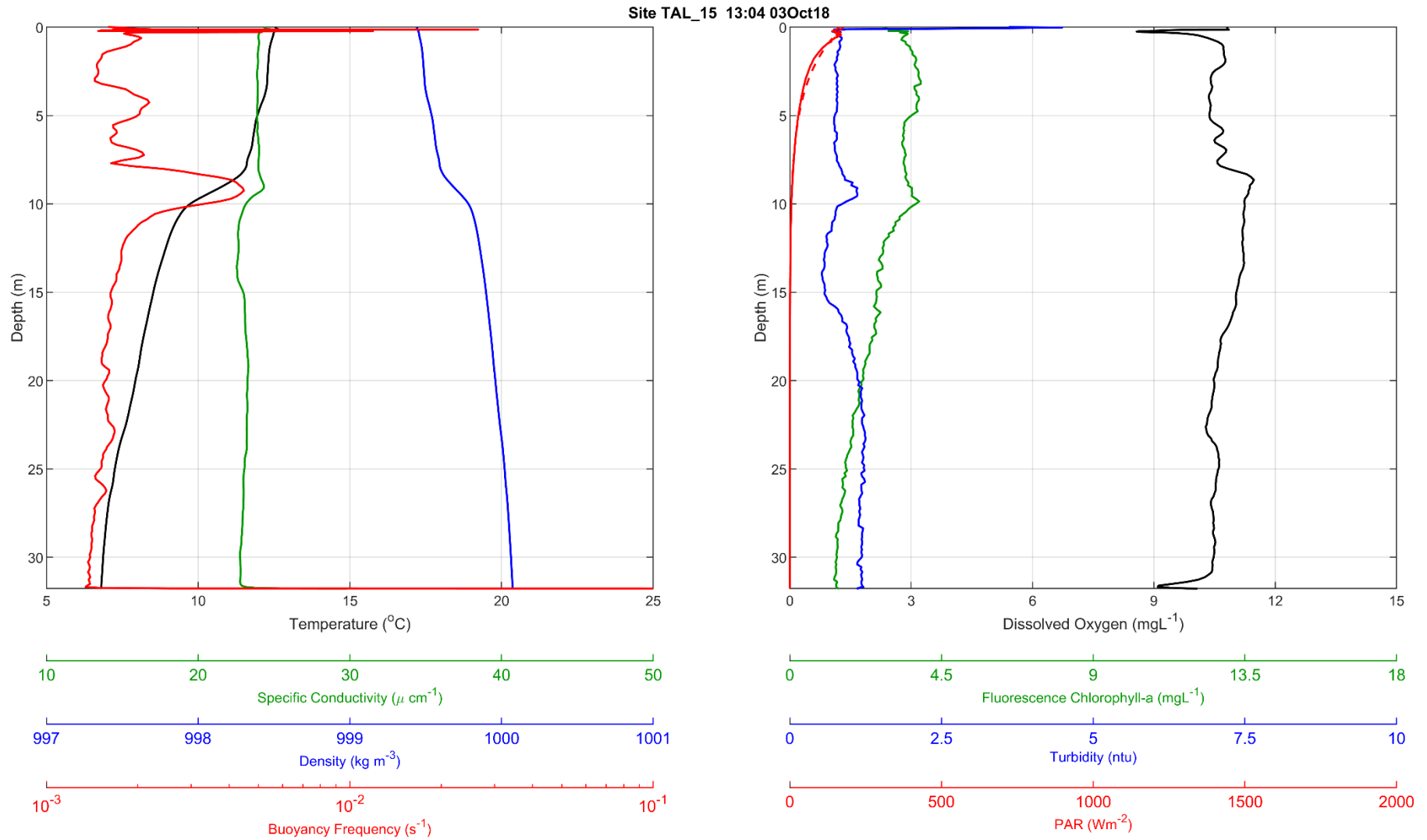


Figure F-30 Talbingo Reservoir CTD Profile, site TAL_17 at 1131 on 3 October 2018

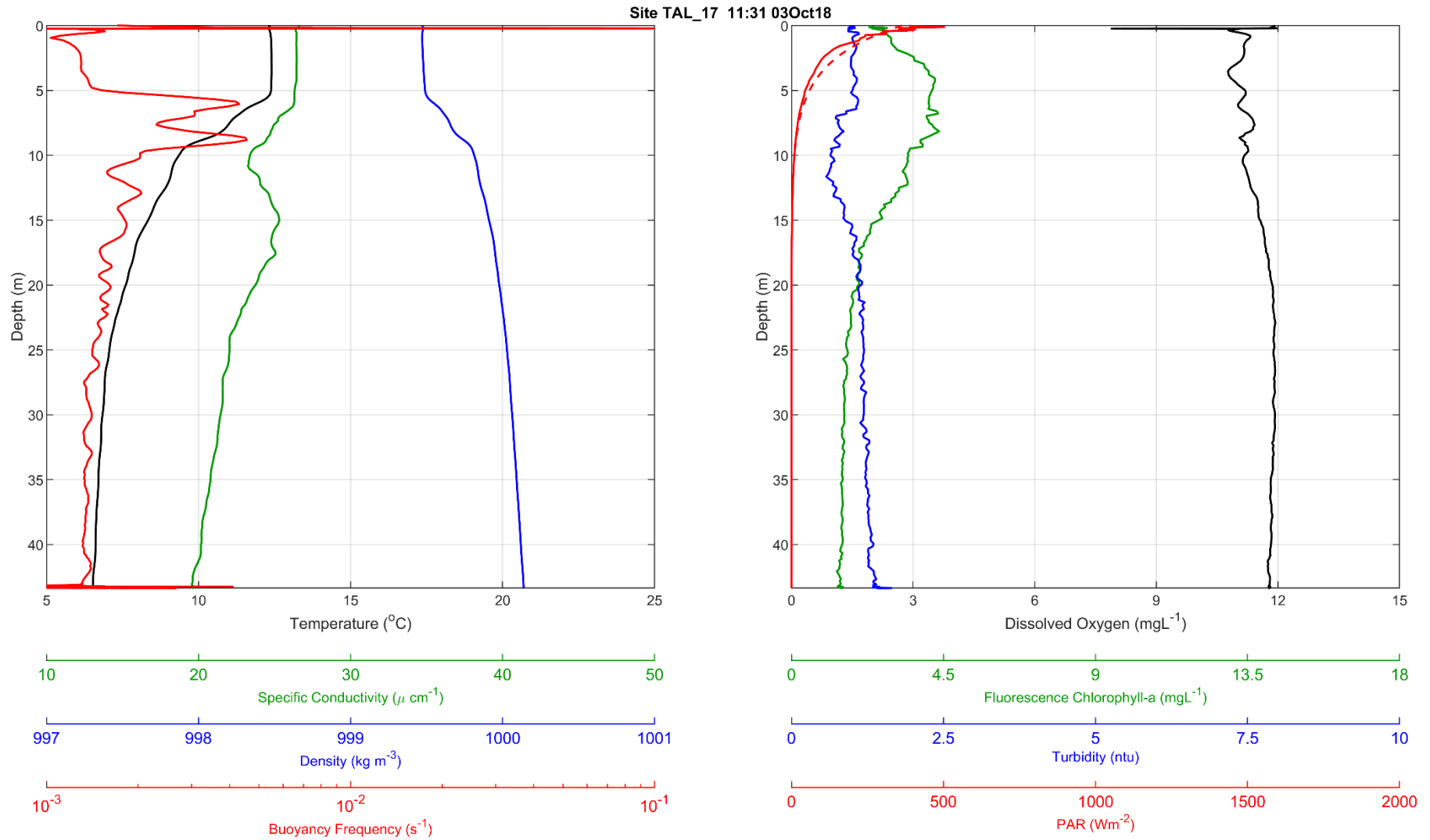


Figure F-31 Talbingo Reservoir CTD Profile, site TAL_18 at 1121 on 3 October 2018

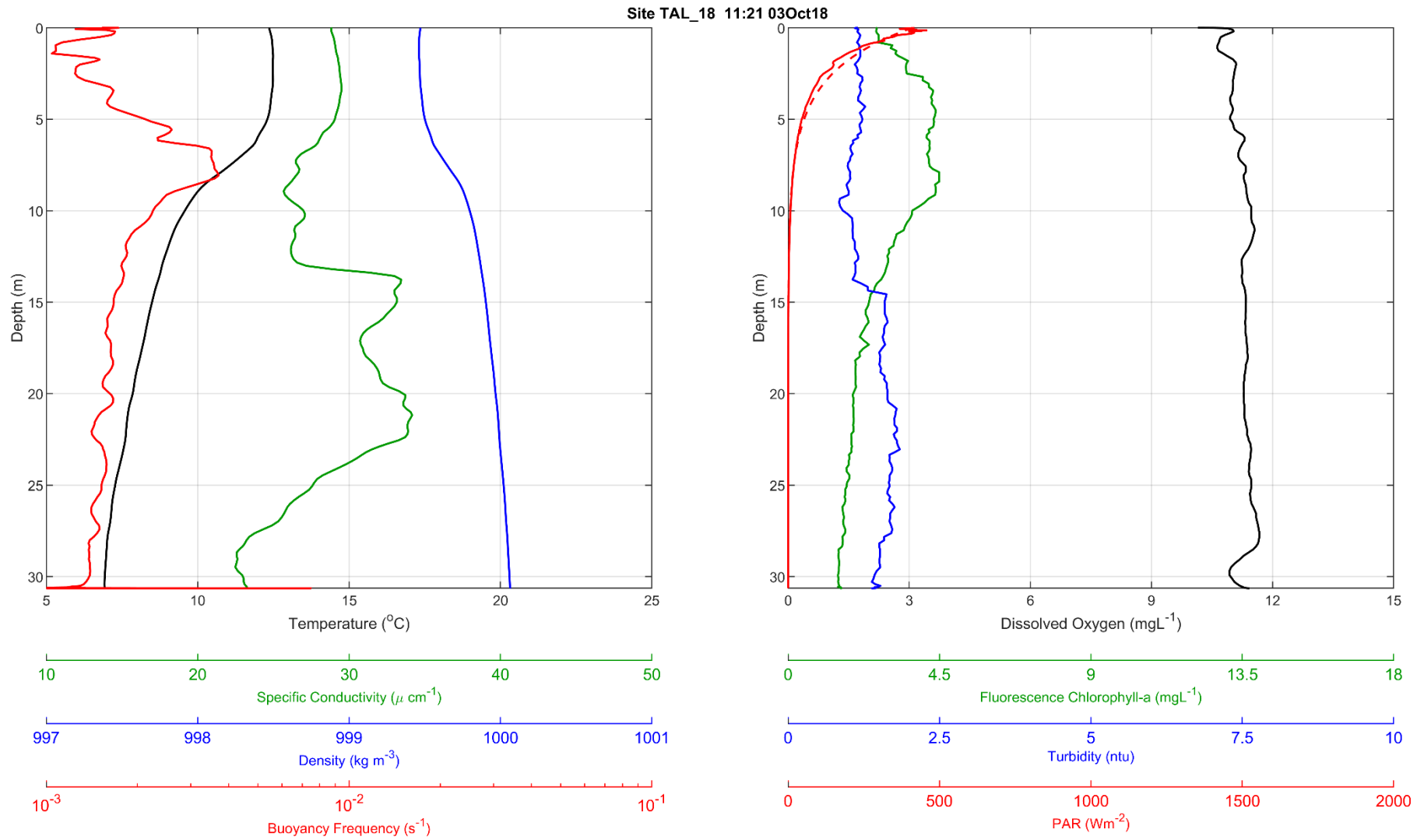


Figure F-32 Talbingo Reservoir CTD Profile, site TAL_19 at 1112 on 3 October 2018

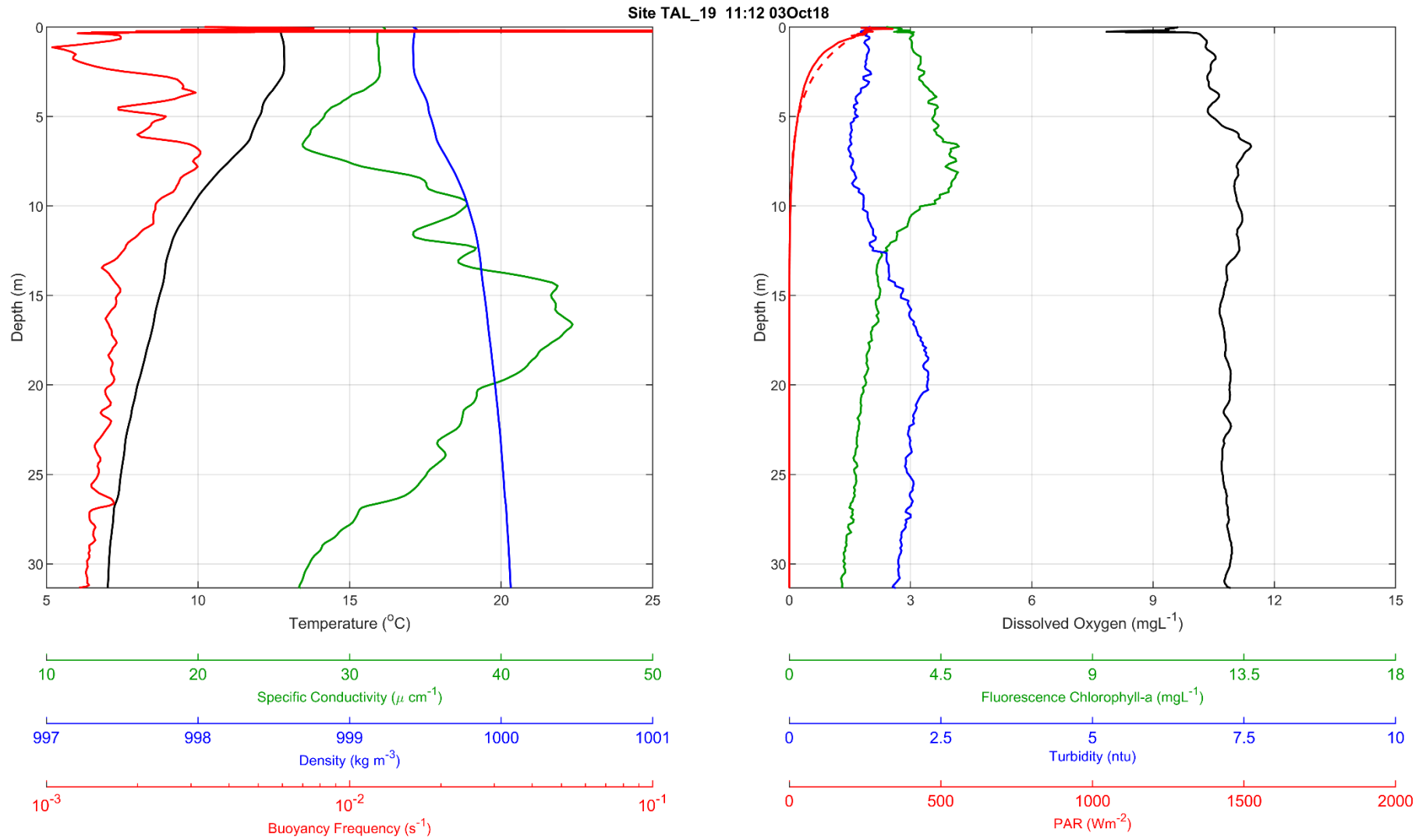
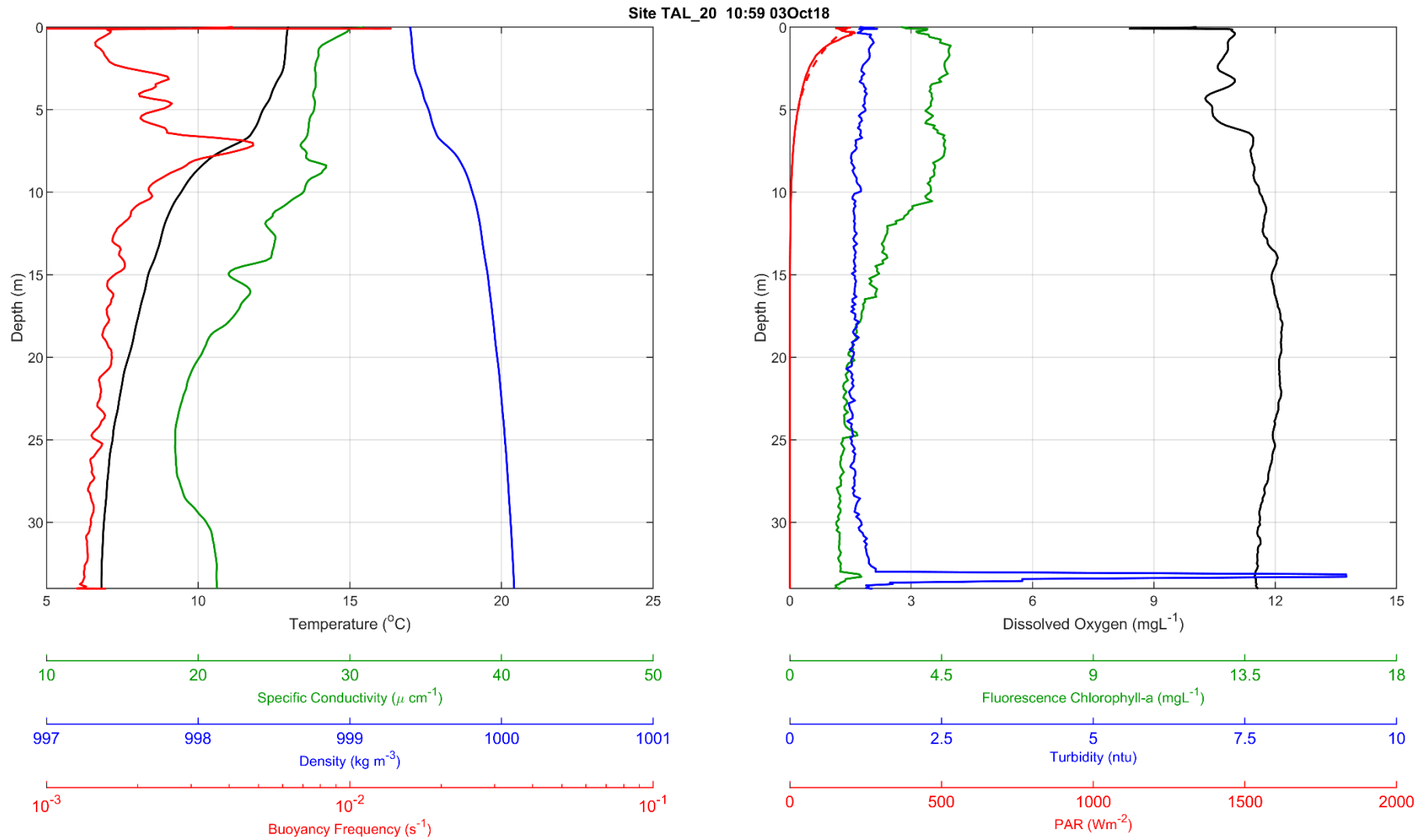


Figure F-33 Talbingo Reservoir CTD Profile, site TAL_20 at 1059 on 3 October 2018



Tantangra Reservoir – 20th March 2018

Figure F-34 Tantangra Reservoir CTD Profile, site TAN_01 at 0940 on 20 March 2018

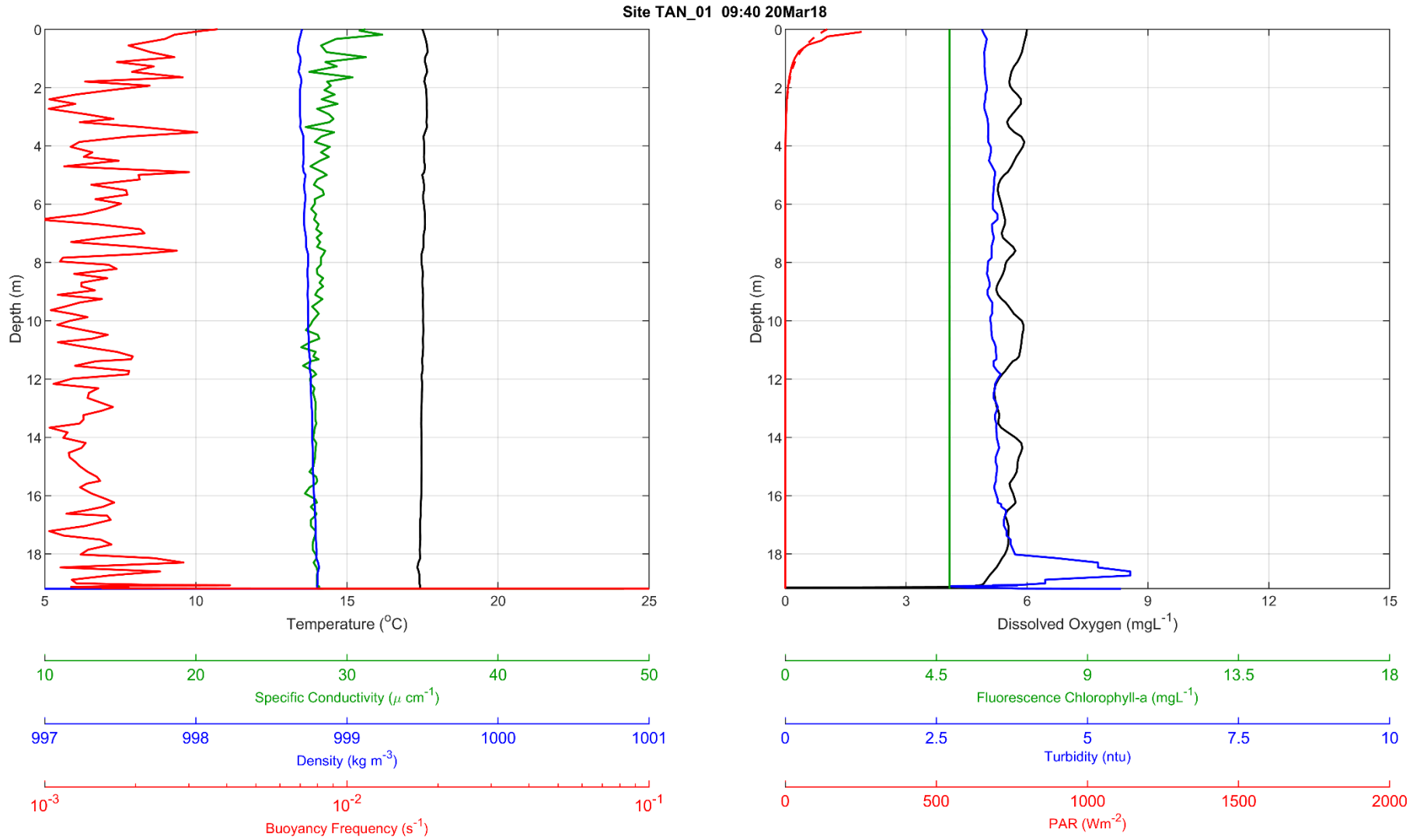


Figure F-35 Tantangra Reservoir CTD Profile, site TAN_01 at 1720 on 20 March 2018

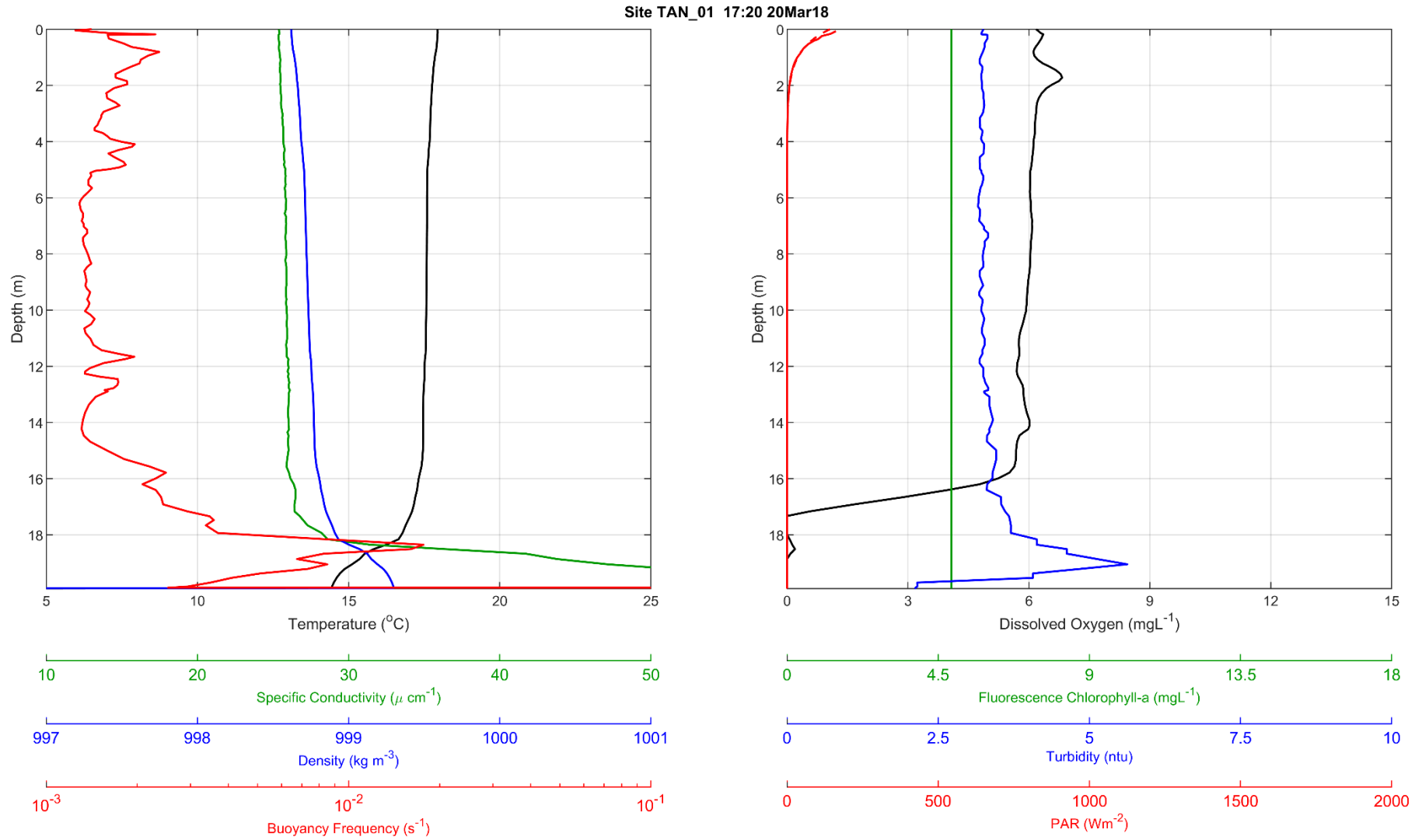


Figure F-36 Tantangra Reservoir CTD Profile, site TAN_01 at 0940 on 20 March 2018

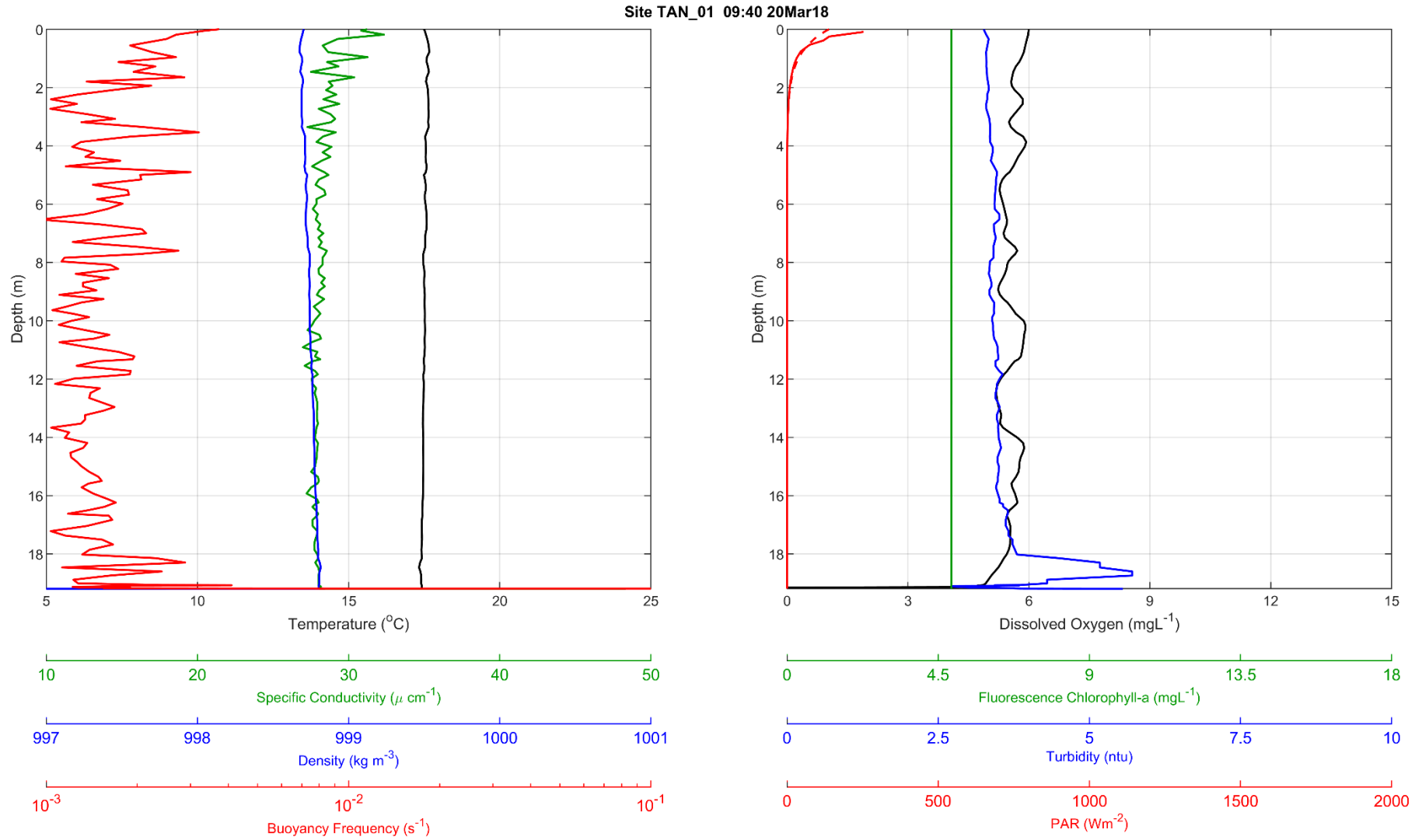


Figure F-37 Tantangra Reservoir CTD Profile, site TAN_02 at 0954 on 20 March 2018

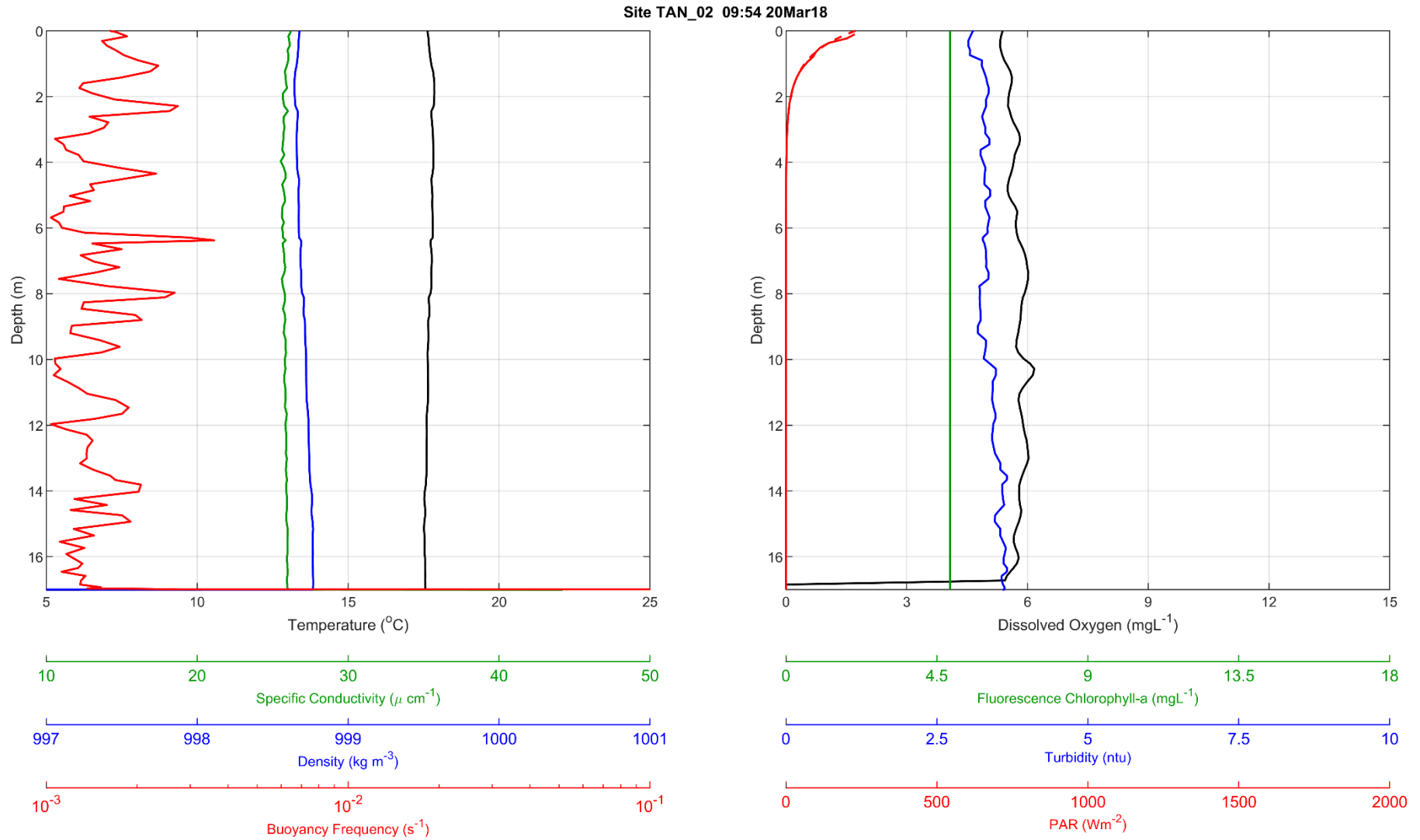


Figure F-38 Tantangra Reservoir CTD Profile, site TAN_03 at 1002 on 20 March 2018

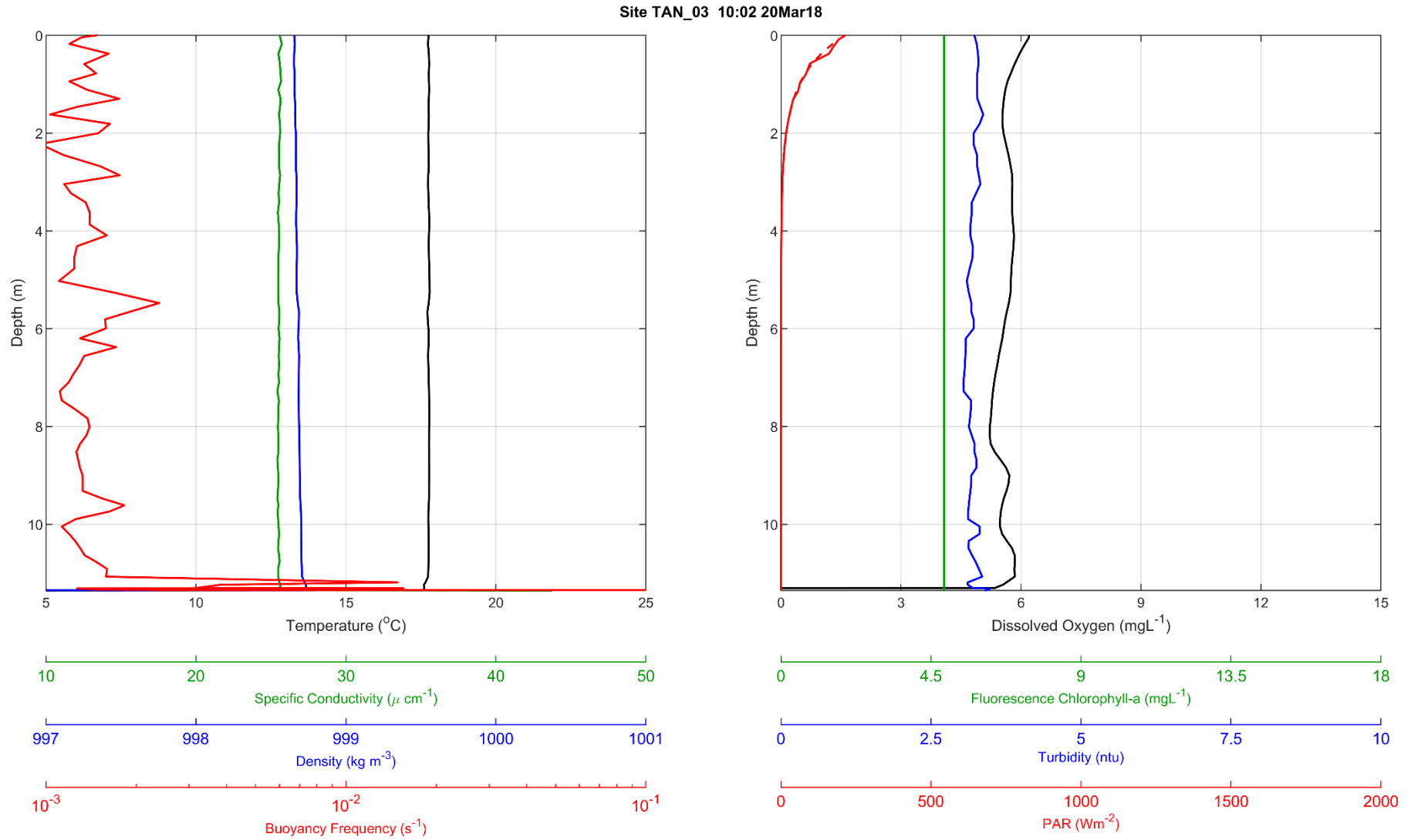


Figure F-39 Tintangra Reservoir CTD Profile, site TAN_04 at 1026 on 20 March 2018

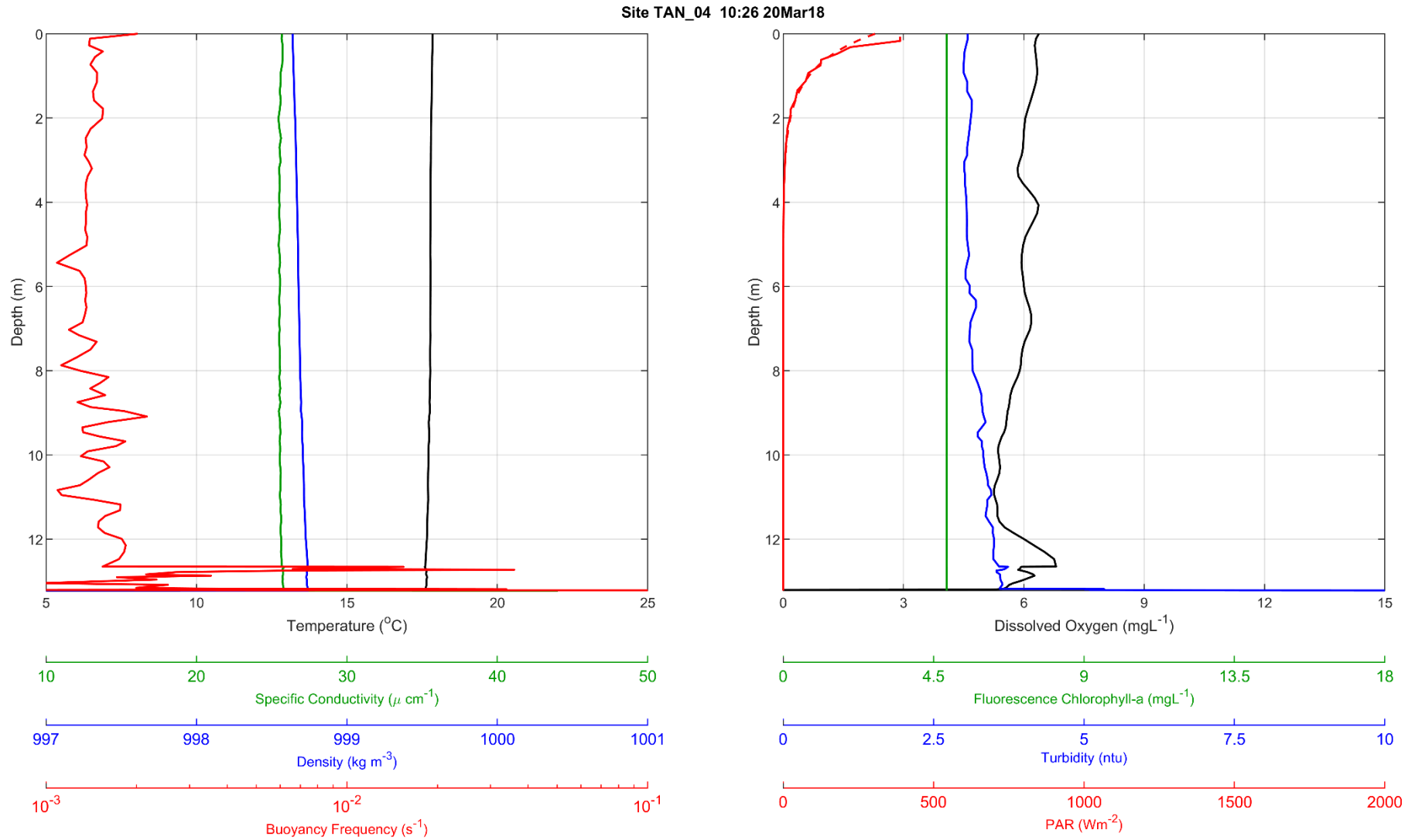


Figure F-40 Tantangra Reservoir CTD Profile, site TAN_05 at 1038 on 20 March 2018

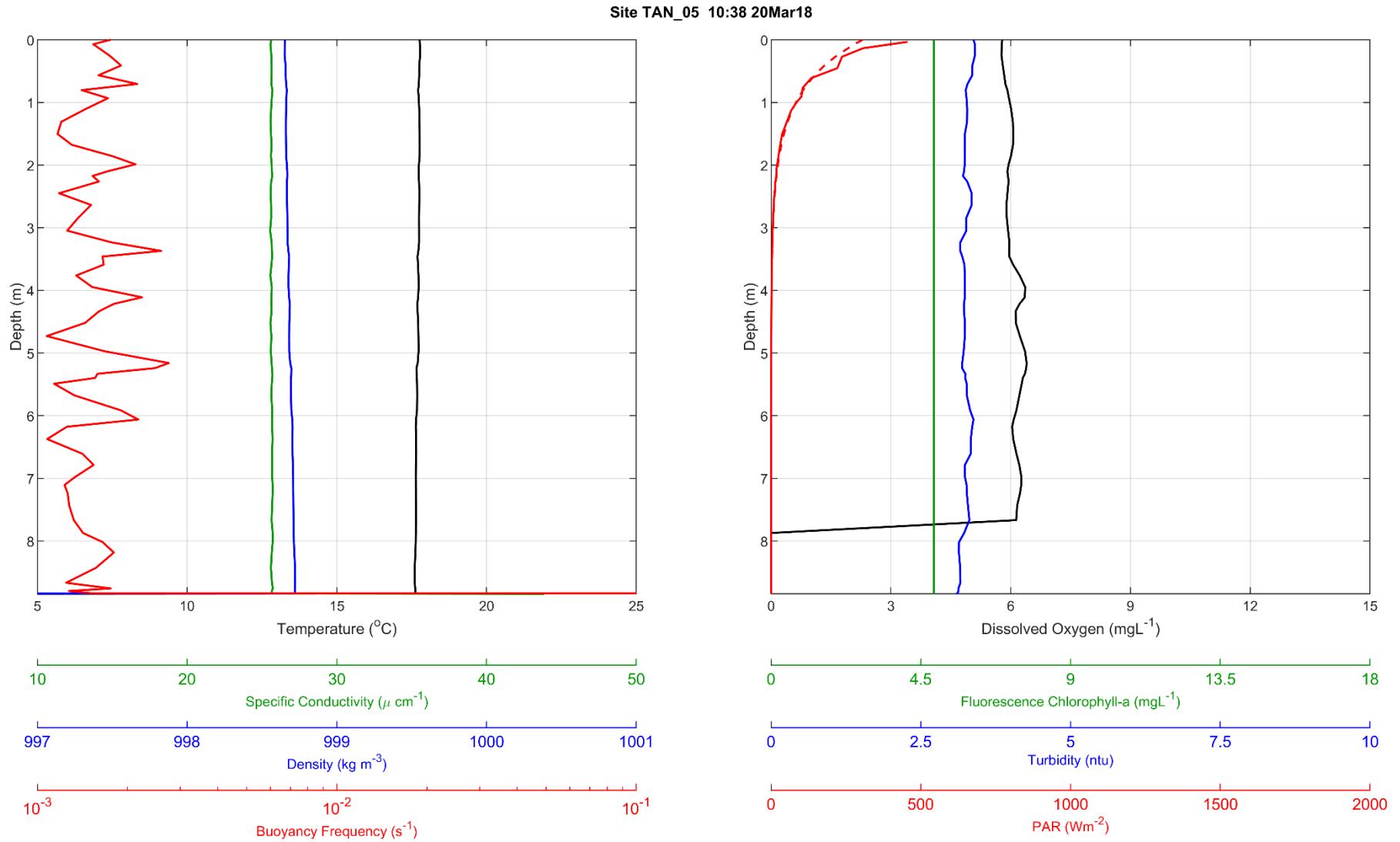


Figure F-41 Tantangra Reservoir CTD Profile, site TAN_06 at 1048 on 20 March 2018

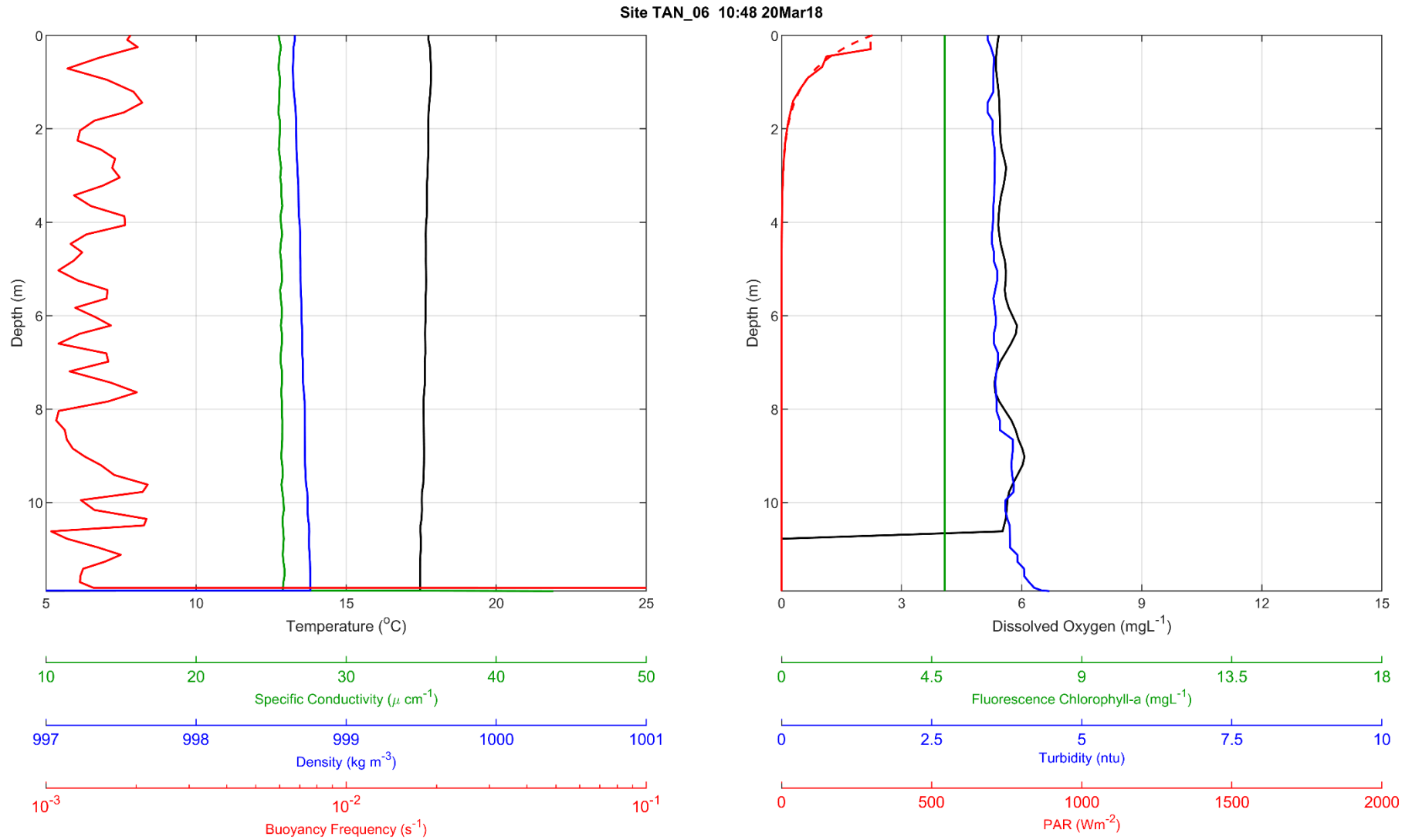


Figure F-42 Tantangra Reservoir CTD Profile, site TAN_06 at 1709 on 20 March 2018

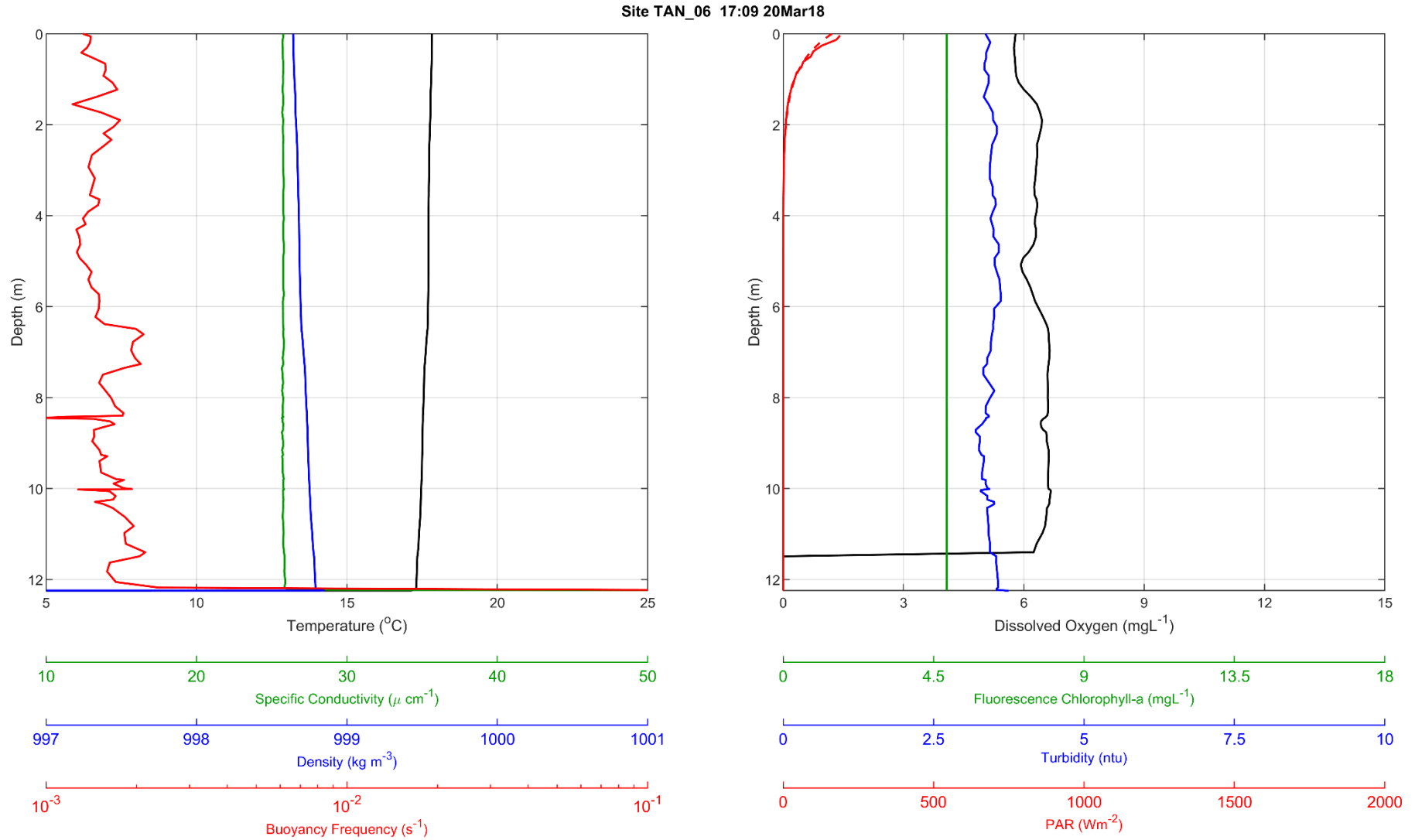


Figure F-43 Tantangra Reservoir CTD Profile, site TAN_07 at 1101 on 20 March 2018

Site TAN_07 11:01 20Mar18

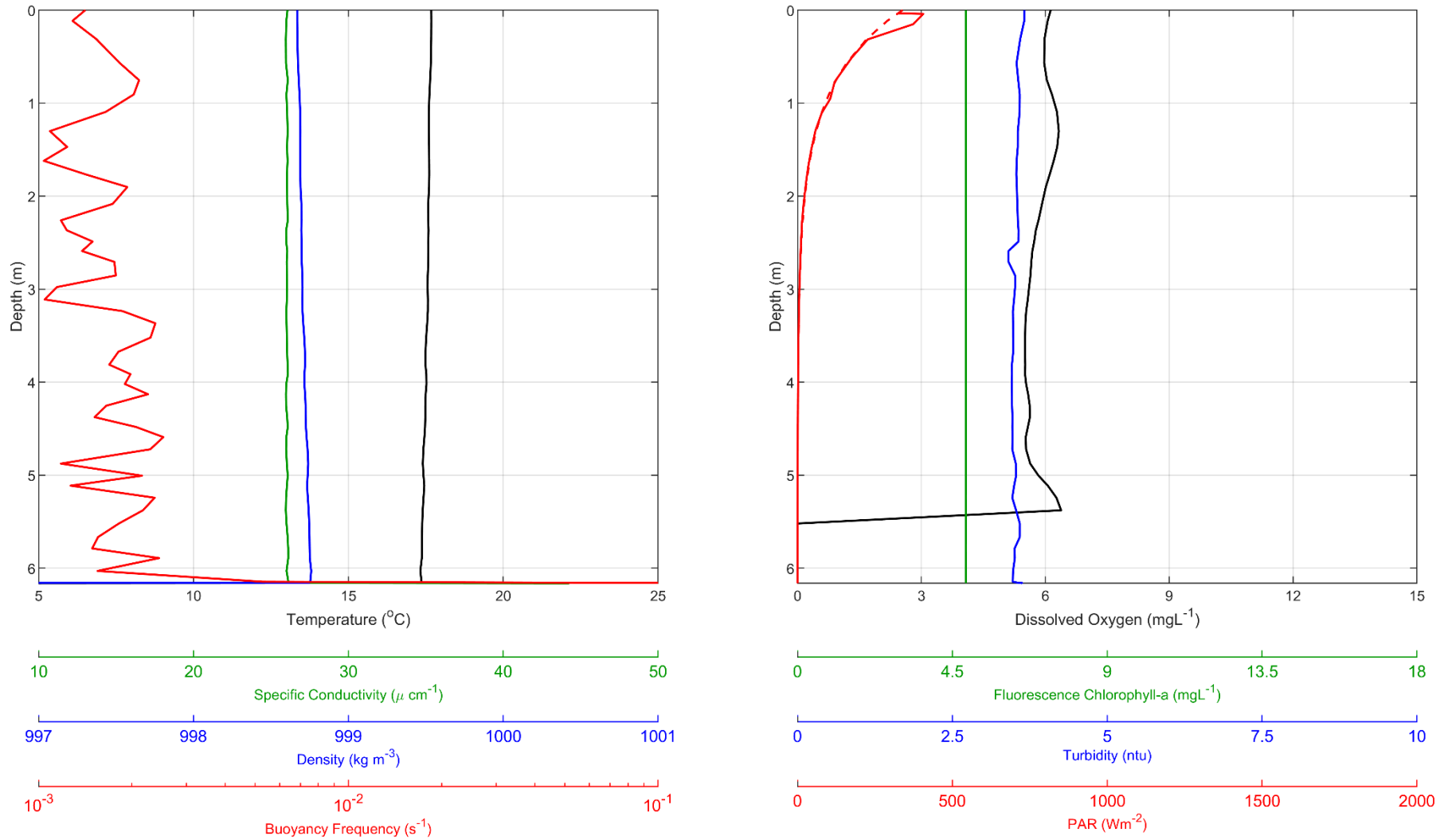


Figure F-44 Tantangra Reservoir CTD Profile, site TAN_08 at 1110 on 20 March 2018

Site TAN_08 11:10 20Mar18

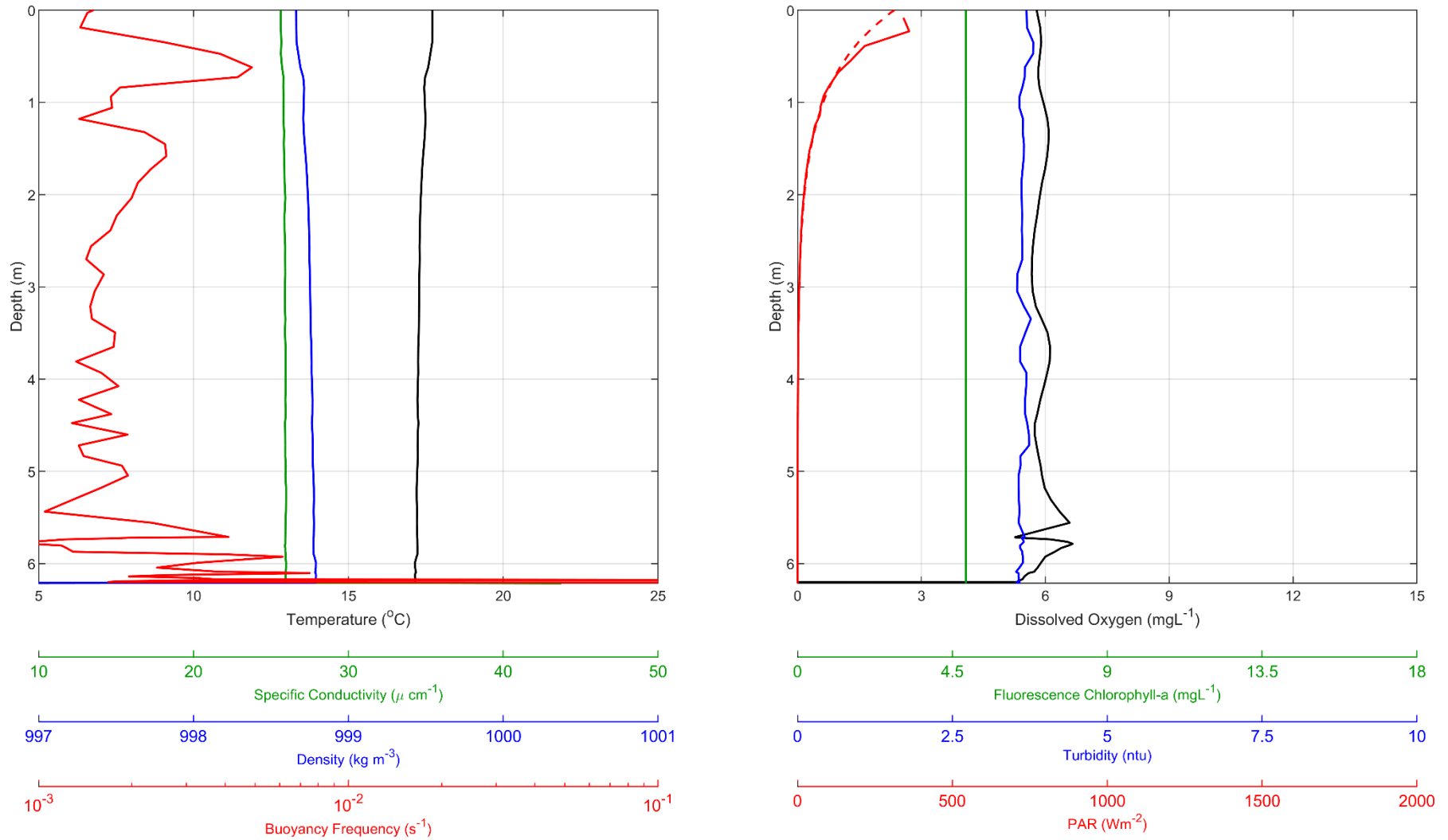


Figure F-45 Tantangra Reservoir CTD Profile, site TAN_09 at 1123 on 20 March 2018

Site TAN_09 11:23 20Mar18

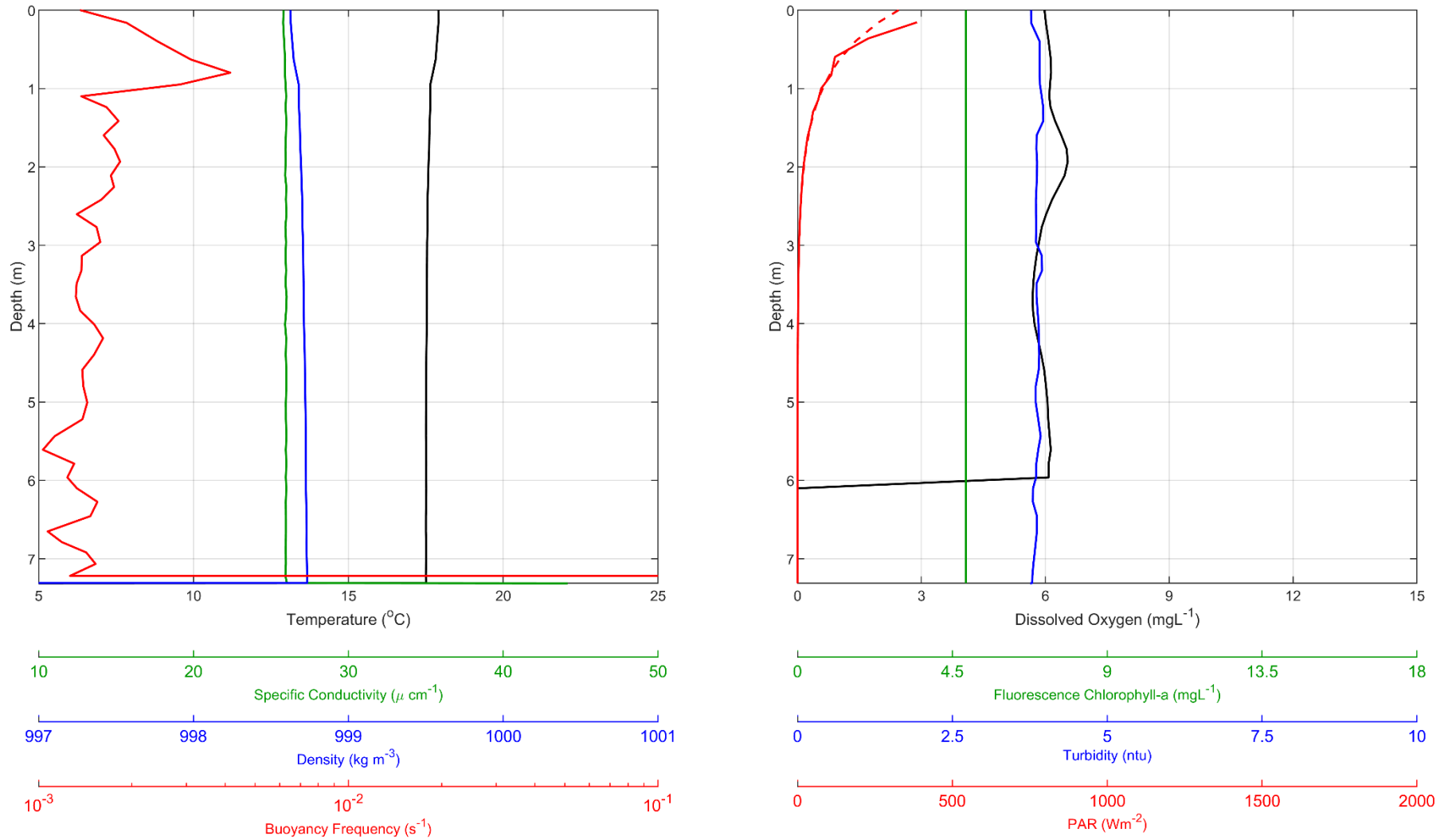


Figure F-46 Tantangra Reservoir CTD Profile, site TAN_09 at 1659 on 20 March 2018

Site TAN_09 16:59 20Mar18

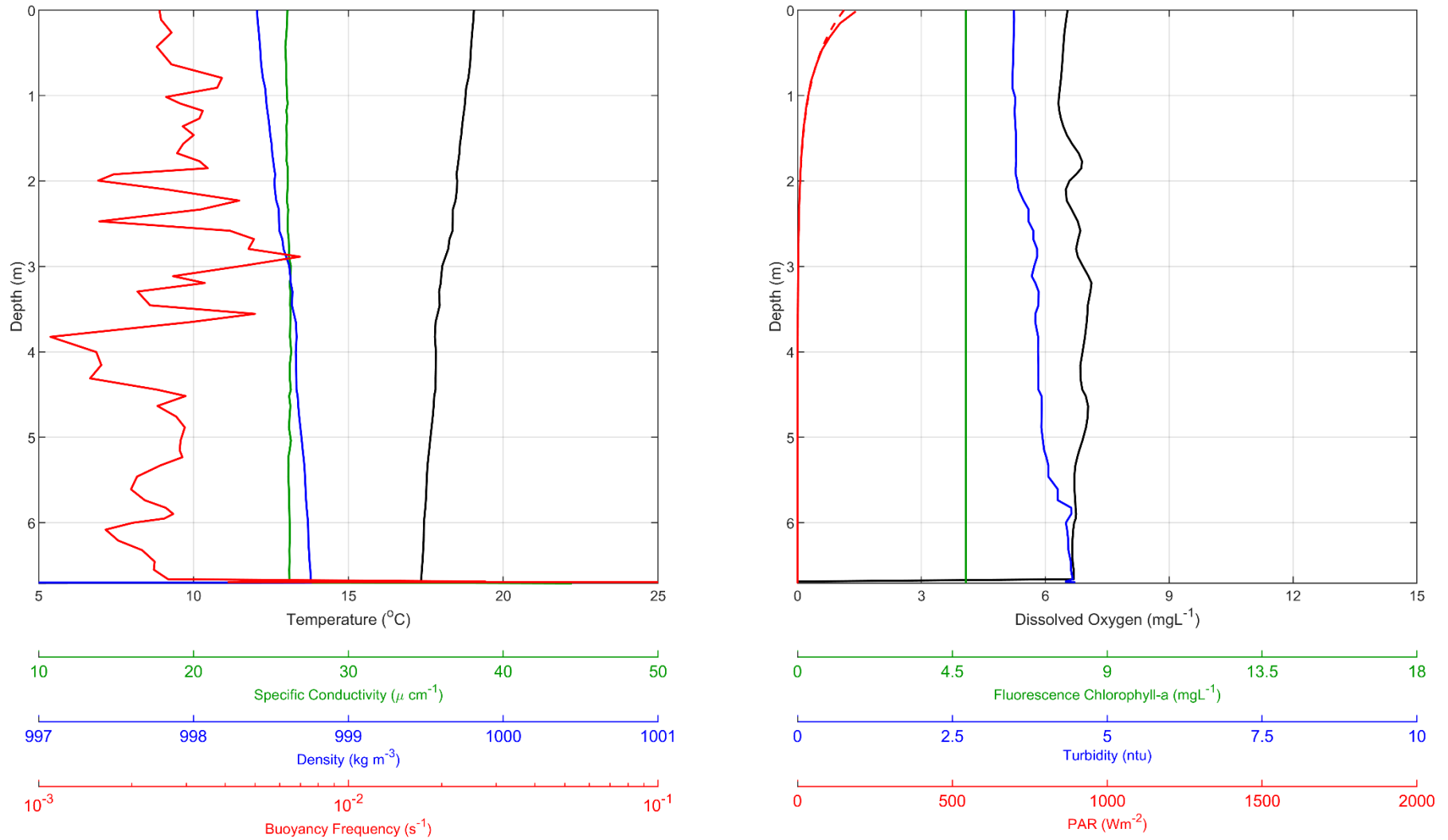
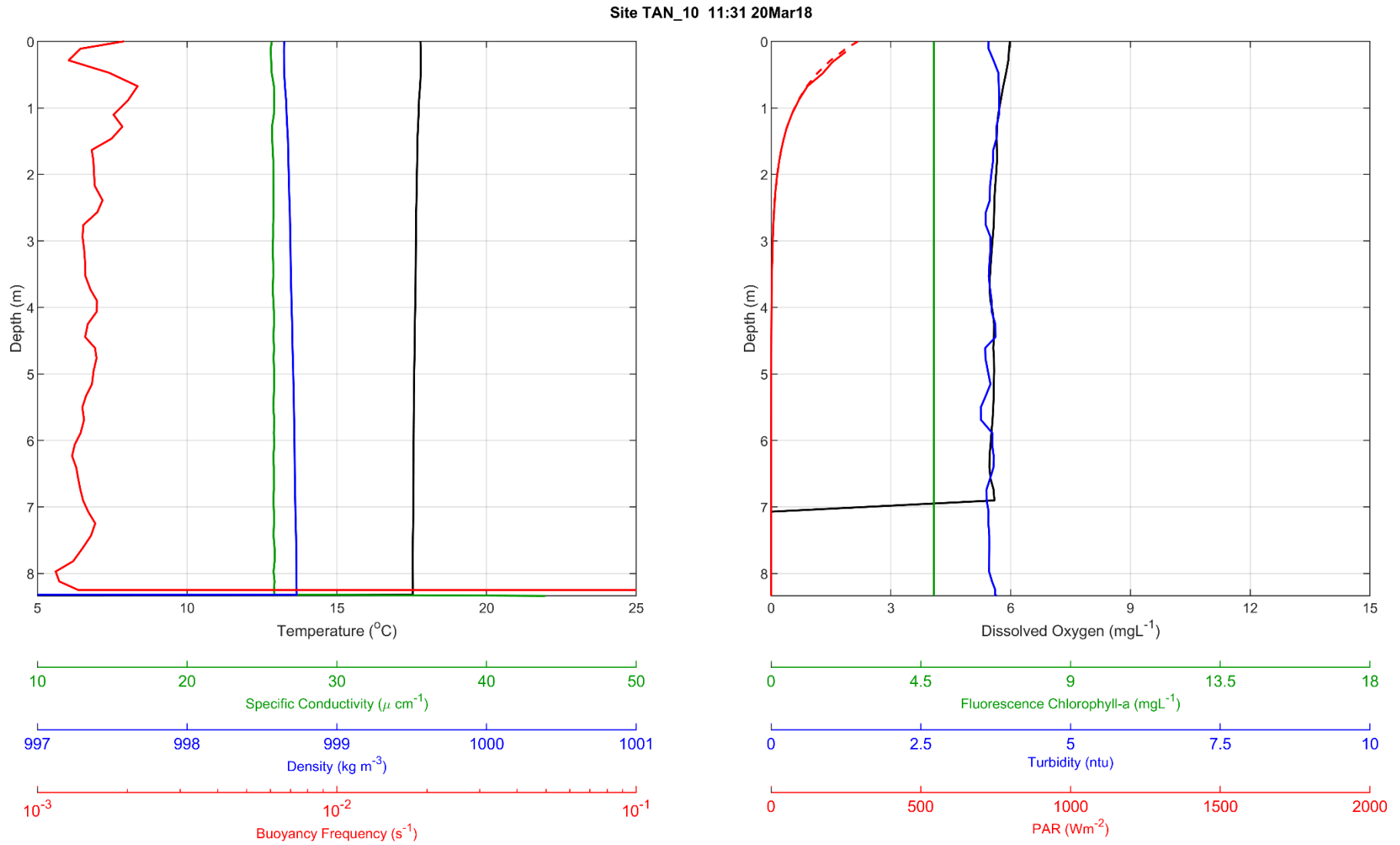


Figure F-47 Tantangra Reservoir CTD Profile, site TAN_10 at 1131 on 20 March 2018



Tantangra Reservoir – 4th October 2018

Figure F-48 Tantangra Reservoir CTD Profile, site TAN_01 at 1153 on 4 October 2018

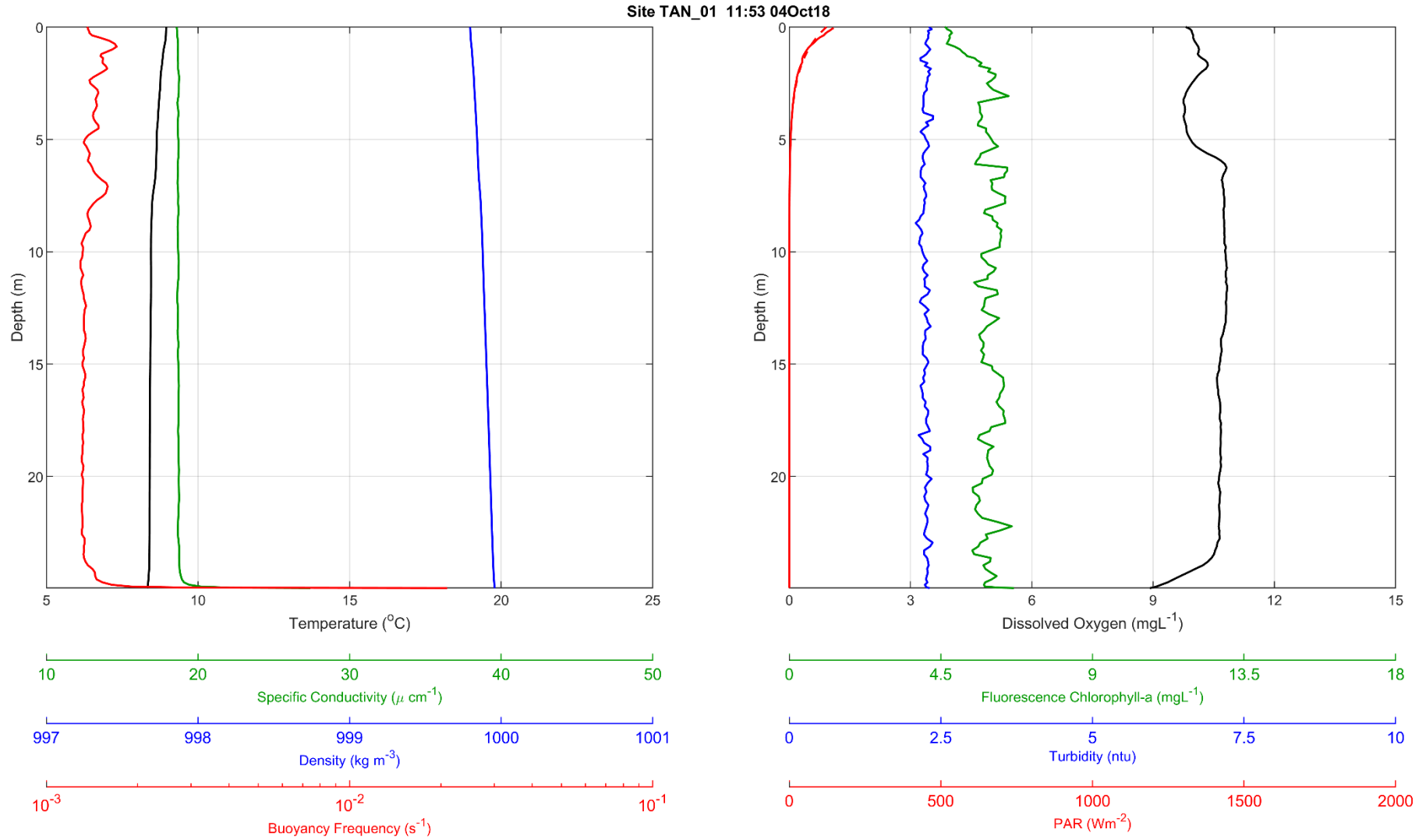


Figure F-49 Tantangra Reservoir CTD Profile, site TAN_02 at 1145 on 4 October 2018

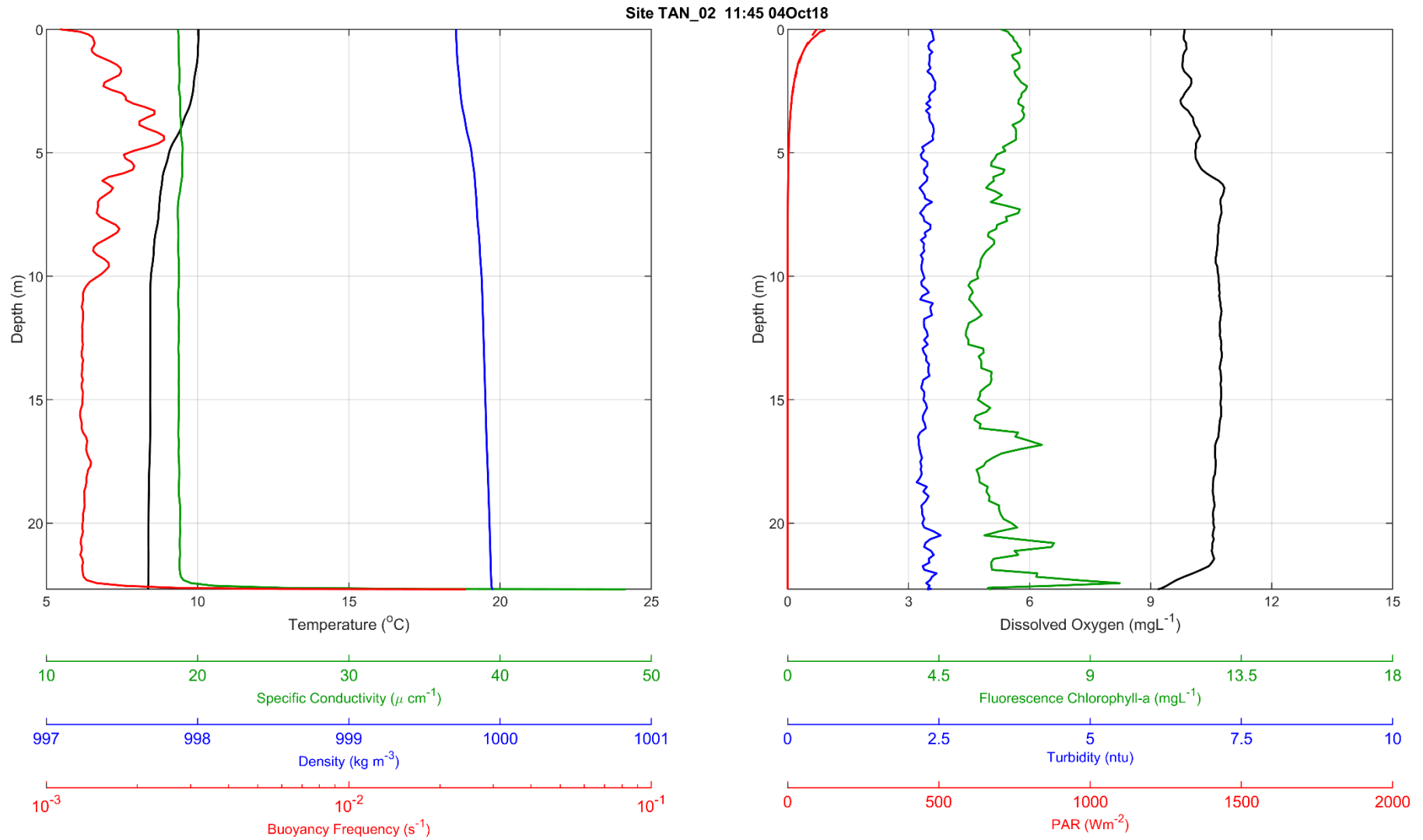


Figure F-50 Tantangra Reservoir CTD Profile, site TAN_03 at 1138 on 4 October 2018

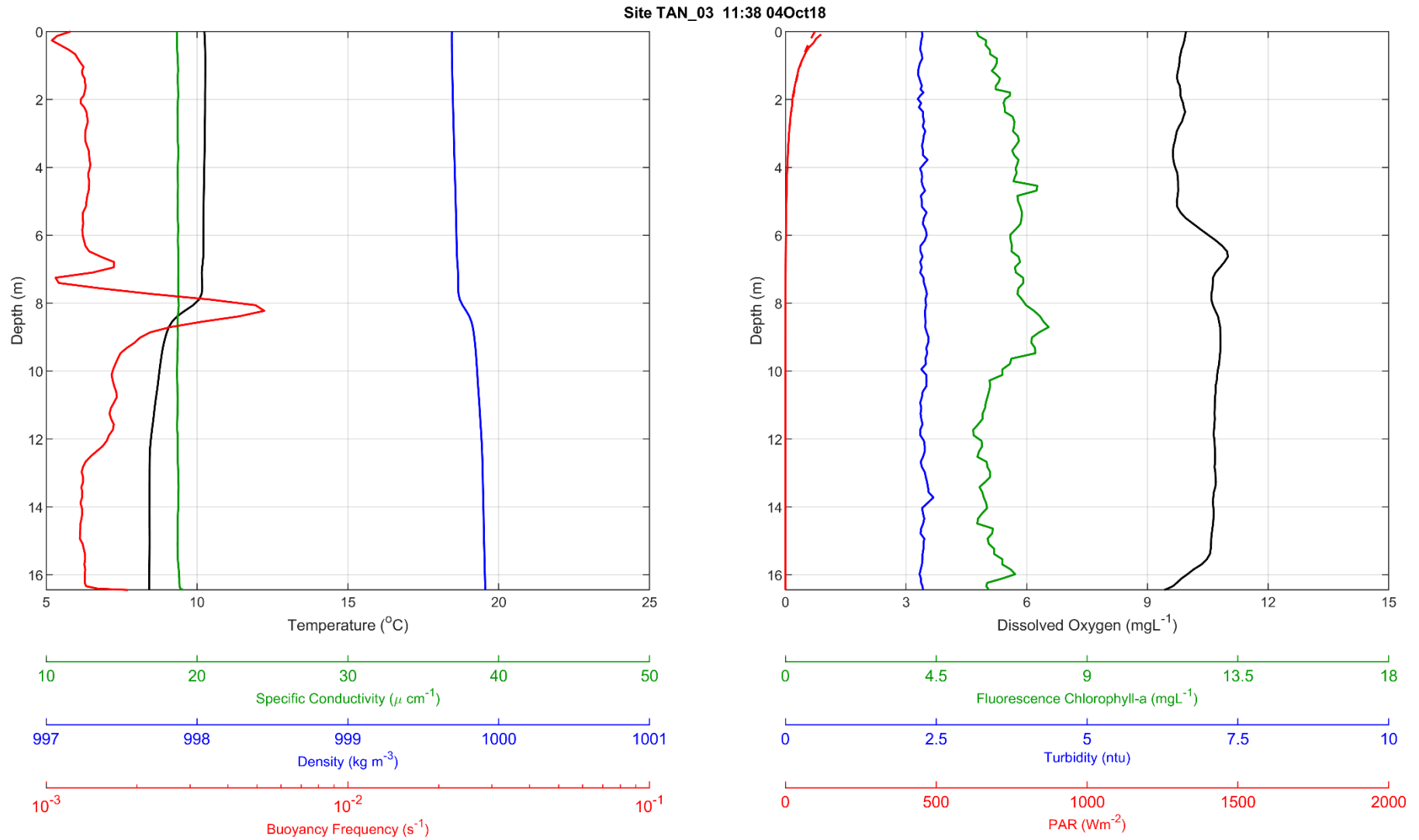


Figure F-51 Tantangra Reservoir CTD Profile, site TAN_04 at 1129 on 4 October 2018

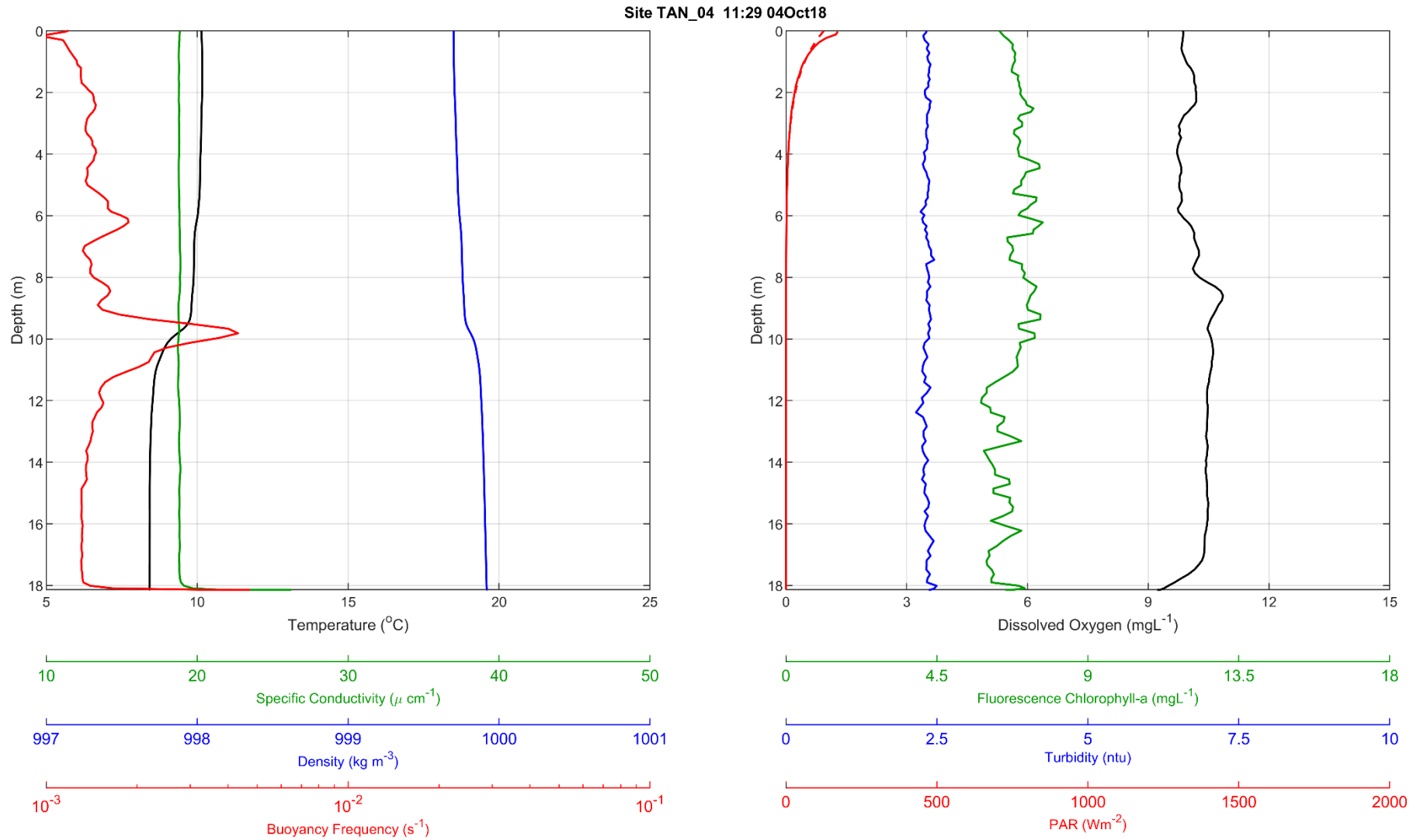


Figure F-52 Tantangra Reservoir CTD Profile, site TAN_05 at 1123 on 4 October 2018

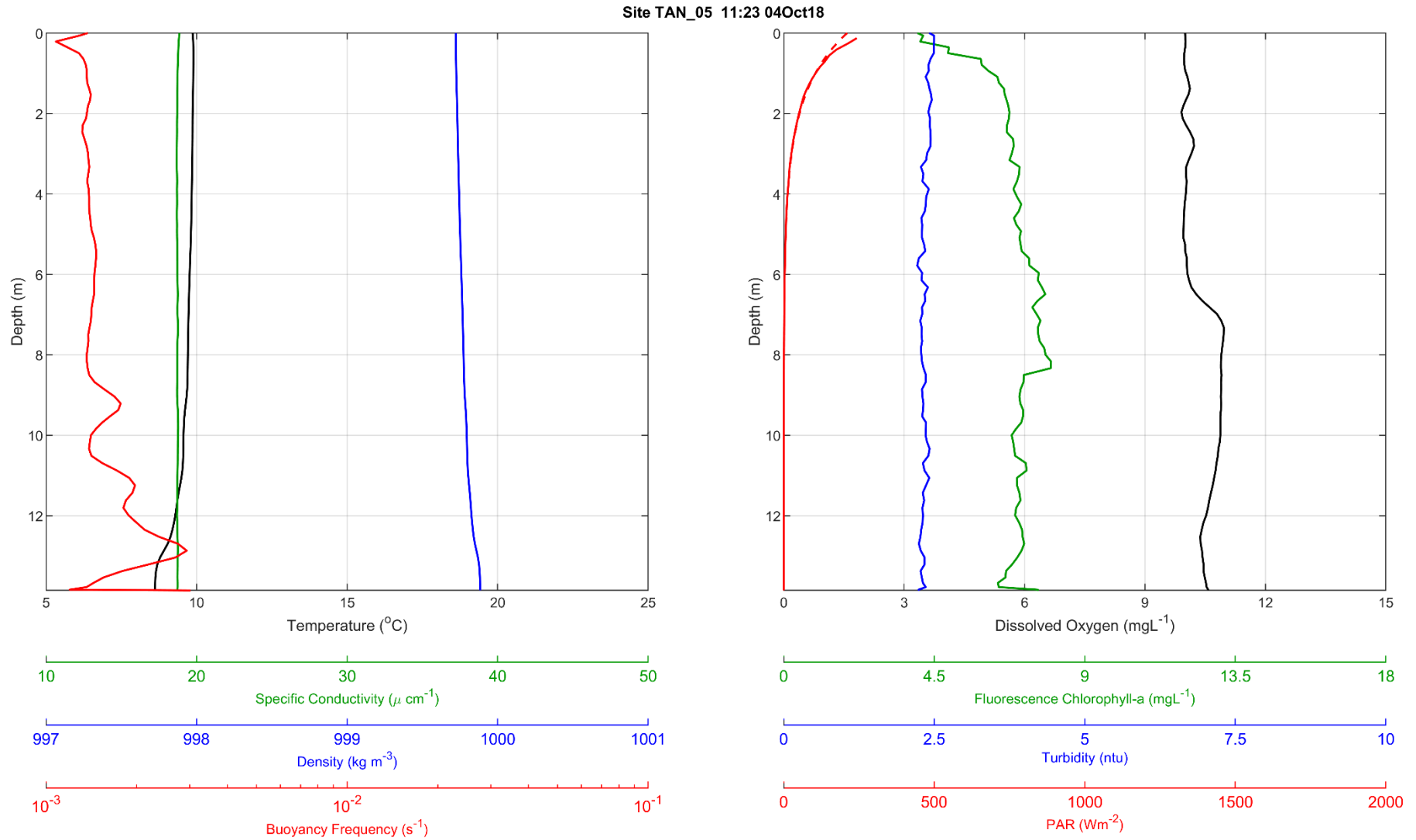


Figure F-53 Tantangra Reservoir CTD Profile, site TAN_06 at 1116 on 4 October 2018

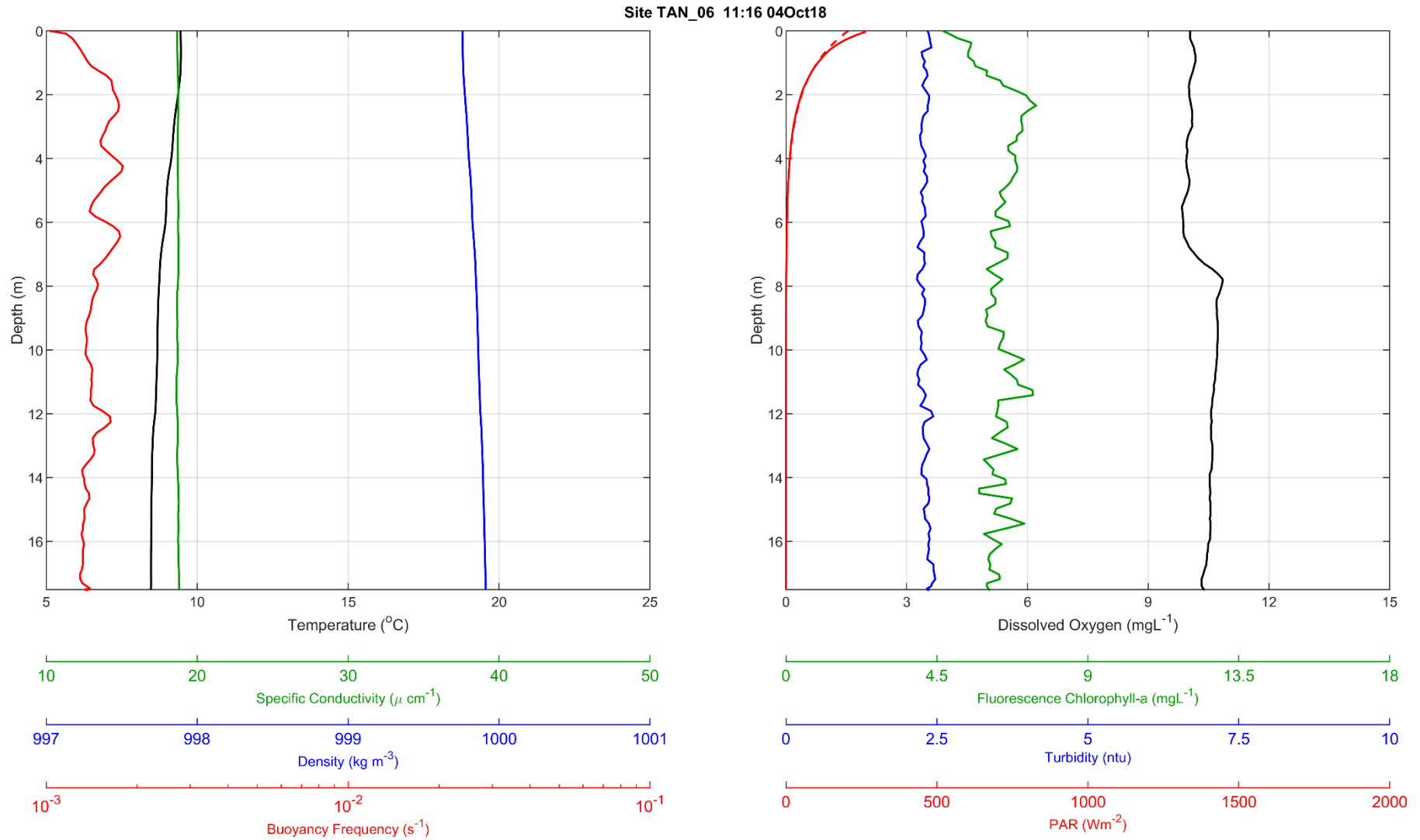


Figure F-54 Tantangra Reservoir CTD Profile, site TAN_07 at 1108 on 4 October 2018

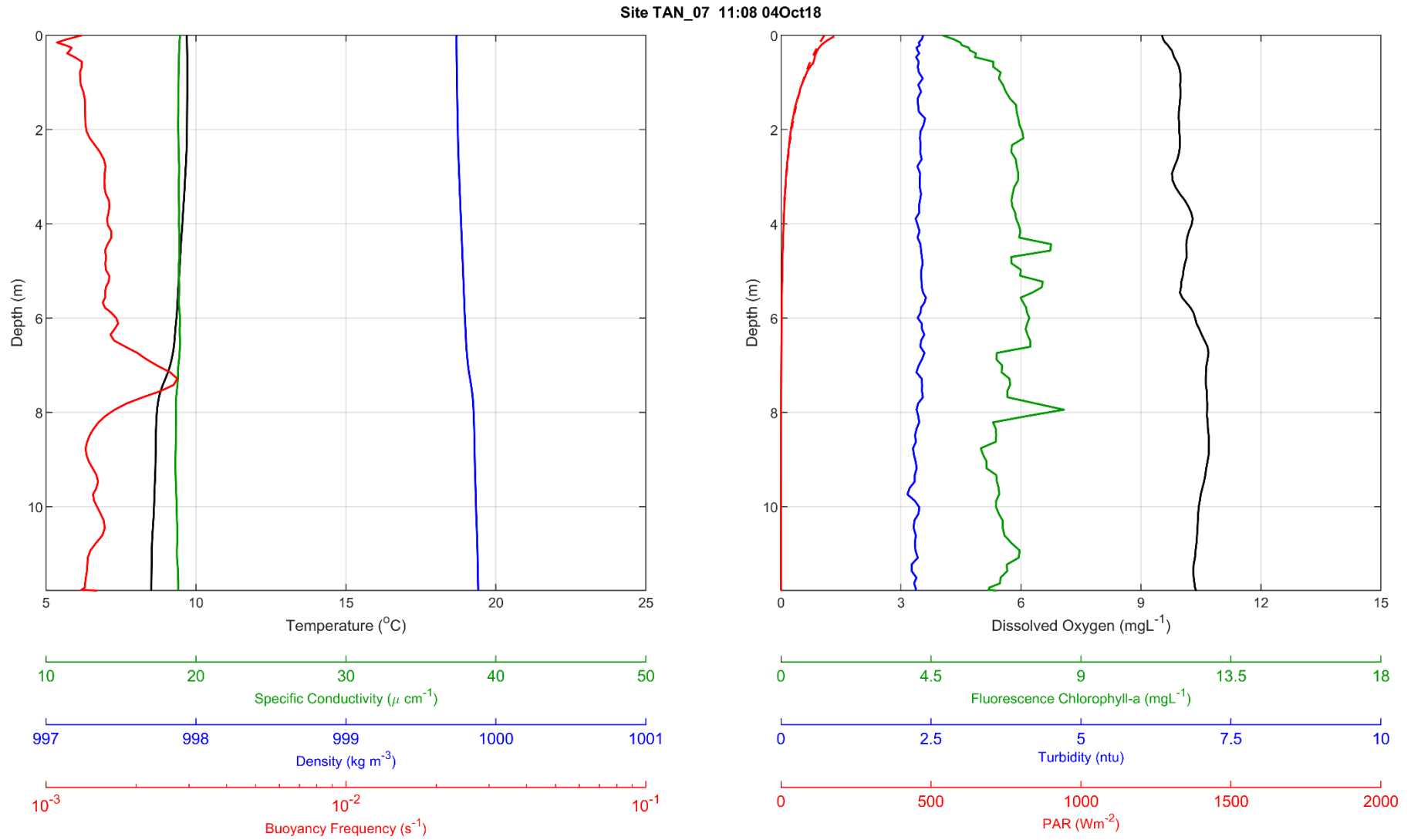


Figure F-55 Tantangra Reservoir CTD Profile, site TAN_08 at 1101 on 4 October 2018

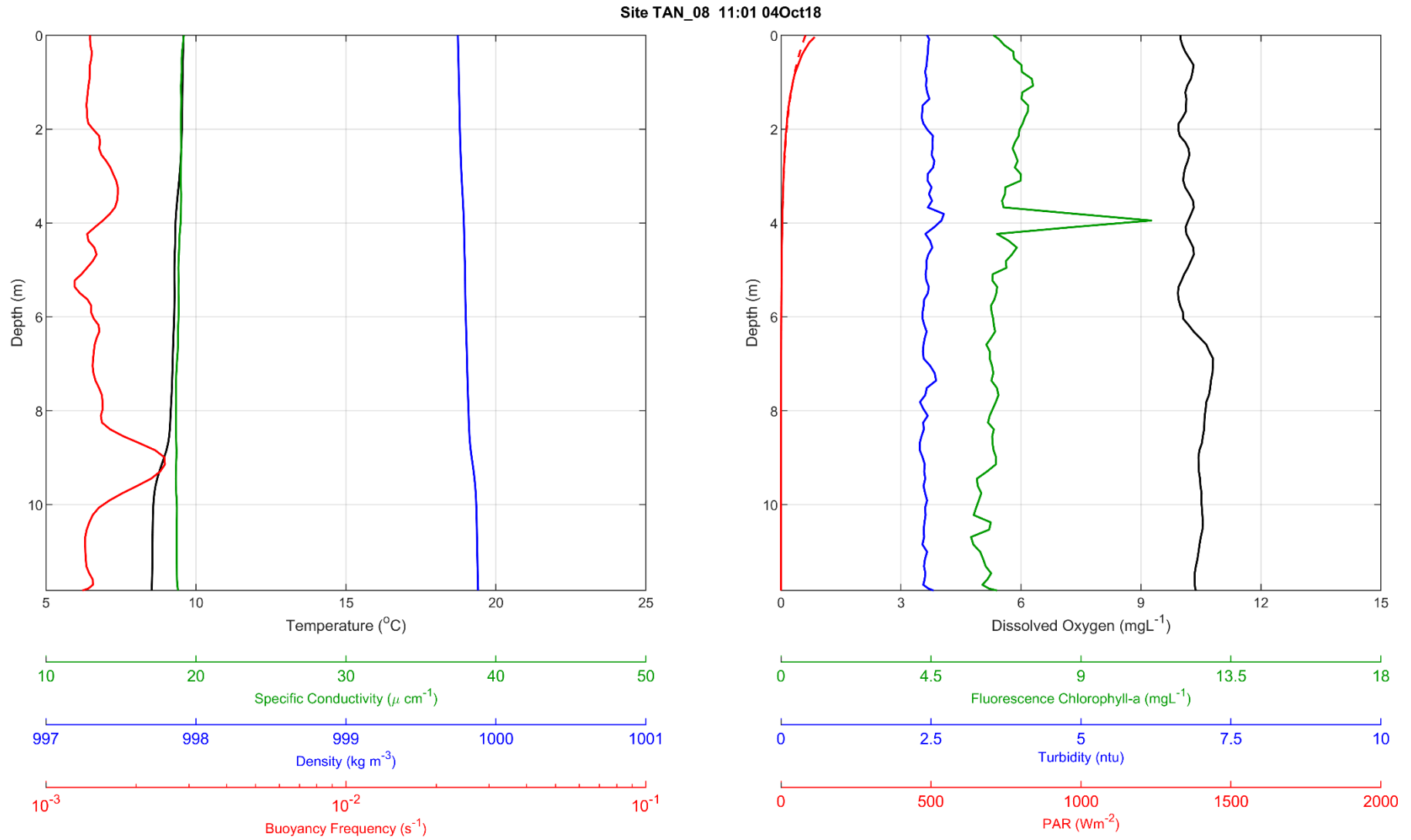


Figure F-56 Tantangra Reservoir CTD Profile, site TAN_09 at 1053 on 4 October 2018

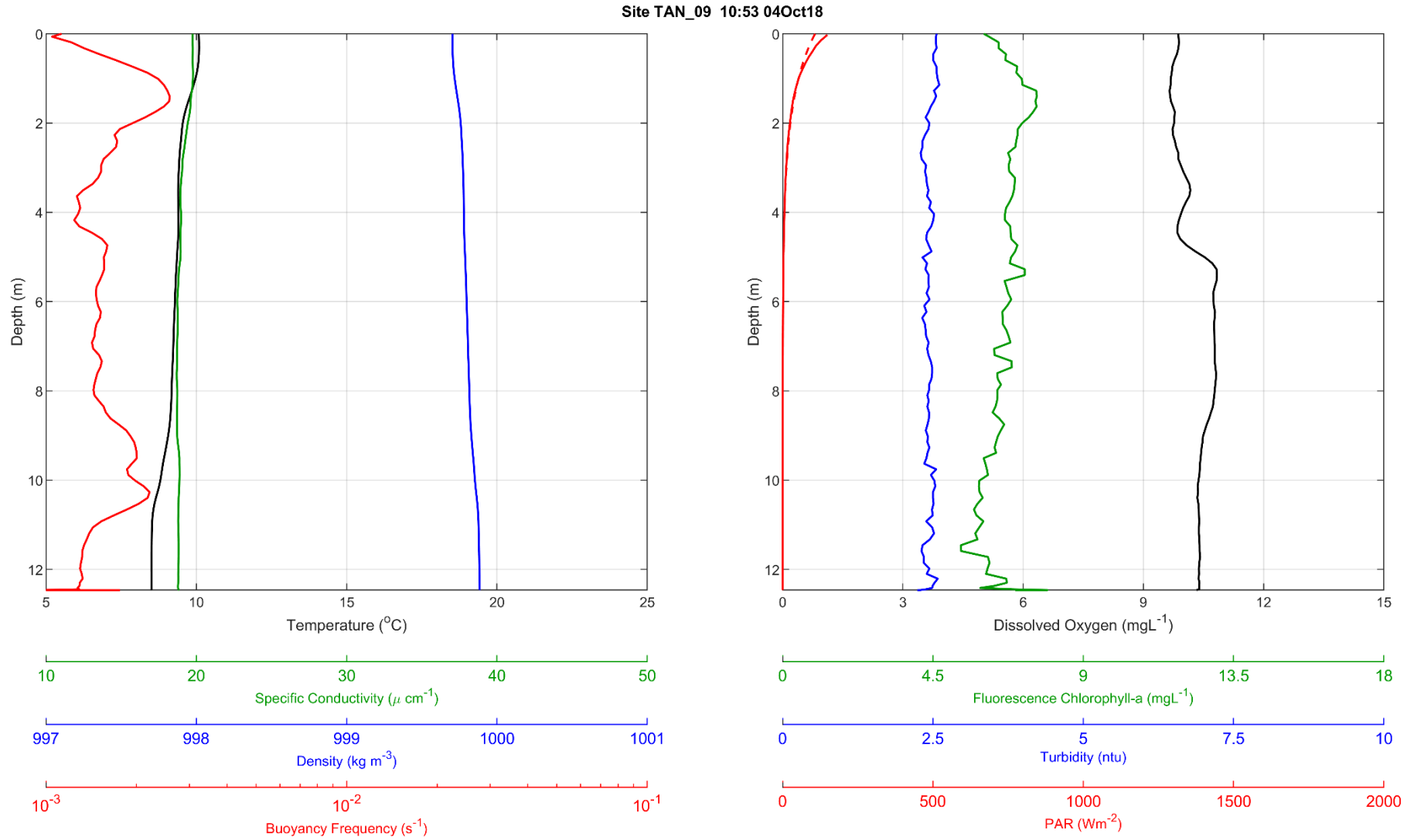
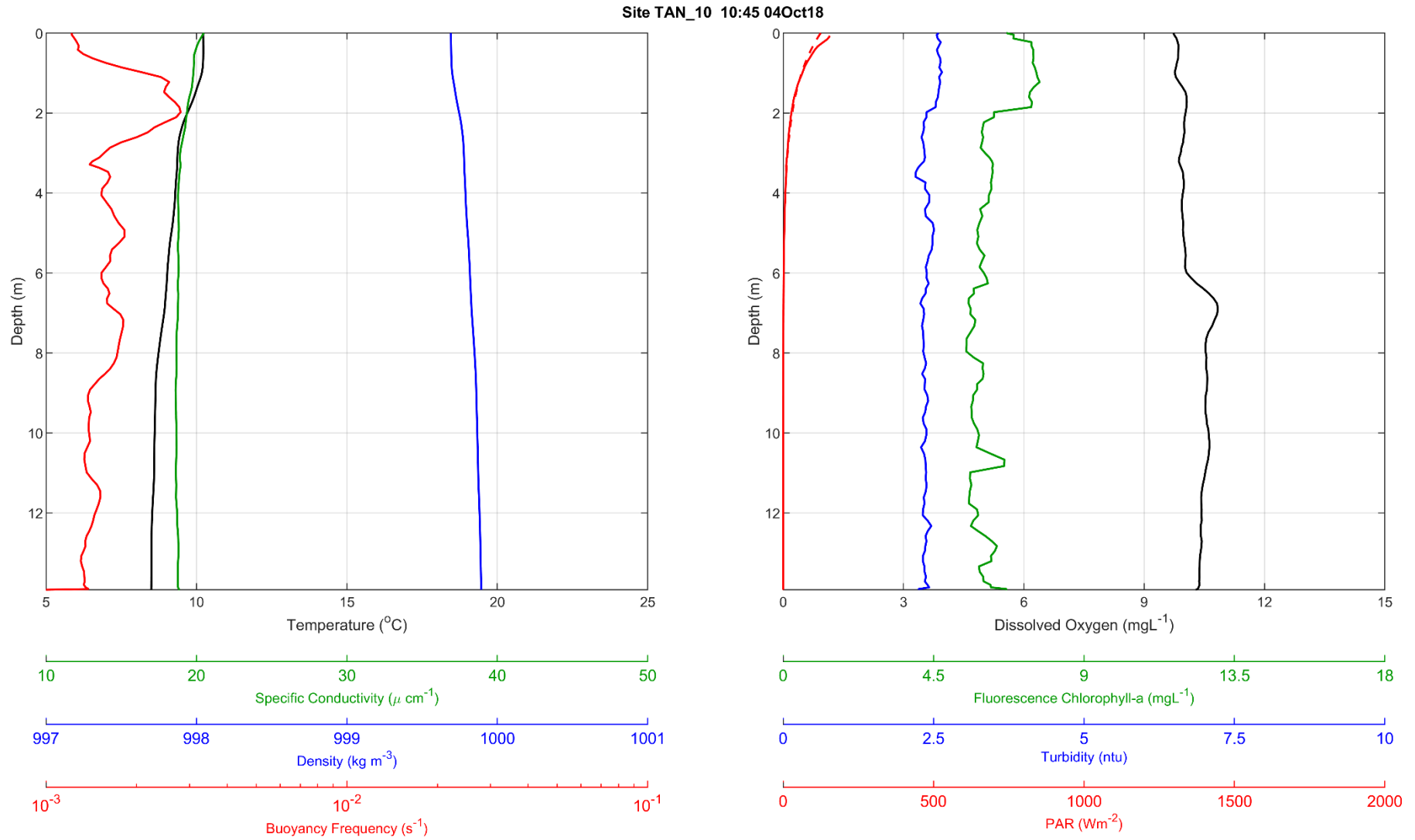


Figure F-57 Tintangra Reservoir CTD Profile, site TAN_10 at 1045 on 4 October 2018



APPENDIX

G

CTD LONG SECTIONS

Talbingo Reservoir 22 March 2018

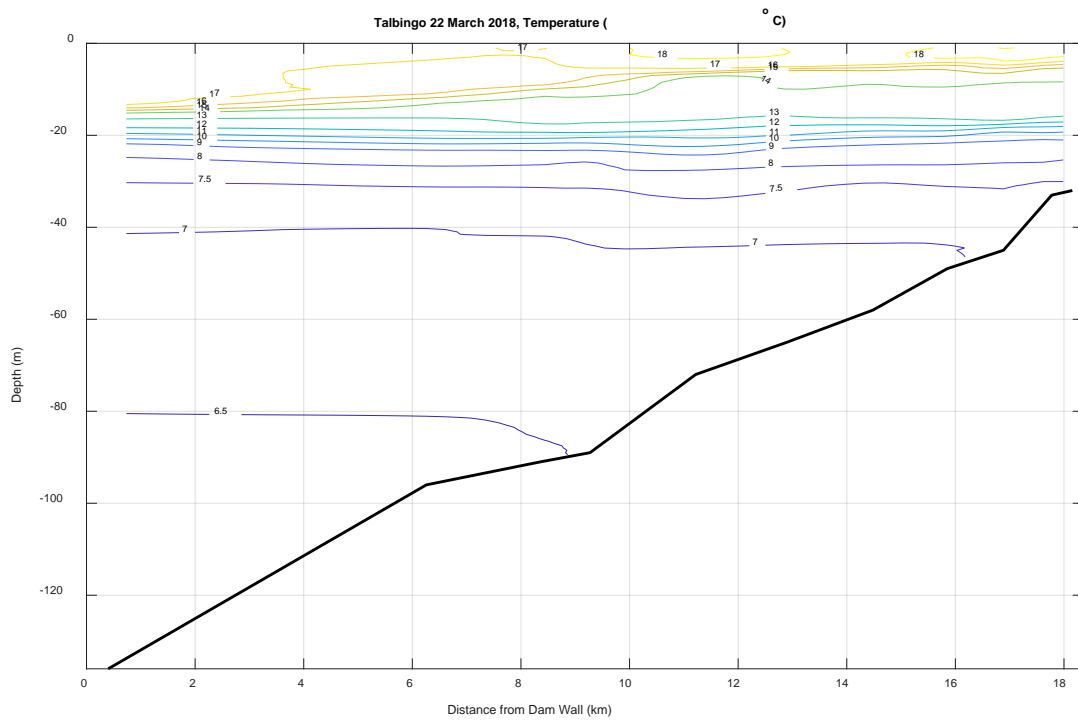


Figure G-1 Temperature contours on 22 March, 2018 in Talbingo Reservoir.

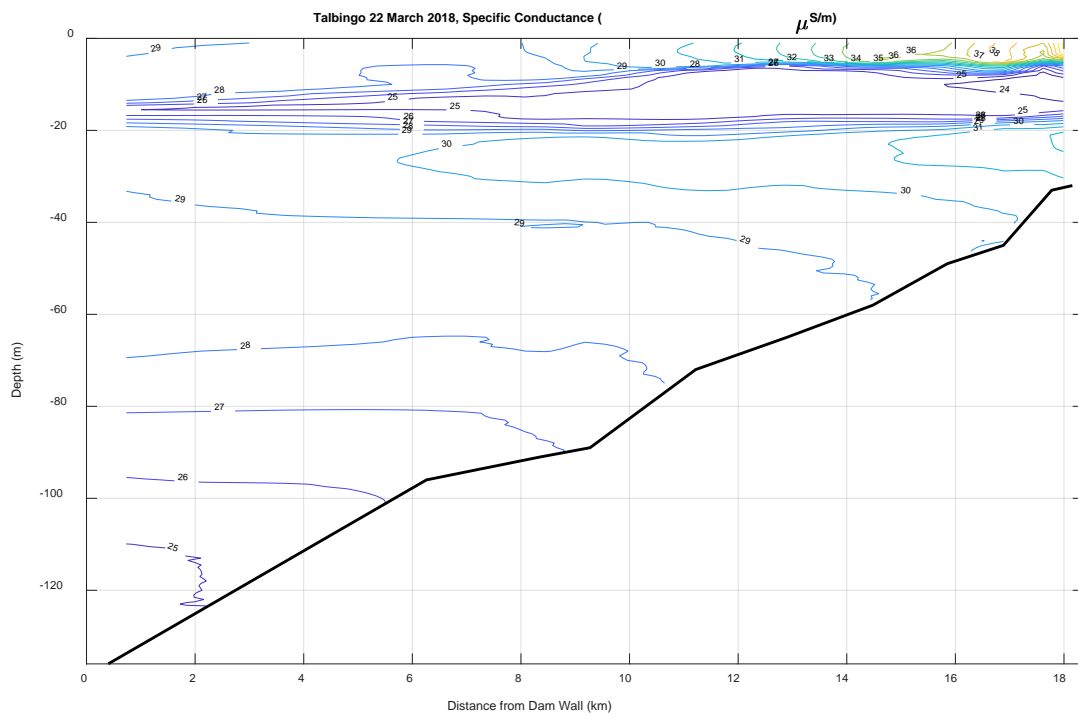


Figure G-2 Specific conductance contours on 22 March, 2018 in Talbingo Reservoir

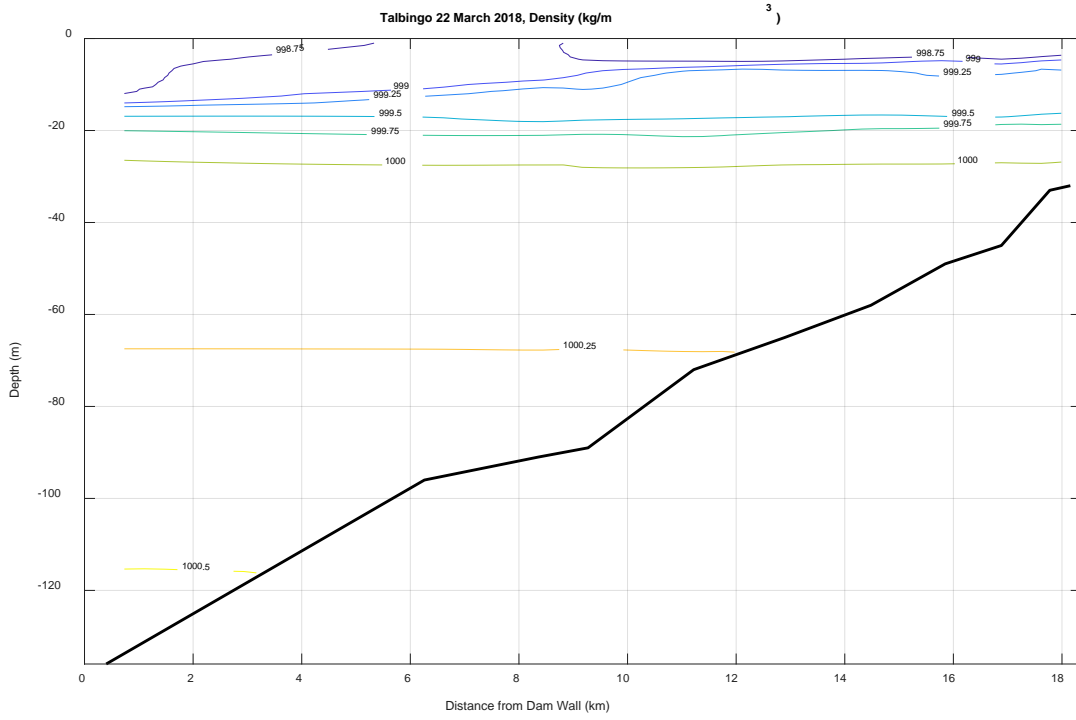


Figure G-3 Water density contours on 22 March, 2018 in Talbingo Reservoir

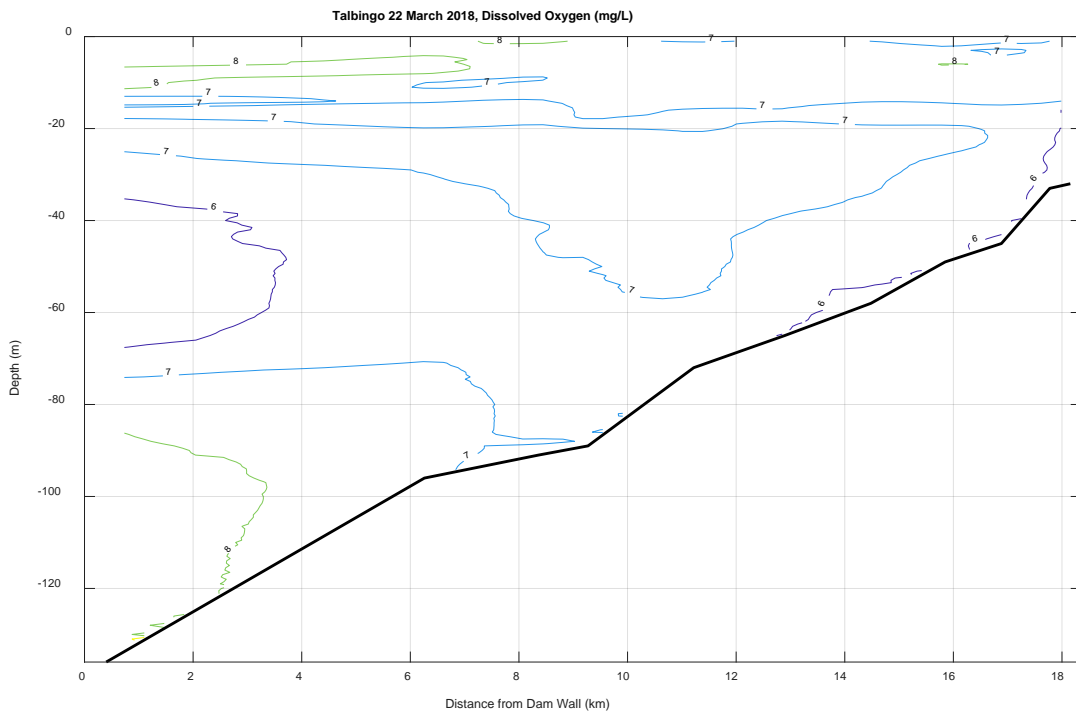


Figure G-4 Dissolved oxygen contours on 22 March, 2018 in Talbingo Reservoir

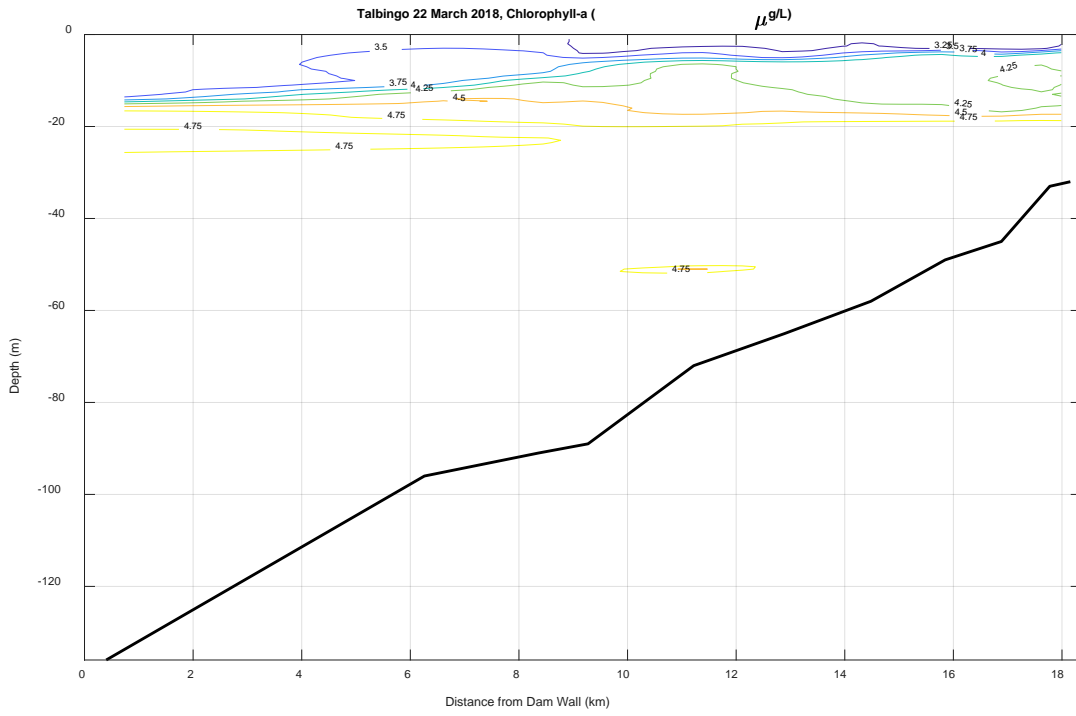


Figure G-5 Fluorescence chlorophyll-a contours on 22 March, 2018 in Talbingo Reservoir

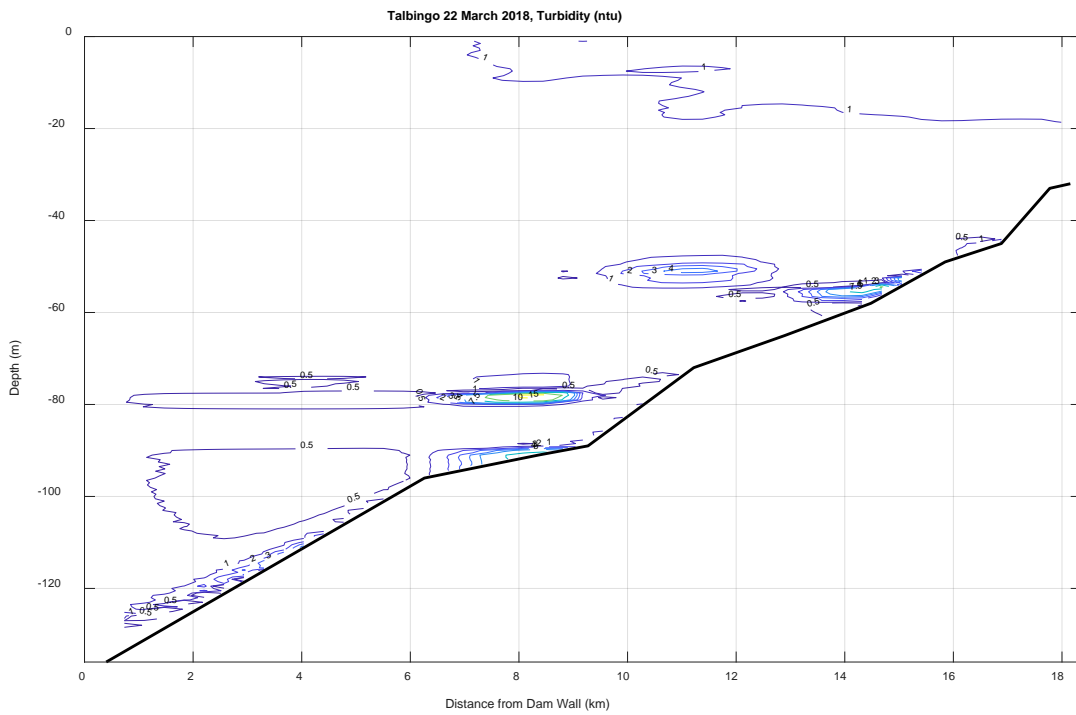


Figure G-6 Turbidity contours on 22 March, 2018 in Talbingo Reservoir

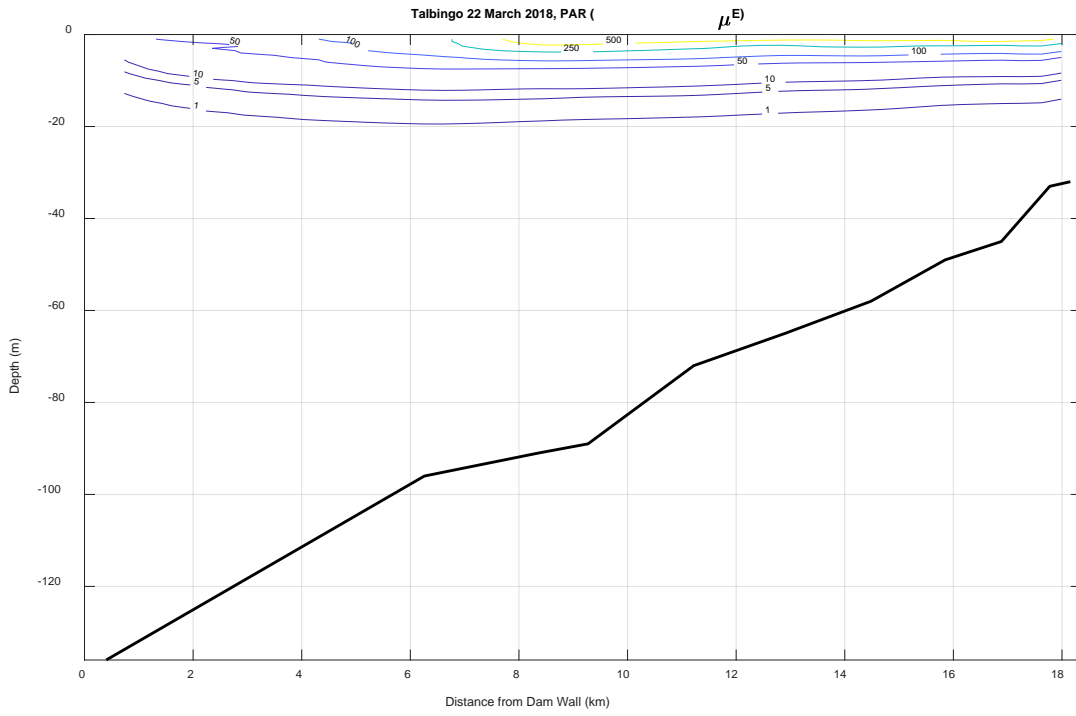


Figure G-7 Photosynthetically active radiation (PAR) contours on 22 March, 2018 in Talbingo Reservoir

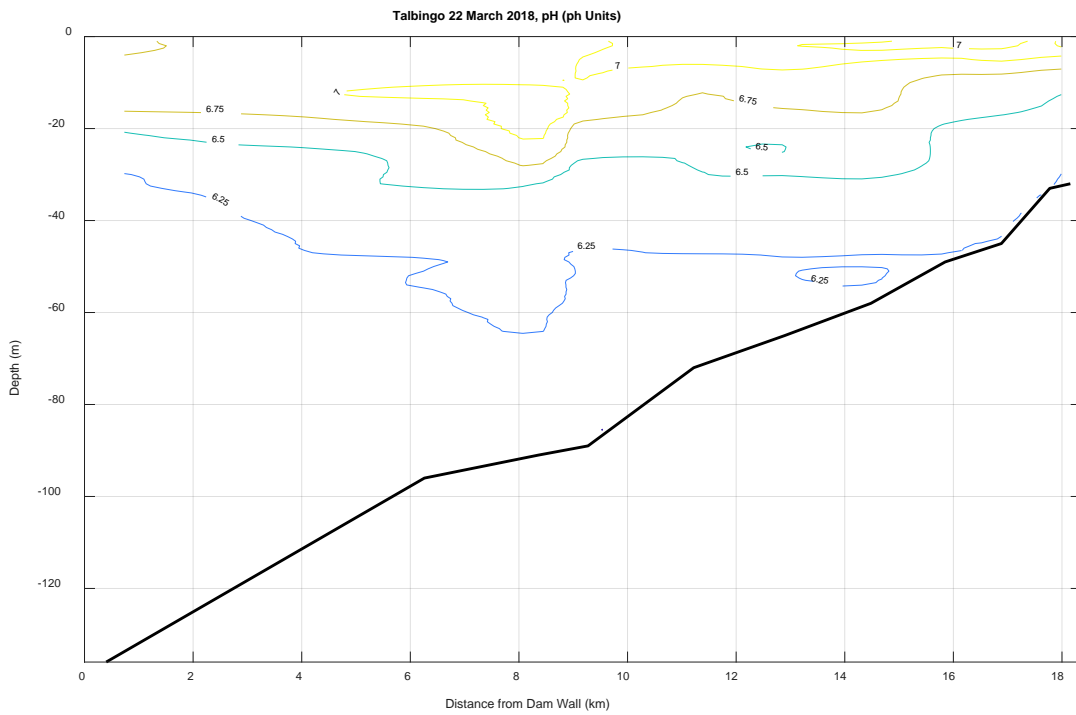


Figure G-8 pH contours on 22 March, 2018 in Talbingo Reservoir

APPENDIX

H

WATER QUALITY TIME SERIES

Talbingo Reservoir

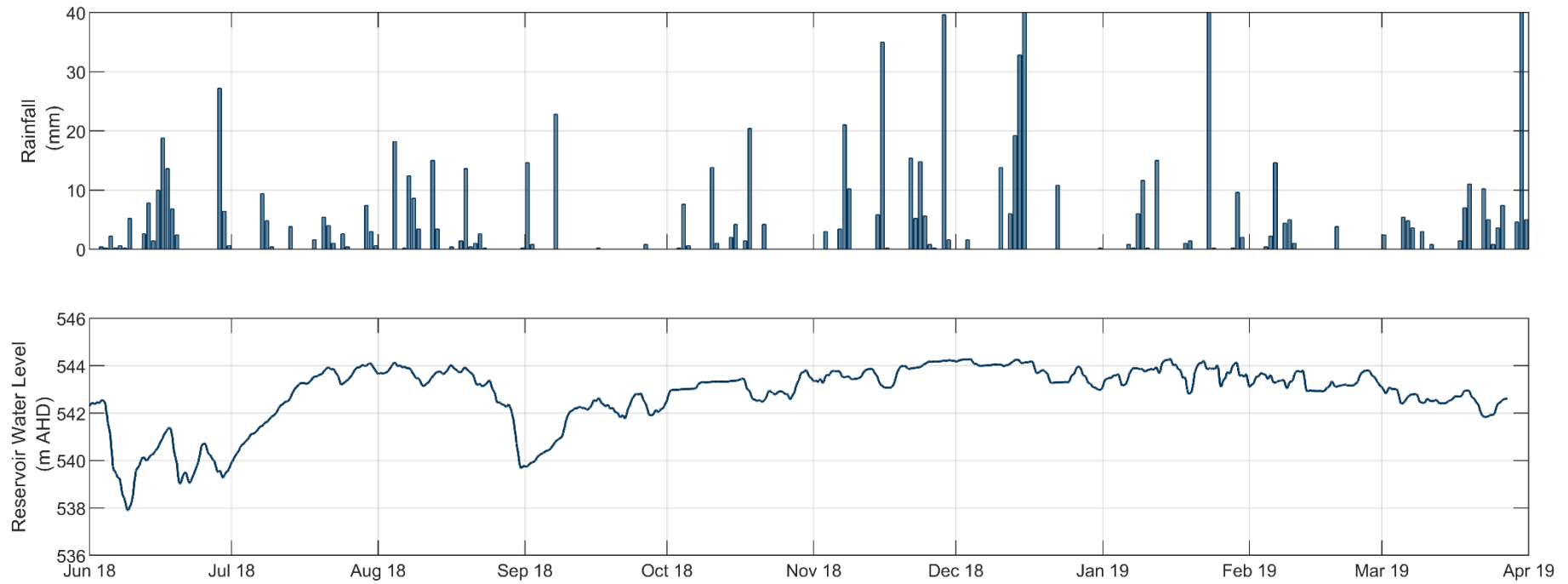


Figure H-1 Rainfall (top) and reservoir water level (bottom) time series at RO Intake near the dam wall

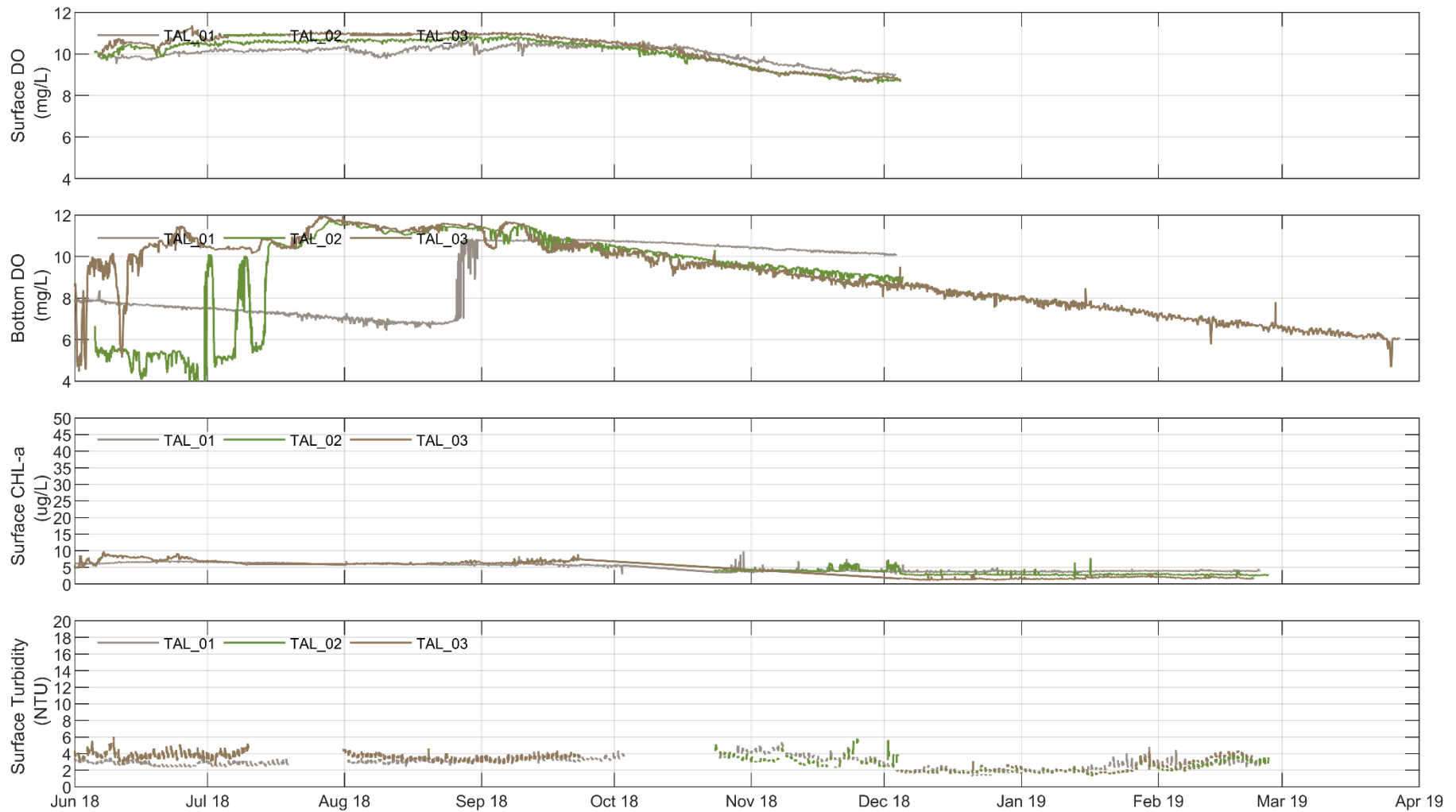


Figure H-2 Surface DO (1 m below surface), bottom DO (4.5 m above bed), surface CHL-a (1 m below surface) and surface turbidity (1 m below surface) time series at Talbingo monitoring sites

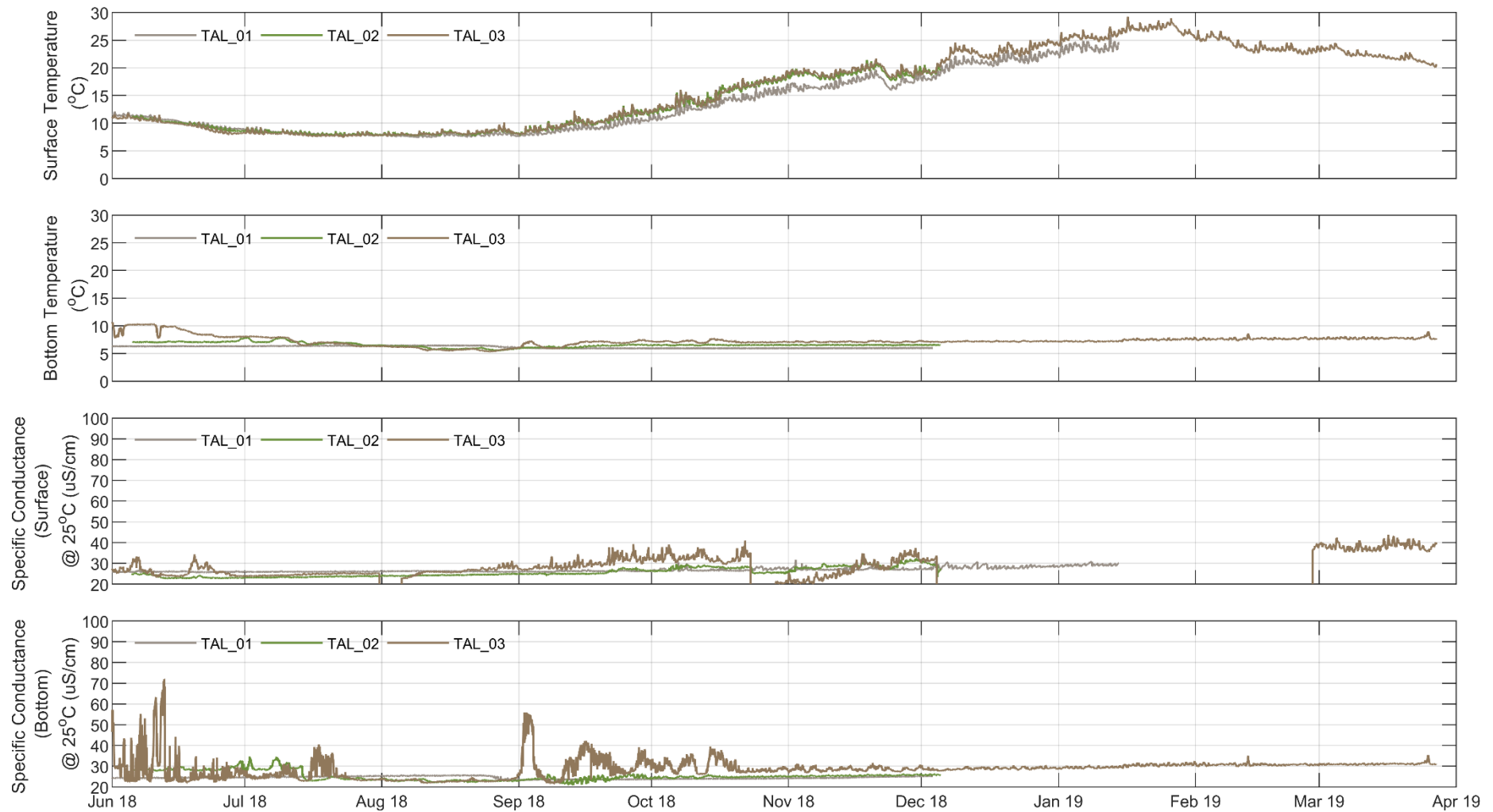


Figure H-3 Surface temperature (0.6 m below surface), bottom temperature (4.5 m above bed), surface specific conductance (0.6 m below surface) and bottom conductance (4.5 m above bed) time series at Talbingo monitoring sites

Tantangara Reservoir

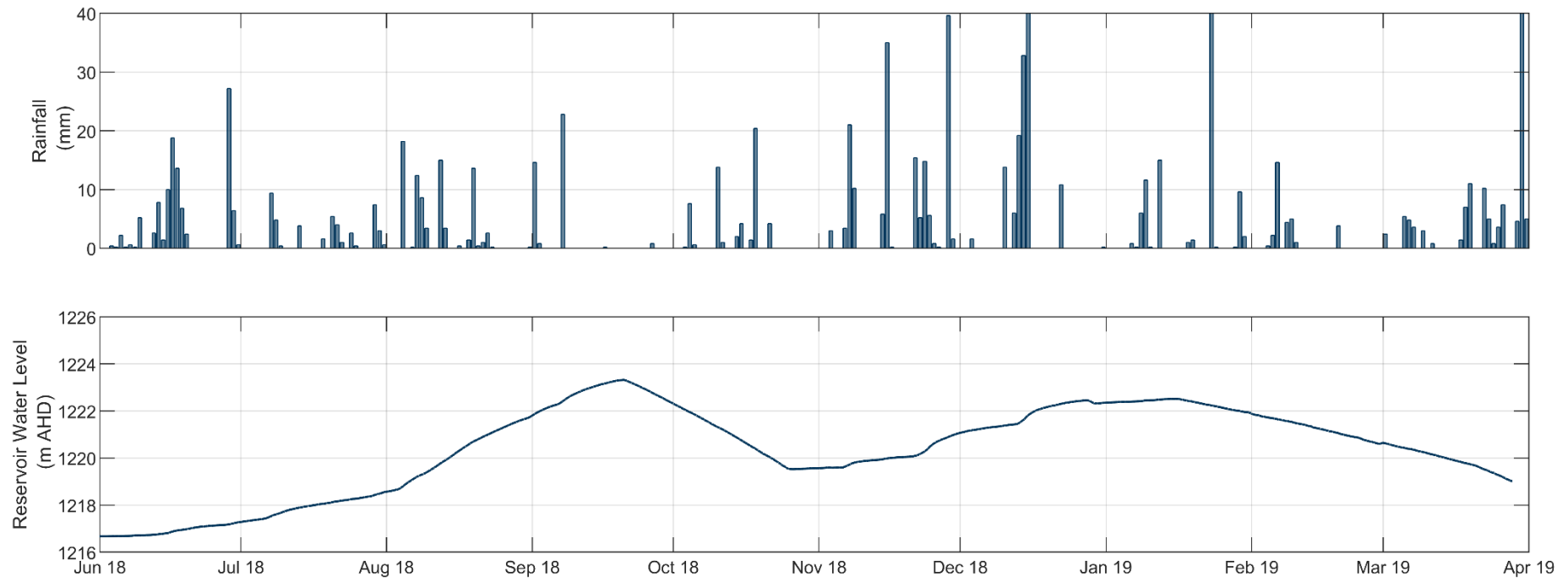


Figure H-4 Rainfall (top) and reservoir water level (bottom) time series at the Tantangara dam wall

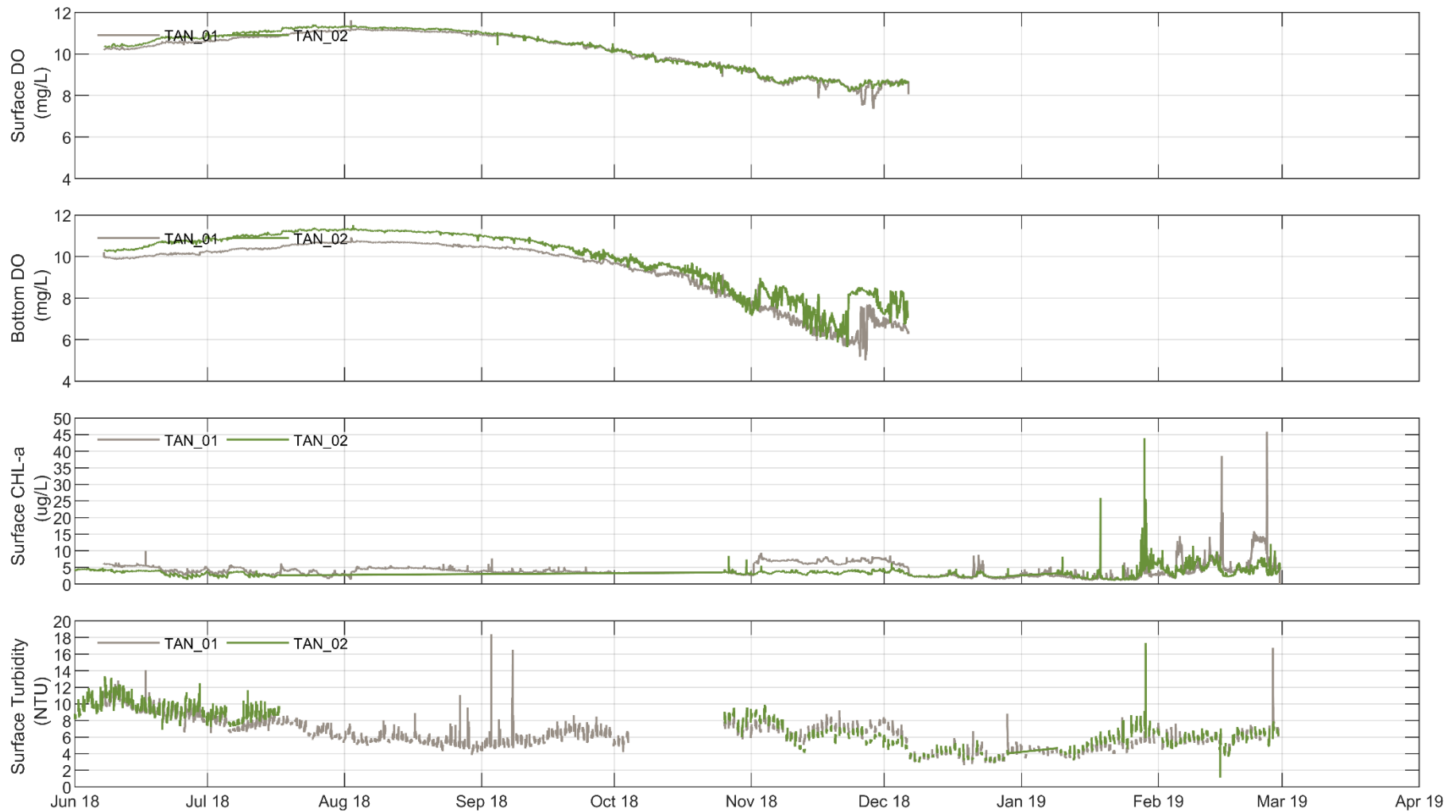


Figure H-5 Surface DO (1 m below surface), bottom DO (4.5 m above bed), surface CHL-a (1 m below surface) and surface turbidity (1 m below surface) time series at Tangara monitoring sites

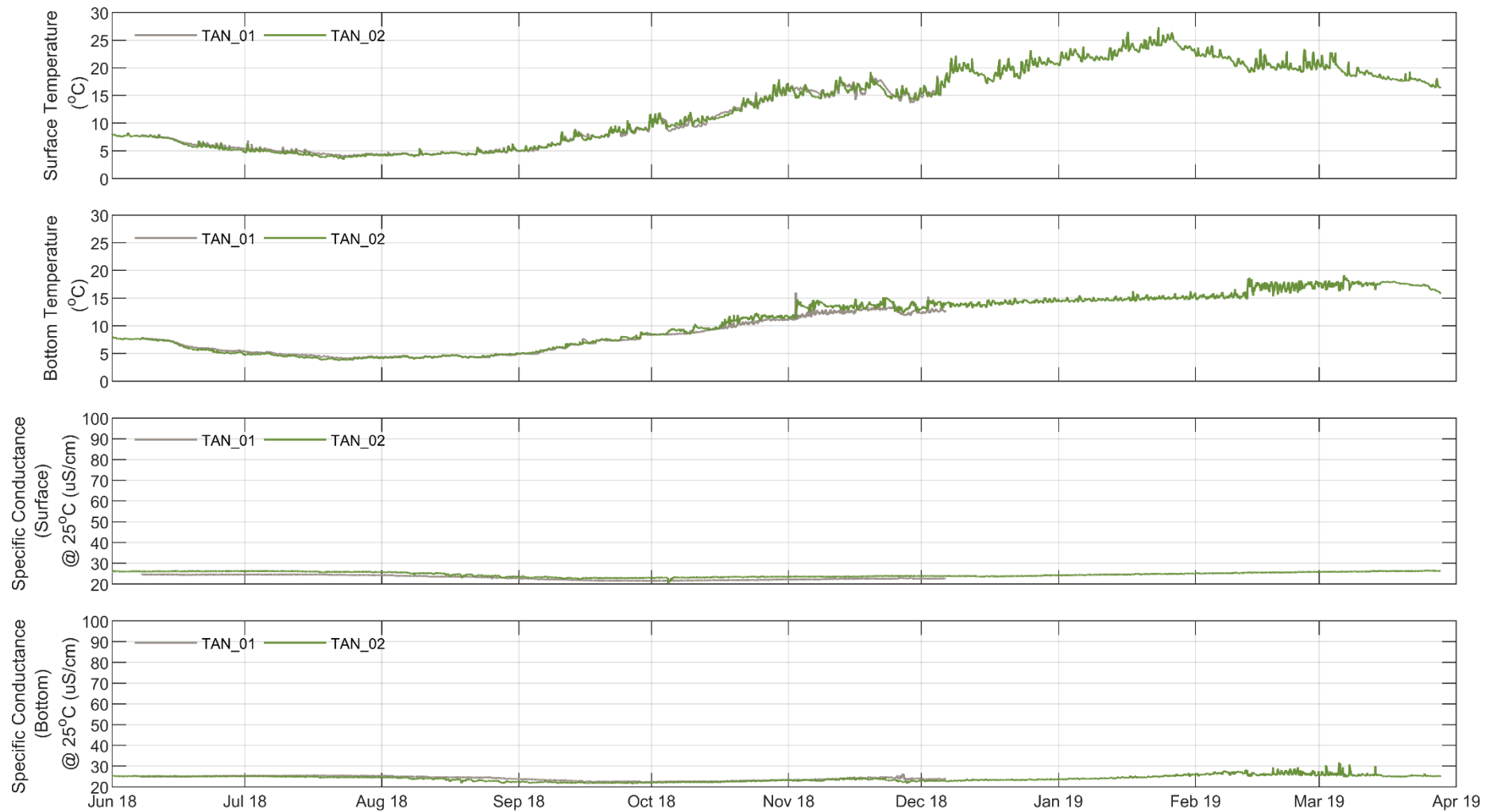


Figure H-6

Surface temperature (0.6 m below surface), bottom temperature (4.5 m above bed), surface specific conductance (0.6 m below surface) and bottom conductance (4.5 m above bed) time series at Tantangara monitoring sites

APPENDIX

I

ADCP CURRENT METER FIGURES

Figure I-1 ADCP current vectors in Talbingo Reservoir at site TAL-01.

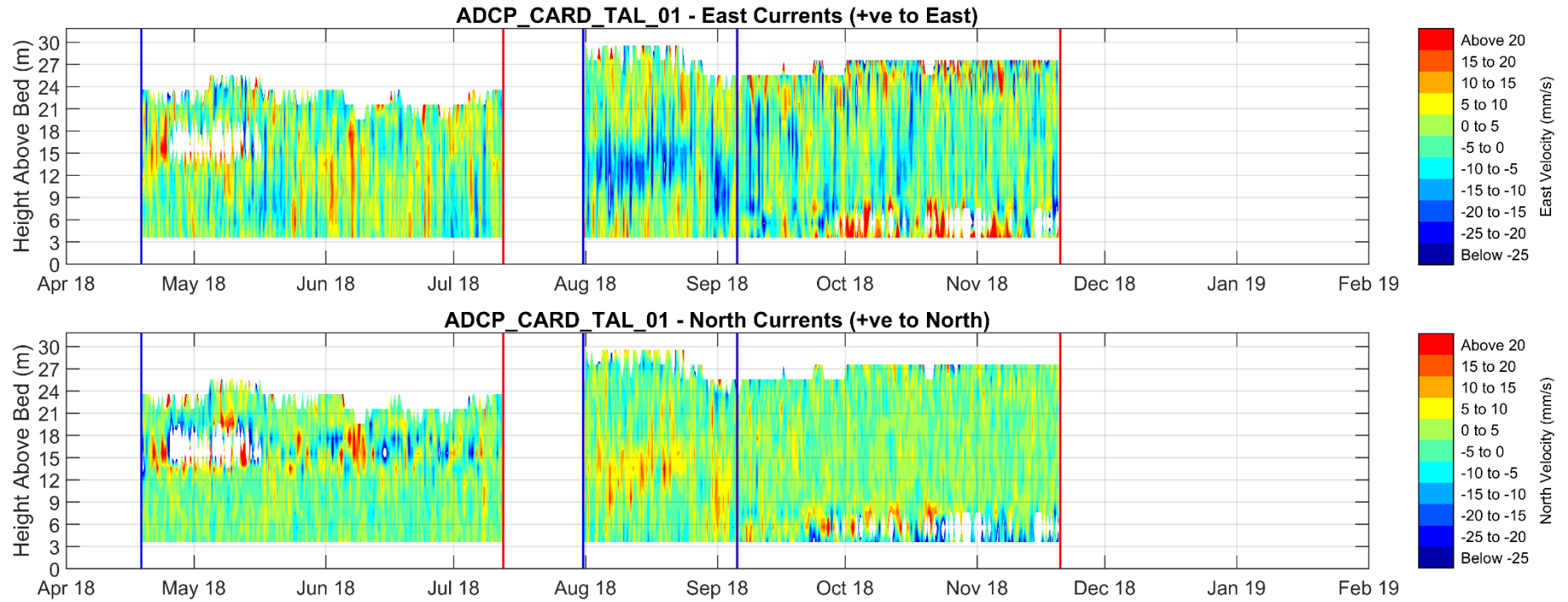


Figure I-2 ADCP current vectors in Talbingo Reservoir at site TAL-02.

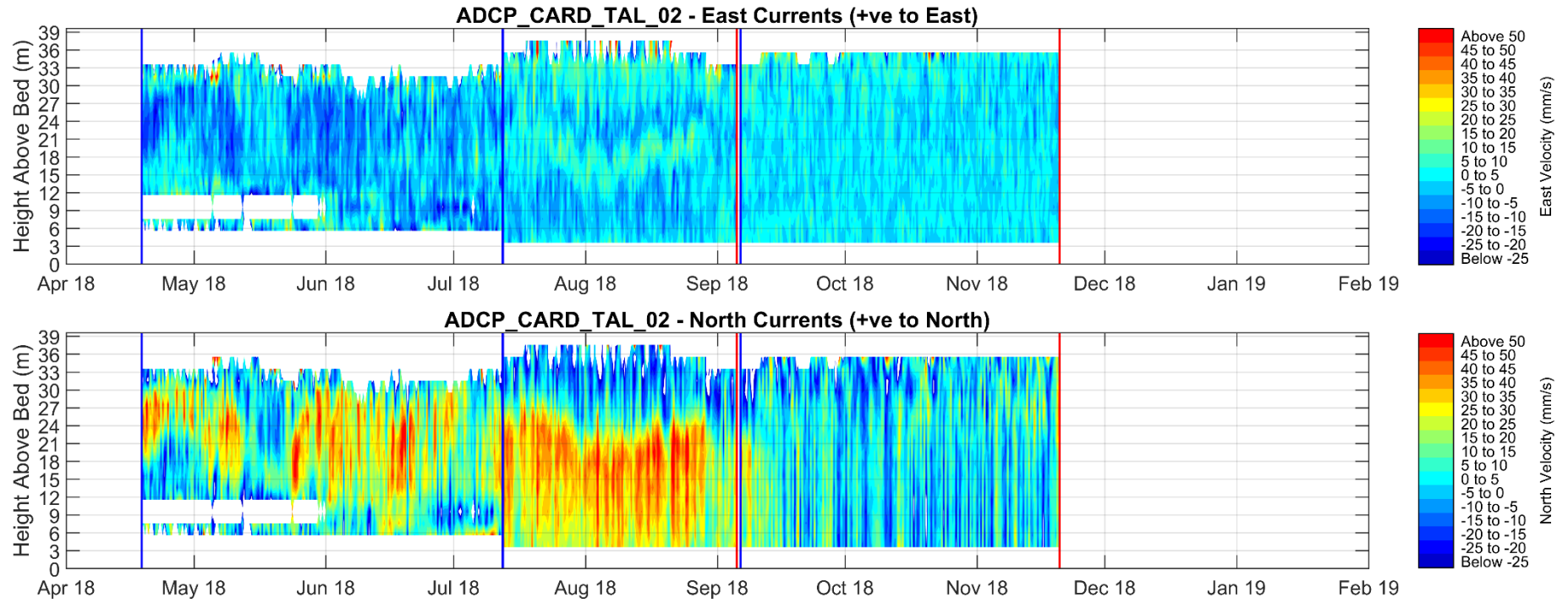


Figure I-3 ADCP current vectors in Tintangara Reservoir at site TAN-01.

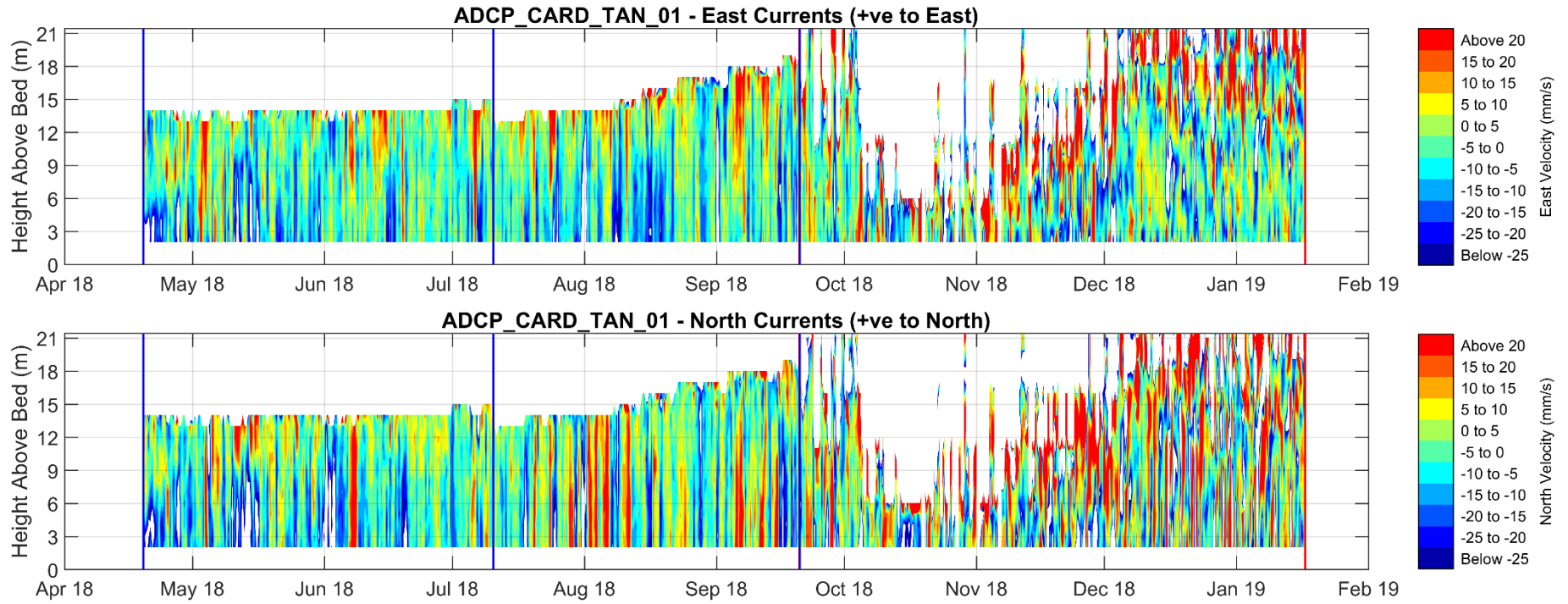
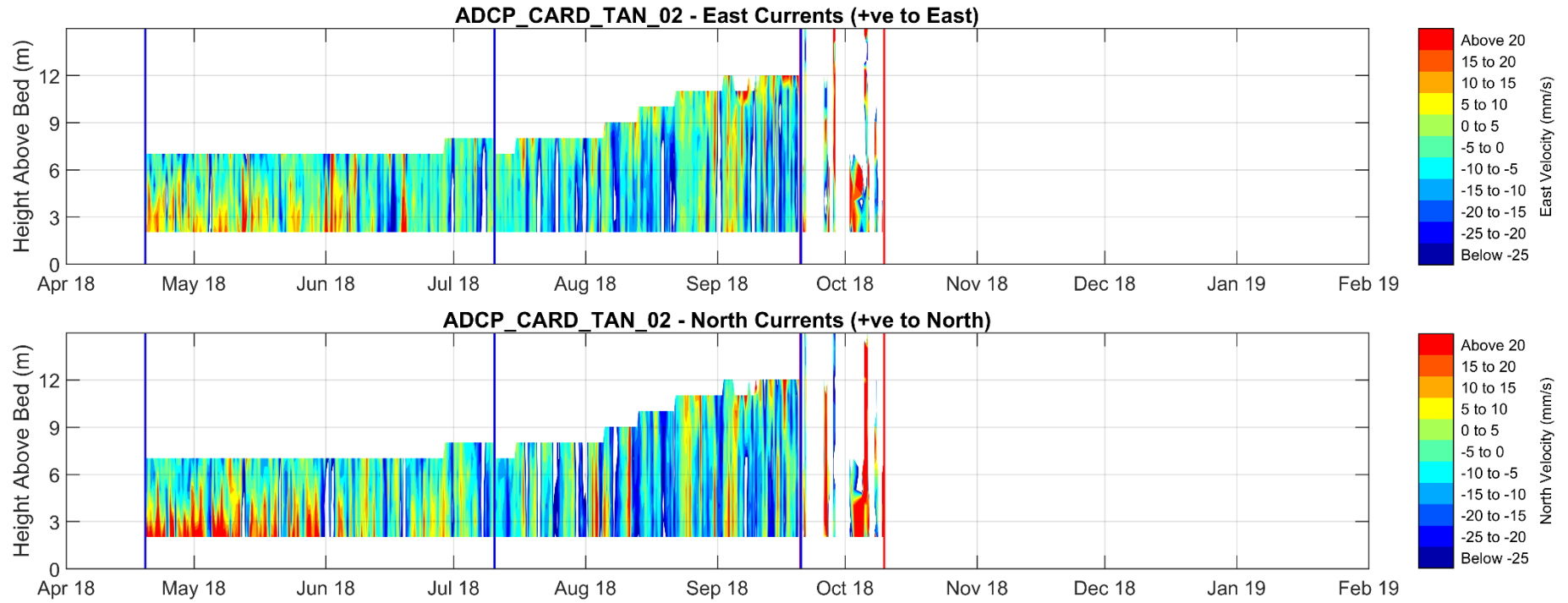


Figure I-4 ADCP current vectors in Tintangara Reservoir at site TAN-02.



APPENDIX

J

MONTHLY SNAPSHOTS

Talbingo Reservoir

Meteorological Conditions

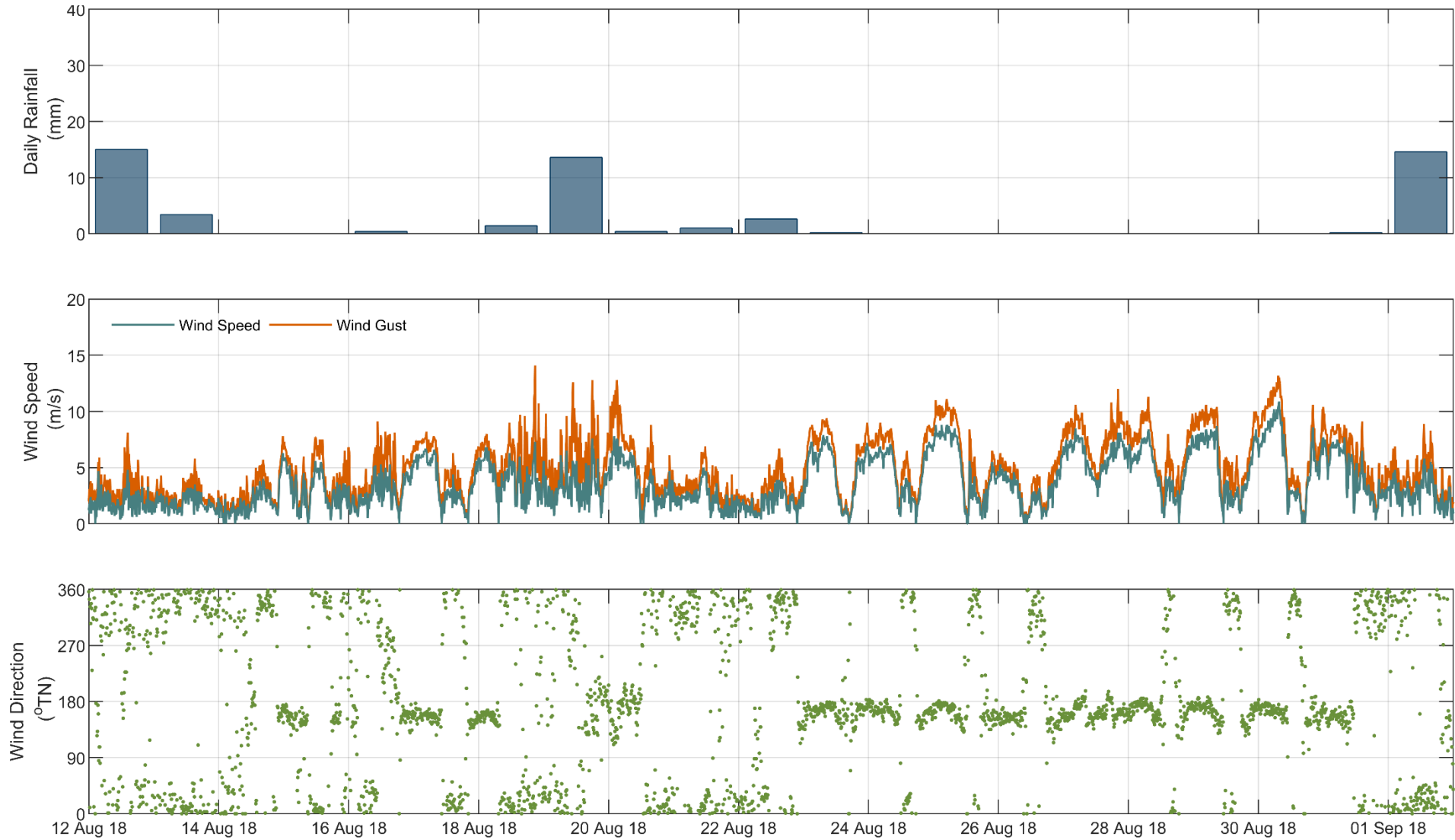


Figure J-1

Daily rainfall (top), wind speed (middle) and wind direction (bottom) time series at site TAL_01 near the dam wall (12th August 2018 to 2nd September 2018)

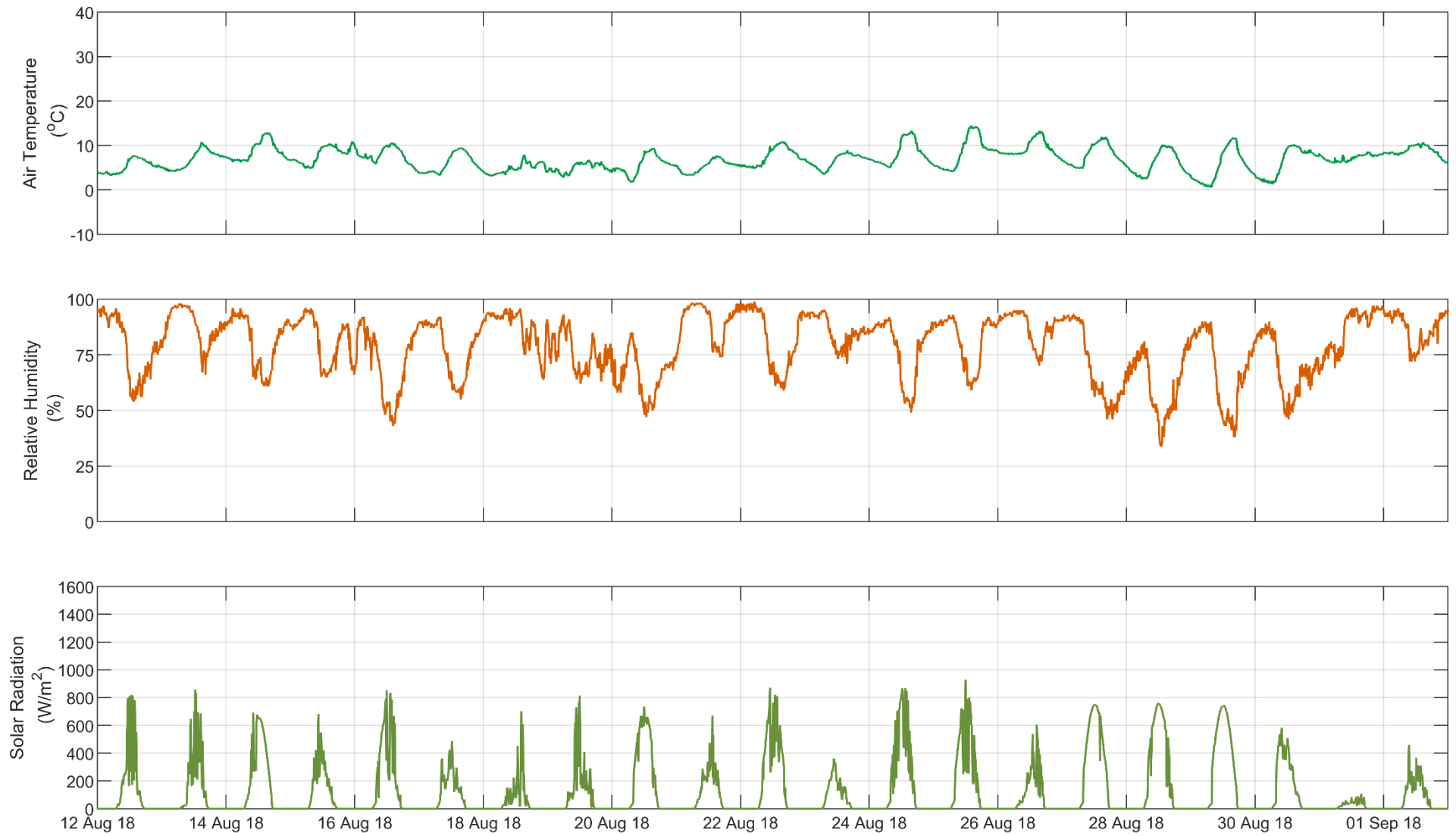


Figure J-2

Daily air temperature (top), relative humidity (middle) and solar radiation (bottom) time series at site TAL_01 near the dam wall (12th August 2018 to 2nd September 2018)

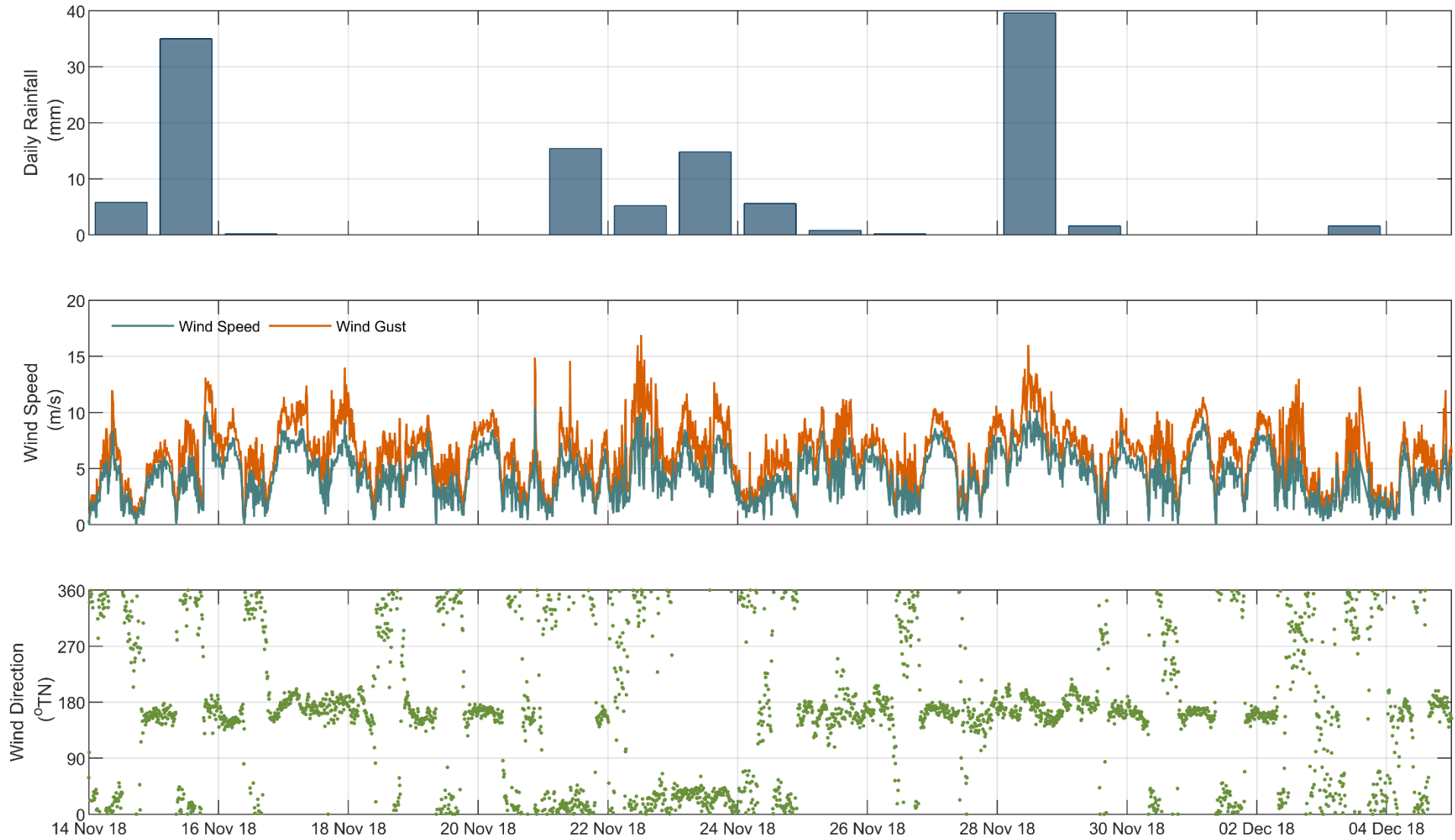


Figure J-3

Daily rainfall (top), wind speed (middle) and wind direction (bottom) time series at site TAL_01 near the dam wall (14th November 2018 to 5th December 2018)

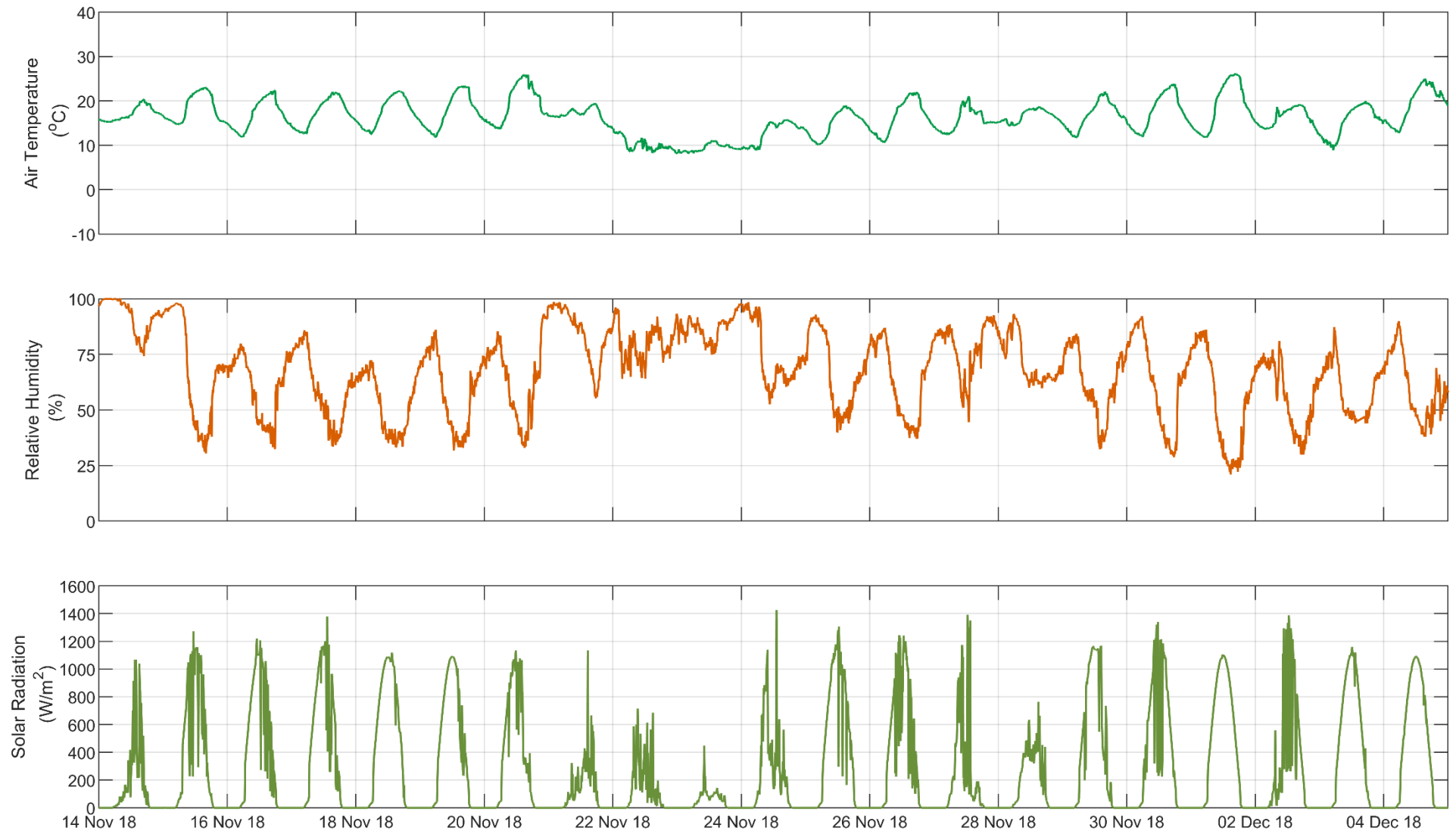


Figure J-4 Daily air temperature (top), relative humidity (middle) and solar radiation (bottom) time series at site TAL_01 near the dam wall (14th November 2018 to 5th December 2018)

Water Quality

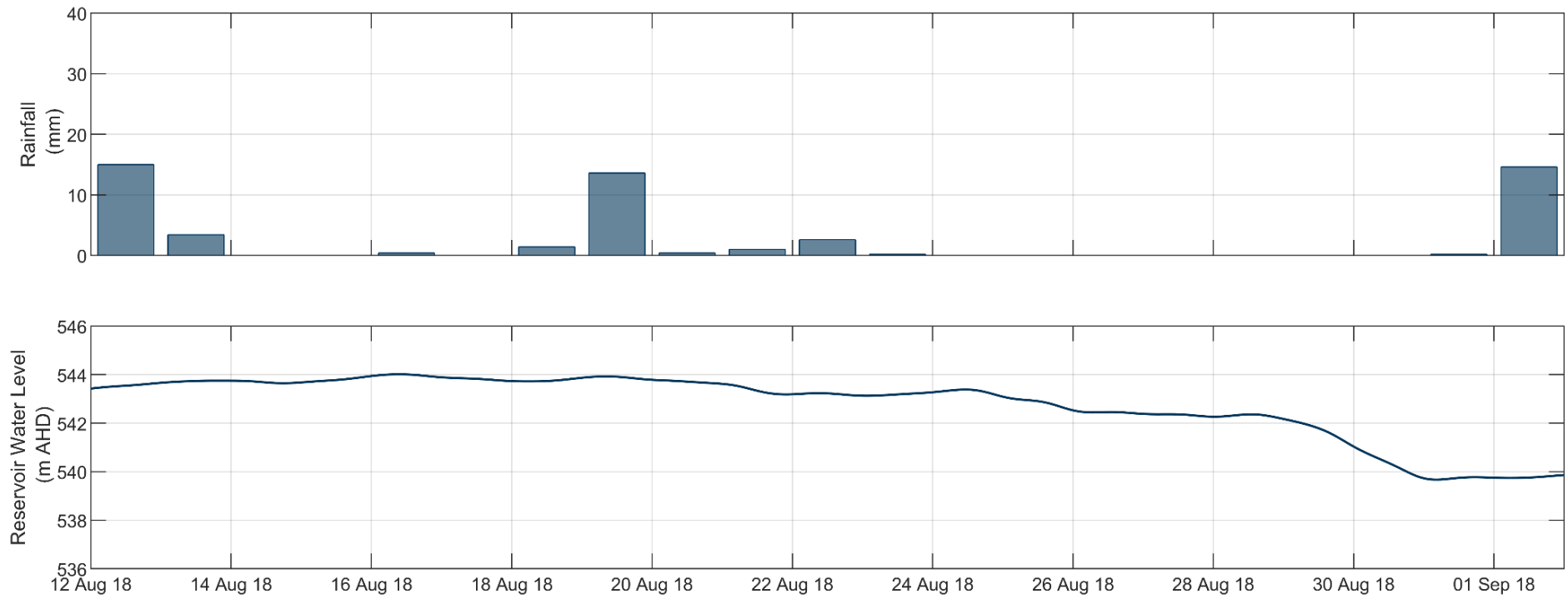


Figure J-5

Total rainfall (top) and water level (bottom) at site TAL_01 near the dam wall (12th August 2018 to 2nd September 2018)

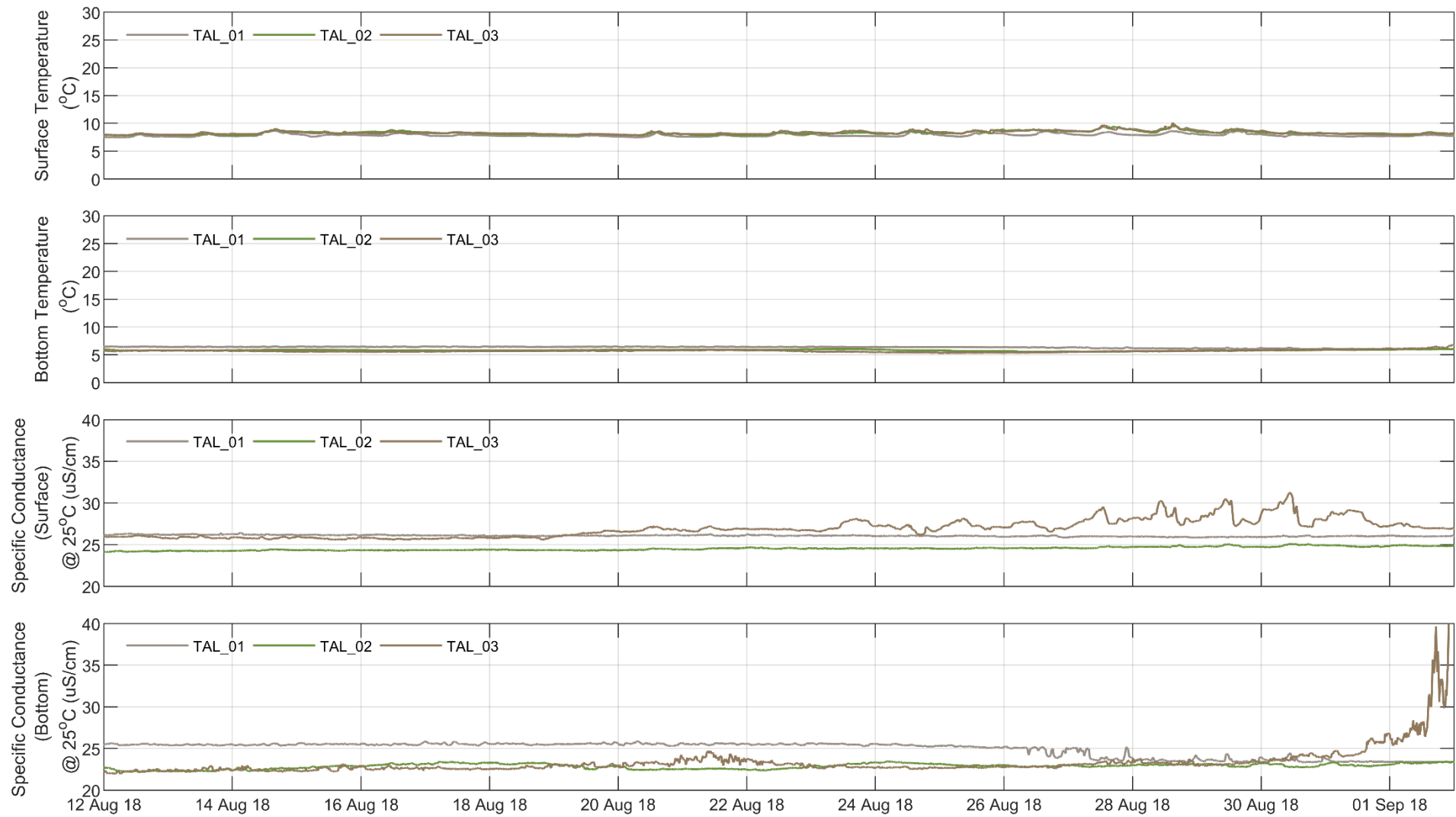


Figure J-6
September 2018)

Surface (0.6 below WL) and bottom (4.5 m above bed) water temperature and specific conductance at Talbingo Reservoir monitoring sites (12th August 2018 to -2nd

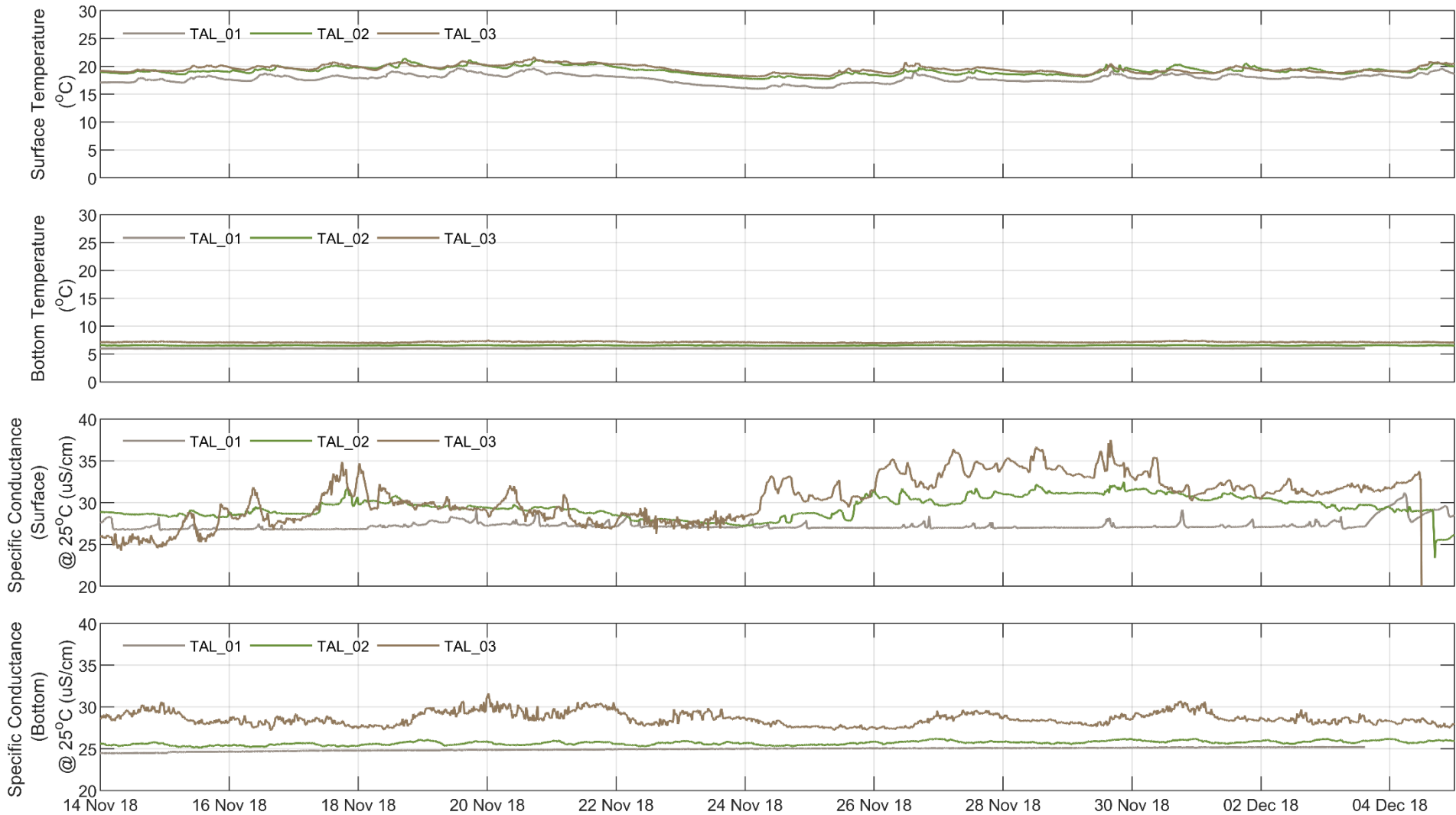


Figure J-7 Surface (0.6 below WL) and bottom (4.5 m above bed) water temperature and specific conductance at Talbingo Reservoir monitoring sites (14th November 2018 to 5th December 2018)

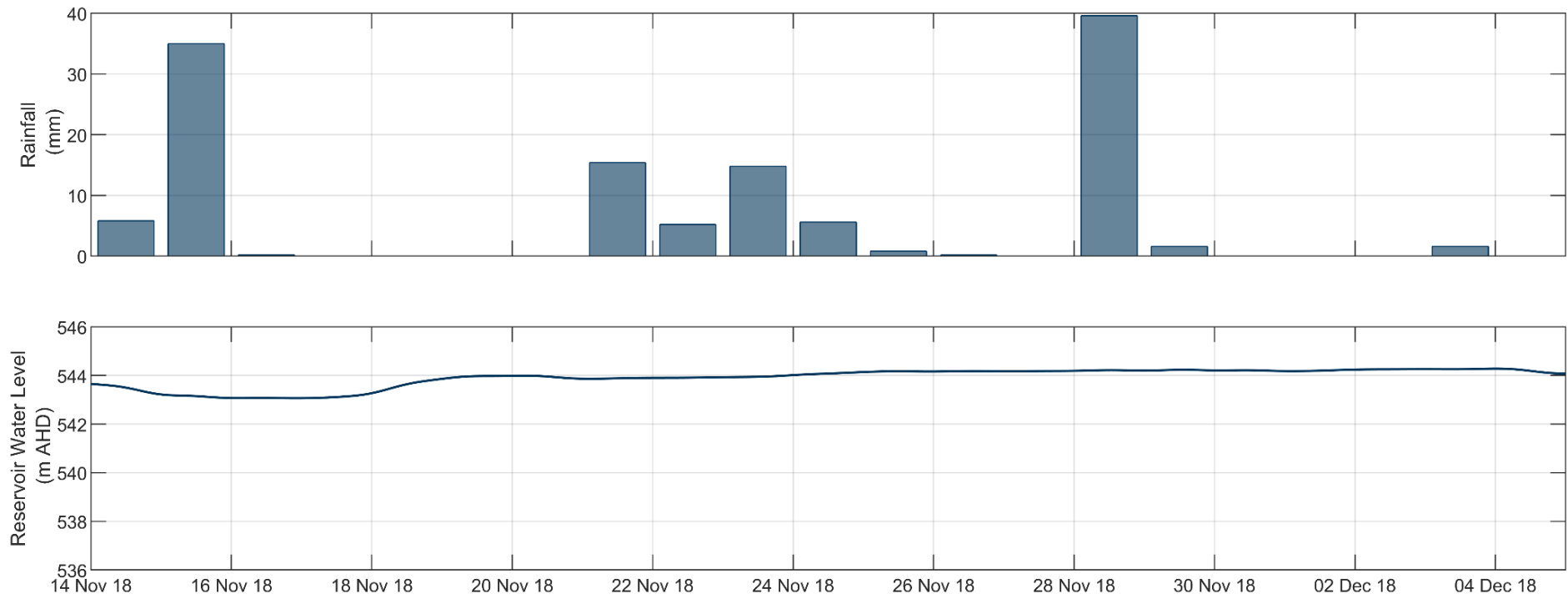


Figure J-8 Total rainfall (top) and water level (bottom) at site TAL_01 near the dam wall (14th November 2018 to 5th December 2018)

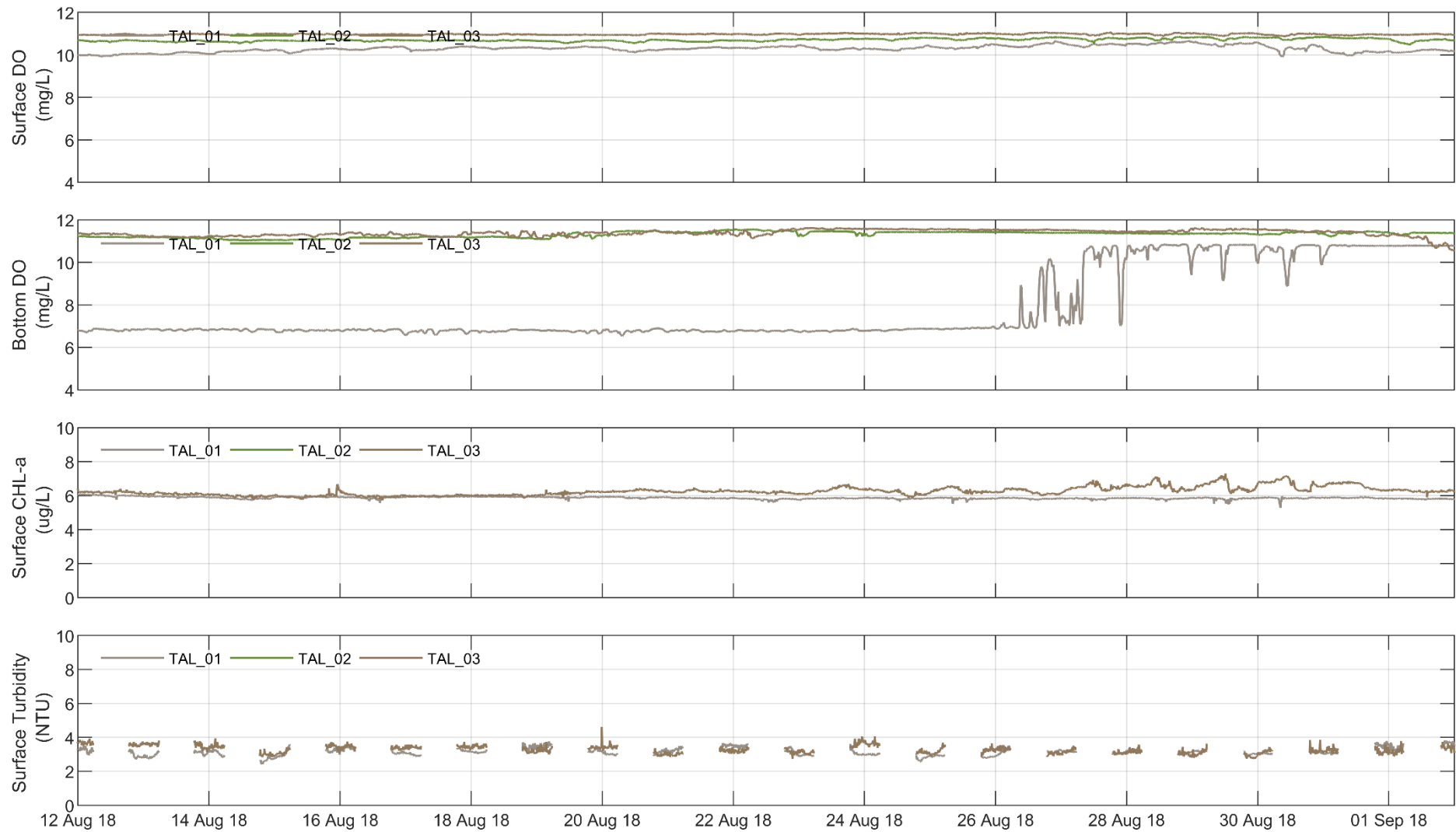


Figure J-9

Surface (1.0 below WL) and bottom (4.5 m above bed) dissolved oxygen concentration and surface (1.0 below WL) CHL-a and Turbidity at Talbingo Reservoir monitoring sites (12th August 2018 to -2nd September 2018)

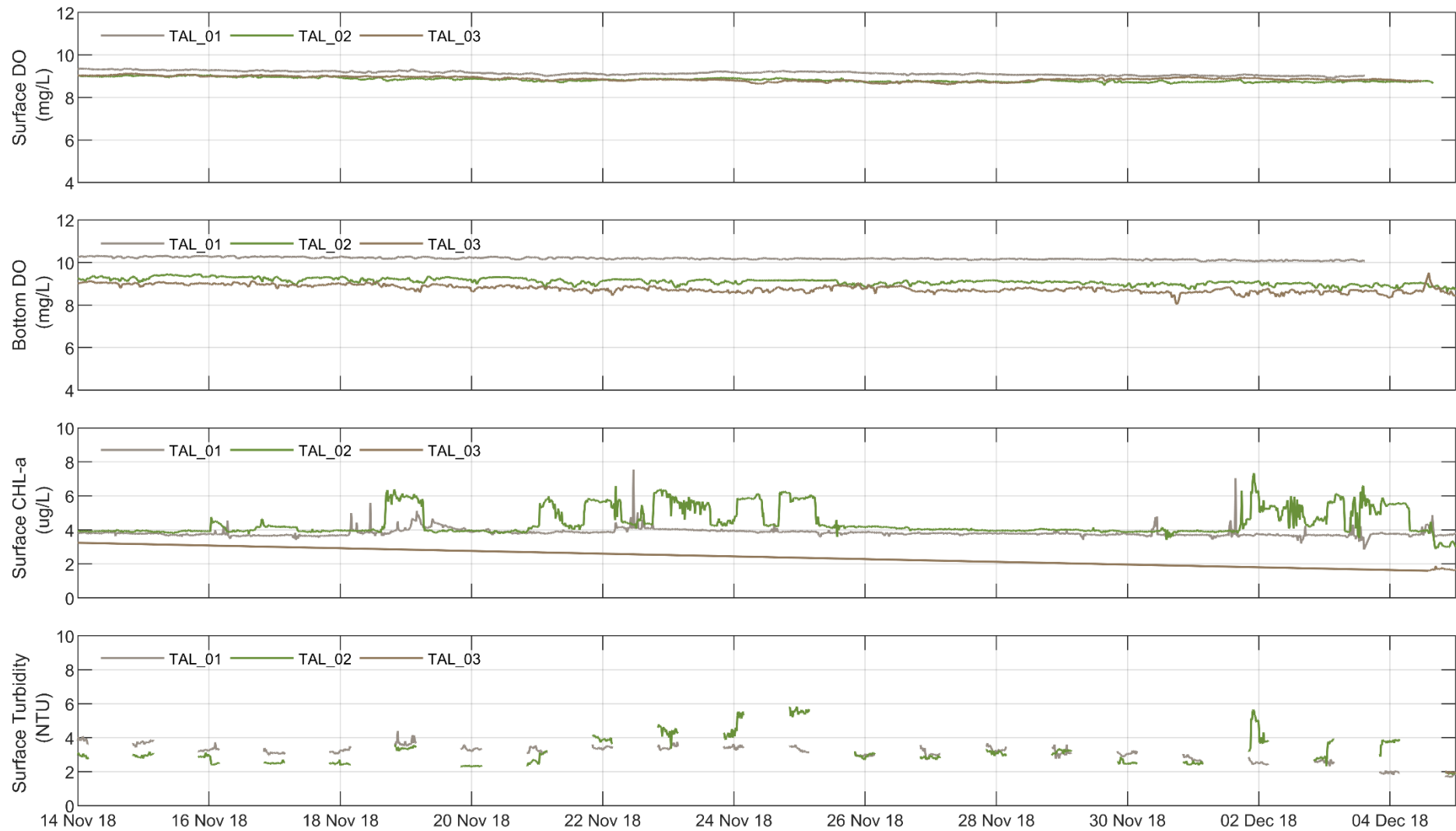


Figure J-10

Surface (1.0 below WL) and bottom (4.5 m above bed) dissolved oxygen concentration and surface (1.0 below WL) CHL-a and Turbidity at Talbingo Reservoir monitoring sites (14th November 2018 to 5th December 2018)

Water Temperature Profiles

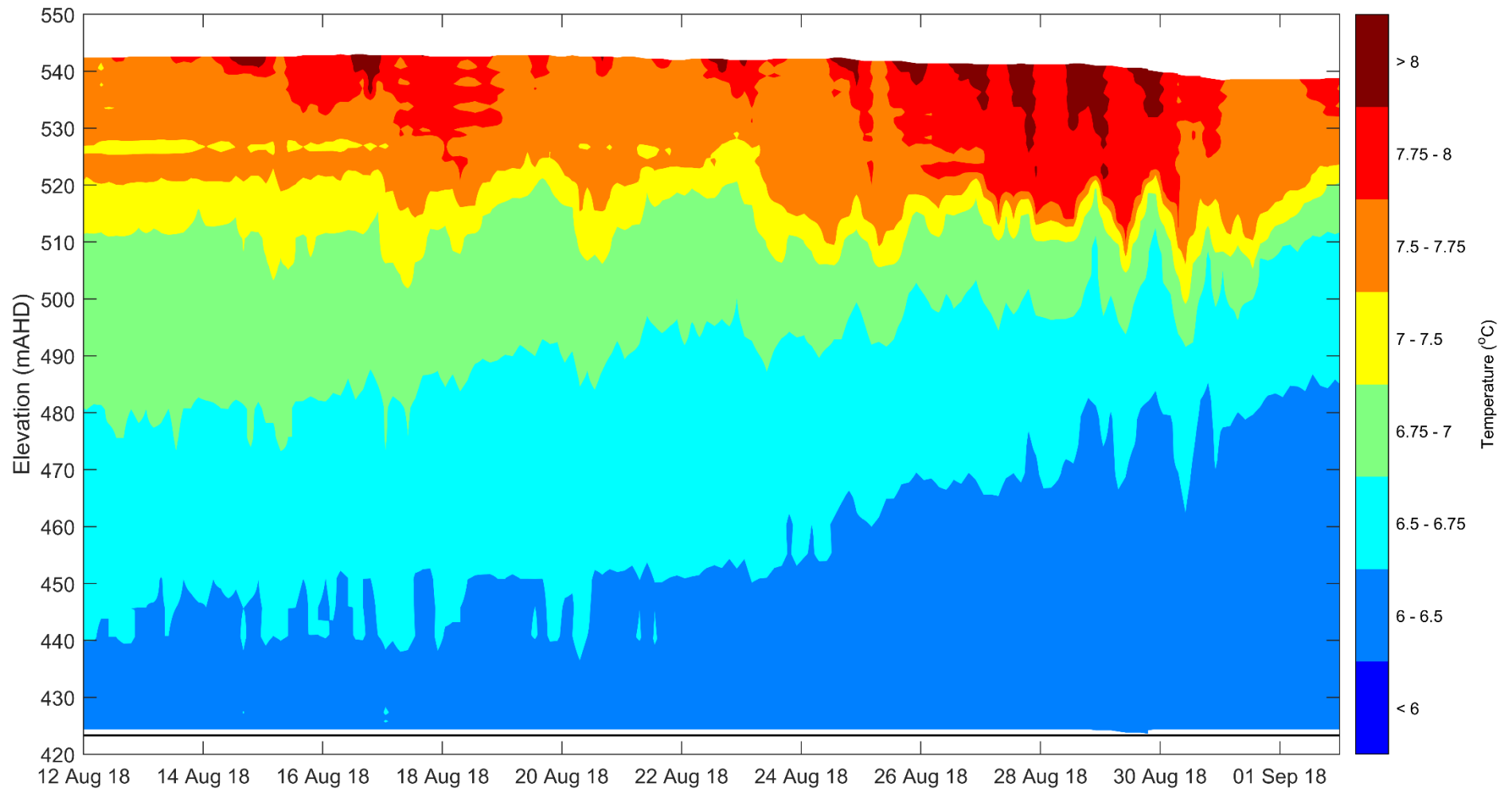


Figure J-11 Water temperature contours at site TAL_01 near the dam wall (12th August 2018 to 2nd September 2018)

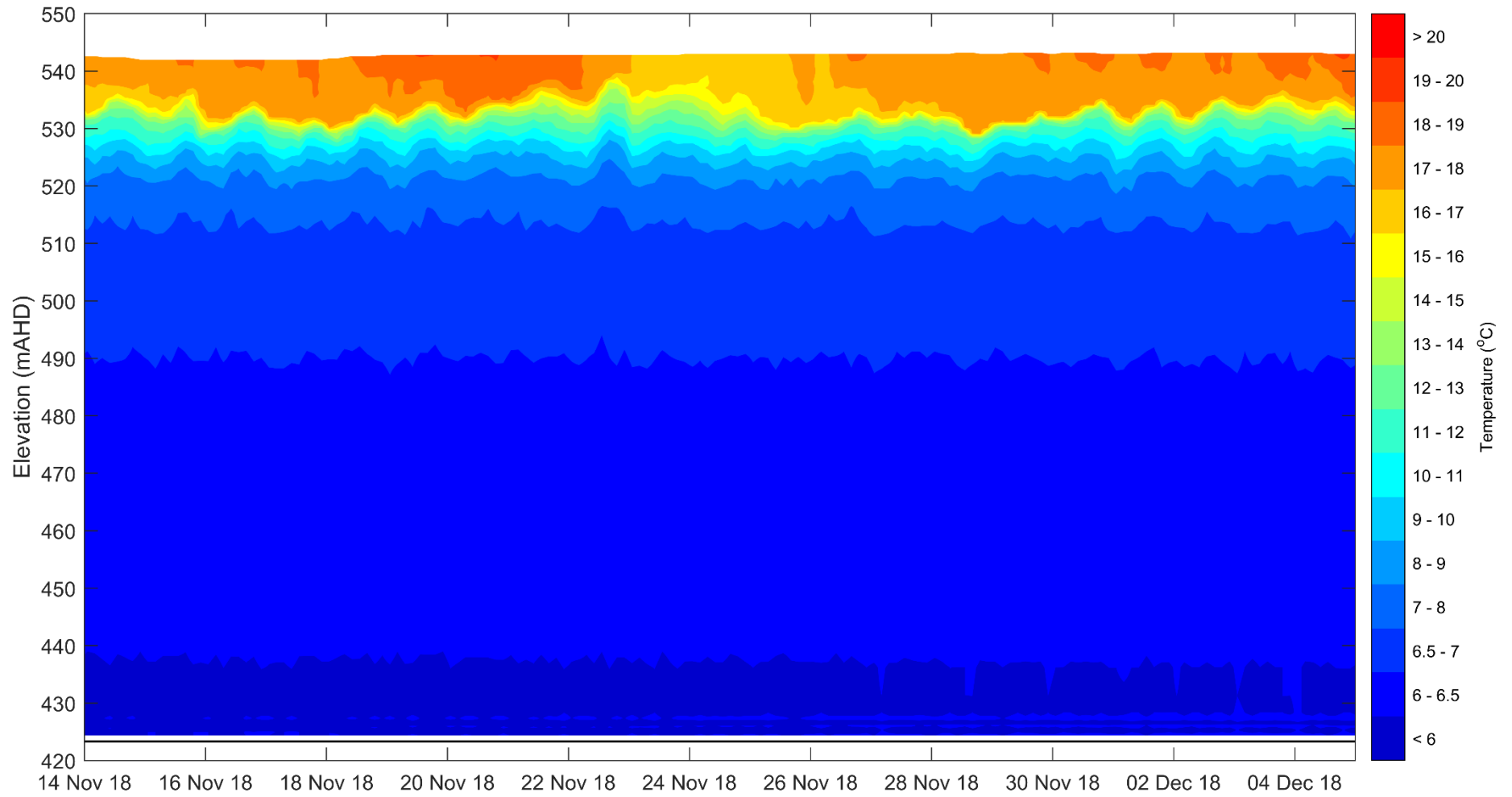


Figure J-12 Water temperature contours at site TAL_01 near the dam wall (14th November 2018 to 5th December 2018)

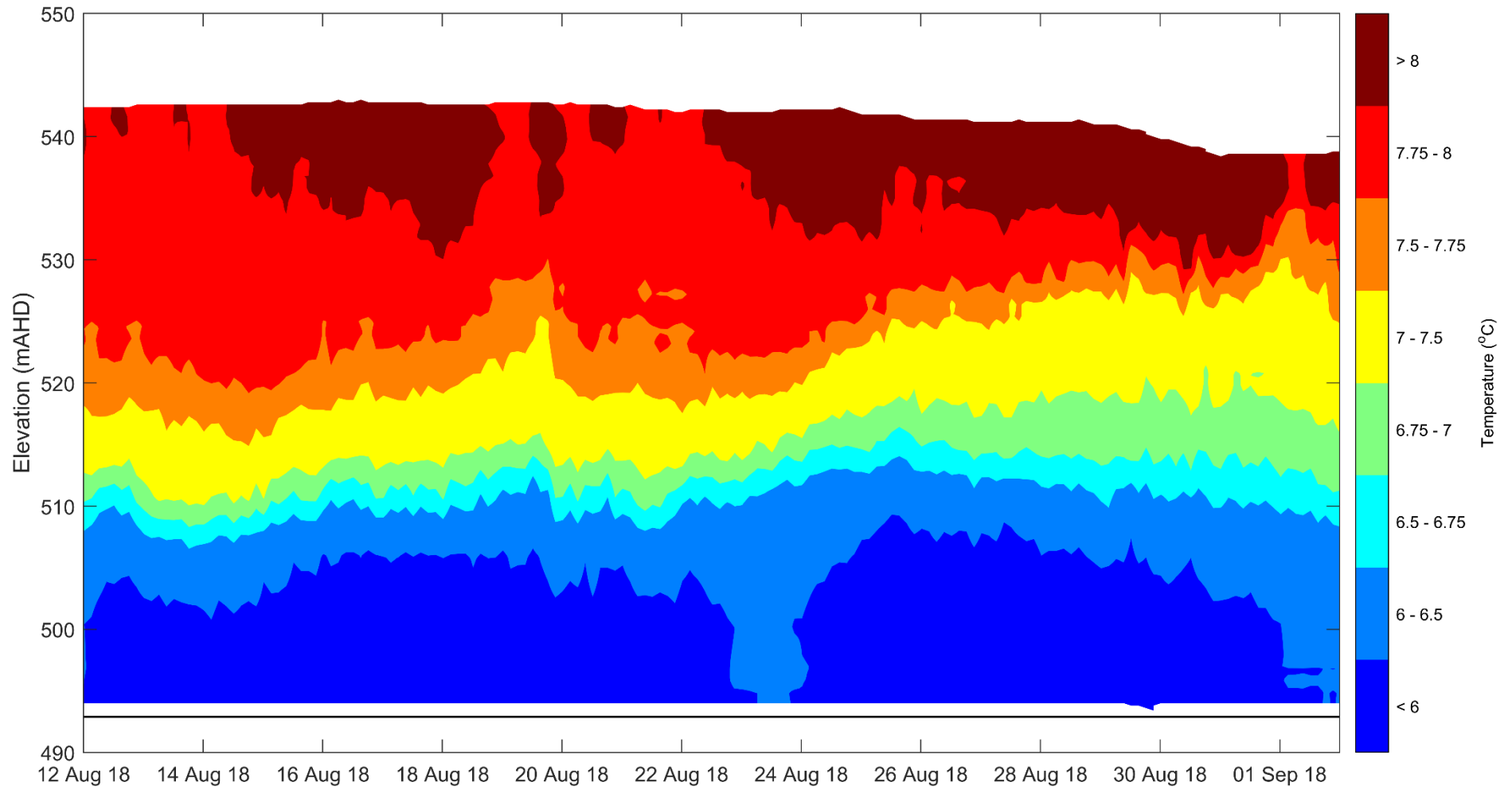


Figure J-13 Water temperature contours at site TAL_02, 14km upstream of dam wall (12th August 2018 to 2nd September 2018)

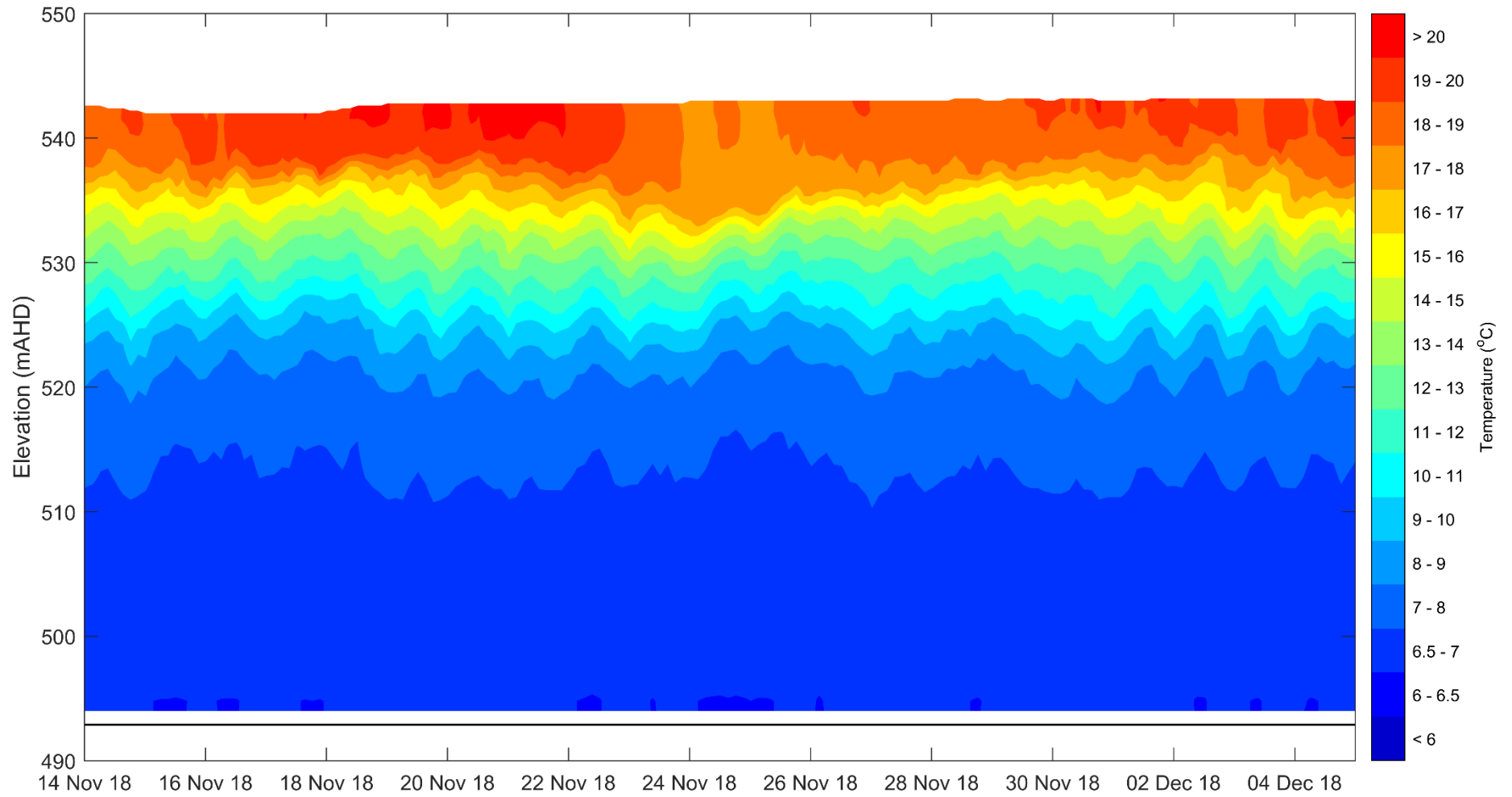


Figure J-14 Water temperature contours at site TAL_02, 14km upstream of dam wall (14th November 2018 to 5th December 2018)

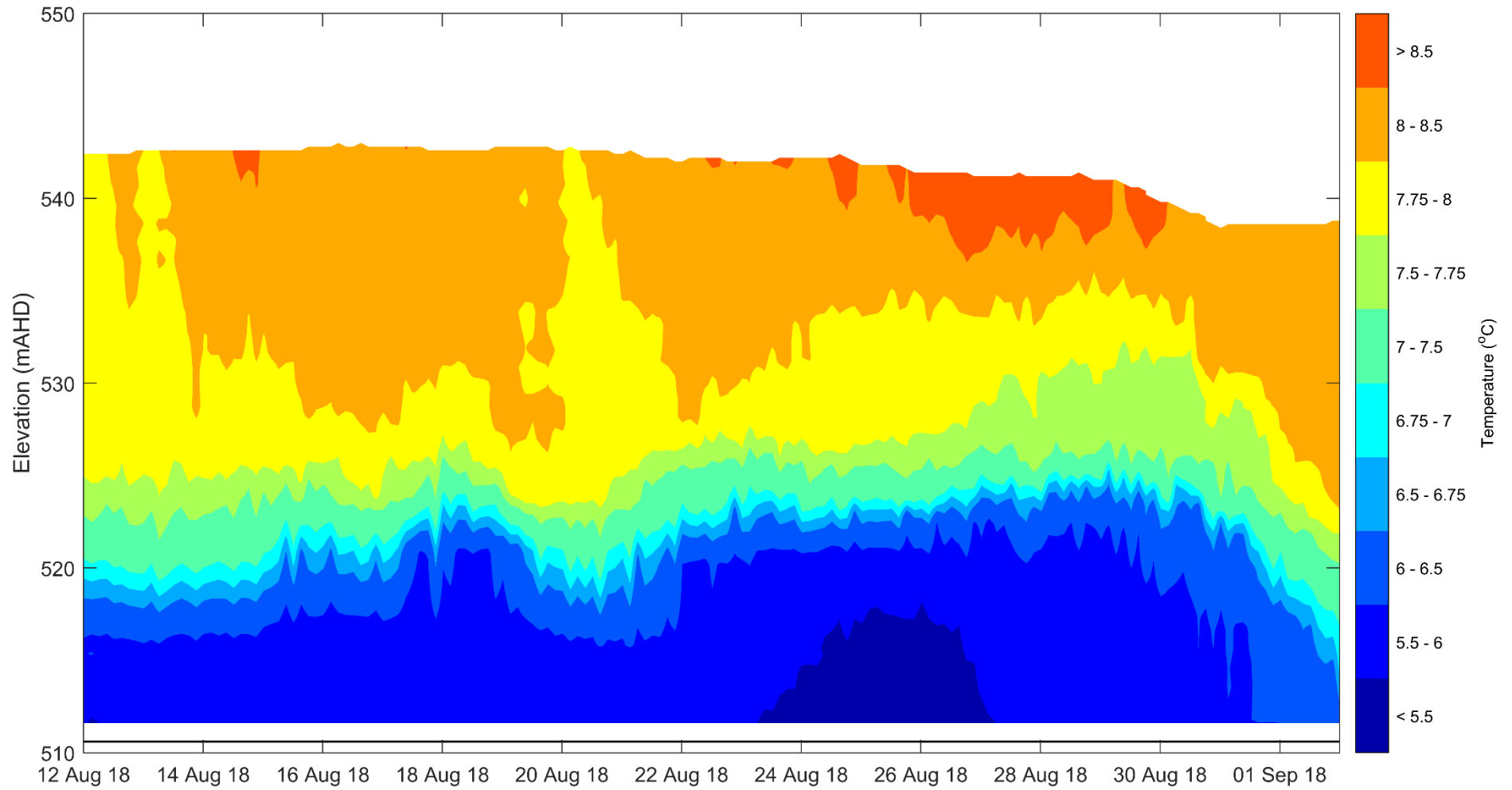


Figure J-15 Water temperature contours at site TAL_03, 17 km upstream of the dam wall (12th August 2018 to 2nd September 2018)

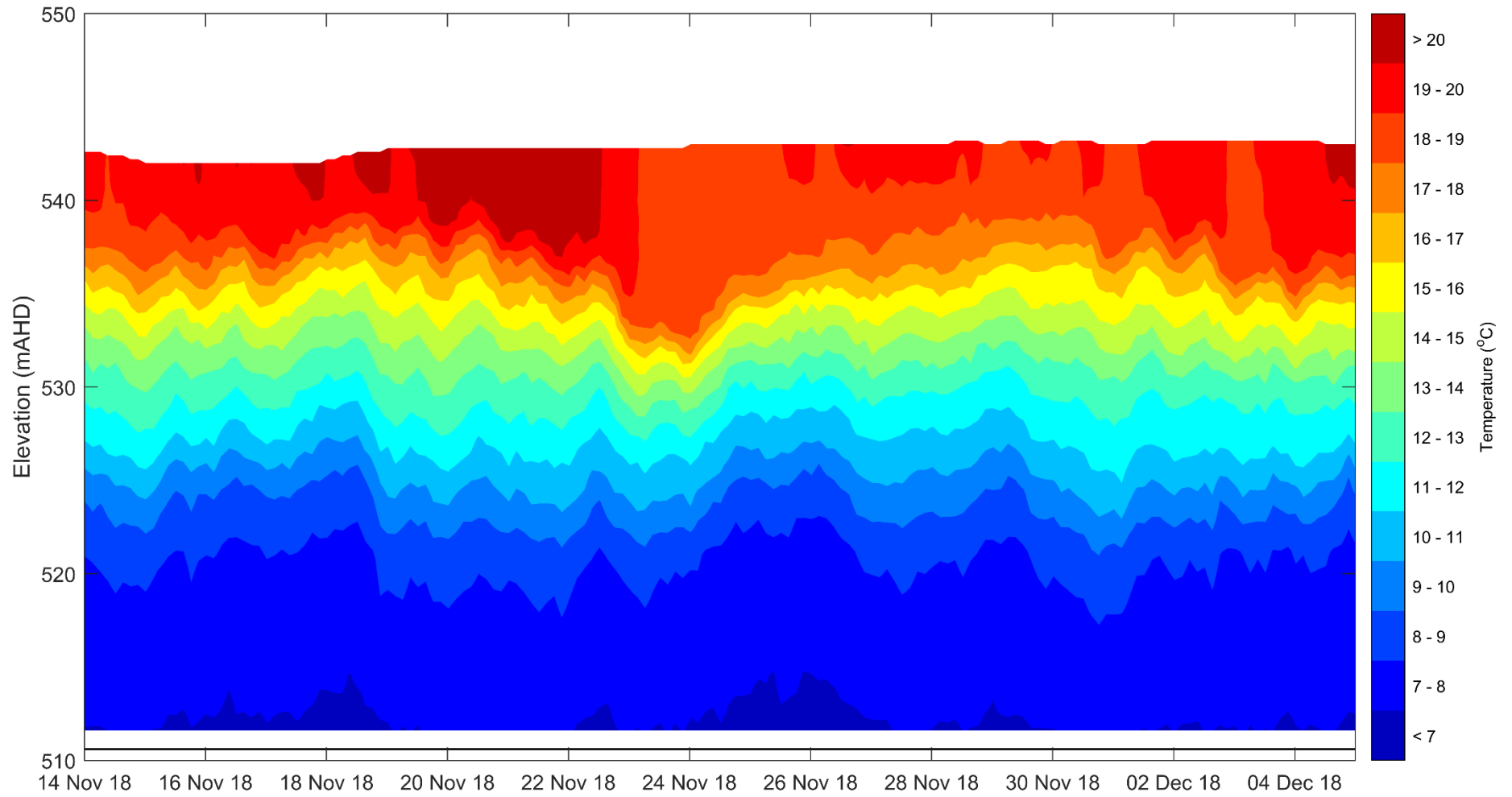


Figure J-16 Water temperature contours at site **TAL_03**, 17 km upstream of the dam wall (14th November 2018 to 5th December 2018)

Tantangra Reservoir

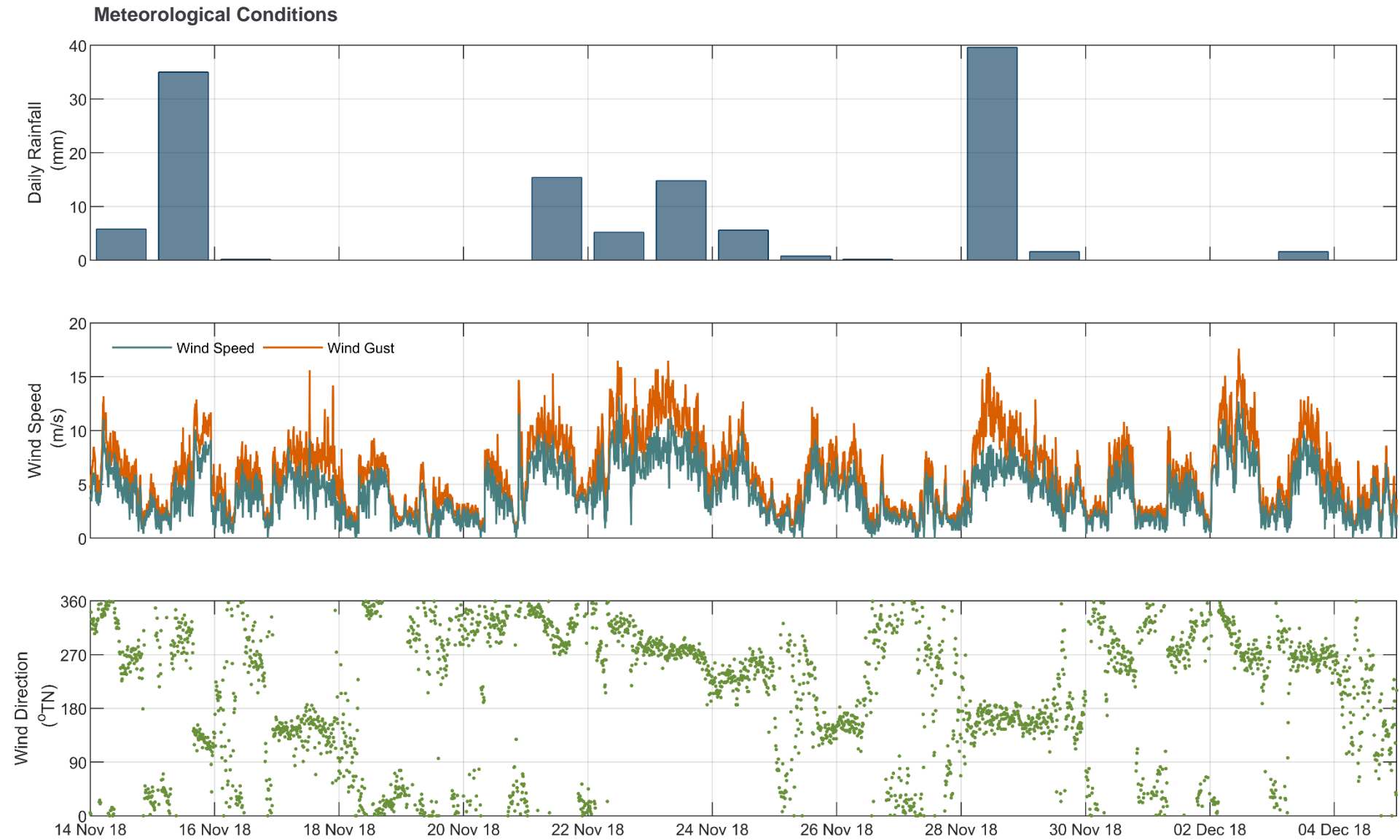


Figure J-17 Daily rainfall (top), wind speed (middle) and wind direction (bottom) time series at site TAN_02, 2 km upstream of the dam wall (14th November 2018 to 5th December 2018)

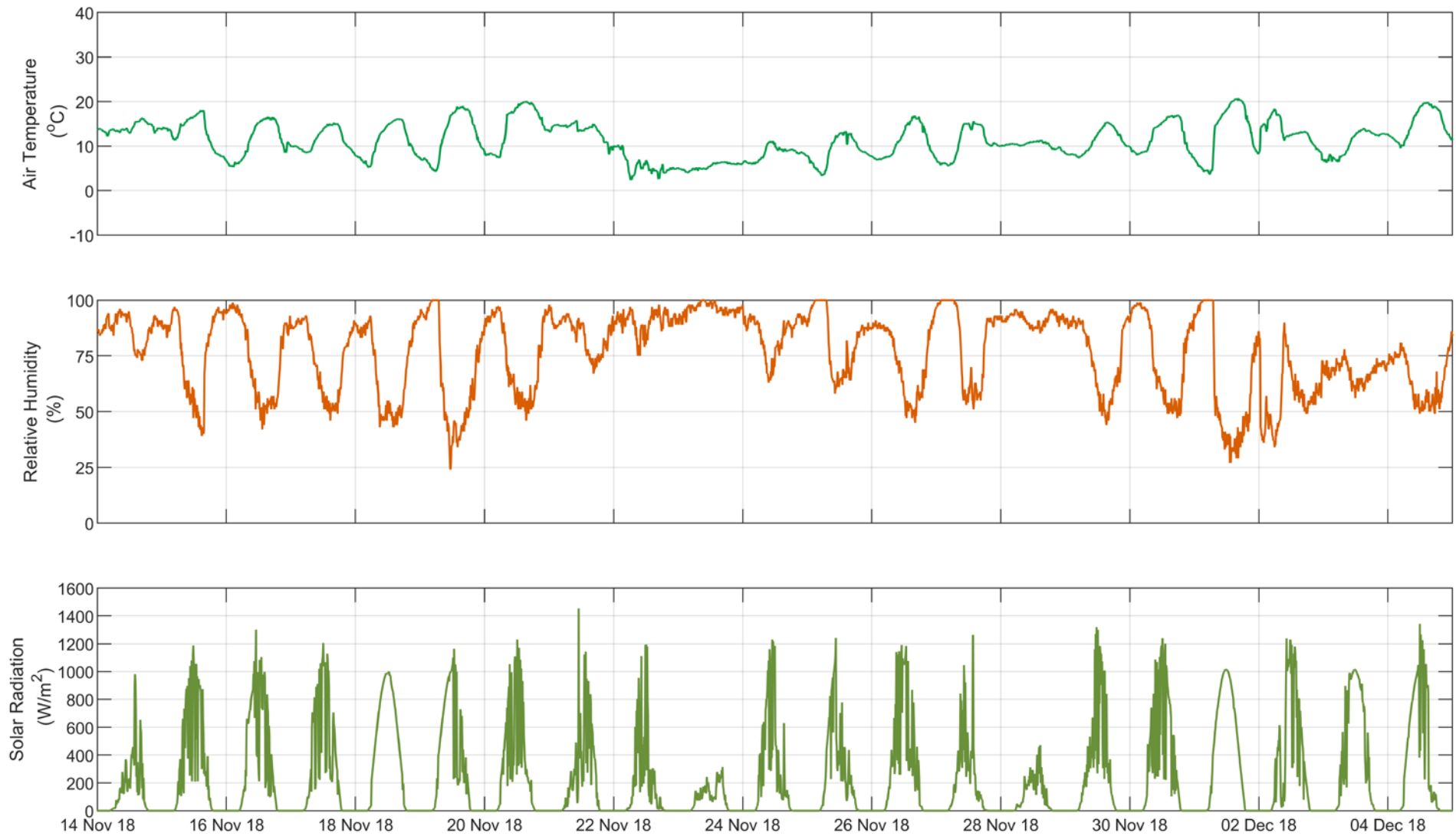


Figure J-18 Daily air temperature (top), relative humidity (middle) and solar radiation (bottom) time series at site TAN_02, 2 km upstream of the dam wall (14th November 2018 to 5th December 2018)

Water Quality

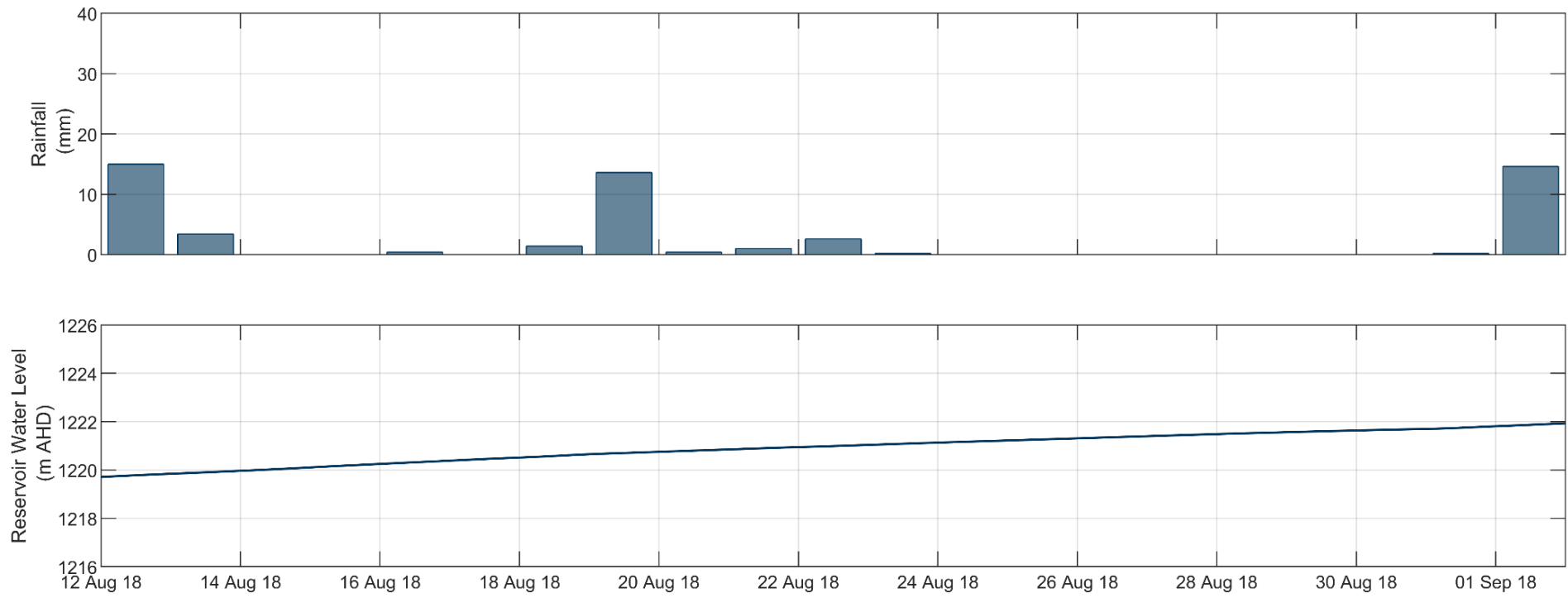


Figure J-19 Total rainfall (top) and water level (bottom) near the Tantangara dam wall (12th August 2018 to 2nd September 2018)

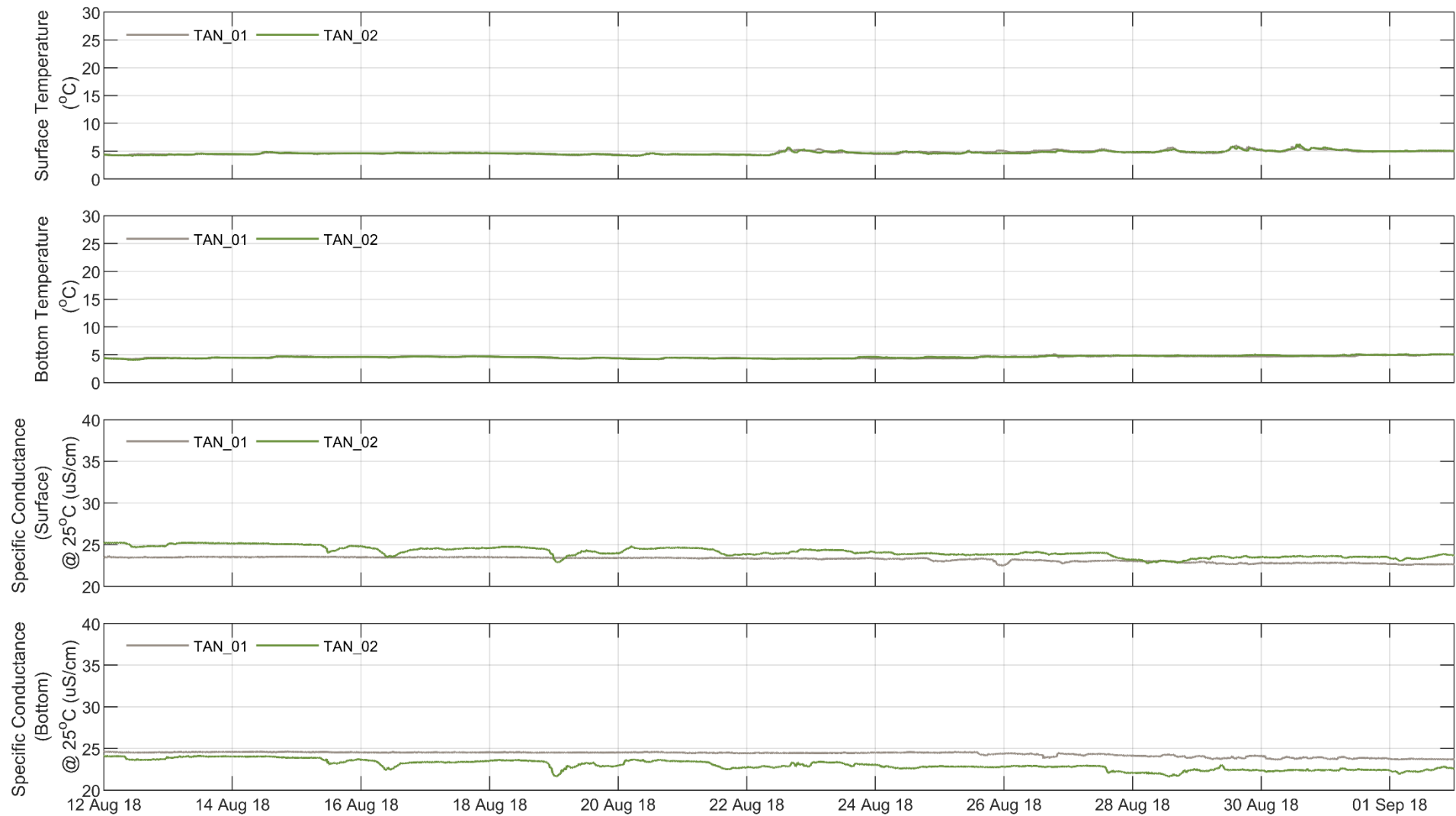


Figure J-20 Surface (0.6 below WL) and bottom (4.5 m above bed) water temperature and specific conductance at Tantangara Reservoir monitoring sites (12th August 2018 to 2nd September 2018)

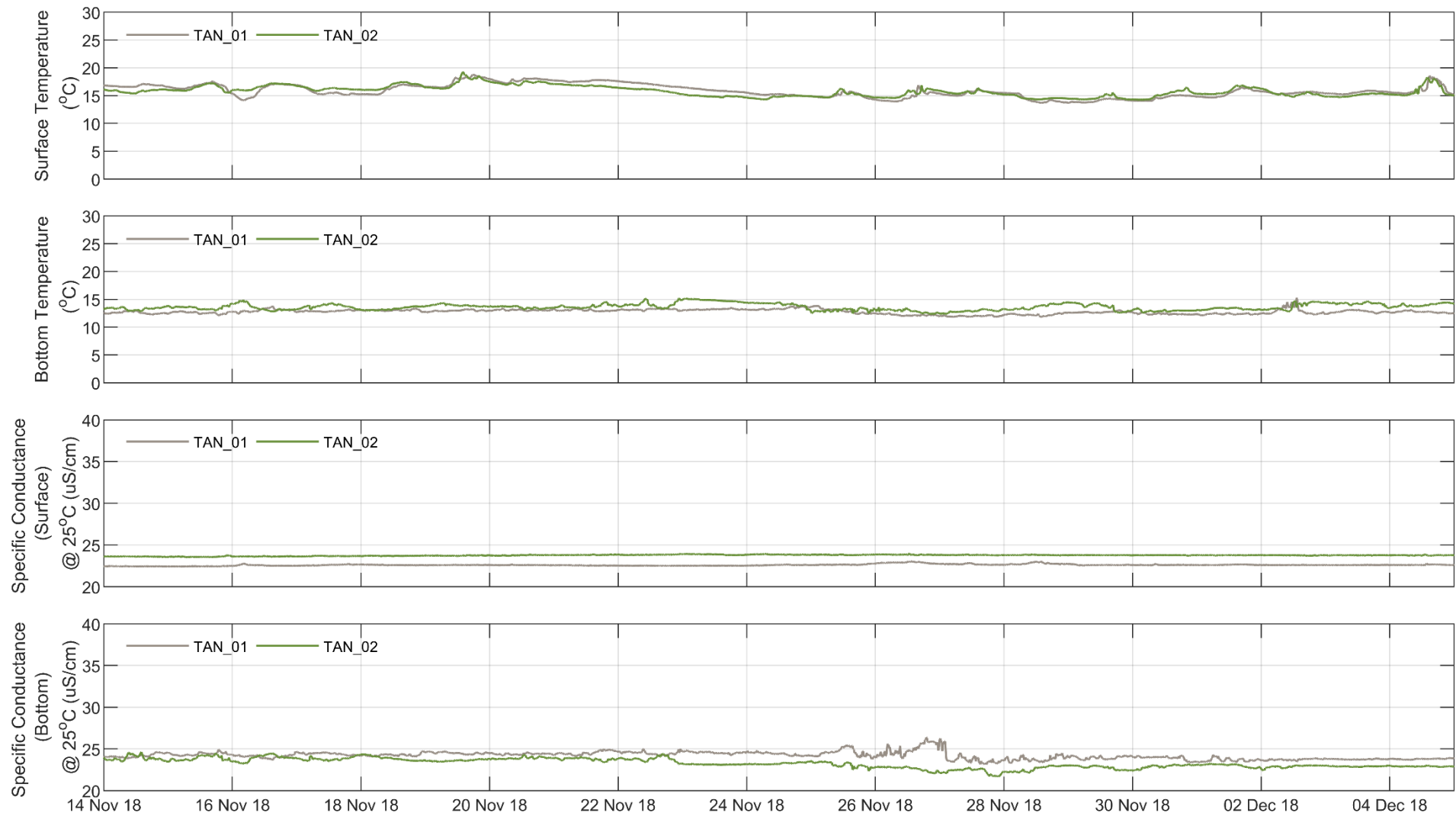


Figure J-21 Surface (0.6 below WL) and bottom (4.5 m above bed) water temperature and specific conductance at Tantangara Reservoir monitoring sites (14th November 2018 to 5th December 2018)

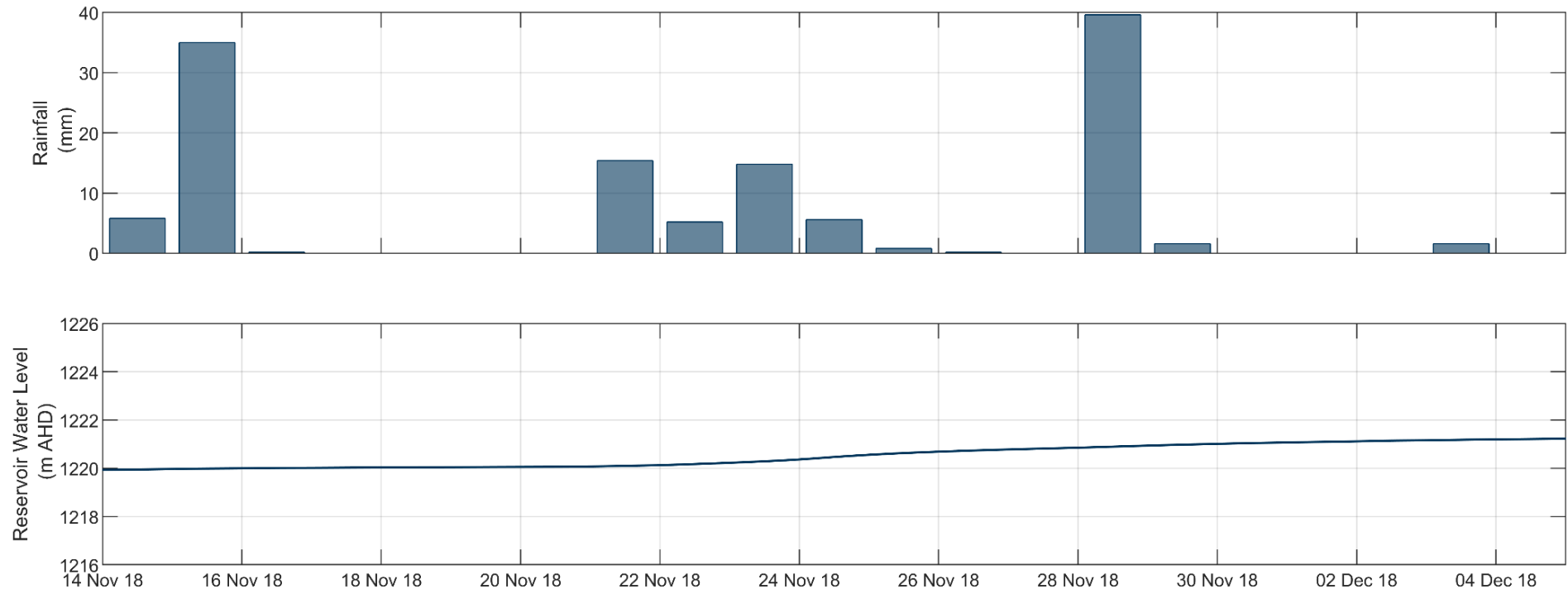


Figure J-22 Total rainfall (top) and water level (bottom) near the Tintangara dam wall (14th November 2018 to 5th December 2018)

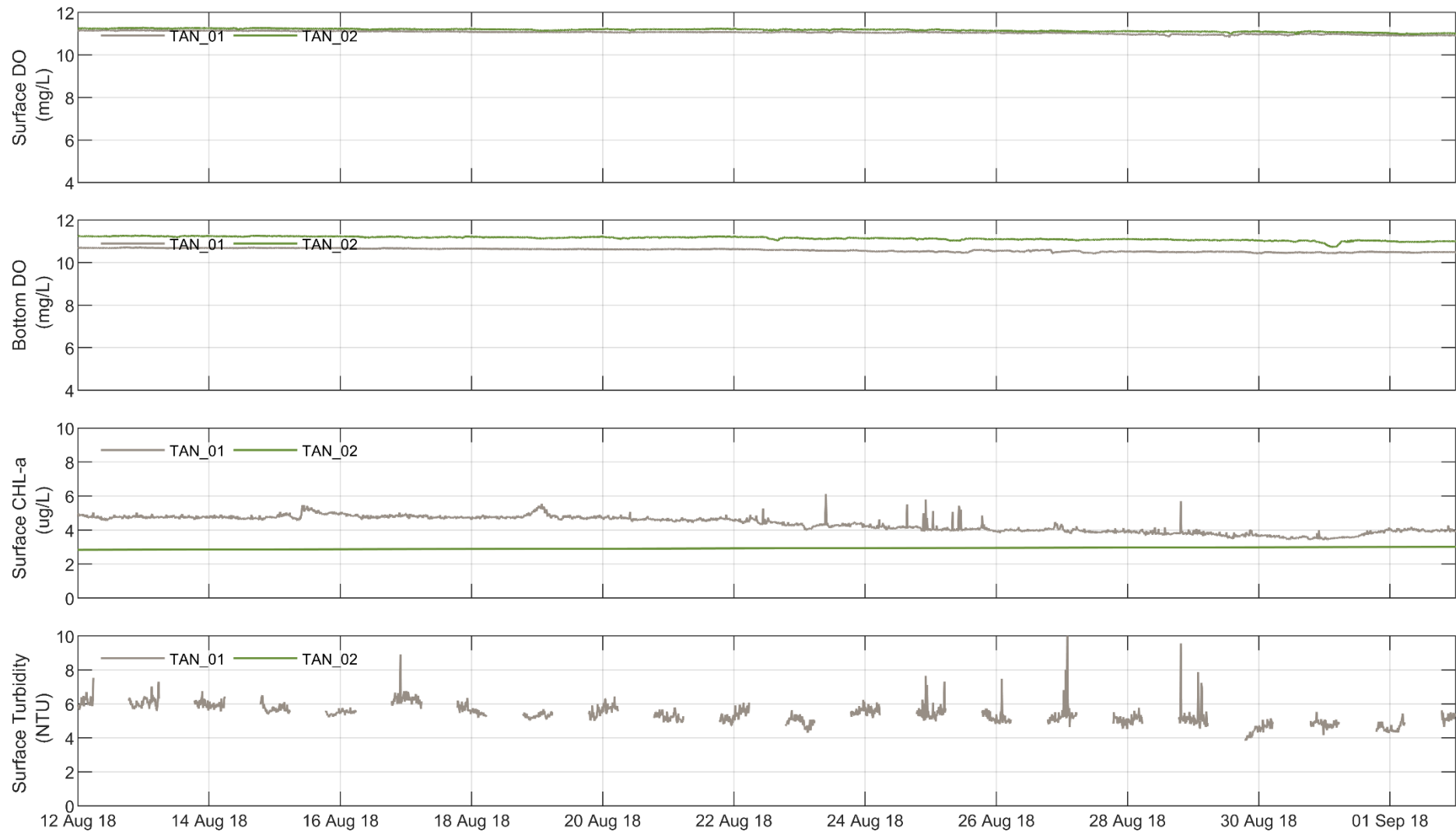


Figure J-23 Surface (1.0 below WL) and bottom (4.5 m above bed) dissolved oxygen concentration and surface (1.0 below WL) CHL-a and Turbidity at Tantangara Reservoir monitoring sites (12th August 2018 to 2nd September 2018)

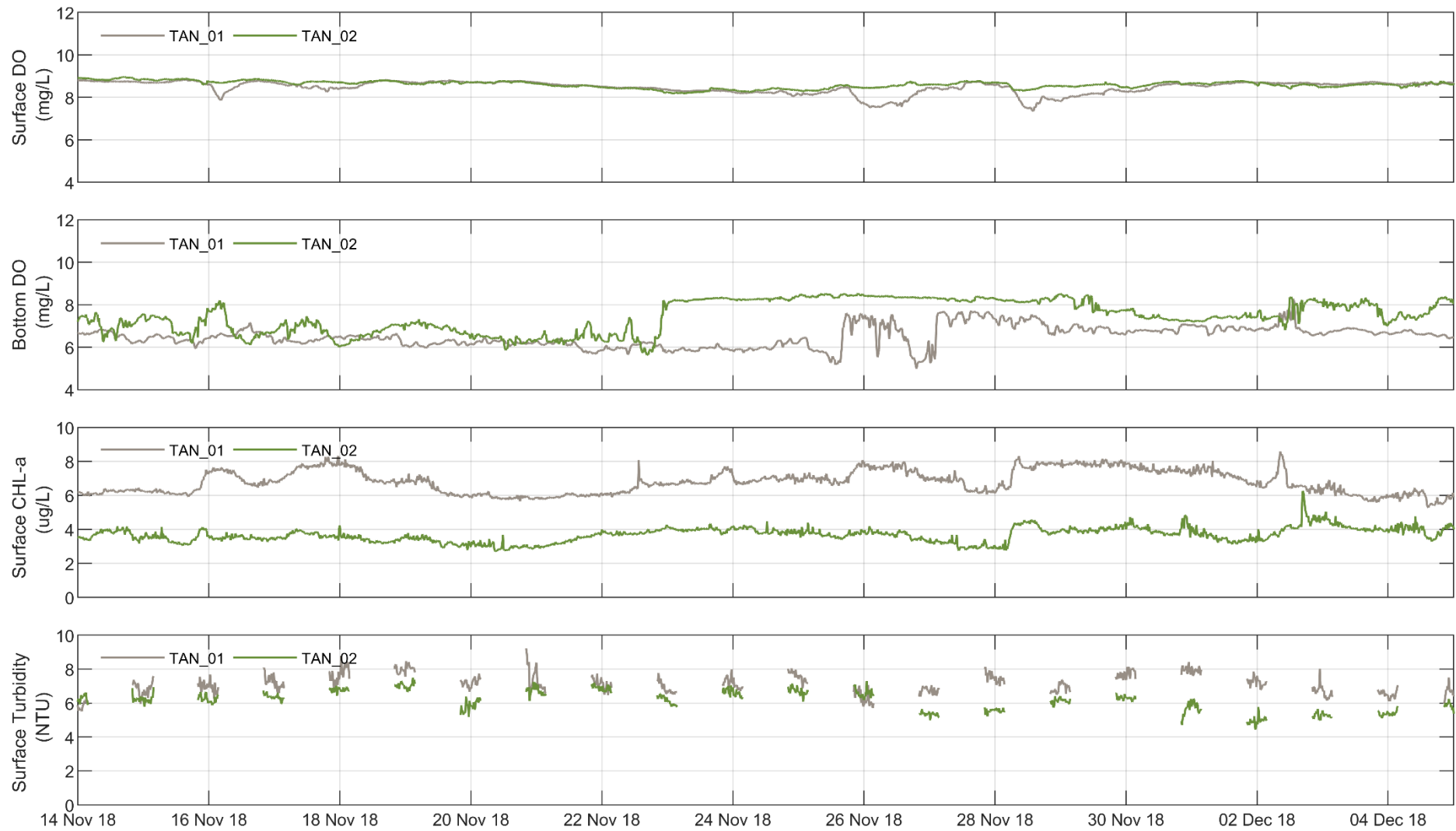


Figure J-24 Surface (1.0 below WL) and bottom (4.5 m above bed) dissolved oxygen concentration and surface (1.0 below WL) CHL-a and Turbidity at Tantangra Reservoir monitoring sites (14th November 2018 to 5th December 2018)

Water Temperature Profiles

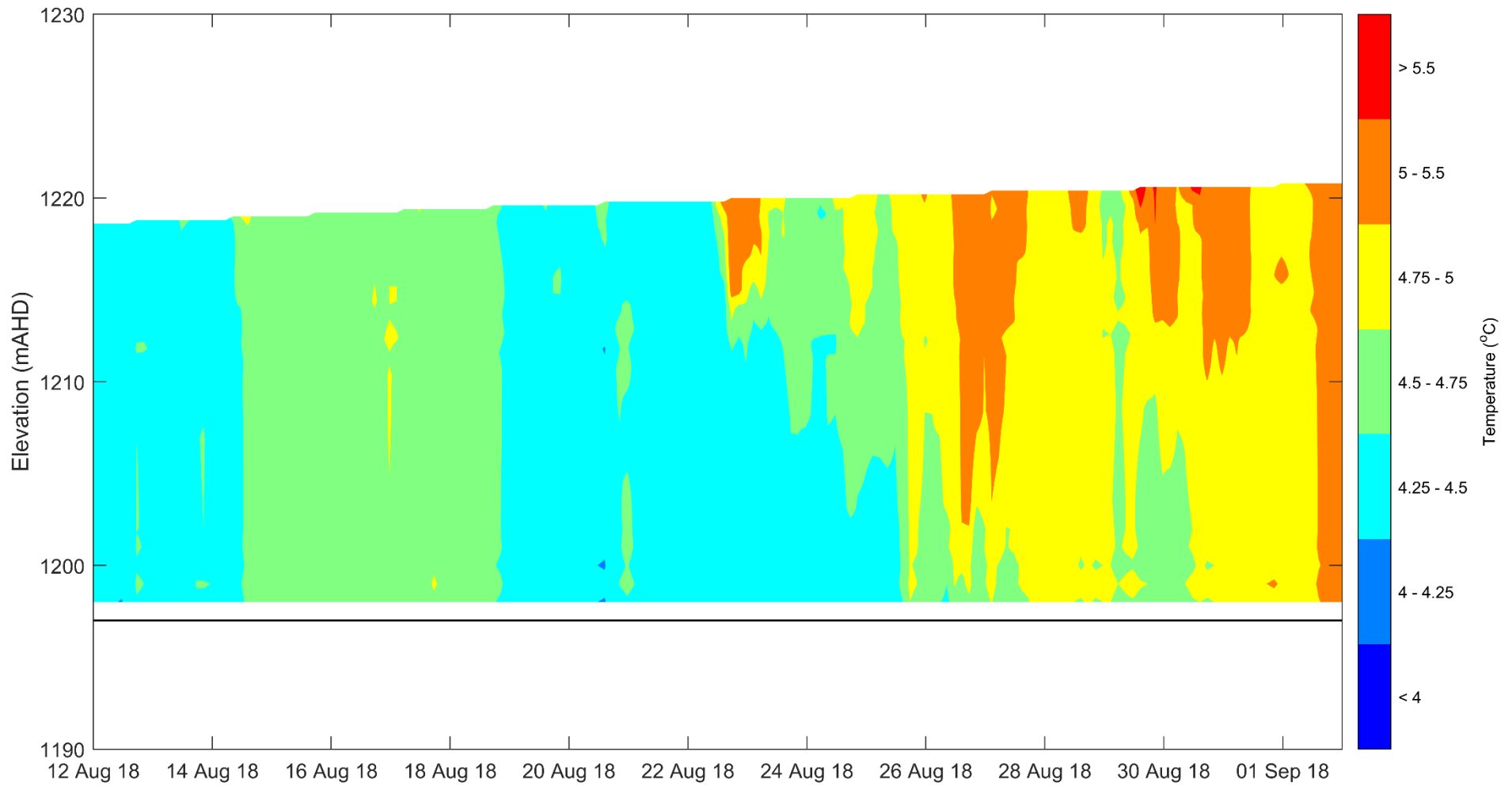


Figure J-25

Water temperature contours at site **TAN_01**, 600 m upstream of the dam wall (**12th August 2018 to 2nd September 2018**)

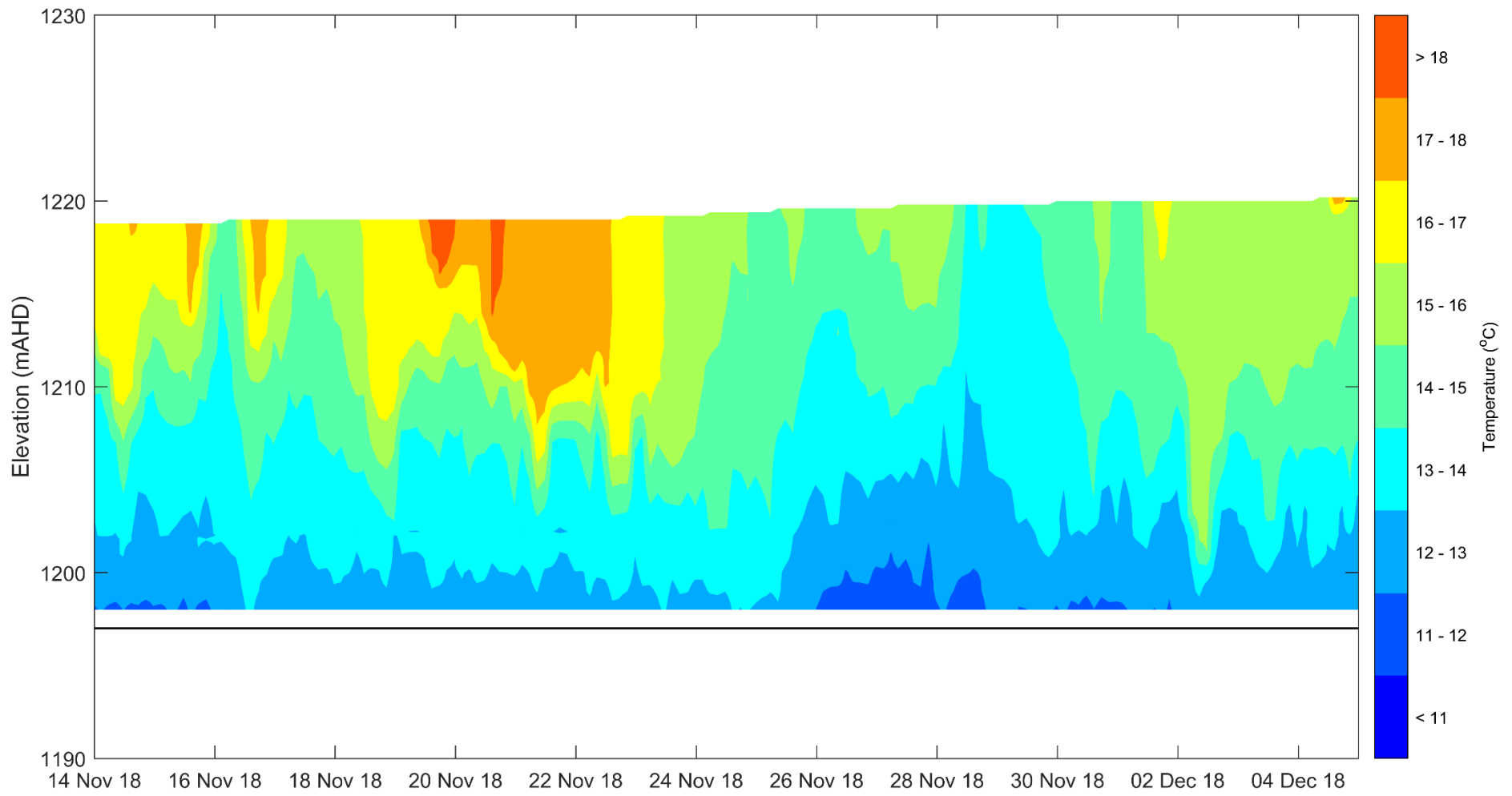
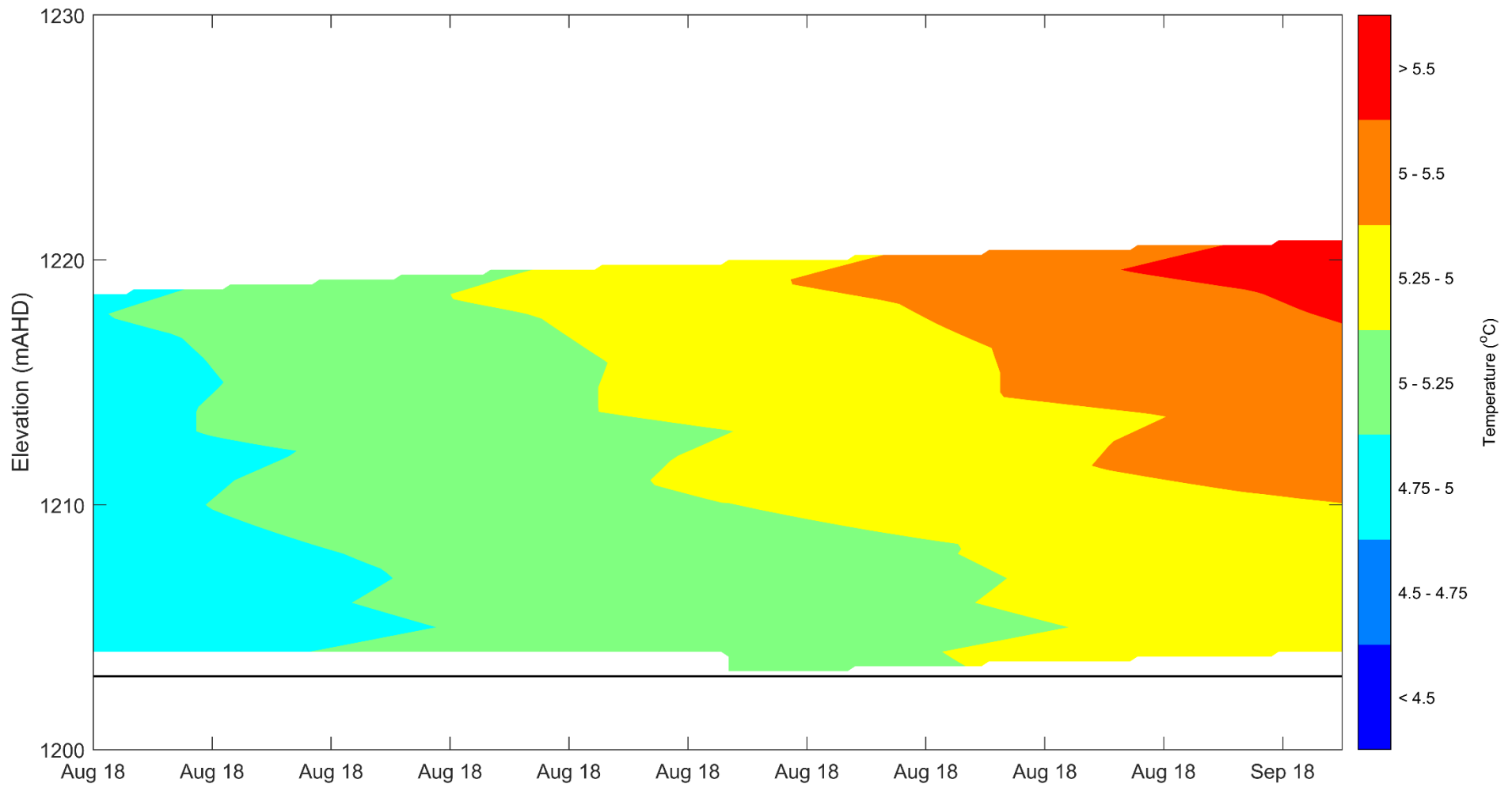


Figure J-26

Water temperature contours at site **TAN_01**, 600 m upstream of the dam wall (**14th November 2018 to 5th December 2018**)



N:\Projects\599\FY18\111_EMMSnowyHydro\Phase 6 - Physical Limnology\Des_An\Matlab\Data Analysis\2. Thermistor\ls_plot_thermister_data.m

Figure J-27

Water temperature contours at site **TAN_02**, 2 km upstream of the dam wall (**12th August 2018 to 2nd September 2018**)

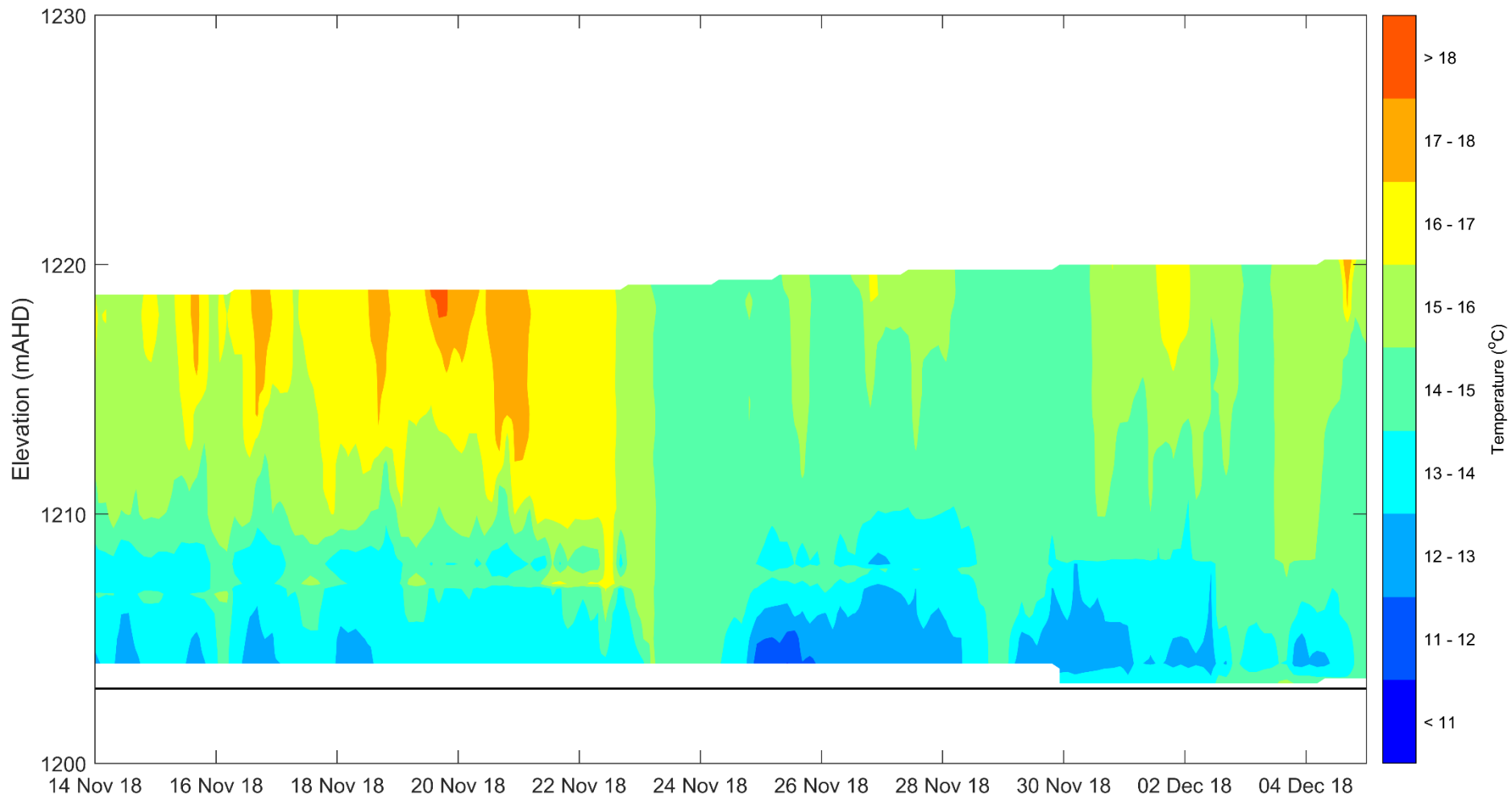


Figure J-28 Water temperature contours at site **TAN_02**, 2 km upstream of the dam wall (14th November 2018 to 5th December 2018)